$p_{n,m}$ is given by the roots of the transcendental equation

$$\alpha p_{n,m}^2 - n^2\pi^2 = \beta\left(p_{n,m}\cot\left(p_{n,m}\right) - 1\right) . \tag{21}$$

Vaidyanathan (1971) discussed the physical significance of the α and β terms. α is the ratio of the time constants for macropore-to-micropore diffusion. For values of α less than 10^{-3}, macropore diffusion is much faster than micropore diffusion and the process can be considered to be a two-step process for all practical purposes. For values of α greater than 10^{+2} , macropore diffusion controls (Ruckenstein et al., 1971). In the range of α between these two limiting cases, both mechanisms are important. The term $\beta/3\alpha$ represents the ratio of sorption in the micropores to macropores at equilibrium. Thus a large value would indicate sorption primarily in the micropores.

Detailed description of other models that were evaluated for potential application to understand the behavior observed for this system may be found in Jubin (1995). These models include

- progressive conversion or volume reaction,
- nonisothermal micropore/macropore diffusion, and
- nonisothermal bed diffusion controlling.

Experimental Objectives

Conditions

As in numerous other studies [Jubin (1980, 1982), Burger and Scheele (1981), Scheele et al. (1983), and Scheele and Burger (1987)], methyl iodide was chosen as the chemical form for the iodine in this study because it is a more difficult form to retain in an adsorption process than elemental iodine. If CH_3I can be successfully retained on the silver mordenite, then the elemental iodine will also be retained (Scheele and Burger, 1987).

Experimental data were collected over a range of conditions selected to differentiate between the anticipated primary controlling mechanisms, and further data were collected to evaluate specific process behavior observed in the initial series of tests. The variables considered were (1) pellet diameter, (2) methyl iodide concentration, (3) gas velocity, (4) temperature, and, later in the study, (5) water vapor content of the carrier gas. The first four conditions were selected to examine the effects of these primary variables by varying each one while holding the others at a standard condition. Two duplicate tests were planned to allow a determination of the level of experimental error. Table 1 provides a listing of the ranges considered for each of the independent variables.

Following the completion of the initial series of tests, T3 to T13, 13 additional tests were conducted to explore specific aspects of this process and to gain further clarification on the behavior observed during the initial tests. Four specific avenues examined (1) the effects of either increasing or decreasing the water vapor content of the air, (2) further lowering of the gas velocity, (3) lower CH_3I concentration, and (4) lower operating temperatures. Two unique runs were also conducted, the first to determine the amount of water adsorbed from the instrument air and the second to determine the CH_3I loading on the zeolite media without chemical reaction occurring. Table 2 presents a listing of the conditions studied in each test.

Table 1 General test conditions.

Variable	Range or values considered
Pellet diameter (in.)	**1/16** and 1/8
Gas velocity (m/min)	1, 2, 5, and **10**
Methyl iodide concentration (mg/m^3)	250, 500, **1000**, and 1500
Temperature (°C)	125, **150**, and 200
Water content [dew point (°C)]	–40, **–15 to –18**, –11

Note: Bold values were considered reference conditions.

Following the completion of the initial series of tests, T3 to T13, 13 additional tests were conducted to explore specific aspects of this process and to gain further clarification on the behavior observed during the initial tests. Four specific avenues examined (1) the effects of either increasing or decreasing the water vapor content of the air, (2) further lowering of the gas velocity, (3) lower CH_3I concentration, and (4) lower operating temperatures. Two unique runs were also conducted, the first to determine the amount of water adsorbed from the instrument air and the second to determine the CH_3I loading on the zeolite media without chemical reaction occurring. Table 2 presents a listing of the conditions studied in each test.

These supplemental tests specifically provided data on the impact of lower gas velocities (T15, T16, and T18) in an effort to resolve any effects of the gas film and lower CH_3I concentrations (T14) on possible reaction rate controlling conditions. The impacts of variations in the water vapor content of the gas stream were examined by adding a small additional amount of water vapor (T13) and by further drying the instrument air carrier gas (T18).

Test Equipment

Figure 1 is a schematic diagram of the process system showing the principal equipment components. The entire system was located inside a walk-in laboratory hood, with the exception of the dry air, hydrogen/argon and nitrogen cylinders, and the process control and data collection instrumentation.

To briefly describe the test system, a stream of dilute methyl iodide was fed into the test reaction chamber in which the bed containing the known quantity of selected sorbent material was located. The test bed, composed of a thin layer of Ag°Z pellets, one to two pellets deep, was supported by a stainless steel wire basket, which was lowered into a glass gas reaction chamber. In this system, a thin layer of adsorbent media was exposed to the sorbate stream such that all pellets were exposed to a uniform gas composition. Thus the effects of a changing gas composition through the test bed were considered to be negligible. This method was selected to provide a constant pressure system and to allow for the direct measurement of the quantity of iodine adsorbed on the bed rather than monitor small changes in gas composition. This is also referred to as a "single pellet system."

The glass gas reaction chamber was connected to the feed gas header. The basket itself was suspended from a tripod device which rested on the pan of the electronic balance (Sartorius Instruments Model LC620P) used to measure the weight changes of the sorbent material. This configuration allowed the basket to be free floating within the reaction chamber. Thus it was possible to directly determine the weight change of the test material in a flowing system. Weight data were collected from the electronic balance via a serial connection to an adjacent personal computer.

Table 2 Summary of single-pellet tests.

Test No.	Size (in.)	Velocity (m/min)	CH_3I concentration (mg/m^3)		H_2O added	Temperature (°C)	Notes
			Planned	Actual[a]			
Initial series							
3	1/16	10	1000	1559		150	
4							Test aborted
5[b]	1/8	10	1000	1275		150	
6	1/16	10	1000	1505		150	
7	1/8	10	1000	1523		150	
8	1/16	5	1000	1675		150	
9							Test aborted
10[c]	1/16	10	1000	1190		200	
11	1/16	10	1500	1634		150	
12[c]	1/16	10	500	837		150	
Supplemental tests							
13[c]	1/16	10	1000	1367	yes	150	
14[c]	1/16	10	250	355		150	
15[c]	1/16	2	1000	1410		150	
16	1/16	1	1000	1124		150	
17	1/16	10	0	0		150	Air only
18	1/16	1	1000	1217	dry	150	
19	1/16	10	1500	2150		150	Short run
20	1/16	10	1500	1636		150	Short run
21[b]	1/16	10	1000			200	
22	1/8	10	1500	1367		150	
23[b]	1/16	10	1000		yes	150	Water data missing
24[b]	1/8	15	1000			150	Data questionable
25	1/16	10	1000			150	NaZ loading
26	1/16	10	1000	1059		125	

[a] Actual CH_3I concentrations determined by pressure drop in the gas supply cylinder vs time measurements.

[b] Data from runs T5, T21, T23, and T24 not used in analysis due to equipment difficulties or questions of validity or conditions.

[c] Data quality may be impacted by possible temperature shift at balance.

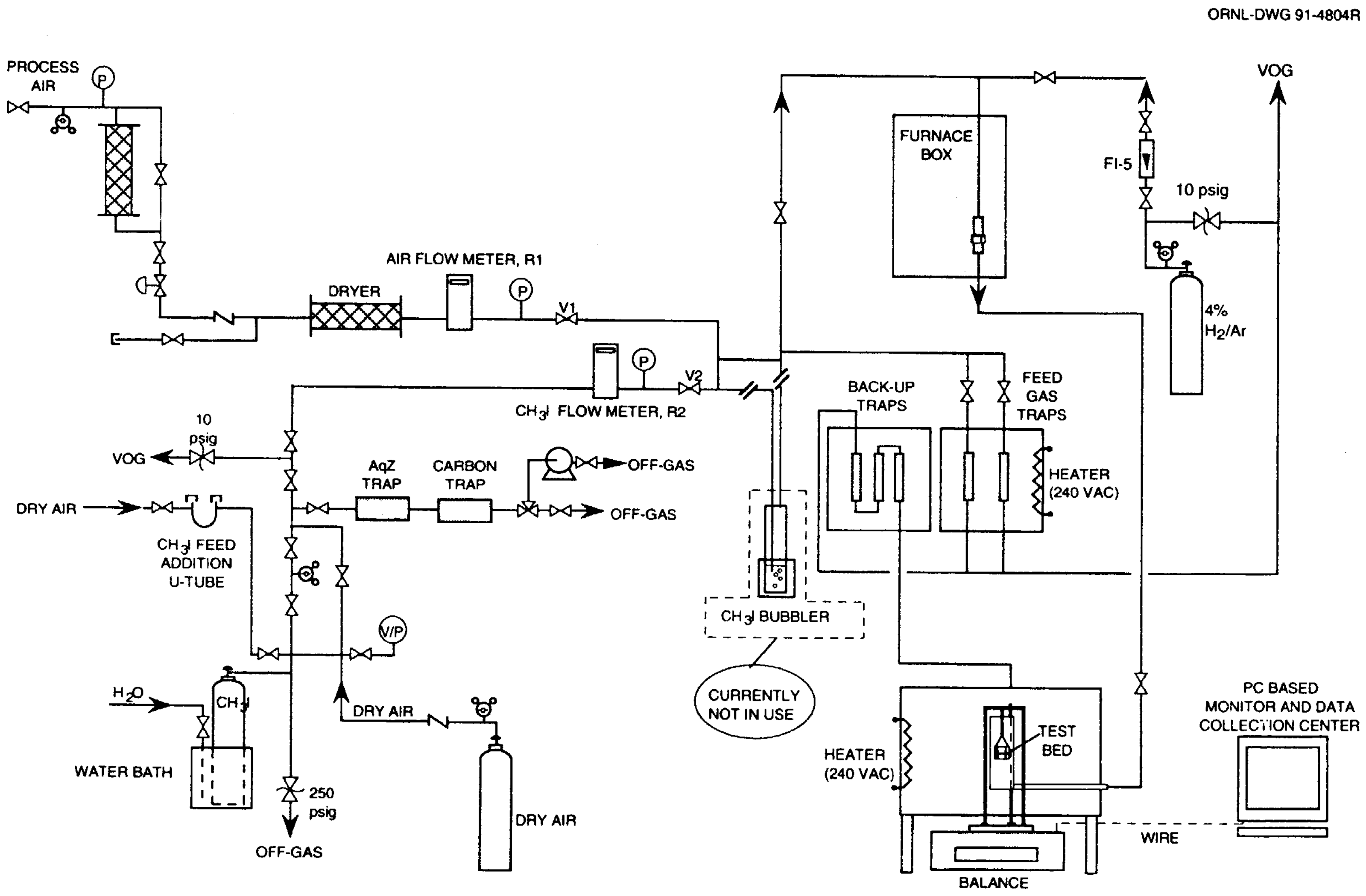

Figure 1 Schematic of experimental setup.

The glass reaction chamber was mounted in an electrically heated enclosure used to control process temperature. The heated enclosure was fabricated from a rigid insulating construction material. A secondary Plexiglas box was placed over this enclosure to prevent disturbances to the balance due to air currents in the hood. The gas that passed through the sorbent test material flowed through a series of 1-in.-I.D. backup filters loaded with either activated charcoal or silver-exchanged faujasite. The gas leaving the backup filters was discharged through the building vessel off-gas system.

The Sartorius Instruments Model LC620P poly-range electronic balance has a capacity of 120/240/620 g. Readability of the balance is 0.001/0.002/0.005 g, and standard deviation or reproducibility is $\leq\pm0.001/0.001/0.003$ g. Gas flowrates were controlled by needle valves and standard gas regulators. Gas flowrates were monitored either by calibrated rotometers or electronic mass flow meters manufactured by Omega Engineering, Inc. The Omega flow meters have an accuracy of ±2% of full scale. Temperature control was accomplished by placing the entire bed in an electrically heated insulated enclosure. Temperature was controlled by a Barber-Coleman controller coupled with a type K thermocouple junction inserted directly into the flowing gas stream above the bed of adsorbent material.

Table 3 presents, in outline form, the sequence of steps used to pretreat the AgZ prior to loading with methyl iodide and the flush or post-treatment steps to flush CH_3I from the bed and thus determine the amount chemisorbed vs physisorbed. Each of these pretreatment, loading, and post-loading steps were monitored for weight changes, with the data being stored in a computer file.

Experimental Results

Optical and Supporting Characterization Studies

Five samples of the mordenite materials used in this study were analyzed for pore size distribution, density, and characterization of the uniformity of silver and iodine distribution where applicable. The samples analyzed were the 1/16-in. sodium mordenite, the 1/16- and 1/8-in. AgZ, and the 1/16- and 1/8-in. AgZ pellets from tests T19 and T20, respectively. The last two samples were analyzed only for silver and iodine distribution.

The topography of the material was shown in secondary electron images (SEI). Back-scattered electron images (BEI) showed variations in the image intensity across a portion of the pellet which is related to variations in the average atomic number in the region under examination. The specific distributions of silver, iodine, silicon, and aluminum across the specimen were shown by elemental maps.

In general, the BEI taken across the entire cross section of several fractured AgZ pellets showed no significant variation in the average atomic number (Walker, 1994). On one or two pellets, some localized accumulation of the silver was noted in a few small areas. Aside from these few areas, no silver gradient was noted within the pellets. Prior to hydrogen pretreatment, the pellets displayed uniform distribution of the silver. However, following pretreatment with 4.5% hydrogen and subsequent loading with methyl iodide (samples from tests T19 and T20), very small particles (<1 or 2 μ) were seen on the surfaces of the larger crystalline structure. An elemental map obtained through energy-dispersive X-ray analysis of one pellet showed that these fine particles contain a higher concentration of silver than the concentration in the surrounding material. In addition to the presence of these fine silver-containing particles, there remained a relatively uniform distribution of silver across the mordenite pellet cross section. No specific area of silver depletion was detected when compared with the silver distribution prior to hydrogen pretreatment and iodine loading.

A low concentration of iodine was also observed to be uniformly distributed in the mordenite pellets analyzed from Test T19 (24% final conversion) and Test T20 (35% final conversion). Examination of the fine silver-containing particles showed that while these are rich in silver, they contained virtually no iodine. Using the same technique on the larger mordenite particles or crystals showed that they, on the other hand, contained a low concentration iodine that appeared to be uniformly distributed.

Table 3 Outline procedure for single-pellet CH_3I loading tests.

- Bed pretreatment (standard for all tests)
  - Drying
    - 24 h air
    - 11.4 L/min of dry instrument air
    - Temperature: 150°C
  - Nitrogen temperature equilibration
    - 4+ h N_2
    - 0.4 L/min
    - Temperature: 200°C
  - Silver reduction
    - 8 to 20 h 4% H_2/Ar
    - 0.4 L/min
    - Temperature: 200°C
  - Second nitrogen temperature equilibration
    - 4+ h N_2
    - Same flow rate as that to be used in CH_3I loading
    - Same temperature as that to be used in CH_3I loading

- Loading conditions (specific test conditions listed in Table 2)
  - H_2O vapor content (dew point)
    - >-15°C (7.3×10^{-5} mol/L) or -40°C (5.6×10^{-6} mol/L)
  - Pellet diameters
    - 1/16 or 1/8 in.
  - Gas velocities
    - 1, 2, 5, or 10 m/min
  - CH_3I gas concentrations
    - 250, 500, 1000, or 1500 mg/m^3
  - Bed temperature
    - 125, 150, or 200°C

- Air flush (standard for all tests)
  - 24+ h air
  - 11.4 L/min or dried instrument air
  - Temperature: 150°C

The SEI of the pellets examined showed the voids and macropores present in this material. The SEI also showed that there was the possibility for significant variation from pellet to pellet. These variations fell into two categories. First there was some variation in the general structure of the pellets. Some were observed to have substantial voids in the pellet interior, while other pellets appeared to contain separate cores. The second type of variation involved the crystalline particles that comprised the overall structure. Some were well formed, and others had very rough and irregular surfaces. In addition, they appeared to vary in size and overall shape. Both the 1/16- and 1/8-in. pellets were composed of individual crystals estimated to be 4.0 μ in equivalent spherical diameter.

What appears to be a shrinking core behavior, as shown by color changes in the pellets, was observed through unpublished optical photographs made during the deep-bed studies previously completed and reported by this author [Jubin (1980, 1982)]. The test from which these pellets were taken was conducted under the following conditions: a bed temperature of 200°C, a CH_3I concentration of 1000 mg/m^3, and a gas velocity of 10 m/min at standard temperature and pressure. The loadings for the individual pellets were not determined, and only the average loading on each of the 2.54-cm-thick bed segments was measured by tracer analysis. At very low CH_3I loadings on the AgZ (~3% average conversion) the pellet from the fourth or last bed segment shows no sign of any visible ring. As the average bed segment loading increases, a clearly developed ring around the core is apparent. This is shown in Fig. 2 at an average bed segment conversion of ~19%. However, at higher average loadings (~40% conversion), the color variation across the diameter of the pellet virtually disappears (Fig. 3). In Fig. 3, which shows several pellets from the first bed segment, it appears that only a very small core remains in one pellet while in the other pellet no core is visible.

Baseline Adsorption Data

Water Uptake by AgZ

One obvious concern in analyzing the CH_3I uptake data was the possible impact of concurrent weight gain by the adsorption of water from the flowing gas stream. Test T17 was performed to measure the quantity of water adsorbed as a function of time. After approximately the first 16 h that the bed was subjected to the flowing instrument air at 150°C, an observed gain of approximately 0.05 g had occurred on the 2.5416-g bed and the loading appeared to have leveled off. After 40 h the total had risen to about 0.07 g. Over the next 50 h, the loading appeared to stabilize at a total weight gain of about 0.075 ± 0.005 g. These values must be compared with the total weight gains observed when CH_3I was present in the flowing gas stream to determine their significance and possible impact on the CH_3I loading data. The typical weight gain was on the order of 0.45 g in 60 h, as in the case of T10.

CH_3I Loading on NaZ

It was assumed at the start of this study that any weight gain on the mordenite pellet was primarily associated with chemical bonding with the silver contained in the pellet. Test T25 was conducted to determine the loading rate and quantity of CH_3I adsorbed on the unexchanged sodium form of the mordenite. In this run, 0.0807 g was loaded over the 22-h test period. Following the loading cycle, an air purge of 70 h was conducted. During this period, a net gain of 0.0353 g was observed that must be attributed to a water vapor. The total CH_3I loading should be compared with loading curves from tests such as T3, in which 0.335 g was gained over the same time period to examine the significance. Based on these data, it would appear relatively safe to assume that the observed weight gains on the beds that were measured during the CH_3I loading tests required a chemical reaction between the CH_3I and the silver.

CH_3I Adsorption Studies

Figures 4 and 5 are examples of the CH_3I loading curves that were obtained for all of the experimental runs. The air flush portions of the tests may also be included in the loading files as this phase of the tests was conducted as a continuation of the test conditions with only the CH_3I flow

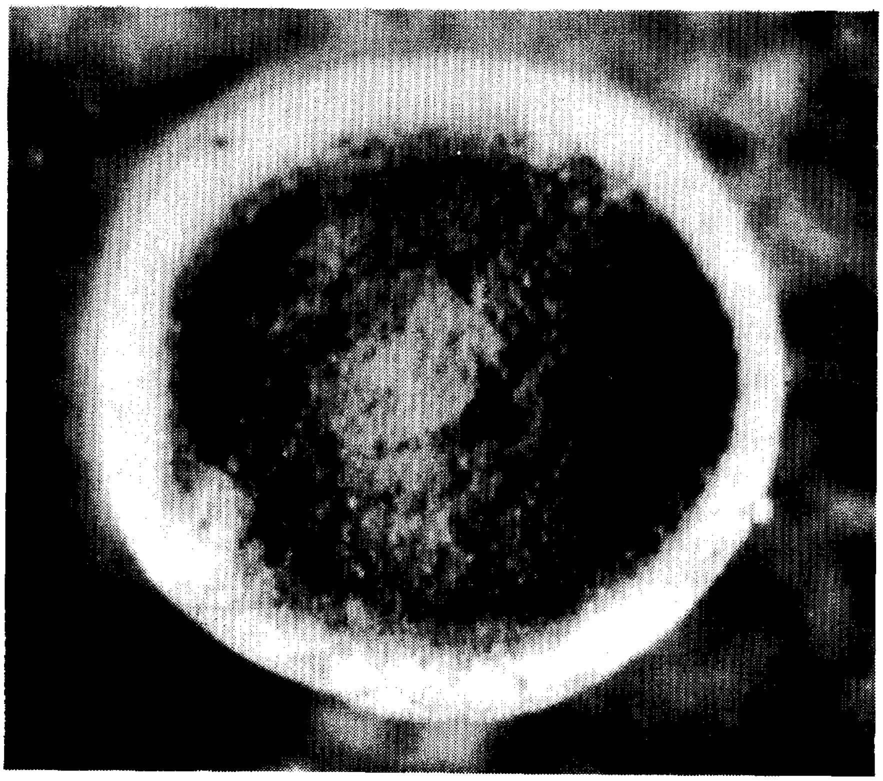

Figure 2 Optical image of 1/16-in. AgZ from bed with an average conversion of ~19%.

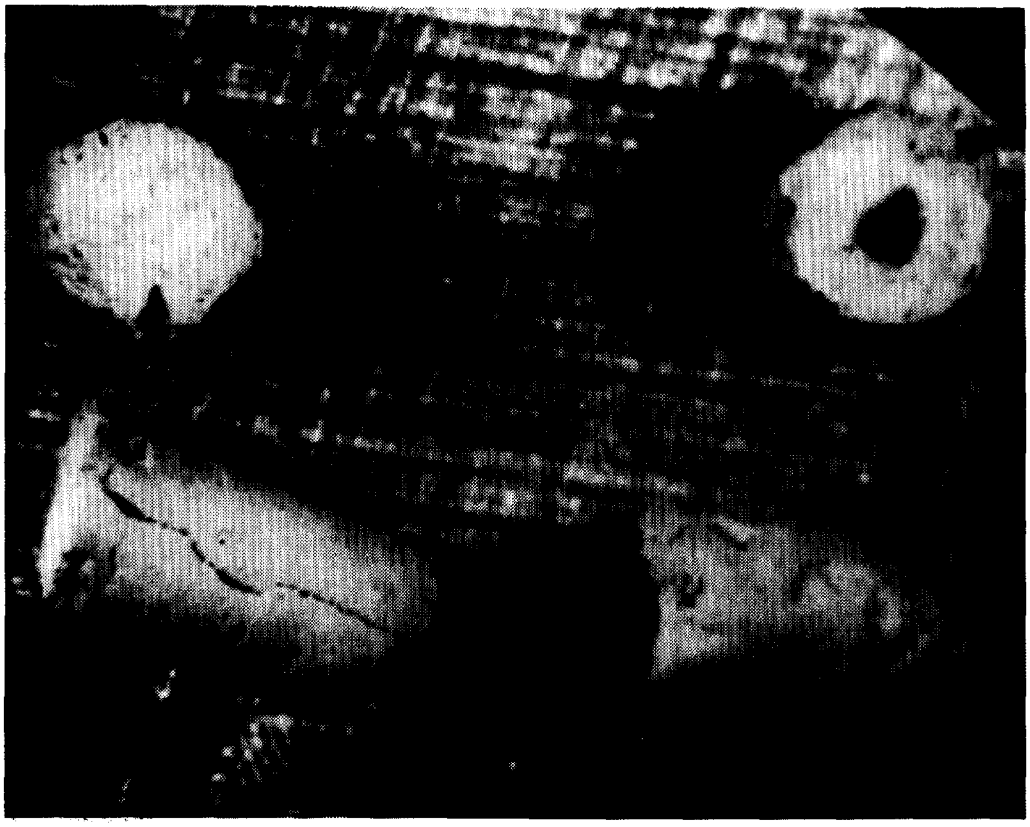

Figure 3 Optical image of 1/16-in AgZ from bed with an average conversion of ~40%.

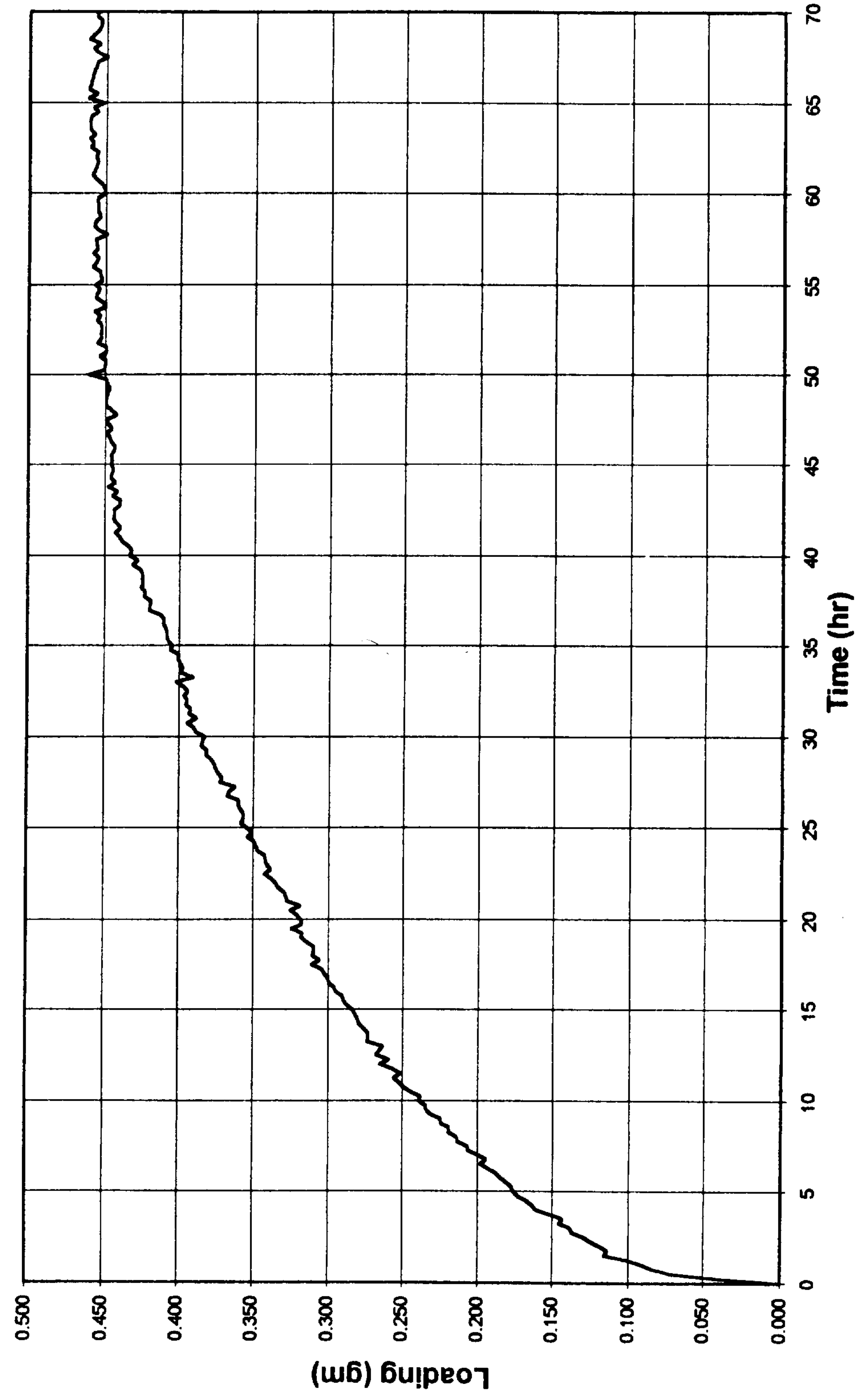

Figure 4 CH_3I loading curve from Test T3.

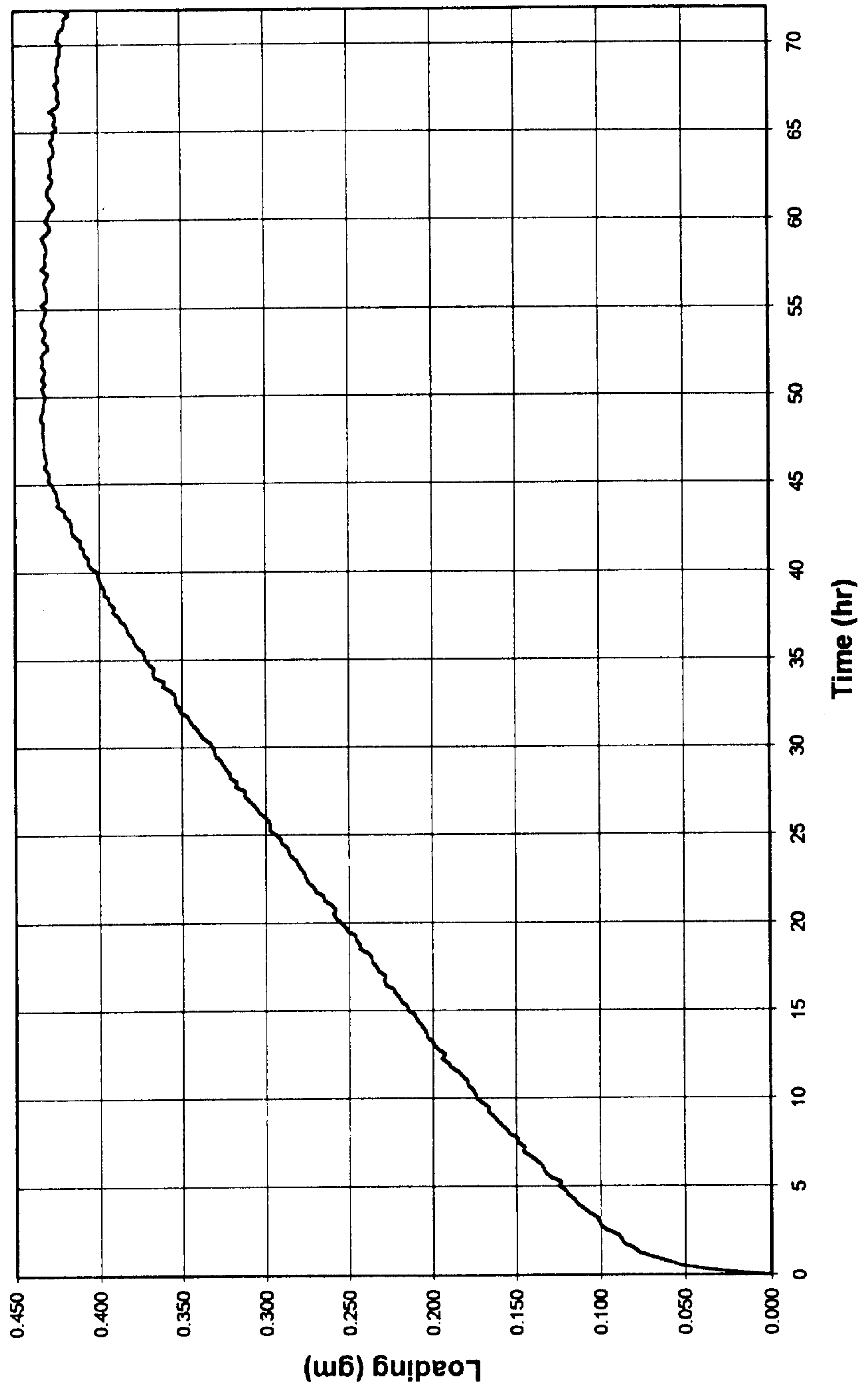

Figure 5 CH_3I loading curve from Test T22.

stopped. The total weight loss from the pellets during the air flush was generally about 1 to 2% of the total iodine loaded. A summary of the actual test conditions is presented in Table 2.

Discussion

Analysis of Optimization Techniques and FORTRAN Implementation of Potential Models

To determine the mechanism(s) controlling the mass transfer of CH_3I onto the silver-exchanged mordenite, the experimentally obtained data were compared against widely accepted models of adsorption behavior. Each of the nine models from the literature was translated into appropriate FORTRAN code using Microsoft Corporation's Powerstation FORTRAN compiler, Version 1.0. In each case, the formulation of the model equations is such that given the appropriate rate-controlling parameters, the degree of conversion or a mass flux at a specific time can be directly or indirectly computed. The term "indirectly computed" means that the conversion cannot be directly computed but must be found by iteration or by some root-finding method. The potential models were evaluated against the observed adsorption uptake curves. The best values for the rate-controlling parameters were determined by linear or multidimensional regression techniques using the experimentally obtained loading data as the reference.

The two primary criteria applied to the selection of the appropriate model for this system were (1) the ability of the model to account for the systematic variation in operating parameters without arbitrary changes in the adjustable parameters and (2) the determination of consistent diffusion coefficients for the experimental conditions evaluated.

Two classes of data fitting models were employed in this study. The first, and by far the simplest, was the single parameter model. In this case, it was a relatively simple matter to find the minimum using any of a variety of minimization techniques. The FORTRAN function FMIN described by Forsythe et al. (1977) was used for all single parameter models. This function used a combination of a golden section search technique and successive parabolic interpolation. This provided a very robust function not requiring the determination of derivatives.

Several of the models required multidimensional minimization to extract the relevant parameters. These models included both the full shrinking core and the bimodal. The determination of "best fit" to the experimental data in the case of a multiparameter model was significantly more complex. Press et al. (1992), in discussing multidimensional minimization, recommend the POWELL method as being faster in most cases and state that it can be used when derivatives are not easy to calculate.

CH_3I Adsorption–Model Comparisons

General Model Requirements

In the identification of a model to describe the adsorption of CH_3I onto silver-exchanged mordenite, it was required that certain general observations be accounted for by the selected model. These were as follows:

1. The possible formation of a rapidly shrinking shell of reacted material as observed in Figs. 2 and 3, noting, of course, that the unreacted core was no longer visible once 30-50 % conversion was achieved.

Table 4 Comparison of the simple sum of the square of the error in the conversion terms for the shrinking core models.

	Gas film		Ash diff		Rxn control		Gas film + Ash + Rxn			
Run No.	k_g (cm/s)	Error[a]	D_e (cm^2/s)	Error	k_s (cm/s)	Error	k_g (cm/s)	D_e (cm^2/s)	k_s (cm/s)	Error
T3	7.44E-02	2.46E+00	1.05E-03	6.89E-03	1.05E-01	1.16E+00	9.90E+99	1.05E-03	1.02E+06	6.89E-03
T6	7.76E-02	3.44E+00	1.33E-03	4.52E-02	1.20E-01	1.16E+00	9.90E+99	1.56E-03	8.42E-01	1.73E-02
T7	1.14E-01	1.74E-01	1.70E-03	6.41E-01	1.36E-01	1.76E-01	9.18E+99	4.72E+11	1.36E-01	1.76E-01
T8	4.20E-02	1.93E-01	3.17E-04	8.44E-01	5.00E-02	2.27E-01	9.20E+99	4.74E+11	5.00E-02	2.27E-01
T10	1.13E-01	4.56E+00	2.75E-03	4.73E-01	2.08E-01	1.85E-01	9.90E+99	8.86E-03	2.99E-01	3.13E-02
T11	8.33E-02	5.30E-01	6.85E-04	4.50E-03	1.01E-01	3.49E-01	9.90E+99	6.85E-04	1.36E+06	4.50E-03
T12	4.74E-02	2.30E-02	1.87E-04	1.91E-01	5.20E-02	1.43E-02	9.90E+99	3.01E-03	5.59E-02	1.27E-02
T13	5.52E-02	3.94E-02	4.85E-04	9.70E-01	6.76E-02	6.93E-02	9.64E+99	4.22E+12	6.76E-02	6.93E-02
T14	1.61E-01	3.17E-01	9.94E-04	8.08E-02	1.86E-01	2.03E-01	9.90E+99	1.66E-03	4.95E-01	3.26E-02
T15	4.82E-02	2.55E-02	3.32E-04	1.19E+00	5.67E-02	9.42E-02	9.89E+99	9.13E+12	5.67E-02	9.42E-02
T16	5.80E-02	4.39E-01	6.59E-04	6.81E-01	7.63E-02	6.20E-02	9.90E+99	4.12E-03	9.24E-02	1.97E-02
T18	5.08E-02	3.32E-02	3.10E-04	4.93E-01	5.87E-02	2.43E-03	9.90E+99	1.35E-02	6.03E-02	1.87E-03
T19	1.14E-01	6.12E-02	5.08E-04	1.60E-04	1.27E-01	4.93E-02	9.90E+99	5.08E-04	6.11E+06	1.60E-04
T20	2.87E-01	2.11E-01	3.88E-03	1.87E-03	3.40E-01	1.44E-01	9.90E+99	4.19E-03	5.05E+00	1.21E-03
T22	9.21E-02	1.05E+00	2.16E-03	2.98E-01	1.23E-01	3.89E-01	9.90E+99	4.38E-03	2.54E-01	9.79E-02
T26	7.36E-02	9.91E-01	5.08E-04	9.40E-02	8.67E-02	7.95E-01	9.90E+99	5.08E-04	2.07E+13	9.40E-02
Total errors		1.46E+01		6.01E+00		5.08E+00				8.87E-01

[a] Error terms are the resultant sum of the square of the error between the experimental data and the proposed model.

2. Fairly uniform iodine loading across the pellet diameter at 30 to 40% conversion of silver or greater.
3. Observation from past studies that higher loading was achieved prior to breakthrough with increased operation temperature.

Shrinking Core Model

The regression analyses for the shrinking core model is presented in Table 4. By examining this table, it is clear that the diffusion through the gas film was not the controlling mechanism. In virtually every case in which the parameters for three terms of the full shrinking core model were used as adjustable parameters in the minimization of the error between the model and experimental data, the computed value for k_g was on the order of 10^{100} cm/s. This value was the upper limit set in the search routines. In the few cases where it did not reach the upper bounds, the value is still above 10^{10} cm/s. The substitution of this value in the Eq. (5) for $\tau_{gasfilm}$ and the subsequent application into summation of the resistances showed that the resistance was mathematically negligible. Further, the values of k_g determined for the gas film alone were compared with the values of k_g as estimated by use of the Sherwood number and the molecular diffusivity D_{AB}. The values of k_g estimated by the Sherwood number were on the order of 3 to 9 cm/s. However, if the assumption was made that the controlling resistance was the gas film, then the values for k_g determined by the least-squares curve fitting method ranged from 0.04 to just over 0.3 cm/s. Finally, the shape of the uptake curve was not indicative of gas film resistance control.

Thus having ruled out gas-phase control and continuing with the shrinking core analysis, there appeared to be two distinct classes of behavior or types of loading curves. The first class may be described by diffusion control through the ash layer, which appeared to describe several of the cases (e.g., T3); however,in most of the runs, the loading curve appeared to have a "knee" which the shrinking core model cannot fit. These uptake curves tended to show a rapid weight gain followed by a slower rate of weight gain. This "knee" may also be an indicator that possibly two or more mechanisms were controlling the adsorption process and that there was a transition from one to the other.

If the ring observed on the pellets, as shown in the Fig. 3, was related to the loading of iodine on the pellet, then it was easily shown that at 40% utilization the radius of the unreacted core should be ~78% of the overall pellet radius. The observed radius in Fig. 3 was only ~27% of the pellet radius for the pellet that still shows a core. This 27% equates to ~93% conversion if a strict shrinking core model was correct. It should also be recalled that the BEI of the pellets from T19 and T20 showed no significant iodine gradient, which appeared to be relatively consistent with the photographic evidence at higher iodine loadings. These data tended to lead to the conclusion that while there may initially be the appearance of the shrinking core-type behavior, there was also a second slower process that accounted for the loading above some nominal level of loading associated with the shrinking core.

The effective diffusivity calculated from the data collected over the time periods of the first 40 data points (10 h) ranges from 1.84×10^{-4} to 3.91×10^{-3} cm^2/s for the runs that did not exhibit any thermal upset in the balance. This effective diffusivity was also compared with that predicted by fundamental analysis of the zeolite pore structure and physical constants for the diffusing component. By comparison of the above effective diffusivities with the combined effective diffusivities for either the Knudsen diffusivity in the micropore/mesopore which are in the range of 5×10^{-5} to 5×10^{-4} cm^2/s or the effective molecular diffusivity of $\sim 1.4 \times 10^{-2}$ cm^2/s in the macropore range, it was observed that the value obtained by curve fitting falls between the two bounding cases. Using the shrinking core model, it was possible to find a set of parameters that seems to successfully model each individual loading curve. However, it was less obvious why some sets of data were diffusion controlled and other similar sets appeared to be reaction controlled. This model by itself was unable to explain the apparent change in controlling mechanism. However, it provides strong evidence that

1. the mass transfer process was not controlled by the gas film resistance; and
2. there was a diffusional component, and the effective diffusivities in the first few hours of loading were in the range of 1.84×10^{-4} to 3.91×10^{-3} cm^2/s for the runs in which the data showed no thermal upset in the balance during the initial period.

Macropore/Micropore Model

Mathematically, these two models are essentially the same. In the micropore diffusion case, the radius of the crystal is the dimensional term used, and in the macropore case, the pellet radius is the relevant term. In the case of the macropore model, the diffusivity term that is obtained from the curve fitting analysis is an effective diffusivity which contains an equilibrium constant. This equilibrium constant, under cases of a linear equilibrium, relates the adsorbed phase concentration q to the gas phase concentration C by

$$q = K^{*}C \ . \tag{22}$$

The results of both micropore and macropore models obviously yield the same error terms (Table 5) and were virtually the same as those obtained for the ash diffusion term of the shrinking core model by itself. It can be noted that neither model provided a particularly good prediction of the overall experimental behavior. However, as noted above, for large values of time, a plot of the term $\ln(1 - X_B)$ vs time should yield a straight line with a slope of $-\pi^2 D_c/r_{i2}$ and an intercept of $\ln(6/\pi^2)$ at a value of time equal to zero if micropore diffusion is the controlling mechanism.

An example of such a plot is shown in Fig. 6. Table 6 is a tabulation of the resulting micropore diffusion coefficients obtained from the slopes of this type analysis of all data sets. The correlation coefficient values, R^2, showed very high correlation for the linear regression of this data. This indicated that after the initial portion of the loading process, the effective micropore diffusivity was constant and, based on the data from this study, fairly consistent over a significant range of operating conditions. All the slopes of the uptake curve plotted as the $\ln(1 - X_B)$ vs time were obtained for values of time greater than 10 h. For all runs except for T12, T14, T16, T18, and T26, the value of D_c was between 2.19×10^{-14} and 3.34×10^{-14} cm^2/s. There was no notable distinction in the values of the determined micropore diffusivity between pellet size or by the addition of supplemental water vapor or any of the variations in the pretreatment steps.

T12 and T14, which utilized low CH_3I gas concentrations, exhibited lower values of D_c, 9.32×10^{-15} and 1.13×10^{-14} cm^2/s, respectively. It has also been noted that both of these runs were subject to some thermal instability in the early readings.

The value of D_c for T26 is also somewhat lower than the rest of the data sets. The calculated value is 1.06×10^{-14} cm^2/s, which in this case could be attributed to the lower bed temperature used in this run since D_c in theory follows an Arrhenius-type temperature response.

T18, which was conducted with a dry air stream, exhibited the same type behavior as the other runs and had a comparable value for D_c of 1.59×10^{-14} cm^2/s, which seemed to indicate that in the long time period, the adsorption rate may also be controlled by micropore diffusion.

T16 yielded values for D_c of 2.98×10^{-14} or 5.39×10^{-14} cm^2/s, depending on which portion of the loading curve is being analyzed. It was noted from the run log that there was some shift in the CH_3I feed rate that may have occurred and was not detected until after the weekend. This may have occurred about the time that the shift in the slope occurred.

Table 5 Micropore and macropore model parameters for the full data sets.

	Micropore		Macropore	
Run No.	D_c (cm^2/s)	Error[a]	D_p (cm^2/s)	Error
T3	1.82E-14	1.16E-02	4.50E-09	1.16E-02
T6	2.26E-14	7.44E-02	5.57E-09	7.44E-02
T7	6.73E-15	6.68E-01	6.23E-09	6.68E-01
T8	5.66E-15	8.75E-01	1.40E-09	8.75E-01
T10	3.43E-14	6.74E-01	8.45E-09	6.74E-01
T11	1.20E-14	5.32E-03	2.97E-09	5.32E-03
T12	1.65E-15	1.95E-01	4.07E-10	1.95E-01
T13	7.18E-15	1.02E+00	1.77E-09	1.02E+00
T14	3.72E-15	8.75E-02	9.17E-10	8.75E-02
T15	4.90E-15	1.22E+00	1.21E-09	1.22E+00
T16	1.17E-14	7.49E-01	2.88E-09	7.49E-01
T18	3.81E-15	5.10E-01	9.39E-10	5.10E-01
T19	1.16E-14	1.31E-04	2.85E-09	1.31E-04
T20	1.66E-14	2.13E-03	1.54E-08	2.13E-03
T22	1.24E-14	3.47E-01	1.15E-08	3.47E-01
T26	5.80E-15	8.86E-02	1.43E-09	8.86E-02
	Error sum:	6.53E+00		6.53E+00

[a]Error terms are the resultant sum of the square of the error between the experimental data and the proposed model.

The value for the y-intercept, however, was somewhat scattered. This was attributed to other mechanisms controlling the initial portions of the uptake curve. In all cases the y-intercept was numerically greater than the expected value of $\ln(6/\pi^2)$. One explanation for this observation was that the observed uptake on the pellets was slower in the initial time periods than would have been observed if all microspheres in the pellet had been exposed to a uniform value of CH_3I at time zero. This could occur if there were a second diffusional process to controll the CH_3I concentration profile across the pellet during the early time periods.

The X-ray fluorescence data indicated a fairly uniform distribution of iodine across the cross section of the pellet. A uniform distribution would not be observed in the case of a strictly shrinking core or in a macropore diffusion-controlled situation. This observation was consistent with micropore diffusion playing a role in the overall controlling mechanism.

Bimodal Model

By examination of Eqs. (18) through (20), it can be observed that the bimodal model is defined by three specific parameters in addition to the physical measurement of the particle sizes and porosities. These parameters are the macropore diffusivity, D_p, the micropore diffusivity, D_c, and an equilibrium

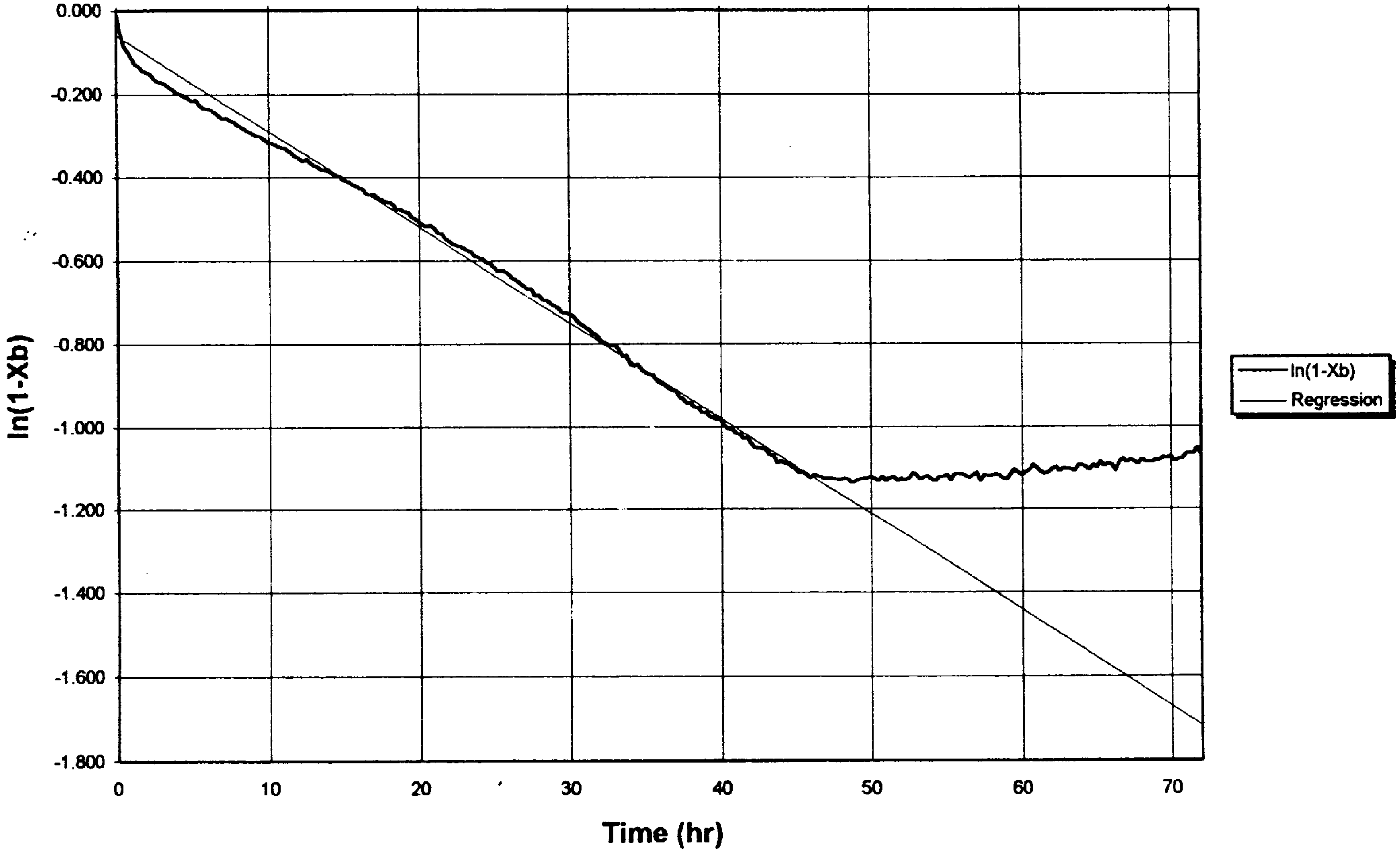

Figure 6 Determination of D_c from slope of the uptake curve plotted as $\ln(1 - X_b)$ vs time for Run T22.

Table 6: Micropore diffusivities calculated from slope of the uptake curve plotted as $\ln(1-X_B)$ vs time.

Run No.	Range considered				Weight adjustment to observed	Linear regression of $\ln(1-X_B)$			
	Beginning time (h)	End time (h)	Beginning conv. (fraction)	End conv. (fraction)	Loading (g)	Slope	Intercept	Correlation coefficient (R^2)	Regressed D_c (cm^2/s)
T3	20	40	0.505	0.685		−5.98E-06	−0.275	0.99	2.42E-14
T6	10	40	0.393	0.744		−7.76E-06	−0.25	0.997	3.15E-14
T7	30	40	0.429	0.571		−8.21E-06	0.331	0.999	3.33E-14
T8	30	80	0.363	0.854		−8.23E-06	0.488	0.998	3.34E-14
T10	10	40	0.082	0.572		−7.10E-06	0.126	0.989	2.88E-14
T10	10	40	0.136	0.621	0.025	−7.73E-06	0.0953	0.991	3.13E-14
T10	10	40	0.185	0.67	0.050	−8.49E-06	0.0669	0.993	3.44E-14
T10	10	40	0.381	0.865	0.150	−1.40E-05	0.0478	0.999	5.67E-14
T11	10	24	0.313	0.475		−5.40E-06	−0.187	0.998	2.19E-14
T12	20	60	0.146	0.384		−2.30E-06	0.00906	0.998	9.32E-15
T13	20	47.25	0.214	0.566		−6.36E-06	0.226	0.997	2.58E-14
T14	10	60	0.159	0.491		−2.78E-06	−0.0698	0.999	1.13E-14
T15	30	80	0.356	0.794		−6.33E-06	0.264	0.998	2.57E-14
T16	30	70	0.525	0.896		−1.07E-05	0.53	0.976	4.34E-14
T16	30	45	0.525	0.678		−7.36E-06	0.0543	0.999	2.98E-14
T16	45	70	0.678	0.896		−1.33E-05	1.1	0.997	5.39E-14
T18	20	70	0.223	0.624		−3.93E-06	0.0409	0.999	1.59E-14
T19[a]									
T20[a]									
T21	45.45	60	0.635	0.772		−9.10E-06	0.454	0.99	3.69E-14
T22	10	40	0.271	0.626		−6.4E-06	−0.0585	0.995	2.57E-14
T26	10	35	0.273	0.428		−2.62E-06	−0.218	0.995	1.06E-14

[a] Not determined due to short run length.

constant, q_∞/C_0. These parameters can be combined along with the physical measurements into the terms α and β. Clearly, however, a difficulty in this system is that α is a function of both D_p and D_c and β is a function of α. Ideally the solution to this model would be greatly simplified if D_c, D_p, and the equilibrium constant could be determined separately.

Determination of the three parameters of the bimodal model, D_c, α, and β, by a multidimensional minimization operation was initially attempted. It was noted during the early attempts to conduct the minimization operations that as the initial search point was varied, the same values of the "optimum" parameters were not always obtained. As a result, each of the data sets was evaluated over the range of anticipated values for α and β for which the full bimodal model must be utilized.

The ranges were selected to examine the behavior of the model between the bounding conditions and thus under conditions where both mechanisms are important. Values of α and β from 10^{-3} to 10^{+2} in six even steps on a logarithmic scale were used to create a "surface map" of the errors resulting from a one-dimensional minimization of the least-squares error with the experimental data by adjusting the micropore diffusion coefficient at each node on the map grid. It was noted in these surface plots that the determination of a "best fit" to the data was not always obvious from the surface formed as a function of α and β. It was observed that there could be numerous combinations of α and β, generated by adjusting D_c, that provided nearly the same sum of the squares of the error. The minimum values for the adjustable parameters of D_c, α, and β obtained from the surface mapping approach are summarized in Table 7. However, based on the surface contours, there could be several values of the adjustable parameters that provided good fits to the experimental data. Therefore, this method provided inadequate resolution to clearly identify any "correct" or "more correct" set of parameters to describe the adsorption process of CH_3I on Ag°Z.

The tables of D_c values determined from the surface mapping approach to locating the best fit to the experimental data were then examined for similarities with the values of D_c determined from the evaluation of the slope of the uptake curve plotted as $\ln(1 - X_B)$ vs time (Table 6). The closest values to the values of D_c determined by the slope method were selected based on the lowest sum of the squares of the errors from the tables of D_c values from the least-squares curve fitting method. As can be seen from Table 7, either the same point in terms of the adjustable parameters α and β or a nearby point yielded virtually the same error term. In most cases the selected values of D_c were associated with α values of 0.001, which indicated primarily micropore diffusion. β values were generally about 10. (Note, however, that an α value of 0.001 is the smallest value evaluated in the table.)

Ma and Lee (1976) reduced the bimodal-type curve fitting problem to one of a single parameter, the micropore diffusion coefficient, D_c, through the use of calculated values for the macropore diffusion coefficient and the use of experimentally determined values for the other parameters in α and β. For the CaX(Na) zeolite in their study, the macropore diffusivity was estimated based on the Knudsen and molecular diffusivities. A similar analysis was conducted with the data obtained in this study. The effective macropore diffusivity for the Ag°Z was calculated to be about 0.014 cm^2/s, and based on the effective Knudsen diffusivity in the mesopores, the overall macropore diffusivity was estimated to be about 5×10^{-4} cm^2/s. Finally using the value of D_c obtained from the slope of the plot of $\ln(1 - X_B)$ vs time, the effective overall macropore diffusivity along with the physical dimensions, values of α on the order of 5×10^{-6} up to about 8×10^{-5} were obtained.

The value of β appeared to be more difficult to establish. Obviously from the definition of β, it was a function of α which in turn was a function of the macropore and mesopore diffusivities. One other significant unknown remained in the β term, which was the value of the adsorption equilibrium constant. This was estimated to be about 3.4×10^5 based on the gas-phase CH_3I concentration from run T16 and the highest loading observed on the Ag°Z. The resulting value of β was about 20. β was the least well-established value, and a third optimization approach was taken to determine if a

Table 7 Bimodal model minimums based on error surface mapping.

	Best fit by mapping surface					Best fit by using closest/best match to D_c calculated by slope							
Run No.	D_c (cm^2/s)	α	β	Error[a]	β/3α	D_c (cm^2/s)	α	β	Error[a]	β/3α	r_a (cm)	r_i (cm)	D_B[b] (cm^2/s)
T3	2.95E-14	1.000	1.000	7.81E-03	0.333333	2.95E-14	1.000	1.000	7.81E-03	0.333333	0.09808	0.0002	7.09E-09
T6	3.22E-14	0.010	1.000	1.40E-02	33.33333	3.22E-14	0.010	1.000	1.40E-02	33.33333	0.09808	0.0002	7.74E-07
T7	4.23E-14	0.001	10.000	3.40E-01	3333.333	4.23E-14	0.001	10.000	3.40E-01	3333.333	0.19715	0.0002	4.11E-05
T8	3.59E-14	0.001	10.000	4.67E-01	3333.333	3.59E-14	0.001	10.000	4.67E-01	3333.333	0.09808	0.0002	8.63E-06
T10	1.49E-13	0.001	10.000	2.96E-01	3333.333	4.64E-14	0.001	1.000	3.54E-01	333.3333	0.09808	0.0002	1.12E-05
T11	2.00E-14	1.000	1.000	4.11E-03	0.333333	2.00E-14	1.000	1.000	4.11E-03	0.333333	0.09808	0.0002	4.81E-09
T12	1.45E-14	0.001	10.000	5.51E-02	3333.333	1.45E-14	0.001	10.000	5.51E-02	3333.333	0.09808	0.0002	3.49E-06
T13	4.23E-14	0.001	10.000	4.81E-01	3333.333	1.23E-14	0.001	1.000	4.81E-01	333.3333	0.09808	0.0002	2.96E-06
T14	2.60E-14	0.100	10.000	1.98E-02	33.33333	2.60E-14	0.001	10.000	2.21E-02	3333.333	0.09808	0.0002	6.25E-06
T15	3.26E-14	0.001	10.000	5.84E-01	3333.333	3.26E-14	0.001	10.000	5.84E-01	3333.333	0.09808	0.0002	7.84E-06
T16	6.27E-14	0.001	10.000	2.02E-01	3333.333	6.27E-14	0.001	10.000	2.02E-01	3333.333	0.09808	0.0002	1.51E-05
T18	2.70E-14	0.001	10.000	1.58E-01	3333.333	2.70E-14	0.001	10.000	1.58E-01	3333.333	0.09808	0.0002	6.49E-06
T19	1.95E-14	1.000	1.000	2.32E-04	0.333333	1.95E-14	1.000	1.000	2.32E-04	0.333333	0.09808	0.0002	4.69E-09
T20	2.18E-14	0.100	1.000	1.71E-03	3.333333	2.18E-14	0.100	1.000	1.71E-03	3.333333	0.19715	0.0002	2.12E-07
T22	6.50E-14	0.001	10.000	8.72E-02	3333.333	1.95E-14	0.001	1.000	1.31E-01	333.3333	0.19715	0.0002	1.89E-05
T26	6.50E-14	0.001	10.000	8.72E-02	3333.333	1.95E-14	0.001	1.000	1.31E-01	333.3333	0.09808	0.0002	4.69E-06
			Error sum:	2.81E+00					2.95E+00				

[a] Error terms are the resultant sum of the square of the error between the experimental data and the proposed model.

[b] Calculated from a by Eq. (19).

correlation existed between the observed behavior in the early time periods and the value of β with the operational or pretreatment conditions. Table 8 is a summary of the bimodal model parameters that were obtained through a one-dimensional least-squares optimization holding D_c to the values established by the slopes of the uptake curve plotted as $\ln(1 - X_B)$ vs time and α as calculated using D_c, the calculated effective macropore/mesopore diffusivity, D_p, the measured pellet diameter, and particle diameter determined from the electron microscope images as noted above. This in essence moved all of the unknowns and variabilities to the equilibrium term contained in the β expression.

Table 8 Optimized fit using bimodal model and fixed parameters of D_c based on the slope from the plot of $\ln(1 \quad X_B)$ vs time in the micropore model value and α based on theoretical computed values

	D_c (cm^2/s)	α	β	Error[a]
T3	2.42E-14	1.28E-05	5.52E-01	4.72E-02
T6	3.15E-14	1.67E-05	8.10E-01	1.77E-02
T7	3.33E-14	7.67E-05	6.80E+00	3.34E-01
T8	3.34E-14	1.77E-05	8.94E+00	4.64E-01
T10	5.67E-14	2.83E-05	1.88E+00	2.56E-01
T11	2.19E-14	1.16E-05	1.02E+00	3.88E-02
T12	9.32E-15	4.94E-06	4.96E+00	5.51E-02
T13	2.58E-14	1.37E-05	4.43E+00	4.70E-01
T14	1.13E-14	5.99E-06	2.46E+00	2.23E-02
T15	2.57E-14	1.36E-05	6.80E+00	5.74E-01
T16	2.98E-14	1.58E-05	2.92E+00	2.02E-01
T18	1.59E-14	8.43E-06	4.24E+00	1.58E-01
T19[b]	2.42E-14	1.28E-05	8.26E-01	6.65E-03
T20[b]	2.42E-14	5.57E-05	4.08E-01	6.41E-03
T22	2.57E-14	5.92E-05	1.98E+00	9.18E-02
T26	1.06E-14	5.81E-06	8.67E-01	2.42E-01
			Total error:	2.99E+00

[a] Error terms are the resultant sum of the square of the error between the experimental data and the proposed model.

[b] Short run D_c from Run T3 was used.

This approach produced relatively good fits to the experimental data. As can be seen by comparing the error terms contained in Table 8 with those in Table 7, the fits obtained by this method were as good as those obtained from the surface mapping approach to the locating of a global minimum. In several cases, notably T3, slightly higher errors resulted from this approach than from the approach in which multiple parameters were allowed to be adjusted, but the fit with the experimental data was still very good. The overall performance of this model using a single parameter was superior to the shrinking core model with all but one parameter fixed. There was, however, no obvious trend in the resulting values of β. These values ranged from 0.4 to about 9.

Further calculation of other parameters such as the equilibrium constant contained in the β term from the values of the parameters determined as described above was thought to be invalid for several reasons. First, when one parameter is determined from a second fitted parameter, the uncertainties tend to accumulate in the resultant value. Second, in this determination, since the value of D_c was determined from the slope of the uptake curve plotted as $\ln(1 - X_B)$ vs time and α was calculated from this value and other theoretical and measured terms, all of the uncertainties will be accumulated in the single adjustable parameter. Third, as noted from the photographs of the pellets, there can be significant variations in the structure, which in turn could impact the macropore diffusivity. Since the theoretical value of D_p was used, any variation from this value would end up being observed in the fitted value of β. It can also be shown that moderate variations in the theoretical values of D_p will not have an impact through α on the least-squares regression of the data to the proposed model (Jubin, 1995). And finally, the nature of the experiments conducted was not directed toward the determination of terms such as the equilibrium constant. Therefore, it is believed that any such secondary value would be of questionable validity.

Conclusions

This study has shown that there is a slow (micropore) diffusional process controlling the latter portion of the uptake curve . This was determined to be 2 x 10^{-14} cm^2/sec, and that the value of the diffusivity associated with this phase of the uptake was consistent over a number of runs. Based on the value of α obtained for the bimodal model, it was also shown that the process can be considered to be occurring in two steps. The time constants for the two processes are such that the macropore diffusion was virtually complete prior to any significant micropore diffusion occurring. Thus there was a shift in time prior to the start of the micropore adsorption.

One measure of this time shift was the observed shift in the y-intercept of the line describing the uptake curve plotted as $\ln(1 - X_B)$ vs time in the long time period. If no macropore diffusional resistance was observed and all microspheres were subject to a bulk gas-phase concentration equal to the bulk gas phase at time = 0, then only the micropore diffusional rate would be observed. In this case, the y-intercept would be the given by $\ln(6/\pi^2)$. However, with macropore diffusional resistance and adsorption occurring in the initial phase, there is some finite time period required before the concentration of the CH_3I becomes nonzero at any point in the pellet and even longer before it reaches the bulk equilibrium concentration. This delay shifts the start of the micropore diffusion and the associated micropore uptake. Thus for any given value of D_c obtained by the slope method, the actual conversion at a given time will be less than that predicted by micropore diffusion model alone using the derived value of D_c.

The quantity and rate at which iodine was adsorbed in the macropores is then a function of the available surface area, the nature of the macropore structure, and the quantity of available silver. Based on photographic evidence, the available surface area and the pore structure was quite variable and could not be predicted by any of the process measurements made during each of the test runs. The available silver may be related to the "nonframework" silver cations in the mordenite structure, to any silver on the surface of the mordenite crystals, and to the silver nodules that appear after the hydrogen pretreatment. This may also be quite variable and the magnitude of the variation was unknown for each run. This macropore diffusion control in the initial time period would also appear to explain the appearance of the shrinking core that vanishes by the time 20 to 30% conversion occurs. One other point on this topic is that the term macropore or bimodal, in the case of this material, is a significant simplification. The pore sizes range from 20 Å to 10 μ, with a peak in the macropore region occurring at about a pore diameter of about 1 μ. Thus a continuum of pore sizes existed.

This study has determined a consistent "micropore diffusion" rate on the order of 2×10^{-14} cm²/s. It has also been shown that the bimodal model adequately explains the observed uptake behavior and the photographic as well as X-ray evidence. It has further been shown that the adsorption process described by this model can be considered a two-step process. This information is important since it is the rate of the second step that ultimately controls the final bed loading rate if high bed loadings are desired. There are, however, several questions concerning the impact of the many process and structural variables still remaining to be answered. But even without answers to every new question raised in this study, a significantly deeper fundamental understanding of the CH_3I adsorption processes onto Ag°Z has been achieved.

In summary, considering the potential sources for experimental variation and the model sensitivity, the values determined for the bimodal model parameters, D_c, α, and β, are very consistent and clearly appear to adequately model the uptake of CH_3I on Ag°Z over the longer time periods. In addition, the bimodal two-step process seems to explain the appearance of a "ring" or shrinking core in the pellets at low conversion and yet a uniform iodine distribution at higher loadings.

The specific conclusions drawn from this study are as follows:

1. It was shown based on both fundamental analysis and on the results of the least-squares curve fitting that the gas film resistance to mass transfer is negligible.
2. It was also shown that the system can be considered virtually isothermal. The maximum calculated temperature difference between the pellet and the bulk fluid was 0.37°C. This is an important determination in that it simplifies the modeling of the process.
3. The micropore diffusivity at 150°C as calculated from the slope of the $\ln(1 - X_B)$ vs time curve is in the range of 1.95×10^{-14} to 3.33×10^{-14} cm²/s. The error in these values as estimated from the duplicate run at the standard conditions is about 30%.
4. The bimodal model, which includes the uptake in both the macropores and the micropores, provides the most uniform ability to model the behavior of the adsorption of CH_3I onto Ag°Z. The model parameters indicate that the uptake is occurring in a two-step manner, with the macropore uptake being much faster than the micropore uptake. This two-step process can account for the shrinking core observed at low conversions and the relatively uniform iodine concentration observed in the pellet at moderate to high concentrations.
5. The impact of the free silver observed in the mordenite structure could not be determined.

References

Burger, L. L., and Scheele, R. D., "Iodine Fixation Studies at the Pacific Northwest Laboratory," *Management Modes for Iodine-129*, W. Hebel and G. Cottone, eds., Harwood Academic Publishers, New York (1981).

Forsythe, G. E. , Malcolm, M. A., and Moler, C. B., *Computer Methods for Mathematical Computations*, Prentice Hall, Inc., Englewood Cliffs, New Jersey (1977).

Jubin, R. T., "Organic Iodine Removal from Simulated Off-Gas Streams Using Silver-Exchanged Mordenite," *Proc. 16th DOE Nuclear Air Cleaning Conference*, CONF-801038, pp. 519–531 (1980).

Jubin, R. T., "Organic Iodine Removal from Simulated Off-Gas Streams Using Partially Exchanged Silver Mordenite," *Proc. 17th DOE Nuclear Air Cleaning Conference*, CONF-820833, pp. 183–198 (1982).

Jubin, R. T., "The Mass Transfer Dynamics of Gaseous Methyl-Iodide Adsorption by Silver Exchanged Sodium Mordenite," Ph.D. Dissertation, University of Tennessee, 1994; also, ORNL-6853 (1995).

Kärger, J., and Ruthven, D. M., *Diffusion in Zeolites and Other Microporous Solids*, John Wiley & Sons, Inc., New York (1992).

Kulkarni, B. D., and Doraiswamy, L. K., "Modeling of Noncatalytic Gas-Solid Reactions," in *Handbook of Heat and Mass Transfer, Volume 2: Mass Transfer and Reactor Design*, Nicholas P. Cheremisinoff, Editor, pp. 1107–1135, Gulf Publishing Company, Houston, Texas (1986).

Lee, Lap-Keung, "The Kinetics of Sorption in a Biporous Adsorbent Particle," *AIChE Journal*, vol. 24, no. 3, pp. 531–533 (1978).

Lee, Lap-Keung, and Ruthven, D. M., "Analysis of Thermal Effects in Adsorption Rate Measurements," *J. Chem. Soc. Faraday I*, vol. 75, pp. 2406–2422 (1978).

Levenspiel, O., *Chemical Reaction Engineering, Second Edition*, John Wiley & Sons, Inc., New York (1972).

Levenspiel, O., *The Chemical Reactor Omnibook*, OSU Book Store, Inc., Corvallis, Oregon (1979).

Ma, Y. H., and Lee, T. Y., "Transient Diffusion in Solids with a Bipore Distribution," *AIChE Journal*, vol. 22, no. 1, pp. 147–152 (1976).

Press, W. H., Teukolsky, S. A., Vettering, W. T., and Flannery, B. P., *Numerical Recipes in FORTRAN: the Art of Scientific Computing, Second Edition*, Cambridge University Press, New York (1992).

Ramachandran, P. A., and Doraiswamy, L. K., "Modeling of Noncatalytic Gas-Solid Reactions," *AIChE Journal*, vol. 28., no. 6, pp. 881–900 (1982).

Ruckenstein, E., Vaidyanathan, A. S., and Youngquist, G. R., "Sorption by Solids with Bidisperse Pore Structures," *Chemical Engineering Science*, vol. 26, pp. 1305–1318 (1971).

Ruthven, D. M., *Principles of Adsorption & Adsorption Processes*, John Wiley & Sons, Inc., New York (1984).

Scheele, R. D., Burger, L. L., and Matsuzaki, C. L., *Methyl Iodide Sorption by Reduced Silver Mordenite*, PNL-4489, Pacific Northwest Laboratory (1983).

Scheele, R. D., and Burger, L. L., *Evaluation of Silver Mordenite for Radioiodine Retention at the Purex Process Facility Modification*, PNL-6261, Pacific Northwest Laboratory (July 1987).

Thomas, T. R., Staples, B. A., Murphy, L. P., and Nichols, J. T., *Airborne Elemental Iodine Loading Capacities of Metal Exchanged Zeolites and a Method for Recycling Silver Zeolite*, Idaho National Engineering Laboratory, ICP-1119 (July 1977).

Vaidyanathan, A. S., *Theoretical and Experimental Investigation of Sorption in Bidisperse Porous Particles*, PhD Dissertation, Clarkson College of Technology (September 1971).

Walker, L. R., personal communication to R. T. Jubin (March 14, 1994).

List of Symbols

b = stoichiometric coefficient for B
C = concentration (g/cm^3)
D_{AB} = molecular diffusion coefficient (cm^2/s)
D_c = intercrystalline or micropore diffusivity (cm^2/s)
D_e = ash layer diffusion coefficient (cm^2/s)
D_p = pore or macropore diffusivity (cm^2/s)
D_∞ = pre-exponential factor in Arrhenius expression for D
E_d = diffusional activation energy (cal/mol)
K^* = Henry's law constant based on q/C (cm)
k_g = gas film mass transfer coefficient (cm/s)
k_s = reaction rate constant for the gas solid reaction (cm/s)
m_t = mass adsorbed at time t
m_∞ = mass adsorbed at time $t \to \infty$
N = moles
p = root to transcendental equations
q = adsorbed phase concentration (g/cm^3)
R = gas constant
R^2 = coefficient of determination
r_a = pellet radius (cm)
r_c = pellet core radius (cm)
r_i = particle radius (cm)
S = surface area (m^2/g) or (m^2/cm^3)
T = temperature (°C or K)
t = time (s)
X = conversion

Greek Symbols:

α = ratio of diffusional time constants $(D_c/r_i^2)/(D_p/r_a^2)$
β = parameter defined by Eq. (20)
ε_p = porosity of pellet
τ = tortuosity factor
ρ_B = molar density of B (gmol/cm^3)

Subscripts:

A = component A (generally CH_3I)
B = component B (generally silver, but in the D_{AB} term is air)
ex = external
g = bulk gas phase
0 = initial
s = surface

Superscripts:

° = metallic form of silver

Other Symbols and Notations:

¯ = average value

DISCUSSION

BARLOW: What capacity do you believe you can be getting with your beds? From the knowledge you have now gained from your modeling, how much do you believe you could increase life? What is the typical utilization of the silver zeolite and does the information presented allow an estimate to be made of the maximum possible incorporation that might be achieved by an understanding of the controlling mechanisms?

JUBIN: In experimental tests with silver exchanged mordenite, loadings in the highest loaded segment of the bed have ranged from ~30% to ~60%, depending in large part on the operating conditions and bed depth. As can be observed from the thin bed loadings, completed as part of this test, silver utilizations of greater than 90% were achieved in numerous cases. The maximum loading that would be achieved in actual practice would be controlled by the bed design and by the operating conditions. By gaining an understanding of the controlling mechanisms through studies such as this one, the equipment and process conditions can be tailored to these mechanisms to achieve the highest practical utilization of the sorbent.

Removal Efficiency of Silver Impregnated Filter Materials and Performance of IodineFilters in the Off-Gases of the Karlsruhe Reprocessing Plant WAK

F.J. Herrmann, B. Herrmann, V. Hoeflich, Ch. Beyer
Wiederaufarbeitungsanlage Karlsruhe

J. Furrer
Forschungszentrum Karlsruhe / Germany

Abstract

An almost quantitative retention of iodine is required in reprocessing plants. For the iodine removal in the off-gas streams of a reprocessing plant various sorption materials had been tested under realistic conditions in the Karlsruhe reprocessing plant WAK in cooperation with the Karlsruhe research center FZK. The laboratory results achieved with different iodine sorption materials justified long time performance tests in the WAK Plant. Technical iodine filters and sorption materials for measurements of iodine had been tested from 1972 through 1992. This paper gives an overview over the most important results.

Extended laboratory, pilot plant, hot cell and plant experiences have been performed concerning the behavior and the distribution of iodine-129 in chemical processing plants (Henrich 1980, 1981, 1988, 1996, and Herrmann 1992). In a conventional reprocessing plant for power reactor fuel, the bulk of iodine-129 and iodine-127 is evolved into the dissolver off-gas. The remainder is dispersed over many aqueous, organic and gaseous process and waste streams of the plant.

Iodine filters with silver nitrate impregnated silica were installed in the dissolver off-gas of the Karlsruhe reprocessing plant WAK in 1975 and in two vessel vent systems in 1988. The aim of the Karlsruhe iodine research program was an almost quantitative evolution of the iodine during the dissolution process to remove as much iodine with the solid bed filters as possible. After shut down of the WAK plant in December 1990 the removal efficiency of the iodine filters at low iodine concentrations had been investigated during the following years.

I. Introduction

In connection with iodine monitoring different methods for sampling iodine in the off-gas streams of the WAK plant were used.

Sampling with caustic scrubbers does not allow to catch the organic iodine. By this method in the off-gas of the Kalrsruhe reprocessing plant WAK only 15 % of the total measured iodine could be trapped. Parallel measurements with a discriminating sampling system for inorganic iodine confirmed that only 10 to 20 % of the total iodine in this vessel off-gas stream was inorganic (Herrmann 1990).

It is well known that sampling and filtering of iodine with charcoal allows to detect organic and inorganic iodine species only at low humidity of the off-gas. Numerous publications in the past years and the following considerations demonstrate some problems encountered utilizing charcoal as sorption material. Charcoal is the most exhaustively studied adsorbent for iodine. High removal efficiencies can be obtained with plain or impregnated charcoal for elemental iodine. However acid vapors, organic vapors, and moisture seriously affect the efficiency of impregnated charcoal. In either case the use of charcoal in off-gas systems containing more than 6 % nitrogen oxides is severely limited (Rodger 1969).

Results of laboratory experiences in the Karlsruhe research center (FZK) have demonstrated that during long-term measurements (about two months) the iodide impregnated charcoal looses most of the inactive iodide impregnation due to the oxidation of the iodide by the air. A break-through of active iodine cannot be excluded.

In the special case of the vessel off-gases of reprocessing plants which are currently saturated with water vapor from the scrubbing columns and kerosene from the solvent, sampling with charcoal is problematic. The influence of the humidity on the removal efficiency of iodine samplers is reported by many authors and quantified by H. Schüttelkopf. At a relative humidity of >90 % iodine sampling is not effective. If 90 % humidity in the off-gas has been overstepped once, the following measuring periods are distinctly influenced. It must be guaranteed that the measuring conditions have a security distance from the dew point of the gas to be measured (Schüttelkopf 1976).

Due to the problems of trapping iodine for measurements and removal of iodine in the off-gases of reprocessing plants, inorganic silver impregnated materials have been developed and were used as sampling and as filter materials in the off-gas streams of the WAK plant (Furrer 1979, Wilhelm 1976 and Herrmann 1995).

II. Testing of Silver Impregnated Iodine Sorption Materials and Iodine Filters

To optimize iodine sorption materials manufactured with different carrier materials and different silver contents, after the preliminary tests in the Karlsruhe research center, the sorption materials had been tested in by-pass streams of the WAK dissolver off-gas and the WAK vessel ventilation system, see figure 1 (Test conditions: temperature 140 °C, residence time 0.4 s; bed depth 0.1 m; gas flow rate 0.7 m^3/h; linear gas velocity 0.24 m/s).

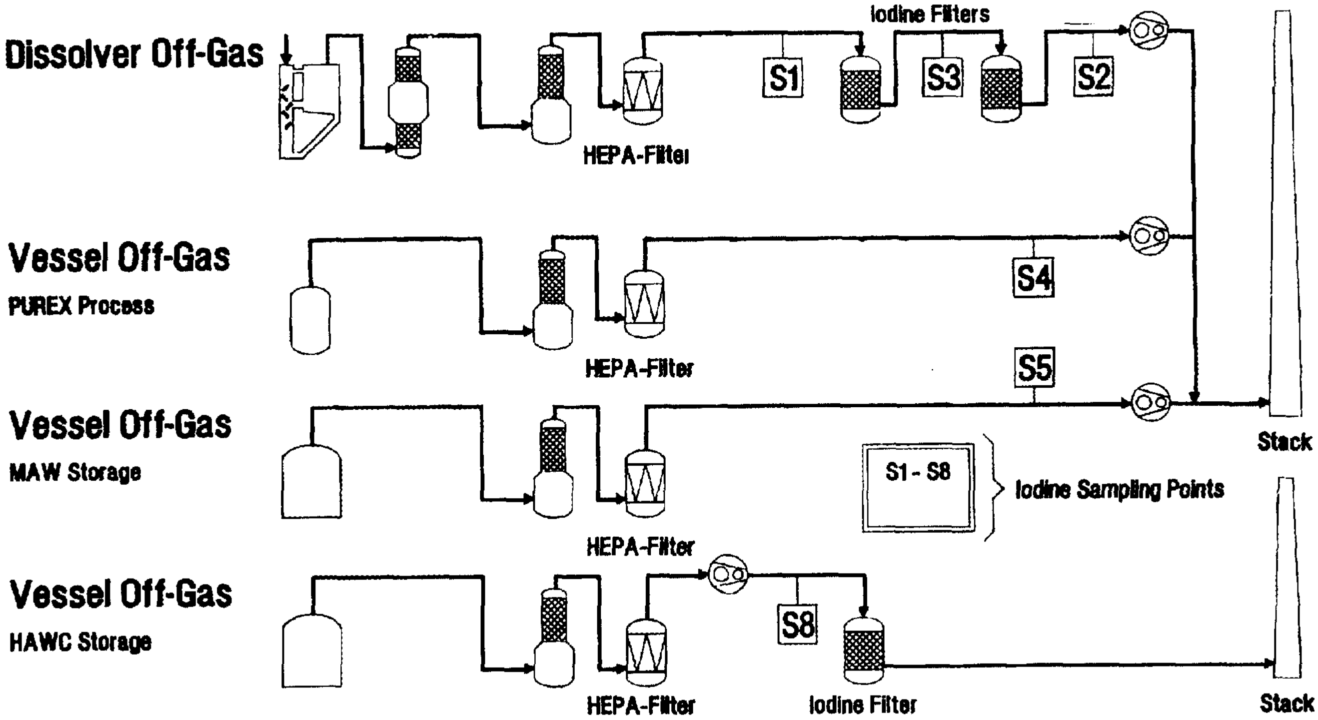

Figure 1 Offgas Cleaning of WAK with Iodine Filters and Iodine Sampling Points

For the investigations of the different sorption materials performed in the by-pass streams of the WAK dissolver off-gas (DOG) and the vessel off-gas (VOG), sampling points are located downstream the HEPA filters (upstream and downstream the iodine filters, see figure. 1). They allow to determine simultaneously the iodine concentration in the off-gas and the removal efficiency of the iodine filters). The gas stream is routed through absorption columns which are located in a heating cabinet. The internal diameter of the columns is 0.032 m. The gas flow rate through the columns is 500 l/h (STP). The column contains six successive beds consisting of the sorption material. Each bed is 0.05 m deep. The calculated residence time per bed is 0.2 s at 140°C. After different exposure times the columns were removed. The beds were emptied individually and the sorption materials were measured on a Intrinsic Germanium Planar Detector to determine its iodine-129 content.

III. Evaluation of Silver Impregnated Iodine Sorption Materials

Experiments concerning the influence of the silver content of the carrier material on the iodine removal efficiency in the vessel off-gas of WAK have shown that an impregnation with 12 % silver is the optimum. Higher silver contents (for example 20 %) increase the risk of the efflorescence of the silver nitrate impregnation taking place in off-gases with 3 to 4 % of water vapor (resulting from the vapor pressure of the scrubbing columns working at 25 to 30 °C).

The essential parameters of sorption materials which may influence the removal efficiency of iodine sorption materials had been investigated. All materials had been impregnated with 12 % silver in form of silver nitrate. The porosity and the inner surface of the carrier material are decisive for the iodine removal efficiency. The alpha alumina shows a lower removal efficiency than the AC 6120.

The properties of the sorption material and the retained removal efficiencies are listened in table 1.

Sorption material	AC6120 (Silica)	Alumina	Sinterglass
Grain size [mm]	1 - 2	2 - 4	1 - 2
Pore volume [ml/g]	0.62	0.45	0.5
BET surface [m^2/g]	65	7	0.15
Maximum of pore distribution [nm]	20 - 40	75	10,000 - 40,000
Silver content [%]	12	12	12
I-129 removal efficiency [%]			
- DOG of WAK	99.8	-----	90.0
- VOG of WAK	99.0	94.0	85.0 - 97.0

Table 1 Properties of sorption materials and iodine removal efficiencies in the off gas of WAK (Bed depth 10 cm, residence time 0.4 s; DOG = dissolver off-gas; VOG = vessel off-gas)

In an earlier paper it has been shown that it doesn't matter whether the carrier material is silica or alumina. A silver impregnated gamma-Al_2O_3 (JFM 1) having a BET surface comparable to the BET surface of AC 6120, showed the same high removal efficiency as AC 6120 (Herrmann 1995). Besides temperature, residence time, silver content, iodine species and concentration in the off-gas,. the decisive parameters for iodine removal efficiency are the porosity and the BET surface.

IV. Transferability of the Removal Iodine Efficiency Obtained by Small Scale Filters and Technical Filters

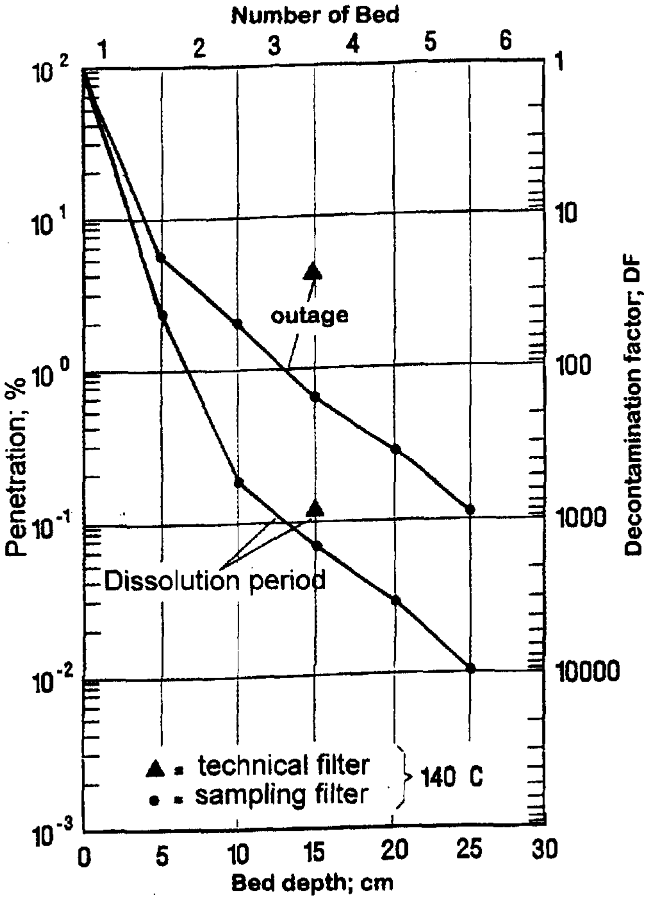

Figure 2 Removal efficiency of AC 6120 in a full size filter and in sampling filters.

The decontamination factors obtained with the small scale columns (sampling filter: inner diameter 0.032 m, bed depth 0.15 m) and the technical iodine filter (annular cylinder with a bed depth of 0.15 m), are traced in figure 2. The small scale filters reveal a higher iodine removal performance than the technical iodine filter. These values result from 12 measuring periods between 1989 and 1991.

The data for the iodine removal efficiency obtained by small sampling tubes (diameter 0,032 m, bed depth 0,1 m) are not directly transferable to the iodine removal performance obtained by full size iodine filters. Table 2 shows the iodine removal efficiency of a small size filter (bed depth 0,15 m, residence time 1.0 s, sorption material 0,078 kg) and a full size filter (annular cylindrical filter with a bed depth of 0.15 m and a filter diameter of 0.4 m, sorption material 35 kg).

	Small size filter	Full size filter
Mass of AC6120/12 % Ag	0.078	35
Bed depth [m]	0.15	0.15
Temperature [°C]	140	entrance: 130, exit: 110
Gas flow rate [m^3/h]	0.5	80 to 120
Linear velocity [m/s]	0.25	0.15
Residence time [s]	0.6	1.0
Iodine removal efficiency [%]		
- during dissolution	99.9-99.95	99.8-99.9
- during outage	98.7-99.3	94-96

Table 2 Comparison of iodine removal efficiency of a small scale and a full size iodine filter with AC6120/12% Ag in the dissolver off gas of WAK

The iodine removal efficiency of the full size filter is distinctly lower than the removal efficiency of the small size filters. The lower removal efficiency of the technical filter can be explained by channeling effects. The differences between laboratory scale filters and full size filters must be taken into consideration for the design of iodine filters in the off-gases of reprocessing plants.

V. Performance of Iodine Filters in the Off-Gas Streams of the WAK Plant

V.1 Dissolver Off-Gas

Two silver impregnated iodine filters in series were in operation in the dissolver off-gas of the WAK plant from 1975 through 1993. The filter material was a silver nitrate impregnated silica (AC 6120/12 % Ag). The filters worked at 110° to 130°C.

The dissolver off-gas filters were annular filters with the following characteristics:

Outer diameter	400 mm
Inner diameter	106 mm
Thickness of annular section	147 mm
Active filter volume	54 l
Number of filters	2 filters in series
Sorption material	AC 6120, 35 kg per filter
Gas temperature	inlet 130 °C, outlet 110 °C
Dissolver off-gas flow rate	80 to 120 m^3/h
Residence time (off-gas)	1.4 s

The sorption material of the first filter was changed when the iodine removal efficiency of the first filter dropped significantly. Under normal operation conditions the iodine filters worked two years without interruption.

During dissolution periods the highest removal efficiencies of 99 to 99.9 % for the first iodine filter had been measured. The average iodine concentrations in the dissolver off-gas upstream of the iodine filter was in the range between 1 and 5 mg/m^3 obtained by discontinuous measurements. The peak values during dissolution were not measured because of the radiation power at the sampling points. They are in the order of 100 mg/m^3. During outage periods the removal efficiency of the first iodine filter was 97 %.

The removal efficiency of the second iodine filter was 90 % during dissolution period and 50 % during outage periods. The average decontamination factor of the second filter between 1989 and 1991 (two years of operation and one year after shutdown) was 4.

Downstream of the two iodine filters iodine-129 concentrations of about 0.005 mg/m^3 were observed during dissolution periods.

During the 15 years of operation a high stoichiometric loading up to 80 % of the first iodine filter had been achieved. The measured values of iodine loading were 17 GBq to 24 GBq. The corresponding service lives were 2 to 4 years for the iodine filter material.

V.2 Vessel Ventilation System of the PUREX Process

In 1987 a prototype iodine filter with a throughput of 35 m^3/h and the following dimensions has been installed in a side stream of the vessel off-gas of the PUREX process:

Diameter	355 mm
Bed depth	150 mm
Sorption material	8.5 kg AC 6120 / 12 % Ag
Operating temperature	140°C
Gas velocity	14 cm/s
Residence time	1 s

The decontamination factor was determined by weekly measurements of the iodine concentration upstream and downstream the prototype iodine filter. The removal efficiency of the prototype filter in this off-gas stream was 90 to 95 %.

The decontamination factors are influenced by the iodine concentrations and by the nature of the iodine species present in the vessel off-gas. Iodine loading after 2.5 years of operation was 21.4 MBq (3.27 g of iodine-129) for the total filter. This corresponds to a stoichiometric loading of 0.33 %.

V.3 Vessel Ventilation System of the Liquid High Active Waste Storage

Up to now the iodine filter with AC6120/12 % Ag in the vessel vent system of the liquid high active waste storage is operating at about 40 °C and a gas flow rate of 180 m^3/h up to now. An iodine removal efficiency of 90 % to 94 % is attained.

Literature

Furrer, J. 1979. Verfahrensentwicklung und Optimierung der Filter zur Auflöserabgas- reinigung. Report KfK 2750.

Henrich, E. and R. Hüfner. 1980 . Improved Procedures for Efficient Iodine Removal from Fuel Solutions in Reprocessing Plants, IAEA-SM-245/16.

Henrich, E., W. Roesch , F.Weirich. 1981. Improved Iodine and Tritium Control in Reprocessing Plants.16th DOE Nuclear Air Cleaning Conference, San Diego, 1980 (Conf-801038), 1981.

Henrich, E., R. Grimm, L. Finsterwalder. 1988. Ioddesorption aus der Brennstofflösung, ein Vergleich von Theorie und Experiment. Report KfK 4476 pp.155-200 (1988).

Henrich, E.1996. Control of Volatile Radionuclides in Reprocessing.
To be published in Kerntechnik, 1996.

Herrmann, F. J., V. Motoi, B. Herrmann, A. van Schoor, D. Fang, H. Fies. 1990. Retention and Measurement of Iodine-129 and of Organoiodine in the Off-gas Streams of the Karlsruhe Reprocessing Plant WAK. 21st DOE/NRC Nuclear Air Cleaning Conference, San Diego 1990, CONF-900813. pp 222-233.

Herrmann, F.J., R. Grziwa, L. Finsterwalder, D. Fang, B. Herrmann, V. Motoi, Ch. Beyer.1992. Iodverteilung in einer Wiederaufarbeitungsanlage am Beispiel der WAK.
Annual Meeting on Nuclear Technology-Jahrestagung Kerntechnik 5.-7. Mai 1992, Karlsruhe
Proceedings 0720-9207.

Herrmann F.J., V.Motoi, B. Herrmann, D. Fang, L. Finsterwalder, K.D. Kuhn, A. van Schoor, Ch. Beyer, J. Furrer, W. Knoch. 1992. Minimizing of Iodine-129 Release at the Karlsruhe Reprocessing Plant WAK. 22st DOE/NRC Nuclear Air Cleaning Conference, Denver 1992.

Herrmann, F.J., B. Herrmann, D. Fang, M. Weishaupt, J. Furrer, T. Engelhardt. 1995.
15 Jahre Erfahrungen mit Iodfiltern im Abgas der Wiederaufarbeitungs- anlage Karlsruhe WAK. Annual Meeting on Nuclear Technology, Nürnberg, 16. - 18. Mai 1995.

Rodger, W.A. and S. L. Reese. 1969. The Removal of Iodine from Reprocessing Plants Effluents. Reactor and Fuel-Processing Technologiy, Vol. 12, No. 2, pp. 173-180, 1969.

Schüttelkopf, H. and H. Fessler. 1976. Die Messung von Iod-131 in der Umgebungsluft kerntechnischer Anlagen. Report KFK 2350.

Wilhelm, J., J. Furrer, E. Schultes. 1976. Head End Iodine Removal from a Reprocessing Plant with a Solid Sorbent. 14th DOE Air Cleaning Conference, Idaho Falls.

DISCUSSION

JUBIN: A point of clarification concerning the difference between your technical filter and your sampling filter, you indicated that the sampling filter always had better performance than the technical filter. Was the technical filter exposed to other contaminants for a longer period of time than the sampling filter? The question is, did they have the same history? Can this be attributed to the length of time the sampling filters were in service or to other contaminants?

HERRMANN: The technical filter has always had distinctly lower removal efficiency than the sampling filter, even for the same experimental conditions and exposure times. Experiments performed with sampling filters of different sizes (diameter 25mm and 33mm) showed the same phenomena. The smaller the filter diameter, the better the removal efficiency. When sampling filters and technical filters had the same service life, the sampling filters always showed a better iodine removal efficiency.

SAKURAI: You use the two DOG filters in series at the WAK reprocessing plant. Why is the DF lower for the second filter than for the first one? Is it a commonly observed phenomenon?

HERRMANN: This has commonly been observed. The iodine concentration entering the second filter is by 3 orders of magnitude lower than the iodine concentration entering the first filter. The iodine species are probably different.

Control of Radio-Iodine at the German Reprocessing Plant WAK during Operation and after Shutdown

F.J. Herrmann, B. Herrmann, K.D. Kuhn, A. van Schoor, M. Weishaupt
Wiederaufarbeitungsanlage Karlsruhe

J. Furrer
Forschungszentrum Karlsruhe/Germany

W. Knoch
Deutsche Gesellschaft für Wiederaufarbeitung von Kernbrennstoffen m.b.H.

Abstract

During 20 years of operation 207 metric tons of oxide fuel from nuclear power reactors with 19 kg of iodine-129 had been reprocessed in the WAK plant near Karlsruhe. In January 1991 the WAK Plant was shut down. During operation iodine releases of the plant as well as the iodine distribution over the liquid and gaseous process streams had been determined. Most of the iodine is evolved into the dissolver off-gas in volatile form. The remainder is dispersed over many aqueous, organic and especially gaseous process and waste streams.

After shut down of the plant in January 1991, iodine measurements in the off-gas streams have been continued up to now. Whereas the iodine-129 concentration in the dissolver off-gas dropped during six months after shutdown by three orders of magnitude, the iodine concentrations in the vessel ventilation system of the PUREX process and the cell vent system decreased only by a factor of 10 during the same period. Iodine-129 releases of the liquid high active waste storage tanks did not decrease distinctly.

The removal efficiencies of the silver impregnated iodine filters in the different off-gas streams of the WAK plant depend on the iodine concentration in the off-gas. The reason of the observed dependence of the DF on the iodine-129 concentration might be due to the presence of organic iodine compounds which are difficult to remove.

I. Introduction

Besides the optimization of the PUREX process particularly by an electrolytic uranium-plutonium separation, an important task for the WAK plant was to demonstrate low iodine releases in view of the project of the German industrial scale reprocessing plant.

In 1975 the yearly iodine-129 release limit of the WAK plant via the off-gas was fixed to 240 MBq (equivalent to 37 g iodine-129). By this reason silver impregnated iodine filters had been installed in the dissolver off-gas.

Main objective of the iodine management during operation of the WAK plant was to obtain a low residual iodine content in the fuel solution after the end of the dissolution process by evolving most of the iodine into the dissolver off-gas and an almost quantitative iodine removal on silver impregnated solid bed filters in the dissolver off-gas. At the beginning of 1988 silver impregnated solid bed iodine filters entered in operation in two vessel ventilation systems.

In the meantime, the licensing authorities had reduced the maximum permissible iodine release of the planned German industrial scale reprocessing plant in Bavaria from 7.4 GBq (200 mCi) to 1.85 GBq per year (50 mCi) for a throughput of 350 tons of uranium from light water reactor fuel (burnup 50,000 MWd/ton U). This value of 1.85 GBq signified that only 0.2 % of the iodine inventory could be released by all off-gas streams of the plant.

After some years of intensive work at the Karlsruhe reprocessing plant WAK in 1989 it was clear that this ambitious aim of 0.2 % release of the iodine inventory could not be demonstrated in the WAK plant. Because of the shortness of time before shut down there was no possibility to install iodine filters in all off-gas lines of the WAK plant. Meanwhile the project of the industrial scale reprocessing plant in Germany had been given up in 1989 after 15 years of intensive development work.

II. Iodine Distribution in the WAK Plant

During fuel dissolution the fission product iodine is present mainly in its volatile elementary form. From the point of view of radio ecology, iodine-129, with a half life period of $1.6*10^7$ years and iodine-131 with a half life period of 8.02 days, are significant. If cooling times are > 1 year, as in the case of commercial reprocessing, practically all of the short life I-131 from uranium fission has decayed.

However, iodine-131 from fission of curium-244 in the fuel is detected and measured in all steps of the PUREX process: in the dissolver off-gas, in the vessel ventilation system, and particularly in the vessel ventilation of the storage tanks of the liquid high active waste (Herrmann 1994).

II.1 Residual Iodine Content in the Dissolver Solution

The chemical behavior of iodine in a nitric acid medium is complex. Particularly at low concentrations, iodine behavior is dominated by the redox potential in combination with unavoidable, mostly organic trace impurities in the solution. The species and the concentration of these impurities depend on the suppliers of nitric acid and on processing details. So the behavior of iodine may deviate largely from expected textbook behavior (Henrich 1996, Comor 1992).

The conditions for evolution of iodine into the off-gas have been examined in laboratory, in inactive pilot plant scale, in the hot cell facilities of the Karlsruhe nuclear research center as well as in the WAK reprocessing plant.

Henrich, Grimm and Boukis (1991) demonstrated with a high burnup fuel (50 GWd/T U) from the BIBLIS light water power reactor in laboratory scale dissolution experiments residual iodine contents between 1.1 % (1.2 mg/l) and 2.2 % (2.3 mg/l) of the inventory of the fuel after dissolution of 80 g of UO_2 fuel in 220 ml HNO_3 (7.5 M). The values of 1.2 mg/l and 2.3 mg/l have been obtained with nitric acid of p.a. quality respectively with recycled acid from the WAK plant (Henrich 1991). After filtration of the fuel solution, addition of iodate carrier, subsequent NOx sparging and a second filtration of the fuel solution the residual iodine content decreased below 0.5 % (0.5 mg/l) of the iodine inventory of the fuel. The residual iodine concentration depends strongly on the quality of the nitric acid.

Because of the extraction behavior of the residual iodine in different extractants, Henrich (1991) and Boukis (1991) conclude that the residual iodine must be a mixture of many iodinated organic species with different extractabilities. Henrich (1988) pointed out that the concentration of organic impurities in a pure nitric acid in a ppm range is by two orders of magnitude higher than the aspired residual iodine content in the dissolver solution ($2*10^{-6}$ mol/l). Henrich's interpretation is supported by the results of Lieser (1989).

The WAK plant experiences (>8 hours boiling time, air sparging, addition of carrier iodine during the last 2 hours of dissolution) showed, that it is difficult to reach residual iodine values in the dissolver solution below 1 % of the inventory for a high burnup fuel (35,000 MWd/T U). This value corresponds to an iodine concentration of approximately 1 mg/l.

For dissolution in WAK lower iodine-129 concentrations than 1 % of the iodine inventory in the feed have been reported by Berg (1977). The discrepancy between the earlier WAK values and the recent values of the Karlsruhe research center and of the WAK plant is not connected with the evolving process but with the usual analytic iodine separation and determination procedure which took into account only the inorganic and soluble iodine compounds (Henrich 1996).

Depending on operation conditions in the WAK plant (8 hours boiling time, air sparging), the residual iodine concentrations in the dissolver solution generally were in the range of 1 to 4 mg iodine per liter. It seems that the residual iodine concentration [g/l] is not influenced by the burnup of the processed fuel; the fraction of the residual iodine in [%] is of course higher for the fuel with a low burn-up and with a low total iodine content. Fuel with a low burn-up of 7 to 14 GWd/t U yielded residual iodine contents of 4 % to 12 % (in average 6 %), whereas high burn-up fuel with 30 GWd/t U yielded average residual iodine contents of 2 to 3 % of the inventory of the fuel after the end of the dissolution. In both cases, high burn-up fuel and low burn up fuel, the range of the residual iodine concentration was 1 to 4 mg/l. (Fission product iodine-127 was taken into account with 25 weight % of the iodine-129 inventory).

Important parameters for the evolution of the iodine during the dissolution process are the quantity of water vapor generated during boiling of the dissolver solution (45 m^3/h), the formation of the nitrous oxides (20 m^3/h) and the duration of the dissolution process. For the standard dissolution conditions 8 hours are required. To obtain low residual iodine values in the dissolver solution it is important to have a high quantity of dissolver off-gas passing through the dissolver and the reflux condenser (80 to 120 m^3/h). The addition of natural iodine as carrier and sparging of the dissolver solution with NO_2 during the last hour of the dissolution resulted in an average iodine content of 1 % (about 1 mg/l) of the iodine-129 inventory in the case of a high burnup fuel.

The percentages employed for the following considerations are average values resulting from the analyses of many liquid and many off-gas samples. These values cover the analyzed iodine fractions obtained by fuel with burn-up between 15,000 MWd/t U and 40,000 MWd/t U.

II.2 Iodine Concentration in the Dissolver Off-Gas

In the Karlsruhe reprocessing plant the bulk of the iodine inventory (in average 94 %) is evolved from the dissolver solution and is transported by the dissolver off-gas DOG through a reflux condenser and two subsequent acid scrubbers on two iodine filters in series. These filters contain a silver nitrate impregnated silica material with a grain size of about 1 mm. The iodine concentration in the dissolver off-gas upstream the iodine filters undergoes big variations. Average values during dissolution periods are in the order of 1 to 5 mg/m^3 with peak values up to 100 mg/m^3.

After shut down of the WAK plant the iodine concentrations upstream the iodine filter in the dissolver off-gas dropped from average values of about 2 mg/m^3 in December 1990 to 0.03 mg/m^3 in January-February 1991 and further to 0.001 mg/m^3 at the end of 1991.

II.3 Iodine Depositions in the Sampling Lines of the Dissolver Off-Gas

Iodine depositions in sampling lines have been studied by Glissmeyer and Sehmel (1991). They occur in the sampling lines because of the high surface/volume ratio of the sampling pipes and the relatively low linear velocity of the sampling gas streams. Iodine depositions in the sampling lines can potentially lead to erroneous results of radioiodine measurements and make dubious all short term measurements concerning the removal efficiency of iodine filters or scrubbers. One example may illustrate the problem of iodine depositions:

Iodine sampling in the dissolver off-gas of WAK is performed discontinuously all 4 to 5 dissolutions. At the beginning of a dissolution campaign in WAK after 5 dissolutions of a fuel with a burnup of 14,000 MWd/t U only about 34 % of the iodine inventory of the fuel could be measured in the dissolver off-gas upstream the iodine filters. (This value can lead to the conclusion that the scrubbers upstream the iodine filters had an iodine removal efficiency of 60 %, assuming an iodine evolution of 94 % of the iodine inventory in the dissolver). After 14 dissolutions about 76 %, and after 32 dissolutions about 84 % of the iodine inventory were found on the sampling filters. These delayed iodine concentrations result from iodine depositions formed in the sampling lines at the beginning of a campaign.

The above cited results had been obtained without heating the sampling lines. To overcome the errors due to iodine depositions in non heated sampling lines, long term measurements have to be performed. By heating the whole sampling lines to > 80 °C, it had been demonstrated that iodine depositions can be prevented and that short term measurements of the removal efficiency of the iodine filters yield reliable results.

After the end of a dissolution period iodine concentrations in the dissolver off-gas system drop slowly. Several days are necessary to attain iodine concentrations comparable to the iodine concentrations in the vessel ventilation system of the PUREX process (0.008 mg/m^3).

II.4 Iodine Behavior in the PUREX Solvent Extraction Process

The percentages of iodine in the following considerations are average values resulting from the last five years of operation. They cover the analyzed iodine fractions obtained by fuel with burn-up between 15,000 MWd/t U and 40,000 MWd/t U (see chapter II.1).

The residual iodine species remaining in the fuel solution (in average about 5 % of the iodine inventory of the fuel; about 1 % is fixed on the dissolver residues) are distributed in the subsequent extraction process operations. About 2 % to 3 % of the iodine inventory of the dissolved fuel were found in the organic solvent (20,000 to 40,000 Bq iodine-129/l corresponding to 3 mg/l to 6 mg/l). The rest of about 2 % are spread over the high active waste and different off-gases. The organic iodine compounds in the solvent contribute to the iodine emitted by the vessel vent system of the PUREX process and the vessel vent of the subsequent medium active waste treatment facility. During solvent wash the iodine content in the organic phase does not decrease considerably. Only about 0.3 % of the iodine inventory of the fuel was found in the alkaline solvent wash streams.

After shut down of the WAK plant the organic solvent, the organic and aqueous wastes have been transferred to the waste treatment facilities of the Karlsruhe Research Center. The iodine releases of this facility had been discussed by Amend (1990).

II.5 Iodine Concentration in the Vessel Ventilation System of the PUREX Process

After 8 hours of dissolution the residual iodine concentration in the dissolver solution is 1 to 4 mg/l. The residual iodine is routed to the extraction process. In 1990 detailed investigations over different reprocessing periods were carried out during reprocessing of about 9 tons of fuel from nuclear power plants (burnup 5.4 to 30 GWd/t) to determine the distribution of iodine in the PUREX process. From the iodine arriving in the separations process, about 50 % are evolved into the vessel vent system. The average iodine concentration in the vessel vent (270 - 330 m^3/h) is between 0.008 and 0.018 mg/m^3. Maximum values measured over a 14 days period attained about 0.03 mg/m^3 (160 Bq/m^3 Iodine-129).

Immediately after shut down the iodine release via this off-gas dropped from about 10 MBq (1.5 g of iodine-129) per month in December 1990 to 5 MBq per month in January 1991 and reached values of about 0.2 MBq/month (= 30 mg/month) after 10 months.

II.6 Iodine in the Vessel Ventilation System of the Medium Active Waste Storage Tanks

The iodine concentrations in this off-gas stream during operation was approximately 0.01 mg/m^3. After shut down this concentration did not drop immediately. One year after shut down the iodine concentration was lower by a factor of 10. No iodine filter was in operation in this off-gas.

II.7 Iodine in the Vessel Ventilation System of the Liquid High Active Waste Concentrate (HAWC) Storage Tanks

Two storage tanks contain the high active waste concentrate of 20 years reprocessing history of the WAK plant (about 60 m^3 HAWC).

During the operation period of WAK the iodine concentration measured in this off-gas stream was between 0.002 to 0.006 mg/ m^3. (iodine-129: 10 to 30 Bq/m^3).

After shut down of the plant in January 1991 the monthly amount of iodine-129 evolved by the HAWC has not decreased considerably during five years. In average 2 MBq of iodine-129 per month (0.3 g I-129) are evolved. Table 1 gives an overview over the iodine-129 evolved.

Year	1991	1992	1993	1994	1995
I-129 evolved [MBq/a]	16.9	16.1	23.7	25.8	26.5

Table 1 Iodine-129 evolution from the liquid high active waste concentrate (HAWC)

The amount of iodine-131 evolved by the HAWC solution in terms of Becquerel is in the same order of magnitude as the amount of Becquerel of iodine 129. Iodine-131 results mainly from the spontaneous fission of Curium-244. Whereas Cm-244 and Cm-246 in the waste solution are the main sources for the generation of iodine-131 by spontaneous fission (Herrmann 1994), the iodine-129 evolved by this off-gas results mainly from the residues of the dissolution processes from 20 years reprocessing, containing some hundred grams of iodine-129.

Up to now the evolution of iodine-129 from these storage tanks show no significant decrease. Due to the iodine filter in this vessel vent system the release values are about 10 % of the amount of the iodine evolved by these solutions.

II.8 Iodine in the Cell Ventilation System

In the cell vent system of the WAK plant during dissolution periods a fraction of 0.3 % of the iodine-129 inventory of the fuel was measured. Iodine monitoring devices in different ventilation systems revealed that the measured iodine (up to 30 mg per day) originated almost exclusively to the shear and dissolver cell. The measured iodine concentrations in this off-gas were $3*10^{-5}$ mg/m³ and reached concentrations up to $18*10^{-5}$ mg/m³ during plant operation. Such high release values have been observed exclusively during dissolution periods. The high releases of 20 to 30 mg of iodine per day had been measured by two independant monitoring systems over a period of 4 to 6 weeks. It can be excluded that the measured iodine was a result of the shearing process itself. Leudet and Leseur (1982) demonstrated that during shearing of high burnup fuel from power reactors fission product iodine release was not detectable.

Two reasons may be responsible for an iodine leaking out of the dissolver:

- A leakage of the dissolver cover seems to be possible at the beginning of dissolution when a high rate of nitric oxides are generated and the reduced pressure of the dissolver off-gas system goes to 0 (related to the pressure in the dissolver cell).
- The reduced pressure cannot be maintained during the opening of the dissolver cover when the fuel is loaded and iodine deposits may come into the cell.

After shut down the iodine-129 release values dropped from about one MBq/month in December 1990 to 0.1 MBq/month in November 1991.

III. Iodine Removal Devices

III.1 Acid Scrubbers and Caustic Scrubber in the Dissolver Off-Gas

Because of the presence of nitric oxides in the off-gases of a reprocessing plant the use of charcoal is prohibited.

Acid scrubbers: Concerning the two acid scrubbers in series located in the dissolver off-gas system of the WAK plant only 0.5 % to 1.5 % of the iodine inventory of the dissolved fuel had been measured in the nitric acid solution of the two packed columns after each dissolution charge. This fact of a low removal efficiency must be seen in connection with the relatively high dissolver off-gas flow rate of the WAK plant of about 100 m³/h.

Caustic scrubber: At the beginning of 1975 during WAK operation it has been tried to remove the iodine evolved from the dissolver by caustic scrubbing. An iodine removal efficiency of 53 % to 71 % could be attained in the dissolver off-gas (Schüttelkopf 1976). Because this iodine removal efficiency was too low, iodine filters with silver impregnated silica entered in operation mid 1975 in the dissolver off-gas. In the vessel ventilation system only 15 % of the total measured iodine could be removed by caustic scrubbing (Herrmann 1990).

III.2 Silver impregnated Iodine Filters in the Dissolver Off-Gas

During dissolution periods the highest removal efficiencies for the two filters in series of 99.5 to 99.9 % related to the iodine concentrations in the off-gas upstream the iodine filter had been measured, the iodine concentrations in the dissolver off-gas varying in average between 1 and 5 mg/m^3. Downstream the two iodine filters in series iodine-129 concentrations of about 0.005 mg/m^3 were observed during dissolution periods.

During outage periods and during the first six months after shut down, iodine concentrations of about 0.01 mg/m^3 (65 Bq/m^3) had been measured upstream the two iodine filters. Downstream the iodine filters iodine concentrations of about 0.0007 mg/m^3 were measured. The removal efficiency of the two iodine filters in series dropped to 90 %.

One year after shut down the iodine-129 concentrations downstream the two iodine filters dropped to about 0.6 Bq/m^3.

III.3 Silver Impregnated Iodine Filter in the Vessel Off-Gas of the PUREX Process

As shown above the iodine concentration in the vessel off-gas varied between 0.008 and 0.018 mg/m^3. The measured removal efficiency of a prototype filter in a side stream of this off-gas has been 90 to 95 % of the iodine concentration in the off-gas upstream the iodine filter.

III.4 Iodine Filter in the Vessel Ventilation System of the High Active Waste Storage

This iodine filter with AC6120/12 % Ag is operating at about 40 °C and has a removal efficiency 90 % to 94 %. The gas flow rate is about 180 m^3/h. The measured iodine contents in the off-gas upstream (evolved) and downstream (released) are shown in table 2.

Year	1990	1991	1992	1993	1994	1995
Iodine-129 evolved [MBq/a]	35.0	16.9	16.0	23.7	23.9	26.5
Iodine-129 released [MBq/a]	2.3	0.9	1.5	2.0	1.72	1.4

Table 2 Iodine contents upstream and downstream the iodine filter in the vessel ventilation system of the storage tanks of the liquid high active waste concentrate (HAWC)

IV. Iodine Release of the Reprocessing Plant WAK during Operation and after Shut Down

The iodine release fraction of a reprocessing plant is defined as the ratio of all iodine leaving the plant to the iodine processed in the plant. It is determined by the efficiency of the iodine removal devices.

Most of the iodine released resulted from the vessel ventilation systems. During the considered period the vessel ventilation system had no iodine filters. Although the iodine removal efficiency of the filter in the dissolver off-gas was high (about 99.5 %), the iodine overall release from the plant was in yearly average 1.8 % of the iodine inventory of the fuel during 14 years of reprocessing. The highest release fraction in one year was 4.1 % of the iodine processed. This high release fraction resulted from an experimental program with the aim of shortening the dissolution time of 7 dissolution charges from 8 hours to 5, 4 and 3 hours. It must be noted that this experimental program concerned only 7 from 25 dissolution charges in one month.

The values of iodine 129 releases during the last year of operation (1990) and the following years after shut down demonstrate clearly a decrease of the iodine-129 concentration by a factor of about 10 in the off-gases.

Table 3 shows the iodine-129 and iodine 131 releases of the WAK Plant from 1990 to 1995.

Year	1990 Operation	1991 shut down	1992	1993	1994	1995
Iodine-129 (MBq/a)	91	33	8.7	6.5	4.3	2.9
Iodine-131 (MBq/a)	12	3.7	4.5	4.5	4.1	2.5

Table 3 Iodine release of WAK Plant from 1990 through 1994 (shut-down January 1991)

After shut down most of the iodine releases is originated from the vessel vent system of the medium active waste storage tanks and the high active waste concentrate (HAWC) storage tanks. The HAWC evolves in average 25 MBq iodine-129 per year. Since this off-gas stream passes through an silver impregnated iodine filter, the releases are lowered by a factor of about 10.

The iodine 131 emissions after shut down result exclusively from the high active waste concentrate. The amount of iodine-131 evolved shows a slight tendency of decrease during the last five years due to the half life period of the nuclide Cm-244 (18 years), generating the iodine-131.

During the last year of reprocessing (1990) the release fraction of the WAK plant for iodine-129 was 2.1 % of the iodine-129 inventory processed. From this 2.1 % two thirds originated to the vessel ventilation system of the PUREX process, one fifth to the storage tanks of the medium active waste and one tenth to the cell ventilation system. Only a fraction of 0.028 of the 2.1 % originates to the iodine filtered dissolver off-gas and a fraction of 0.018 to the iodine filtered vessel ventilation system of the liquid high active waste concentrate storage tanks.

Literature

Amend, J., V. Motoi, F.J. Herrmann, J. Furrer. 1990. Iodine-129 Distribution and Retention during Evaporation of MLLW Solutions. 21st DOE/NRC Nuclear Air Cleaning Conference, San Diego 1990.

Berg, R., H. Schüttelkopf. 1977. Die Messung der Verteilung von Iod-129 in der WAK, Seminar on Radioactive Effluents from Reprocessing Plants. Karlsruhe, November 1977, pp. 81 f.

Boukis, N., and E. Henrich. 1991. Two-Step Procedure for the Iodine Removal from Nuclear Fuel Solutions. Radiochimica Acta 55, 37 - 42 (1991).

Comor, J.J, E. Henrich, R. Grimm, L. Stieglitz. 1992. Further Investigations on the Iodine Species Formed in the Nitric Acid/Nitric Oxide System. Radiochimica Acta 57 (1992) pp. 207-212.

Glissmeyer, J. A., and G. A. Sehmel. 1991. Line-Loss Determination for Air Sampler System. NUREG/CR-4757; PNL-5797.

Henrich, E., R. Grimm, L. Finsterwalder. 1988. Ioddesorption aus der Brennstofflösung, ein Vergleich von Theorie und Experiment. Report KfK 4476 pp.155-200 (1988).

Henrich, E., R. Grimm, N. Boukis, W. Zetzel, F. Leonhard, D. Ertel. 1991. Experimente zur Ioddesorption aus hochaktiven und simulierten Brennstofflösungen und Entwicklung der zugehörigen Iodanalytik. Primärbericht Kernforschungszentrum Karlsruhe PWA 29/91 (Okt. 1991).

Henrich, E.1996. Control of Volatile Radionuclides in Reprocessing. To be published in Kerntechnik 1996.

Herrmann, F. J., V. Motoi, B. Herrmann, A. van Schoor, D. Fang, H. Fies. 1990. Retention and Measurement of Iodine-129 and of Organoiodine in the Off-gas Streams of the Karlsruhe Reprocessing Plant WAK. 21st DOE/NRC Nuclear Air Cleaning Conference, San Diego 1990, CONF-900813. pp 222-233.

Herrmann, B., F.J. Herrmann, W. Knoch, A. Stollenwerk. 1994. Iodine-131 in the Off-Gas of Karlsruhe Reprocessing Plant. RECOD '94, Vol. III. London

Leudet, A. and A. Leseur. 1982. Comportement des radionuclides gazeux dégagés pendant les opérations initiales de retraitement. Rapport EUR 7822 FR.

Lieser, K. H., et al., 1989. Radioiodine in Nitric Acid, Radiochimica Acta 48. 193-199.

Schüttelkopf, H. 1976. Jahresbericht 1975 - Abteilung Strahlenschutz und Sicherheit: Emissions- und Immissionsmessungen von I-129. pp. 142-146. Report KFK 2266 (Mai 1976).

DISCUSSION

SAKURAI: At the WAK reprocessing plant, was the expulsion of iodine from the spent-fuel solution performed by NO_x sparging? And what was the effect?

HERRMANN: It was an experimental program which took a lot of preparation because we must make the demand to the authorities. But we have already made ten dissolutions with additions of I-127 and NO_2. NO_2-sparging and simultaneous addition of iodine-127 to the dissolver resulted in a residual iodine content in the feed solution of 1 mg/l.

JUBIN: I have a question on the high active waste concentrate. Have you had a chance to analyze the iodine content in the HAWC?

HERRMANN: The problem with the iodine-129 analysis was the biggest problem we had because the analytical procedure, by extracting and reextracting the iodine from the high activity solutions did not catch the organic species. And as far as I remember, in the high active waste solutions, we found between 500 and 5,000 B8/l before the concentration step (HAWC). But this was not compatible with the continuous evolution of iodine-129 tanks. (The measurement of iodine-129 in the offgases is reliable because after the HEPA filters, there is no other activity on these sampling filters.) The continuous evolution of I-129 from HAWC results from the solid residues in the HAWC containing iodine.

KNOCH: Iodine depositions can occur also in the main ducts of the offgas.

HERRMANN: In our case the linear velocity in the sampling lines is lower than the gas velocity in the main line. I agree, we cannot exclude depositions in the main pipes.

FUKASAWA: In Table 3 of your manuscript, I-129 release decreased more rapidly than I-131. (I-129: 91 MBq/y (‘90) ⇨2.9 (‘95); I-131: 12 (‘90)⇨2.5 (‘95) What is the reason for this phenomenon?

HERRMANN: The rapid decrease of I-129 releases is conspicuous after shutdown of the plant in January, 1991. The I-131 releases after shutdown result from the spontaneous fission of Cm-244 present in the high level liquid waste HAWC.

CLOSING COMMENTS OF SESSION CHAIRMAN

I would like to thank all of the speakers for their effort in attending this conference and for the quality of their presentations. I think that iodine studies continue to be important. In the United States we are moving toward looking at waste. A number of the statements by Dr. Herrmann are relevant to the work that is going on in waste and most certainly in the iodine content of the tanks. As we look at adsorbents we find that they all have potential application when there is a significant quantity of iodine that has to be removed from the waste. Other countries are proceeding with reprocessing and adsorbents can become important in their applications.

In this session we have heard five papers describing very interesting work from around the world. I found the studies concerning the continued release of iodine from the waste tanks at WAK very interesting and in particular the data that indicated the continued generation of iodine 131 from the tanks. While I am not aware of other reports of similar observations, I certainly recognize this as relevant to activities currently underway in the U.S. and warranting further investigation. Clearly this could have impact on the processing of the millions of gallons of waste currently stored within the DOE complex. The first paper of the session provided an update on the research into the behavior of iodine in the dissolver solution. This work continues to shed light on some of the reported variations in the observed iodine evolution from dissolver solutions. The second paper is also a continuation of previously reported work on the silver impregnated alumina iodine sorbents. This paper focused on the impact of NO_x, water vapor, and pre-exposure times. Other off-gas impurities were also investigated. The third paper reported on a fundamental study into the controlling mechanisms of methyl iodide adsorption on silver exchanged mordenite. Micropore diffusion was identified as the rate controlling process for the adsorption of methyl iodide in the long term. The fourth paper looks back over an extensive experience base on iodine removal efficiencies in actual operations. I want to thank the speakers for their effort and interesting research and evaluations.

SESSION 11

FILTERS

Wednesday July 17, 1996
Co-Chairmen: R. Dorman
J. Slawski
J. Dyment

A REVIEW OF DOE HEPA FILTER COMPONENT TEST ACTIVITIES: FY- 1994
J.W. Slawski, J.F. Bresson, and R.C. Scripsick

IN-PLACE HEPA FILTER EFFICIENCY TESTS
W. Bergman, K. Wilson, J. Elliot, and J.W. Slawski

METHOD FOR HEPA FILTER LEAK SCANNING WITH DIFFERENTIATING AEROSOL DETECTOR
B.J. Kovach , E.M. Banks, and W.O. Wikoff

UNCERTAINTY IN IN-PLACE FILTER TEST RESULTS
R.C. Scripsick, R.J. Beckman, and B.V. Mokler

VALIDATION TESTING OF RADIOACTIVE WASTE DRUM FILTER VENTS
L.D. Weber, R.S. Rahimi, and D. Edling

A GENERAL CORRELATION OF MPPS PENETRATION AS A FUNCTION OF FACE VELOCITY WITH THE MODEL 8140 USING THE CERTITEST 8160
N. Lifshutz, and M.E. Pierce

FURTHER DEVELOPMENT OF THE CLEANABLE STEEL HEPA FILTER AND COMPARISON WITH COMPETING TECHNOLOGIES

W. Bergman, K. Wilson, and G. Larsen

THE EFFECT OF MEDIA AREA ON THE DUST HOLDING CAPACITY OF DEEP PLEAT HEPA FILTERS

J. Dyment, and D. Loughborough

POTENTIAL FOR HEPA FILTER DAMAGE FROM WATER SPRAY SYSTEMS IN FILTER PLENUMS

W. Bergman, J.K. Fretthold, and J.W. Slawski

SIMULATION TEST OF AEROSOL GENERATION FROM VESSELS IN THE PRE-TREATMENT SYSTEM OF FUEL REPROCESSING

S. Fujine, K. Kitamura, and T. Kihara

EXTENDED-LIFE NUCLEAR AIR CLEANING FILTERS VIA DYNAMIC EXCLUSION PREFILTERS

S.W. Wright, H.S. Crouch, and J.H. Bond

A REVIEW OF DOE HEPA FILTER
COMPONENT TEST ACTIVITIES
FY 1992-FY 1995

James W. Slawski, CIH, CSP[1]
James F. Bresson[2]
Ronald C. Scripsick[3]

[1]**Defense Programs (DP-45)**
United States Department of Energy

[2]**Informatics Corporation, Inc.**
Albuquerque, New Mexico

[3]**Industrial Hygiene and Safety Group (ESH-5)**
Los Alamos National Laboratory

ABSTRACT

The Department of Energy (DOE) HEPA Filter Test Facilities have continued to operate in a changing political and operational environment. All HEPA filters purchased for installation in DOE nuclear facilities are required to be tested at a DOE Filter Test Facility (FTF) prior to installation, but the program is changing. Due to changes in its primary mission, the numbers of HEPA filters purchased by DOE each year since FY 1991 have been substantially reduced, to the point where one of the FTFs (Hanford) was closed in FY 1995 due to lack of filters to test. During the period FY 1992 - FY 1994, DOE funding was not provided to support the FTF Technical Support Group at the Los Alamos National Laboratory. As a consequence, Round Robin Tests (RRTs), performed twice each year by the FTFs in order to assess constituency of test results among the FTFs, were not performed in FY 1992 and FY 1993. The Annual Reports, summary reports of FTF test activities reports prepared and statistically analyzed by the TSG, were not prepared for fiscal years 1992 - 1995. Technical support provided to the FTFs was minimal. Currently, there is talk of closing a second FTF, and there are ongoing discussions as to whether the DOE will continue to fund operation of one or more of the FTFs.

In FY 1994, DOE Defense Programs commenced funding the TSG. The Round Robin Test Program is again administered by the TSG. RRT data for the years FY 1994 and FY 1995 have been retrieved and entered into the RRT data base; the FY 1994 RRT report has been issued; and the FY 1995 RRT report is in progress. Data from Semi-annual reports prepared by the FTFs have been retrieved, and entered into the FTF data base at LANL. Standards related to HEPA filter test and procurement activities(1-4), which had been written, peer reviewed, and recommended for implementation by DOE (but never "officially" issued) are now scheduled for issuance by the end of CY 1996. Continuation of these activities, however, depends on whether DOE will continue to support the HEPA filter test program.

The history and activities of the FTFs and the Technical Support Group (TSG) at Los Alamos have been reported at previous Air Cleaning Conferences(5-13). Data from the FY 1991 Annual Report of FTF activities was presented at the 22nd DOE/NRC Air Cleaning Conference in 1992(14). Preparation of the Annual Reports was temporarily suspended in 1992. However, all of the FTF Semi-annual report data have been retrieved and entered into the Los Alamos data base. This paper focuses primarily on the results of HEPA filter tests conducted by the DOE FTFs during the period FY 1992 - FY 1995, and the possible effects of the DOE program uncertainties on the quality of HEPA filters procured for installation at the DOE sites.

I. INTRODUCTION

Twice each year the DOE HEPA Filter Test Facilities (FTFs) must prepare a summary report of HEPA filter test activities. Each year, the Technical Support Group (TSG) at the Los Alamos National Laboratory is tasked with compiling the two Semi-annual Reports from the FTFs into an Annual Report. The objective of the annual report is to provide information on the performance and quality of High Efficiency Particulate Air (HEPA) filters being purchased and installed at DOE facilities. Current DOE policy requires that every HEPA filter be tested at one of the FTFs prior to acceptance and installation at a DOE user facility. With the exception of the summary data which appears in Section III, Table 1, below, this report focuses primarily on the period FY 1992 through FY 1995.

II. ORGANIZATION OF THE REPORT

The combined data from tests performed at the DOE FTFs for fiscal years FY 1983 - FY 1995 are presented in Section III A of this report. In Section III-B, summary data for the period FY 1992 - FY 1995 is presented, together with a general discussion of these data. In Sections IV-VII, in order to readily compare the test data with data in previous reports, and to analyze them accordingly, the test data is presented, analyzed and discussed by individual fiscal years. Results of a multi-year trend analysis are presented in Section VIII, and overall summary statements and conclusions regarding the HEPA filter test data appear in Section IX.

III. ANALYSIS OF THE FTF DATA

A. Summary of Overall DOE FTF HEPA Filter Test Activities

Annual reporting of DOE HEPA filter test data commenced in FY 1983. From the program's inception in FY 1983, through FY 1995, the DOE FTFs tested a total of 131,218 filters. The average number of filters tested per year during the period FY 1982-FY 1990 was 12,465. The total number of filters tested during the period FY 1992-FY 1995 was 23,948, an average of just under 6000 filters per year. A significant decrease in numbers of HEPA filters tested each year began in FY 1991, when the total number of filters tested was 7,551, which was a new annual low. The downward trend has continued, such that in FY 1995, only 3,758 filters were tested at the DOE FTFs. Table 1 presents the overall HEPA filter test history for the period FY 1983 - FY 1995.

In FY 1991 and FY 1992, the decrease in filter test activities was attributed primarily to cessation of weapons production activities at the Rocky Flats Plant, resulting in a significant decrease in numbers of HEPA filters procured for installation at Rocky Flats. However, the downward trend continued in the years FY 1993 - FY 1995, reflecting the general curtailment of nuclear activities at several DOE sites. The frequency of HEPA filter changes in facility air handling systems has, in some cases, been sharply reduced, perhaps compounded by the fact that HEPA filters in radioactively contaminated systems at several sites remained in place for extended periods. This latter practice has also caused a decrease in the numbers of HEPA filters procured by DOE sites and tested at the FTFs. In July, 1995, the DOE FTF located at Richland, Washington was closed, due to lack of filters to test. There have been recent discussions within DOE which could result in closing a second FTF, or both of them.

Possible actions which could reverse the downward trend in HEPA filter procurement and testing might include: 1) an increase in treatment operations for radioactive and mixed wastes at several DOE sites; 2) an increase in decontamination and deconstruction activities at DOE nuclear facilities; and 3) a commitment to comply with previously established frequencies for replacing filters in radioactively contaminated air handling systems.

Table 1
Annual Filter Test Results- FY 1983 - FY 1991

Period	N[1]	NIA/%[2]	NAW/%[3]	NR/%[4]
10/82-9/83	10,468[5]	9,811/94	291/2.8	366/3.5
10/83-9/84	12,223[6]	11,657/95	310/2.5	255/2.1
10/84-9/85	13,762[7]	12,141/88	1014/7.4	597/4.3
10/85-9/86	14,500[8]	13,263/91	847/5.8	392/2.7
10/86-9/87	13,656	13,161/96	235/1.7	260/1.9
10/87-9/88	11,822	10,847/92	745/6.3	230/1.9
10/88-9/89	12,538	12,042/96	139/1.1	347/2.8
10/89-9/90	10,750[9]	10,398/97	52/0.5	352/3.3
10/90-9/91	7,551	7,353/97	0/0.0	198/2.6
10/91-9/92	6,221	5,868/94	0/0.0	353/5.7
10/92-9/93	8,683	8,028/92	0/0.0	655/7.5
10/93-9/94	5,286	4,763/90	0/0.0	523/9.9
10/94-9/95	3,758	3,082/82	0/0.0	676/18
TOTALS	131,218	122,414/93	3,633/2.8	5,204/3.9

1. Number of Filters Tested
2. Number Initially Accepted/ %
3. Number Accepted with Waiver/ % (Category Deleted in FY 1991)
4. Number Rejected/ %
5. Does Not Include FY 1983 Data From Oak Ridge FTF
6. Does Not Include Oak Ridge FTF Data for the First Half of FY 1984
7. Disposition of One Filter was Not Given in FTF Reports
   Disposition of 10 Filters was not given in the FTF Reports
8. Per DOE Direction, Two Filters were Reported as Both NAW and NR. The Sum of NIA, NAW and NR Exceeds N by 2.
9. Per DOE Direction, Fifty-Two Filters Were Reported as both NAW and NR. The Sum of NIA, NAW and NR Exceeds N by 52.

B. Summary of DOE HEPA Filter Test Activities: FY 1992 - 1995

Summary HEPA filter test data for the period 1992-1995 appears in Table III-2.

TABLE 2
HEPA FILTER TEST RESULTS FY 1992 - FY 1995

FY	# Rec.	# Acc./%[1]	Rejections			
			Penetration/%[2]	Resistance/%[3]	Other/%[4]	Overall/%[5]
1992	6,221	5,868/94.3	280/4.5	0/0	73/1.2	353/5.7
1993	8,683	8,028/92.4	145/1.7	0/0	510/5.9	655/7.5
1994	5,286	4,763/90.1	103/1.9	2/0.04	418/7.9	523/9.9
1995	3,758	3,082/82.0	68/1.5	479/12.8	129/3.6	676/18.0
TOT.	23,948	21,741/90.8	596/2.5	481/2.0	1130/4.7	2,2079.2

1 Number of Filters Accepted/% Accepted
2 Number of Filters Rejected for High Penetration/ % Rejected
3 Number of Filters Rejected for High Resistance to Airflow/% Rejected
4 Number of Filters Rejected for "Other" reasons/% Rejected
5 Overall Number of Filters Rejected for All Reasons/% Rejected

Of the 23,948 filters tested during the period FY 1992 - FY 1995, 21,741 or 90.8% were initially accepted by the FTFs (NIA), 2,207 or 9.2 % were rejected (NR), and no filters were accepted with waiver or repair (NAW).

The overall rejection rate during the period FY 1992 - FY 1995 was 9.2%, ranging from a low of 5.7% in FY 1992 to a high of 18.0% in FY 1995. These results represent a marked increase over rejection rates for the three previous years, which ranged from 2.6 % to 3.3%, or for the overall period FY 1983 - FY 1991, in which the filters were rejected at a rate of 2.8%.

Review of the test data identified no single cause for the increasing rate of HEPA filter rejection. In FY 1992, high penetration constituted the highest component (4.5%) of the overall rejection rate (5.7%). In both FY 1993 and FY 1994, the highest failure rate was attributed to the general category called "Other" (5.9% and 7.9% respectively). The "Other" category includes but is not limited to: media damage, carrier damage, failure to comply with specifications in purchase orders, physical dimensions which are out of tolerance, and poorly installed or damaged gaskets. Specific details on why filters, or lots of filters, are rejected for "Other" reasons are recorded in the Semi-annual Reports submitted by the FTFs, but have not been specifically broken out in the LANL data base or in the Annual Reports. The specifics for "Other" rejection can be (and were) retrieved, if deemed necessary, from the Semi-annual reports.

In FY 1995, the highest cause for test failure was resistance to airflow (12.8%). More detailed discussion of these failure rates appears in Sections IV-VII of this report.

The category "Accepted with Waiver (NAW)" was abolished in FY 1991, following a revision to the DOE HEPA filter procurement standard(4). From FY 1987 through FY 1990, filters Size 4 and above, which had been initially rejected for high resistance to airflow, were allowed to be tested at decreasing airflow rates until the resistance to airflow across the filter was equal to the applicable limit of 1" w.g.. Therefore, under this provision, every HEPA filter ultimately "passed" the resistance test. The downrated filters were to be installed in air handling systems which would not expose the filters to flow rates in excess of the established downrated test airflows. This technique was not successful; some downrated filters were installed in systems which exposed them to airflows in excess of their downrated airflow values. At an FTF managers meeting in 1990, it was agreed to eliminate both downrating and the "Accepted with Waiver" test category. From that point forward, HEPA filters tested at the DOE FTFs either must either meet the applicable limit of 1" w.g., at rated airflow or be rejected. The DOE Procurement Standard(4) was revised to reflect this change in 1991. Commencing in FY 1992, the category "Accepted with Waiver" is no longer reported.

Strict adherence to the modified test standard for resistance to airflow did not immediately result in higher HEPA filter rejection rates. This was primarily because only one of the FTFs reported tests of HEPA filters Size 7 (1500 cfm) or Size 8 (2000) cfm) during the period FY 1992-FY 1994. Specifically, Rocky Flats reported testing one lot of 24 Size 7 filters in FY 1993, all of which were accepted. However, further review of the circumstances related to this test batch brought forth the information that the filters had been designated as "special" filters, not to be subject to the 1" w.g. test limit for resistance to airflow. None of the filters would have been accepted had the applicable standard for resistance to airflow been applied.

In FY 1995, the Oak Ridge FTF did test one lot of 506 Size 7 (1500 cfm) filters, and a total of 35 Size 8 filters. The Size 8 filters were designated as "special" filters, not subject to the applicable criterion of 1" w.g.. None of the Size 8 filters would have been accepted had the DOE criterion been applied. In fact, none of the Size 8 filters would have been accepted had the criterion of 1.3" w.g. which appears in a once-applicable Military Specification(14) , or its successor, (15) been applied, because the measured resistances in all of the tests were either 1.7" w.g., or 1.8" w.g.. The test history of the 506 Size 7 filters is discussed in more detail in Section VII-C of this report.

IV. FY 1992 HEPA FILTER TEST DATA

A. Summary of Test Results by FTF

FY 1992 test results, by individual FTF, appear in Table 3.

Table 3
FY 1992 HEPA Filter Test Results by FTF

FTF	N[1]	NIA[2]/%	NAW[3]/%	NR[4]/%
HANFORD	1,018	1,007/99	0/0.0	11/1.1
OAK RIDGE	3,217	3,056/95	0/0.0	161/5.0
ROCKY FLATS	1,986	1,805/91	0/0.0	181/9.1
TOTALS	6,221	5,868/94	0/0.0	353/5.7

1 Number of Filters Tested
2 Number Initially Accepted/% Accepted
3 Number Accepted With Waiver (Now 0)
4 Number Rejected for All Reasons/% Rejected

The overall rejection rate was 5.7%, which is more than twice the overall rejection rate of 2.8% for the period FY 1983-1991 (hereinafter the "Reference Rate"). Review of the results listed in Table 3 indicates a broad range of rejection rates, namely 1.1% at Hanford, 5.0% at Oak Ridge, and 9.1% at Rocky Flats. Review of additional test records indicates a rejection rate of 4.5% due solely to penetration, which by itself is about 1.5 times the "Reference Rate". This subject is further discussed Section IV-D of this report.

In FY 1992, the Oak Ridge FTF tested more filters (52% of the total tested) than the other two FTFs. This was only the second time since the filter test records data base program was initiated in FY 1883 that the Rocky Flats FTF was not the leader in total filters tested

B. Summary of Test Results by Manufacturer

Table 4 presents the overall FY 1992 HEPA filter test data by manufacturer. In FY 1992, Manufacturer # 7 supplied 4,995 of the 6221 (81%) HEPA filters tested by the FTFs; Manufacturer # 3 was second with 663 filters (10.6%); Manufacturer # 4 was third with 240 (3.8%); and Manufacturer # 19 was fourth with 137 (2.2%). The overall rejection rate for Manufacturer # 7 was 2.7%, compared to the overall FY 1992 rejection rate of 5.7%, however high rejection rates for filters supplied by Manufacturer # 3 (13%), Manufacturer # 4 (7.1%) and Manufacturer # 19 3M (75%) served to raise the overall rejection rate to 5.7%.

Table 4
FY 1992 HEPA Filter Test Results by Manufacturer

Manufacturer	N[1]	NIA[2]/%	NAW[3]/%	NR[4]/%
7	4,995	4,860/97	0/0.0	135/2.7
3	663	574/87	0/0.0	89/13
4	240	223/93	0/0.0	17/7.1
19	137	34/25	0/0.0	103/75
29	78	76/97	0/0.0	2/2.6
32	46	43/93	0/0.0	3/6.5
17	24	24/100	0/0.0	0/0.0
21	18	17/94	0/0.0	1/5.6
13	9	9/100	0/0.0	0/0.0
9	4	4/100	0/0.0	0/0.0
16	4	4/100	0/0.0	0/0.0
14	3	0/0.0	0/0.0	3/100
TOTAL	6,221	5,868/94	0/0.0	353/5.7

[1] Number of Filters Tested
[2] Number Initially Accepted/% Accepted
[3] Number Accepted With Waiver (Now 0)
[4] Number Rejected for all Reasons

C. Summary Discussion - FY 1992

The FY 1992 Semi-annual Report data was analyzed to identify statistically significant differences in HEPA filter test data among the FTFs, or among manufacturers. Statistical analysis was performed by use of an Analysis of Variance technique (ANOVA). When statistical differences are identified, the Semi-annual report data and/or individual test records are further reviewed to determine their cause and practical significance. Statistical analysis of FY 1992 test data identified several significant differences among manufacturers, but not among the FTFs. Chief among them were:

- An extremely low (64.3%) acceptance rate at the Oak Ridge FTF for Size 1 (25 cfm) filters supplied by Manufacturer # 3.
- An extremely low (17.6%) acceptance rate at the Rocky Flats FTF for Size 3 (125 cfm) filters supplied by Manufacturer # 19.
- Acceptance of only six of eleven Size 4 (500 cfm) filters supplied by Manufacturer # 4 at the Oak Ridge FTF.

The statistical analysis described above helped to focus further review on specific filter test data. This review confirmed a higher than usual rejection rate due to high penetration. Review of past test records indicates that although the rejection rates due to high penetration for the period FY 1983 - FY 1991 were typically less than 2.0%, the rejection rate due to high penetration in FY 1992 was 4.5%.

Review of the FY 1992 Semi-annual report data indicates that the high overall rejection rate was due chiefly to filters from four specific shipment lots. All the filters in these lots were rejected for high penetration. Three of the lots were tested by the Rocky Flats FTF; the fourth was tested by Oak Ridge.

Two of the lots tested at Rocky Flats were composed of Size 3 HEPA filters supplied by Manufacturer # 19. In one lot, 61 of 71 filters (85.9%) were rejected for high penetration; in the second lot, 42 of 54 filters

(77.8%) were also rejected for high penetration. This represents an average rejection rate of about 82% for the two lots. In the third lot tested by Rocky Flats, 45 of 242 Size 5 filters (19%) supplied by Manufacturer #7 were rejected for high penetration. In the fourth lot tested by Oak Ridge, 73 of 140 Size 1 HEPA filters (52.1%) supplied by Manufacturer # 3 were rejected for high penetration. The four lots in question accounted for 221 of the 280 (78.9%) filters rejected for penetration in FY 1992.

It is noteworthy that none of the 6,221 HEPA filters tested in FY 1992 failed the test for resistance to airflow. The rejection rate for "Other" causes in FY 1992 was 1.2%.

V. FY 1993 HEPA FILTER TEST DATA

A. Summary of Test Results by FTF

FY 1993 test results, by individual FTF, appear in Table 5.

Table 5
FY 1993 Test Results by FTF

FTF	N	NIA/%	NAW/%	NR/%
HANFORD	903	882/98	0/0.0	21/2.3
OAK RIDGE	3,564	3,330/93	0/0.0	234/6.6
ROCKY FLATS	4,216	3,816/91	0/0.0	400/9.5
TOTALS	8,683	8,028/92	0/0.0	655/7.5

The overall rejection rate for all causes was 7.5%, or about 2.6 times the "Reference Rate". The predominant reason for rejection in the FY 1993 tests was attributed to the "Other" category for which the rejection rate was 5.9%.

B. Summary of Test Results by Manufacturer

Table 6 presents the overall FY 1993 HEPA filter test results by manufacturer.

Manufacturer # 7 supplied 6,980 of the 8,683 HEPA filters (80.4%) tested at the FTFs in FY 1993. Of these, 570 (8.2%) were rejected, nearly three times the "Reference Rate". Manufacturer # 3 supplied 619 (7.1%) of the tested filters. Of these 12 (1.9 %) were rejected. Manufacturer # 32 provided 434 filters (5%), of which 51 (12%) were rejected. Manufacturer # 5 supplied 250 filters (2.9%), of which nine (3.6%) were rejected, and Manufacturer # 4 supplied 158 filters (1.8%) of which four (2.5%) were rejected. The remaining 242 filters (2.8%) were supplied by twelve different vendors, and nine of these (3.7%) were rejected.

Table 6
FY 1993 HEPA Filter Test Results by Manufacturer

Manufacturer	N	NIA/%	NAW/%	NR/%
7	6,980	6,410/92	0/0.0	570/8.2
3	619	607/98	0/0.0	12/1.9
32	434	383/88	0/0.0	51/12
5	250	241/96	0/0.0	9/3.6
4	158	154/97	0/0.0	4/2.5
11	72	72/100	0/0.0	0/0.0
19	60	60/100	0/0.0	0/0.0
10	29	26/90	0/0.0	3/10
23	20	18/90	0/0.0	2/10
21	18	17/94	0/0.0	1/5.6
29	11	11/100	0/0.0	0/0.0
14	9	6/67	0/0.0	3/33
16	8	8/100	0/0.0	0/0.0
33	6	6/100	0/0.0	0/0.0
17	6	6/100	0/0.0	0/0.0
9	2	2/100	0/0.0	0/0.0
25	1	1/100	0/0.0	0/0.0
TOTAL	8,683	8,028/92	0/0.0	655/7.5

C. Summary Discussion - FY 1993

The FY 1993 Semi-annual Report data was analyzed to identify statistical differences among the FTFs or the manufacturers. There were no statistically significant differences among the FTFs, however, there was a statistical difference identified among the manufacturers for Size 5 (1000 cfm) filters. It was determined that the acceptance rates for filters supplied by Manufacturer # 7 were lower than usual especially at Rocky Flats and Oak Ridge.

Further review of the FY 1993 test data indicates that the high rejection rates for the Size 5 filters occurred in the "Other" category, and were primarily related to two shipment lots. The first lot was tested at Rocky Flats. Of a shipment lot of 1,358 filters, 304 (22.4%) were rejected because of media damage. The second lot was tested by the Oak Ridge FTF. Of 930 tested filters, 80 were rejected because of missing extraction clips, 25 for defective fluid seal gaskets, and 1 for frame damage, a total of 106 rejects (11.4%). The overall rejection rate for the year FY 1993 was 7.5%, about 2.7 times the "Reference Rate", of which 5.9% was due to "Other" causes, and 1.7% was due to high penetration. No filters tested in FY 1993 were rejected for high resistance to airflow.

VI. FY 1994 HEPA FILTER TEST DATA

A. Summary of Test Results by FTF

FY 1994 HEPA filter test results by FTF appear in Table 7. The overall rejection rate for filters tested in FY 1994 was just under 10%. This rate is more than three times the "Reference Rate". The highest rejection rate component (8%) was the "Other" category.

Table 7
FY 1994 HEPA Filter Test Results by FTF

FTF	N	NIA/%	NAW/%	NR/%
HANFORD	708	681/96	0/0.0	27/3.8
OAK RIDGE	1,371	1,175/86	0/0.0	196/14
ROCKY FLATS	3,207	2,907/91	0/0.0	300/9.4
TOTALS	5,286	4,763/90	0/0.0	523/9.9

B. Summary of Test Results by Manufacturer

Table 8 presents the overall FY 1994 filter test results by manufacturer.

Table 8
FY 1994 HEPA Filter Test Results by Manufacturer

Manufacturer	N	NIA/%	NAW/%	NR/%
7	3,752	3,616/96	0/0.0	136/3.6
3	937	718/77	0/0.0	219/23
32	313	229/73	0/0.0	84/27
19	111	52/47	0/0.0	59/53
4	54	52/96	0/0.0	2/3.7
29	41	41/100	0/0.0	0/0.0
5	20	0/0.0	0/0.0	20/100
10	20	19/95	0/0.0	1/5.0
23	13	12/92	0/0.0	1/7.7
16	11	11/100	0/0.0	0/0.0
13	9	9/100	0/0.0	0/0.0
21	4	4/100	0/0.0	0/0.0
6	1	0/0.0	0/0.0	1/100
TOTAL	5,286	4,763/90	0/0.0	523/9.9

Of the 5,286 filters tested, Manufacturer # 7 supplied 3,752 (71%); Manufacturer # 3 supplied 937 (17.7%); Manufacturer # 32 supplied 313 (5.9%); Manufacturer # 19 supplied 54 (0.1%); and various other manufacturers supplied 119 filters (2.3%). Of the 3,752 filters supplied by Manufacturer # 7, 136 (3.6%) were rejected. Of the 937 filters supplied by Manufacturer # 3, 219 (23.4%) were rejected. Of the 313 filters supplied by Manufacturer # 32, 84 (26.8%) were rejected. Of the 111 filters supplied by Manufacturer # 19, 59 (53.2%) were rejected. Of the 54 filters supplied by Manufacturer # 4, two (3.4%) were rejected, and of the 119 filters supplied by various other manufacturers, 23 (19.3%) were rejected. Of these, an entire shipment of 20 filters supplied by Manufacturer # 5, was rejected.

C. Summary of Test Results - FY 1994

The FY 1994 test data was analyzed to determine whether there were statistical differences among the FTFs or among the manufacturers. There were strong differences among the FTFs for Size 5 (1000 cfm) filters, and among manufacturers for Size 3 (125 cfm) filters.

The high rejection rates for both Size 3 and Size 5 filters were due primarily to the "Other" category and were related to two specific shipments. At Rocky Flats, an entire shipment of 200 Size 3 filters supplied by Manufacturer # 3 was rejected. There was no further explanation available from the Rocky Flats FTF regarding the specific problem or problems which led to rejection of the entire batch of filters. At Oak Ridge, 100 filters of a shipment of 126 Size 5 filters (79.4%) supplied by Manufacturer # 7 were rejected because the gaskets had not been installed according to purchase specifications.

The rejection of all thirty-five filters in a lot of Size 6 filters for "Other" reasons is also noteworthy. The filters were supplied by Manufacturer # 33, and tested at Oak Ridge. Further review of the test records indicates that 34 of the filters had splintered frames and/or improperly seated gaskets. The remaining filter was rejected because it was not a "Nuclear Grade" filter. The cause of the splintered frames was not documented, and it is not known whether the filters were damaged during shipping and handling, or simply not properly inspected prior to shipment.

The overall rejection rate for HEPA filters tested in FY 1994 was 9.9%, more than three times the "Reference Rate". The overall rejection rate includes: 1.9% for high penetration, 2.0% for high resistance to airflow, and 7.9% for "Other" reasons. This was the first of the four years in which filters were rejected for high resistance to airflow.

VII. FY 1995 HEPA FILTER TEST DATA

A. Summary of Test Results by FTF

Table 9 presents the overall FY 1995 HEPA filter test data by FTF. 3,758 filters were tested, the lowest test total since LANL initiated the HEPA filter test data base in FY 1983. Of these, 2,471 (65.8%) were tested by Oak Ridge, 1,197 (31.9%) were tested by Rocky Flats, and 90 (2.4%) were tested by Hanford. Of the 2,471 filters tested by Oak Ridge, 62 (12.5%) were rejected; of the 1,197 filters tested by Rocky Flats, 46 (3.8%) were rejected; and of the 90 filters tested by Hanford, nine (10%) were rejected. FY 1995 was the first of the years covered in this report in which a significant number of filters was rejected for high resistance to airflow.

Table 9
FY 1995 HEPA Filter Test Results by FTF

FTF	N	NIA/%	NAW/%	NR/%
HANFORD	90	81/90	0/0.0	9/10
OAK RIDGE	2,471	1,850/75	0/0.0	621/25
ROCKY FLATS	1,197	1,151/96	0/0.0	46/3.8
TOTALS	3,758	3,082/82	0/0.0	676/18

B. Summary of Test Results by Manufacturer

FY 1995 HEPA filter test data by Manufacturer appears in Table 10.

Of the 3,758 filters tested by the FTFs, 2,794 (74.3%) were supplied by Manufacturer # 7; 751 (20%) were supplied by Manufacturer # 3; 56 (14.9%) were supplied by Manufacturer # 33; and 52 (13.8%) were supplied by Manufacturer # 32. Other manufacturers supplied smaller quantities of filters in FY 1995 as follows: Manufacturer # 19supplied 26 filters (0.7%); Manufacturer # 23 supplied 22 filters (0.6%); Manufacturer # 12 supplied 14 filters (0.4%); Manufacturer # 29 supplied 12; Manufacturer # 21 supplied 12; Manufacturer # 25 supplied 8; Manufacturer # 1 supplied 7; Manufacturer # 14 supplied 2; Manufacturer # 4 supplied one; and Manufacturer # 9 supplied one. Of the 3,758 filters tested in FY 1995, 676 (18%) were rejected for all reasons.

Table 10
FY 1995 HEPA Filter Test Results by Manufacturer

Manufacturer	N	NIA/%	NAW/%	NR/%
7	2,794	2,233/80	0/0.0	561/20
3	751	712/95	0/0.0	39/5.2
33	56	39/70	0/0.0	17/30
32	52	37/71	0/0.0	15/29
19	26	12/46	0/0.0	14/54
23	22	10/45	0/0.0	12/55
12	14	14/100	0/0.0	0/0.0
29	12	12/100	0/0.0	0/0.0
21	12	12/100	0/0.0	0/0.0
25	8	0/0.0	0/0.0	8/100
1	7	0/0.0	0/0.0	7/100
14	2	0/0.0	0/0.0	2/100
4	1	1/100	0/0.0	0/0.0
9	1	0/0.0	0/0.0	1/100
TOTALS	3,758	3,082/82	0/0.0	676/18

Of the 2,794 filters supplied by Manufacturer # 7, 561 (20%) were rejected. Of the 751 filters supplied by Manufacturer # 3, 39 (5.2%) were rejected. Of the 56 filters supplied by Manufacturer # 33, 17 (30.4%) were rejected. Of the 52 filters supplied by Manufacturer # 32, 15 (28.8%) were rejected. Of the 26 filters supplied by Manufacturer # 19, 14 (54%) were rejected. Of the 22 filters supplied by Manufacturer # 23, 12 (54.5%) were rejected. All of the eight filters supplied by Manufacturer # 25, the seven filters supplied by Manufacturer # 1, the two filters supplied by Manufacturer # 14, and the single filter supplied by Manufacturer # 9 (a total of 18 filters) were rejected.

C. Summary Discussion - FY 1995

The overall rejection rate for FY 1995 was 18%, more than six times the "Reference Rate", and by far the highest rejection rate encountered in the test program. The FY 1995 Semi-annual report data was analyzed to determine whether there were statistical differences among the FTFs or the manufacturers. Statistically significant differences were identified among the FTFs and the manufacturers for Size 5 (1000 cfm) filters. For Size 7 (1500 cfm) filters, 518 of the 524 Size 7 filters tested in FY 1995 were rejected. The remaining six filters were accepted, but only because they were designated as "special case" filters. All six of these filters also exceeded the criterion for resistance to airflow.

Further review of the actual test data for Size 7 filters confirmed that high resistance to airflow was the largest contributor to the overall FY 1995 rejection rate of 18%; this category accounted for just under 13% of the rejected filters. The rejection rate due to high penetration was 1.8% (about average), and the rejection rate due to "Other" causes was 3.4%, which was higher than noted in previous years. Of a single lot of 506 Size 7 HEPA filters supplied by Manufacturer # 7, 476 were rejected for excessive resistance to airflow. In the same lot, seven additional filters (1.4%) were rejected for high penetration, 18 filters (3.6%) were rejected for defective fluid seals, four filters were rejected for shipping damage and one was "out of square". Thus, the entire lot of 506 filters was rejected.

This manufacturer's lot raises a serious question concerning purchase of HEPA filters at DOE sites in general, and at the Savannah River Site in particular. The purchase order for these filters specified a nominal airflow rating of 1500 cfm, but a limit for resistance to airflow of 1.3" w.g.. Procurement organizations at WSRC apparently do not recognize the applicable limit for resistance to airflow (1" w.g. for filters Size 4 and above) which appears in the DOE HEPA filter procurement standard(4). Instead, WSRC chose to specify the limit of 1.3" w.g. which appears in the former Military Specification, MIL 51068F(14) and the current specification (ASME AG-1 Code, Section FC)(15).

The limit for resistance to airflow which appears in the DOE Standard was carefully considered and approved by consensus. Filter manufacturers were included in the Technical Review Committee which recommended that DOE adopt the standard. The DOE FTFs are directed to apply the DOE limit for resistance to airflow as a basis for HEPA filter acceptance/rejection. The operating contractor, when notified that the filters had been rejected, directed the testing FTF to place rejection labels on the shipping containers, but not on the individual filters (contrary to established policy), and to ship the 476 filters which had been rejected for high resistance to airflow to the contractor site. The request was complied with, under protest from the Oak Ridge FTF, the FTF Coordinator at Los Alamos, and the HEPA Filter Performance Assurance Program Manager at DP-45.

It should be noted that the filters in question are intended for use in the Defense Waste Processing Facility (DWPF), which is designed to process highly radioactive High Level Waste. It is suspected that the rejected filters have or will find their way into the safety class exhaust system(s) of the DWPF.

The statistically significant differences for the Size 5 (1000 cfm) filters, which were identified by the statistical analysis of the FY 1995 test data, did not appear to be traceable to one specific cause. A review of the test data produced the following information:

- Of 206 Size 5 filters supplied by Manufacturer # 3, 171 (83%) were rejected by Oak Ridge because of "Other" reasons. The gaskets did not meet specifications.
- Of 73 Size 5 filters supplied by Manufacturer # 7, six (8.2%) were rejected by Oak Ridge for "Other" reasons, in this case because of general deterioration due to long term storage, a situation not necessarily related to the manufacturing process.
- Of 24 Size 5 filters supplied by Manufacturer # 33, 12 were rejected by Oak Ridge because of "Other" reasons, related to splintering and rough edges of the plywood filter frames.
- The totals for these three batches are: 303 filters received with 189 (62.4%) rejected for "Other" reasons.

VIII. MULTI-YEAR TREND ANALYSIS

A statistical trend analysis of the consolidated Annual Report data for the five year period FY 1991-1995 (a slightly different time frame than that of this report) was performed. Data from these years were combined and then analyzed to identify statistically significant differences between FTFs and manufacturers for each filter size (Sizes 1-8. Following is a summary of the major conclusions from the Trends Analysis:

- There is a strong statistically significant difference among manufacturers for Size 1 (25 cfm) filters. This is caused primarily by the low acceptance rates for filters supplied by Manufacturer #3 (64%) and Manufacturer #4 (51%) by the Oak Ridge FTF. All three FTFs accepted Size 1 HEPA filters supplied by Manufacturer #1 at about the same rate (95-97%).
- There are statistically significant differences between among manufacturers and among FTFs for Size 3 (125 cfm) filters, caused primarily by the low acceptance rates for filters supplied by Manufacturer # 3 (59%) and # 19 (25%) at the Rocky Flats FTF. All three FTFs accepted Size 3 filters supplied by Manufacturer # 7 at about the same rate (98-99%).
- There is a statistically significant difference in acceptance rates for Size 5 (1000 cfm) filters, for the manufacturers and for the FTFs. The Oak Ridge FTF accepted a lesser percentage of filters supplied by Manufacturer #3 (92%) than the other two FTFs. The Oak Ridge FTF also tested far more filters from Manufacturer # 3 (1995) than the other two FTFs combined (253). Oak Ridge accepted a lower percentage of

filters from Manufacturer # 4 (85%) than did Rocky Flats (96%), however, in this instance, Oak Ridge tested only 26 filters from this manufacturer compared to 159 tested by Rocky Flats.

- The acceptance rate for Size 5 filters supplied by Manufacturer # 7 was fairly consistent among the FTFs, with Hanford accepting 99%, and Oak Ridge and Rocky Flats each accepting 95%. However, the 5% rejection rate for filters from Manufacturer # 7 at Oak Ridge and at Rocky Flats is significantly above the overall failure rate for HEPA filters (2.8%) noted during the period FY 1983 - FY 1991.

In order to further examine the history and trends of HEPA filters supplied to DOE in the recent past, Tables 11 - 13 were prepared to present the overall acceptance/rejection history for the three major suppliers of HEPA filters for the period FY 1992 - FY 1995. These three manufacturers supplied 94.9% of the filters tested in FY 1992, 91.5% of the filters tested in FY 1993, 92.3% of the filters tested in FY 1994, and 97% of the filters tested in FY 1995. Manufacturer # 7, with overall filter supply percentages ranging from 71% to 80.4%, is by far the major supplier. Manufacturer #3 supplied from 7.7% to 20% of the filters tested during the period covered by this report, and the third manufacturer, a combination of Manufacturers # 4 and # 33 (one bought the other during the report period), supplied from 2.7% to 3.9%.

Table 11
Overall FY 1992 - FY 1995 Acceptance/Rejection Rates for Manufacturer # 7

Fiscal Year	# Received	Number Accepted/%	Number Rejected/%
1992	4,995	4,860/97.3	135/2.7
1993	6,980	6,410/91.8	570/8.2
1994	3,752	3,616/96.4	136/3.6
1995	2,794	2,233/79.9	561/20.1
TOTALS	18,521	17,119/92.4	1402/7.6

Manufacturer # 7 is by far the largest supplier of HEPA filters to the DOE complex, and, in general, has had the best overall acceptance rate of the major filter suppliers. The 2.7% rejection rate for FY 1992 is similar to the "Reference Rate", and the rejection rate of 3.6% in FY 1994 is marginally (0.8%) higher. However the rejection rates for FY 1993 (8.2%) and FY 1995 (20.1%) further support the conclusion that the quality of HEPA filters supplied to DOE has diminished. In fairness to the manufacturer, it can be argued that the two lots of size 7 filters, in which 518 of 524 filters were rejected due to a disagreement over the applicable criterion for resistance to airflow, should be removed from the FY 1995 statistics, because rejection of these filters is not directly related to the manufacturing process. If this is done, then only 43 of the remaining 2270 filters (1.9%) were rejected. On the other hand, the manufacturers are well aware of the DOE specification for resistance to airflow, and know that the filters they provide do not meet the DOE specifications. It would appear that this issue should be resolved by further review of all the applicable filter performance specifications, leading to technical consensus, such that there is no longer a conflict among the applicable standards.

The decreasing numbers of Manufacturer # 7 filters tested at the DOE FTFs each year during the period covered by this report reflects the diminishing DOE market for HEPA filters.

Table 12
Overall FY 1992 - FY 1995 Acceptance/Rejection Rates for Manufacturer # 3

Fiscal Year	# Received	Number Accepted/%	Number Rejected/%
1992	663	574/86.6	89/13.4
1993	619	607/98.1	12/1.9
1994	937	718/76.6	219/23.4
1995	751	712/94.8	39/5.2
TOTALS	2,970	2,611/87.9	359/12.1

Manufacturer # 3 was the second largest supplier of HEPA filters to the DOE complex during the period FY 1992 - FY 1995. The acceptance rates for Manufacturer # 3 filters have been highly variable, and the overall rejection rate of 12.1% is more than four times the "Reference Rate". Of the 89 filters rejected in FY 1992, 84 were tested and rejected by Oak Ridge. Of the 84 filters rejected at Oak Ridge, 78 were rejected for high penetration. Seventy-three of these were from one lot of 140 25 cfm filters, which was discussed in the summary report section for the year FY 1992. Two hundred of the 219 Manufacturer # 3 filters which were rejected in FY 1994 constituted an entire batch which was rejected at Oak Ridge for "Other" reasons. This situation was earlier discussed in the summary report section for FY 1994. The test data for Manufacturer # 3 filters further support the conclusions that the quality of filters supplied to DOE during FY 1992 - FY 1995 has lessened, and that filter failures tend to occur in batches.

Table 13
Overall FY 1992 - FY 1995 Acceptance/Rejection Rates for Manufacturer # 4-33

Fiscal Year	# Received	Number Accepted/%	Number Rejected/%
1992	240	223/92.9	17/7.1
1993	298	251/84.2	47/15.8
1994	186	114/61.3	72/38.7
1995	103	71/68.9	32/31.1
TOTALS	827	659/79.7	168/20.3

Manufacturer # 4 became Manufacturer # 33 in 1993. This manufacturer combination accounts for the third highest total of filters supplied to DOE in the period FY 1992 - FY 1995. Individual records from the Semi-annual Reports were reviewed, and the combined totals were compiled and appear in Table 14. The combined test history for Manufacturer # 4-33 during the reporting period of FY 1992 - FY 1995 constitutes the highest rejection rate of the major suppliers. Review of the individual test reports again indicates batch, not random type failures, and further demonstrates the general lessening of HEPA filter quality.

IX. SUMMARY AND CONCLUSIONS

This combined Annual Report presents summary results of HEPA filter tests performed by the DOE Filter Test Facilities for the four year period FY 1992 - FY 1995. Test results for each year are discussed separately in specific sections (IV-VII) of the report, including a trend analysis. The test results for each fiscal year were analyzed in order to identify statistical differences, either among the FTFs by manufacturer and filter size, or by manufacturer. In Section VIII, a more general multi-year trend analysis for the four year period is presented.

The FTF program was instituted in the late 1960s and early 1970s when it became apparent that the HEPA filters supplied to the Department of Energy for installation in its nuclear facilities were not always of the high quality required to adequately protect workers, the environment, and the general public from the hazards associated with release of radioactive materials. The FTFs have been instrumental in identifying HEPA filters which do not meet required performance standards and preventing their installation in critical safety systems.

IX. SUMMARY AND CONCLUSIONS

This combined Annual Report presents summary results of HEPA filter tests performed by the DOE Filter Test Facilities for the four year period FY 1992 - FY 1995. Test results for each year are discussed separately in specific sections (IV-VII) of the report, including a trend analysis. The test results for each fiscal year were analyzed in order to identify statistical differences, either among the FTFs by manufacturer and filter size, or by manufacturer. In Section VIII, a more general multi-year trend analysis for the four year period is presented.

The FTF program was instituted in the late 1960s and early 1970s when it became apparent that the HEPA filters supplied to the Department of Energy for installation in its nuclear facilities were not always of the high quality required to adequately protect workers, the environment, and the general public from the hazards associated with release of radioactive materials. The FTFs have been instrumental in identifying HEPA filters which do not meet required performance standards and preventing their installation in critical safety systems.

The changing nature of the Department of Energy's overall mission is apparent when the number of HEPA filters procured and tested is reviewed and compared to previous years. Review of the test records indicates a significant decline in the numbers of filters tested during the period addressed in this report. Prior to FY 1991, the numbers of HEPA filters tested each year were on the order of 10,000-14,000 filters. These numbers have declined steadily over the past four years, such that in FY 1995, only about 3,800 filters were tested. In FY 1995, one of the FTFs was closed, due to lack of filters to test. In FY 1996, there have been ongoing discussions concerning the future of the FTFs and the HEPA filter test program, and there have been recommendations to close one or both of the remaining FTFs.

The recent FTF test data verifies that the quality of the HEPA filters supplied to the DOE has diminished substantially. Review of the test data indicates that annual average rejection rates due to all causes, during the period FY 1992 - FY 1995 have increased from two to more than six fold. over the rejection rates observed during the period FY 1983 - FY 1991. Had there been no FTFs, the numbers of substandard filters installed in DOE's nuclear facilities could have increased significantly, leading to an increase in the probability that higher concentrations of radioactive materials could have been released to work stations, the on-site worker populations, or to the public and general environment.

References

1. DOE F 3-42, "Operating Policy of DOE Filter Test Programs" (1991).
2. DOE F 3-43, "Quality Assurance Testing of HEPA Filters" (1991).
3. DOE F 3-44, "DOE Filter Test Facilities Quality Program Plan" (1991).
4. DOE F 3-45, "Specifications for HEPA Filters Used by DOE Contractors" (1991).
5. Gilbert H., "The Filter Test Program, An Installation Manual, and Filter Research," published in the Proceedings of the 6th AEC Air Cleaning Conference, (July 7-9, 1959) United States Atomic Energy Commission Division of Technical Information, ed. TID 7593, October 1960, pp 161-181.

6. Gilbert, H., and Hurwitz, G. J., "Filter Rating and Testing Program," published in the Proceedings of the 7th AEC Air Cleaning Conference, Brookhaven National Laboratory (October 10-12, 1961), United States Atomic Energy Commission Division of Technical Information, ed. TID-7627, pp 74-81.

7. Collins, J. T., Bellamy R. R., and Allen, J. R., "Evaluation of Data From HEPA Filter Quality Assurance Testing Stations," published in the Proceedings of the 15th DOE Nuclear Air Cleaning Conference, Boston, Massachusetts (August 7-10, 1978), M. W. First, ed., February, 1979, pp. 1159-1176.

8. Bresson, J. F., "DOE Filter Test Program-Policy for the '80s," published in the Proceedings of the 17th DOE Nuclear Air Cleaning Conference, Denver, Colorado (August 2-5, 1982), M. W. First, ed., February, 1983, pp 788-789.

9. Burchsted, C. A., "A Review of DOE Filter Test Facility Operations 1970-1980," published in the Proceedings of the 17th DOE Nuclear Air Cleaning Conference, Denver, Colorado, (August 2-5, 1982), M. W. First, ed., February 1983, pp. 775-787.

10. Bresson, J. F., "Department of Energy Filter Test Program Policy for the '80s," published in the proceedings of the 18th Nuclear Airborne Waste Management and Air Cleaning Conference, Baltimore, Maryland, (August 12-16, 1984) M. W. First, ed., March, 1985, pp. 1144-1148.

11. Bresson, J. F., "HEPA Filter Activities at the Department of Energy," published in the Proceedings of the 19th DOE/NRC Nuclear Air Cleaning Conference, Seattle, Washington, (August 18-21, 1986), M. W. First, ed., May 1987, pp. 852-862.

12. McIntyre, J. A., "Review of Department of Energy Filter Test Facility and Filter Test Facility Technical Support Group Activities FY 1986-1989," published in the Proceedings of the 21st DOE/NRC Nuclear Air Cleaning Conference, San Diego, California, (August 13-16, 1990), M. W. First, ed., February, 1991, pp. 385-393.

13. McIntyre, J. A., "Review of Department of Energy HEPA Filter Test Activities FY 1990-FY 1992," published in the Proceedings of the 22nd DOE/NRC Nuclear Air Cleaning and Treatment Conference, Denver, Colorado, August 24-27, 1992, M. W. First, ed., March, 1993, pp 177-187.

14. MIL F 51068F "Military Specification, Filters, Particulate (High Efficiency, Fire Retardant)" April 1988.

15. American Society of Mechanical Engineers (ASME) AG-1 Code, Section FC, "HEPA Filters" December, 1995 [draft]).

DISCUSSION

FRANKLIN: We sold a lot more filters to DOE facilities than were evidently tested. Is this a trend?

BRESSON: I think it has to do with whether they are procuring specification HEPA filters and the intended use. I hope that it is not a trend, but I suspect that procurement people at DOE sites are finding ways to get around testing of filters, and having to deal with rejected filters, the latter to avoid delays caused by replacing defective filters. There does not appear to be consistency any more among the DOE sites with respect to procurement activities. In addition, HEPA filters are often purchased for installation in non-nuclear facilities, and these filters do not have to be tested at a DOE FTF.

FRANKLIN: Some of our filters may have been rejected for not meeting specifications, but they met the user's purchase order . In those cases, we didn't even know they were rejected.

BRESSON: The records that I have reviewed indicate that when the filter test facilities perform their tests, they test all the filters the same way, regardless of whether they are specification filters or how they were procured. Consequently, the filter test data remain consistent.

FIRST: I listened to all your problems and now I am going to ask you the question that always gets asked at DOE, "What are the lessons learned here?"

BRESSON: I think the lesson that should have been learned is that air cleanup in nuclear facilities is a very important part of environmental and health protection activities at the sites. There is a move afoot, and I do not know how it is going to come out, within the Department of Energy, to do away with the DOE HEPA filter test facilities, and to rely instead on QA tests, QA inspections, manufacturers' data and in-place testing. To my mind, this would be a much different, less effective, and probably more expensive program than the current component assurance test program in which every filter is tested at the FTFs, and at a reasonable cost. I can not think of a better, more reliable QA program than the current test program, rather than one which relies on tests performed at the beginning of a QPL qualification cycle, followed by vendor inspections. One of the messages in my presentation is that, in recent years, the FTFs have rejected a higher percentage of HEPA filters, for all reasons. Given this fact, it makes little sense to me to back off on the quality test program.

SLAWSKI: I can add something to the discussion. We have a working group at DOE looking at this question explicitly. It looks like we will continue to test every filter. Where we will do it, we do not know at this time. We are considering other things. There are some people that are very emphatic that the QA/QC program should be placed exclusively on the manufacturers. We have considered that. I think we know how we are going to proceed on it but the decision has yet to be made.

GILLES: Over the past 4 years, what percentage of all the filters rejected were rejected due to flaws found visually?

BRESSON: Failures due to visual inspection are a part of the category called "Other" in the summary test data for the years FY 1992 - FY 1995. Failure reasons which are lumped together into the "Other" category include, but are not limited to, carrier damage, media damage, failure to comply with purchase specifications, dimensional problems, and improperly installed gaskets. With the exception of procurement specifications, some or all of these failure modes are detected by visual inspection. Note that

Table 2 of my presentation shows that, for the years FY 1992 - FY 1995, filter failure rates due to "Other" category causes have ranged from about 1% to 8% per year, the average being nearly 5%. A cursory review of individual test records, which provide additional information on the causes for failures recorded in the "Other" category, leads me to conclude that the visual inspection process detects a high percentage of these failures, perhaps as high as 75-80% of them.

IN-PLACE HEPA FILTER PENETRATION TEST*

by

W. Bergman, K. Wilson, J. Elliott, B. Bettencourt and J. W. Slawski[1]
Lawrence Livermore National Laboratory
Livermore, CA 94550

Abstract

We have demonstrated the feasibility of conducting penetration tests on high efficiency particulate air (HEPA) filters as installed in nuclear ventilation systems. The in-place penetration test, which is designed to yield equivalent penetration measurements as the standard DOP efficiency test, is based on measuring the aerosol penetration of the filter installation as a function of particle size using a portable laser particle counter.(1) This in-place penetration test is compared to the current in-place leak test using light scattering photometers for single HEPA filter installations and for HEPA filter plenums using the shroud method. Test results show the in-place penetration test is more sensitive than the in-place leak test, has a similar operating procedure, but takes longer to conduct. Additional tests are required to confirm that the in-place penetration test yields identical results as the standard dioctyl phthalate (DOP) penetration test for HEPA filters with controlled leaks in the filter and gasket and duct by-pass leaks. Further development of the procedure is also required to reduce the test time before the in-place penetration test is practical.

I. Introduction

Before a HEPA filtration system can be used in a DOE nuclear facility, the ventilation system and the HEPA filters must pass acceptance tests described in ASME N510 or AG1, and the HEPA filter must pass the MIL-STD-282 penetration test. (1-3) The acceptance tests consist of leak tests of ducts and housings, airflow capacity and distribution tests, and air-aerosol mixing uniformity tests. The airflow distribution test is designed to insure that HEPA filters see a uniform air flow, while the air-aerosol mixing test is performed to insure that the concentration of aerosols challenging the filter is uniform. This will insure that representative samples can be obtained before and after the filter for computing the filter penetration.

---

[1] U.S. Department of Energy, Defense Programs(DP-45), Germantown, MD 20874

*This work was performed under the auspices of the U.S. Department of Energy by Lawrence Livermore National Laboratory under contract no. W-7405-ENG.45. The work was supported by DOE's Defense Program Office of Technical and Environmental Support, DP-45.

The HEPA filter penetration test is given in MIL-STD-282.(1) This test requires HEPA filters to have less than 0.03% penetration for 0.3 μm DOP aerosols as measured by a light scattering photometer. The 0.3 μm aerosols were originally selected because they were believed to be the most penetrating aerosols and would yield the most conservative penetration values for the HEPA filters. These aerosols were generated in a very large machine by a controlled condensation of DOP vapor and were thought to be monodisperse.

After the HEPA filter is installed in a certified ductwork, and once a year thereafter, the filter installation must be tested for leaks.(2-4) This in-place leak test is performed to insure that the HEPA filter is properly installed and has not been damaged, that there are no leaks in the mounting frame or between the mounting frame and the housing, and that the system contains no bypassing that would reduce the system penetration. The in-place leak test is not a filter penetration test and can not be used in determining the penetration of HEPA filters. The difference between the two tests is the particle size and the type of aerosol generator used to challenge the filter: the DOP penetration test uses near monodisperse 0.3 μm particles generated by a very large vapor condensation generator, while the in-place test uses heterodisperse 0.7 μm particles generated by small portable air or thermal generators.(2-4) ERDA 76-21 recommends an acceptance criterion of 0.03% maximum penetration for the in-place DOP test.(4)

The HEPA filter leak test was implemented in 1960 in the U.S. to verify that the installed filtration systems did not have leaks.(5) This test represented a second-best choice at that time since it was not possible to conduct in-place penetration tests using the available test equipment. The problem was that the particle measuring instruments at that time could not distinguish between particle sizes, and monodisperse 0.3 μm aerosol generators were not portable. The available light scattering photometers were portable but could not distinguish between different particle sizes. To measure HEPA filter penetration at 0.3 μm diameter, it was necessary to have a monodisperse 0.3 μm diameter generator, which were not portable. The only portable aerosol generators at that time produced heterodisperse aerosols.

Now, a variety of instruments and aerosol generators are commercially available that can be used for measuring in-place filter penetration. Portable particle spectrometers are available that can measure specific particle sizes in heterodisperse aerosols. Portable aerosol generators are also available that can generate monodisperse aerosols. Thus it is now possible to measure in-place HEPA filter penetration at 0.3 μm using portable equipment consisting of either a particle size spectrometer and a heterodisperse aerosol generator or an integrated particle analyzer (e.g. photometer, condenstation nuclei counter) and a monodisperse aerosol generator. We will only address the in-place penetration method using laser spectrometers and heterodisperse aerosols in this paper.

II. Difference Between Penetration, In-Place Leak, and In-Place Penetration Tests

The difference between the results of the penetration and the in-place leak tests can be illustrated with a typical HEPA filter penetration curve shown as a function of particle size in Figure 1. The penetration is a maximum at 0.15µm, decreases rapidly with increasing particle size and is negligible at 0.7 µm for HEPA filters with no leaks. Although the penetration measurement at 0.3 µm is significantly less than the maximum, it still provides a sensitive measurement of the filter penetration. In contrast to the in-tact HEPA filter installation in Figure 1, particle penetration through leaks is independent of particle size. Thus any penetration that is measured at 0.7 µm diameter during the in-place leak test can be attributed to leaks.

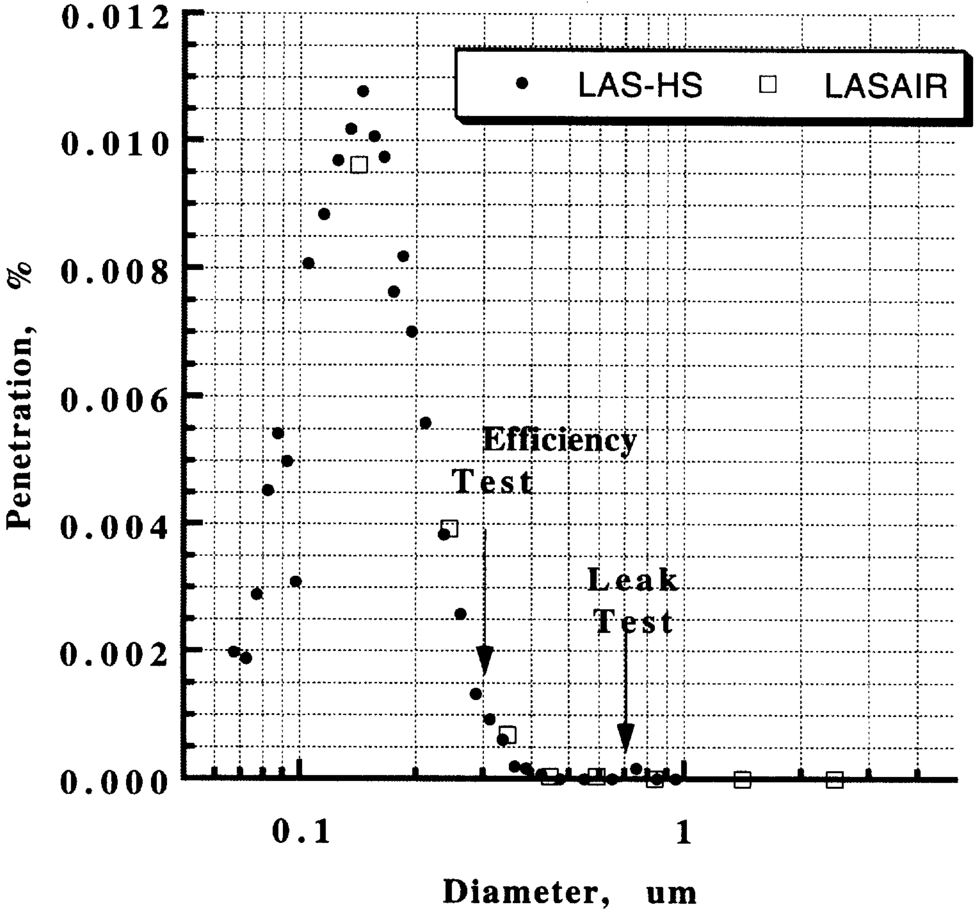

Figure 1. Plot of HEPA filter penetration measurements as a function of particle size for dioctyl sebacate (DOS) aerosols with two different laser spectrometers. Nuclear grade, 1,000 cfm HEPA filter.

Two different laser particle counters (Particle Measurement Systems, Bolder, CO) were used to generate the curve in Figure 1: the LAS-HS laser counter, which measures particles from 0.067 to 0.95 μm diameter and the LASAIR laser counter, which measures particles from 0.14 to 2.4 μm diameter. The diameter measurements are based on the logarithm midpoint of each of the counter channels. A 100:1 diluter (TSI, Minneapolis, MN) was used to dilute the upstream measurements to avoid coincidence counting. The dioctyl sebacate aerosols were generated with a Laskin nozzle aerosol generator (Virtis, Gardiner, NY). Details of the test procedure are described in previous reports.(6,7) The agreement between the two instruments is good.

It is possible to conduct filter penetration tests as described in ASME N-510 and ASME AG-1 using a laser particle counter during in-place filter tests.(2,3) If the laser counter is used for measuring the total number of particles without regard to particle size, then the filter test becomes another leak test. However, if the laser counter is used to discriminate between different particle sizes, such as 0.3 μm, then the laser test becomes an in-place penetration test. Using the laser particle counter also allows the maximum filter penetration, as shown in Figure 1, to be determined with the in-place penetration test. A description of the filter efficiency test using the laser particle counter is given by Bergman and Biermann and by Scripsick et al.(6-8)

The in-place penetration test using the laser particle counter is a measurement of the penetration of the total filtration system. This test incorporates the aerosol penetration from both the HEPA filter and leaks in the filter housing or gaskets. In separate filter penetration and leak tests, the total penetration of the filtration system is determined from the sum of the filter penetration and the leak penetration. In separate penetration and leak tests, once the filter is installed, it is only possible to determine system leaks with the light scattering photometer and assume the filter penetration remains the same. The in-place leak test using the light scattering photometer can only detect a major deterioration in filter penetration.

The increased sensitivity of the laser particle counter allows filter penetration measurements of two stages of HEPA filters for both the leak test and the penetration test. This capability, which is not possible for the standard photometer based leak test, is advantageous because of the reduced testing time and the difficulty in measuring the penetration of individual stages in systems having minimal space between stages. Schuster and Osetck were the first to use a laser particle counter to measure the filter penetration of one-stage and two-stage, size 1 HEPA filters.(9) They found typical DOP penetrations of 0.003% for single stage and 0.000005% for two stage HEPA filters. However measurements of penetration versus particle size were only reported for the single stage HEPA filters.(9)

Ortiz determined the filter leaks in a number of 20,000 cfm two-stage HEPA filter systems.(10) He did not discriminate between particle size, but rather used the total particle count before and after the filters to determine the system leaks. The test was therefore a leak test and not a penetration test. The leak measurements for ten systems varied from 0.0067% to 0.00000009%. The maximum allowable leakage for two stage HEPA filters is 0.000009%. This study was significant not only because the test system was demonstrated under field conditions, but also because it showed the laser particle counter detected filter system failures that were not seen with the standard single stage method described in ASME N510.(2)

Ortiz et al also conducted a round robin test of two-stage HEPA filtration system in which they measured filter penetration as a function of particle size using a laser spectrometer.(11) In this configuration, the filter test was an in-place penetration test. To avoid coincidence counting, the upstream concentration was diluted. The test apparatus and procedure were incorporated into an ASTM test method for evaluating HEPA filters.(12)

The Los Alamos National Laboratory (LANL) uses a laser spectrometer and heterodisperse aerosols as developed by Ortiz and incorporated in the ASTM standard for conducting in-place HEPA filter leak tests in all of their facilities.(10-13) Since the particle measurements are made by adding all of the sizes into a single count, the LANL in-place filter measurements can not be used for determining filter penetration, but rather for leaks. Adding together the particle counts in the different particle size bins destroys the ability to measure filter penetration with heterodisperse aerosols. However, by keeping the particle counts in the different size bins separate, the LANL test procedure for leaks can be converted to a test of filter penetration test.

III. Correlation of In-Place Penetration Test With Standard Penetration Test

In order to claim that an in-place filter penetration test is equivalent to the standard HEPA filter penetration test at 0.3 µm, it is necessary to establish a correlation between the in-place penetration test with the standard penetration test specified in MIL-STD-282.(1) Such a correlation would include penetration measurements on HEPA filters with varying defects in the filter and the gasket as well as by-pass leaks in the ventilation ducting. These correlation tests have not yet been completed. However Scripsick et al conducted tests on 849 new HEPA filters using laser measurements at 0.31 µm and the standard Q-107 measurements at 0.3 µm.(8) The correlation between the laser measurements at 0.31 µm and the Q-107 measurements at 0.3 µm is good, as shown in Figure 2.(8) Note that the correlation becomes worse at smaller penetration values. This is not surprising considering the photometer in the Q-107 measurements is increasingly noisy below 0.01% penetration. We plan to conduct similar correlations using filters with controlled leaks in the media and gaskets and using controlled by-pass leaks in the ducting.

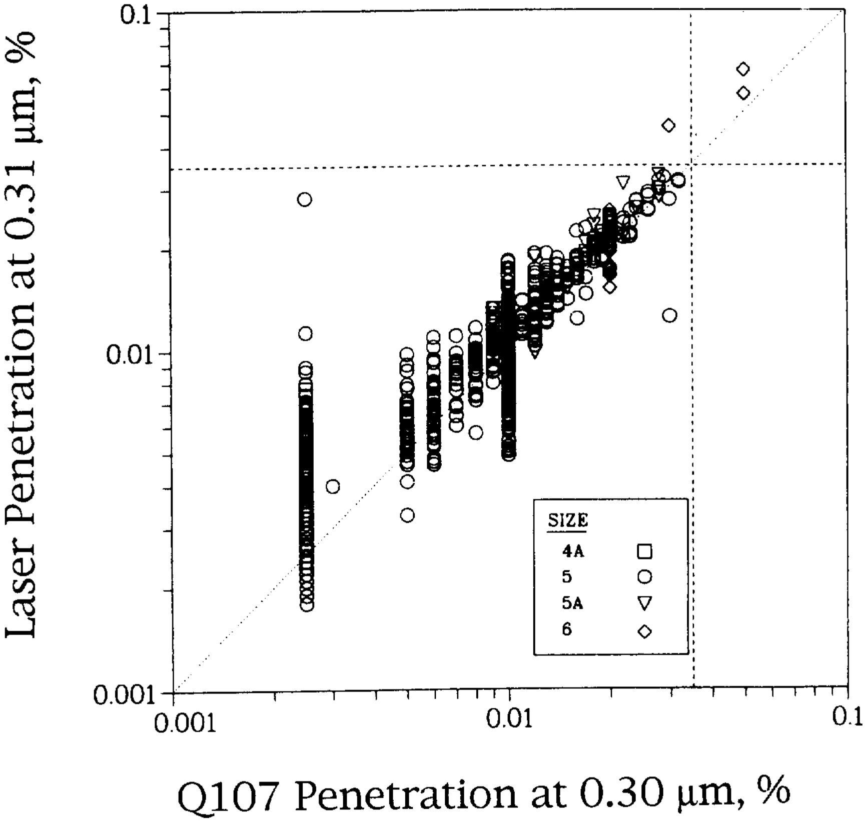

Figure 2. Correlation of HEPA filter penetration between laser spectrometer and Q107 photometer.(8)

For measurements of the maximum filter penetration, it is not necessary to conduct correlation tests with the Q107 tester because it only measures the penetration at 0.3 μm. The Q107 can not be used to determine the maximum filter penetration at 0.15 μm, as seen in Figure 1. In fact, there are no standard reference tests for the maximum filter penetration. The laser spectrometer can be used in a primary test standard for the maximum filter penetration if the particle size range is sufficient to clearly show a maximum as seen in Figure 1.

IV. Correlation of In-Place Penetration Test With Standard Leak Test

We have conducted a series of filter penetration tests on a HEPA filter with an increasing number of pin holes to establish a correlation between the in-place penetration test and the standard leak test. A nuclear grade, 1,000 cfm HEPA filter was used in these correlation tests. Two different laser spectrometers were used to determine the in-place filter penetration as a function of size: the LAS-HS laser counter, which measures particles from 0.067 to 0.95 µm diameter and the LASAIR laser counter, which measures particles from 0.14 to 2.4 µm diameter. A 100:1 diluter (TSI, Minneapolis, MN) was used to dilute the upstream measurements to avoid coincidence counting. The dioctyl sebacate aerosols used in the in-place penetration tests were generated with a Laskin nozzle aerosol generator (Virtis, Gardiner, NY). Filter penetration was determined from the ratio of the downstream concentration divided by the upstream concentration after correcting for the upstream dilution and subtracting background aerosols. Figure 1 shows the penetration of the new HEPA filter as a function of particle size.

The standard leak test was conducted using a TDA-2GN light scattering photometer (ATI, Owings Mills, MD) to obtain aerosol measurements before and after the HEPA filter. A TDA-5B aerosol generator (ATI, Owings Mills, MD) was used to generate the alpha-olefin (Emery 3004) aerosols for the in-place leak tests. Filter leak measurements were made by electronically setting the photometer upstream concentration to 100% and reading the downstream concentration directly. The in-place leak test yielded a leak of 0.01% for the test shown in Figure 1.

Following the initial test on the new HEPA filter, we made a single pinhole in the filter medium using a 0.025 inch diameter needle and repeated the in-place penetration and in-place leak tests. Additional pin holes were then made in the filter, and the filter was retested each time for penetration and leakage. The test results for the in-place penetration measurements are shown in Figure 3 for the filter having 0, 1, 2, and 6 pin holes and in Figure 4 for the filter having 9, 13, 19, 27, and 40 pin holes. The photometer measurements for each of the filter tests are shown in Table 1 along with the designated number of pinholes. Table 1 also shows the filter pressure drop and the penetration measured at 0.15, 0.3, and 0.7 µm diameter. Note that the pressure drop is not affected by the pin holes, whereas the laser penetration and photometer leaks show large increases with increasing number of pin holes.

The agreement between the HS-LAS and the LASAIR laser counters is very good over the overlapping size range as seen in Figures 3 and 4. The HS-LAS and LASAIR data are indicated by the open and closed data points, respectively. Both laser counters also yield the same value at the maximum filter penetration. However, the maximum penetration for the LASAIR occurs in the first size channel (0.1-0.2 µm), which will not allow verification of maximum penetration when the LASAIR instrument is used alone. This is not a serious problem since the maximum penetration occurs at 0.15 µm diameter for filters with and without pin holes. The preferred laser counter should have several measurements between 0.1 and 0.2 µm to verify that the maximum filter penetration is bracketed.

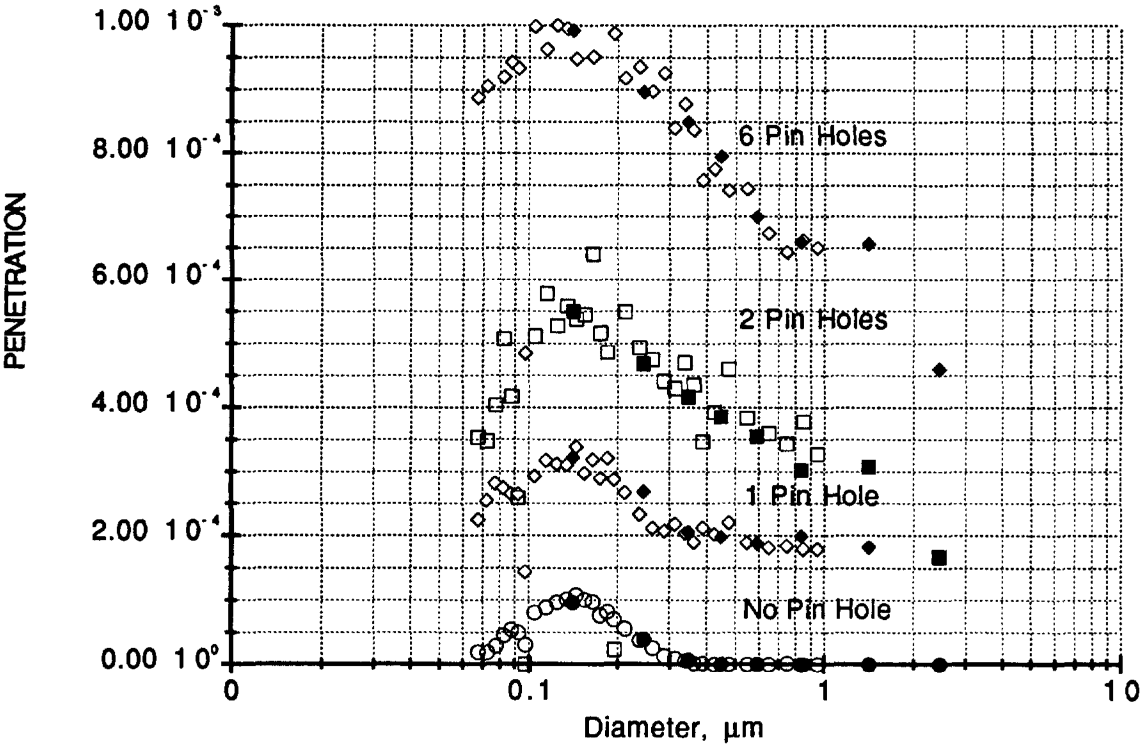

Figure 3. Penetration of DOS aerosols as a function of aerosol diameter for the same HEPA filter having 0, 1, 2, and 6 pin holes produced with a 0.025 inch needle. HS-LAS, open points, LASAIR, closed points.

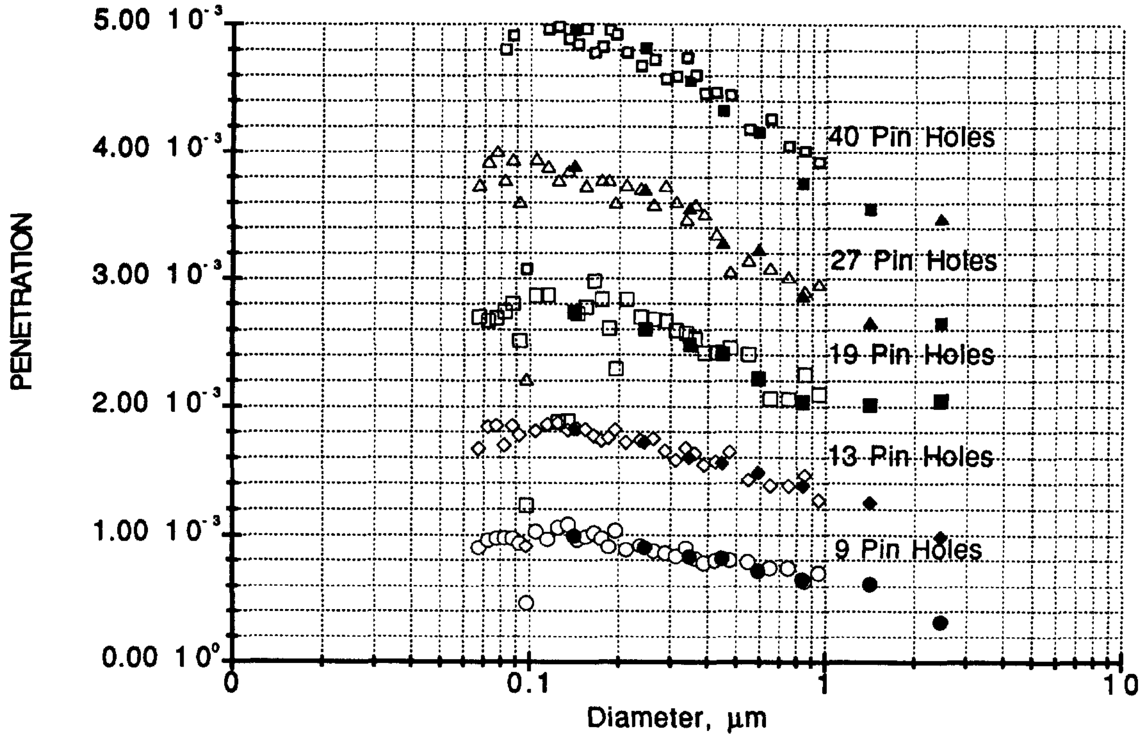

Figure 4. Penetration of DOS aerosols as a function of aerosol diameter for the same HEPA filter having 9, 13, 19, 27, and 40 pin holes produced with a 0.025 inch needle. HS-LAS, open points, LASAIR, closed points.

Table 1. Penetration and leak measurements on a HEPA filter with varying pin holes .

Pin Holes	ΔP, inches	Laser Penetration at Diameter			Photometer Leak
		0.15 µm	0.3 µm	0.7 µm	
0	1.06	1.5 x 10-4	1.0 x 10-5	1.0 x 10-6	1 x 10-4
1	1.06	3.2 x 10-4	2.2 x 10-4	1.8 x 10-4	2 x 10-4
2	1.06	5.8 x 10-4	4.5 x 10-4	3.5 x 10-4	2 x 10-4
6	1.06	1.00 x 10-3	8.8 x 10-4	6.5 x 10-4	8 x 10-4
9	1.07	1.03 x 10-3	8.8 x 10-4	7.5 x 10-4	9 x 10-4
13	1.07	1.85 x 10-3	1.65 x 10-3	1.40 x 10-3	1.1 x 10-3
19	1.06	2.9 x 10-3	2.6 x 10-3	2.3 x 10-3	1.2 x 10-3
27	1.06	3.8 x 10-3	3.6 x 10-3	3.0 x 10-3	1.3 x 10-3
40	1.06	4.9 x 10-3	4.6 x 10-3	4.1 x 10-3	1.7 x 10-3

We have plotted the threee different penetration measurements versus the photometer measurements from Table 1 in Figure 5 to examine the correlation between the various measurements.

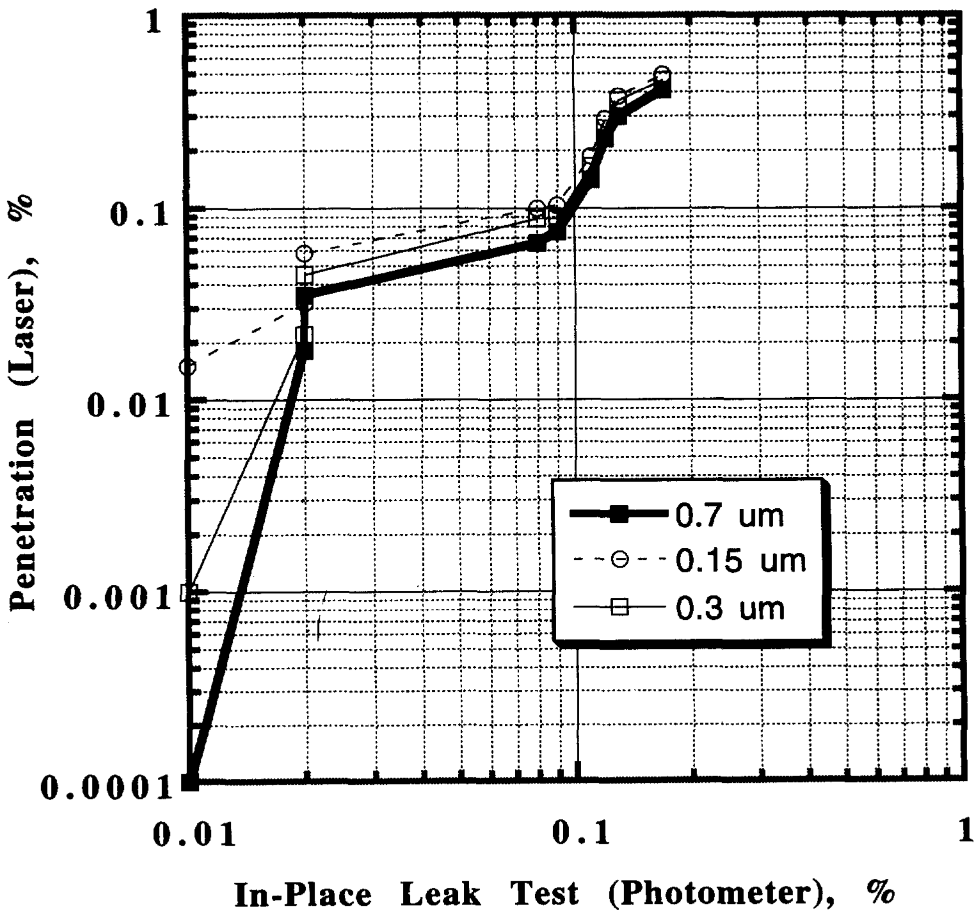

Figure 5. Correlation of laser penetration test with in-place leak test.

In general, there is poor correlation between the photometer leak and the laser penetration measurements, even for the 0.7μm data, which is supposed to represent the average size of the test aerosol in the photometer test. One of the reasons for the poor correlation is the lack of sensitivity of the photometer for penetration measurements less than 0.01%. However, the major reason for the poor correlation between the photometer leak and the laser penetration measurements is due to the fundamental difference between differential and integrated size measurements with heterodisperse aerosols. Bergman and Biermann have shown that large variations in the photometer measurements are possible compared to laser or condensation nuclei counters depending on the degree of aerosol heterodispersion and the extent of filter leaks.(7,14) Figure 5 also shows that the photometer measurements, although still not satisfactory, correlate better with the maximum penetration measurements at 0.15 μm than with the measurements at 0.3 or 0.7 μm. The lack of correlation between the in-place penetration test and the in-place leak test illustrates that the present leak test provides only an approximate measure of the sytem penetration.

V. Field Evaluation of In-Place Penetration and In-Place Leak Tests

We have conducted in-place penetration and leak tests on two typical HEPA filter installations at LLNL, a single HEPA filter system and a two-stage HEPA filter plenum, to evaluate the practicality of the in-place penetration test. The single HEPA filter system located on the roof of a LLNL building is shown in Figure 6 with the HS-LAS laser counter on the HEPA filter, the LASAIR laser counter on the blower, and the TSI aerosol diluter on the floor. The Laskin nozzle aerosol generator, not shown, was placed inside a ventilation hood in one of the building laboratories. After several in-place penetration tests were completed, the standard in-place leak test was performed using a TDA-2GN aerosol photometer (ATI, Owens Mills, MD) and a TDA-4A aerosol generator (ATI, Owens Mills, MD) with Emery 3004. The in-place leak test indicated the HEPA filter system had 0.006% leakage.

Several in-place penetration tests were conducted on the single HEPA filter system to determine the effect of challenge concentration and the repeatability of the test results. The challenge concentration is an important factor in the in-place penetration test because it affects the accuracy of the data and the duration of the test. Higher aerosol concentrations result in shorter and more precise tests but also result in instrument error due to coincidence counting. Counting errors due to coincidence occur at higher concentrations when two or more particles are counted as a single particle. Since filter penetration measurements involve two measurements at significantly different concentrations, one upstream and one downstream of the filter, separate optimizations are required for each measurement. In theory, the challenge concentration is adjusted so the downstream concentration after the filter is just below coincidence counting. The upstream concentration then has to be diluted to avoid coincidence counting. However, since the commercially available diluters have a fixed dilution ratio; e.g. 100:1 for one stage dilution, 10,000:1 for two stages of dilution; the challenge concentration must be adjusted to avoid coincidence in both the upstream (challenge) and downstream measurements.

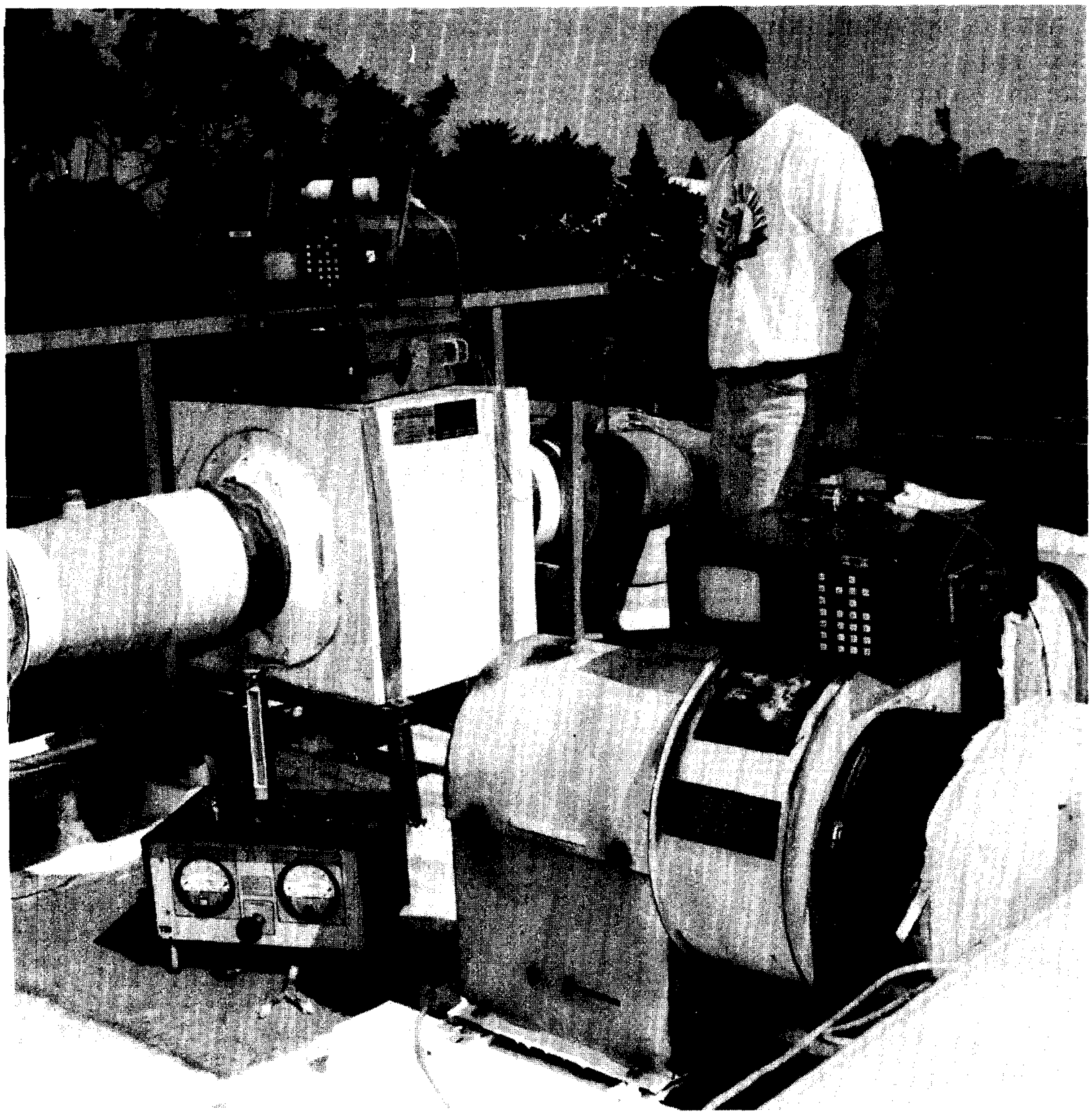

Figure 6. Photograph of the in-place penetration test apparatus on a single HEPA filter system using laser counters. The HS-LAS laser counter is on the HEPA filter, the LASAIR laser counter on the blower, and the TSI aerosol diluter on the floor.

The available dilution ratios did not allow for optimization of the concentration measurements as shown with the following illustration. Figure 7 shows the filter penetration curve derived from measurements using a 100:1 dilution of the upstream (challenge) aerosols for a single HEPA filter system which is similar to the system shown in Figure 6. The filter penetration curve is extremely noisy, even with a 1 minute upstream and a 15 minute downstream sample, because the low downstream aerosol concentration is at the background level. This resulted from reducing the challenge concentration to avoid coincidence counting. Increasing the sampling time did not help in this case because the measurement of background aerosols also increased. Using a 10,000:1 diluter on the upstream sample significantly improved the precision of the data and also reduced the sampling time as seen in Figure 8. The upstream and downstream sample times for that test were 2 and 6 minutes, respectively. An optimized diluter between 1,000:1 and 2,000:1 would reduce the sample time to about 1 minute for each measurement. The optimized diluter and associated calibration procedure must be developed before the in-place penetration method is adopted for routine measurements.

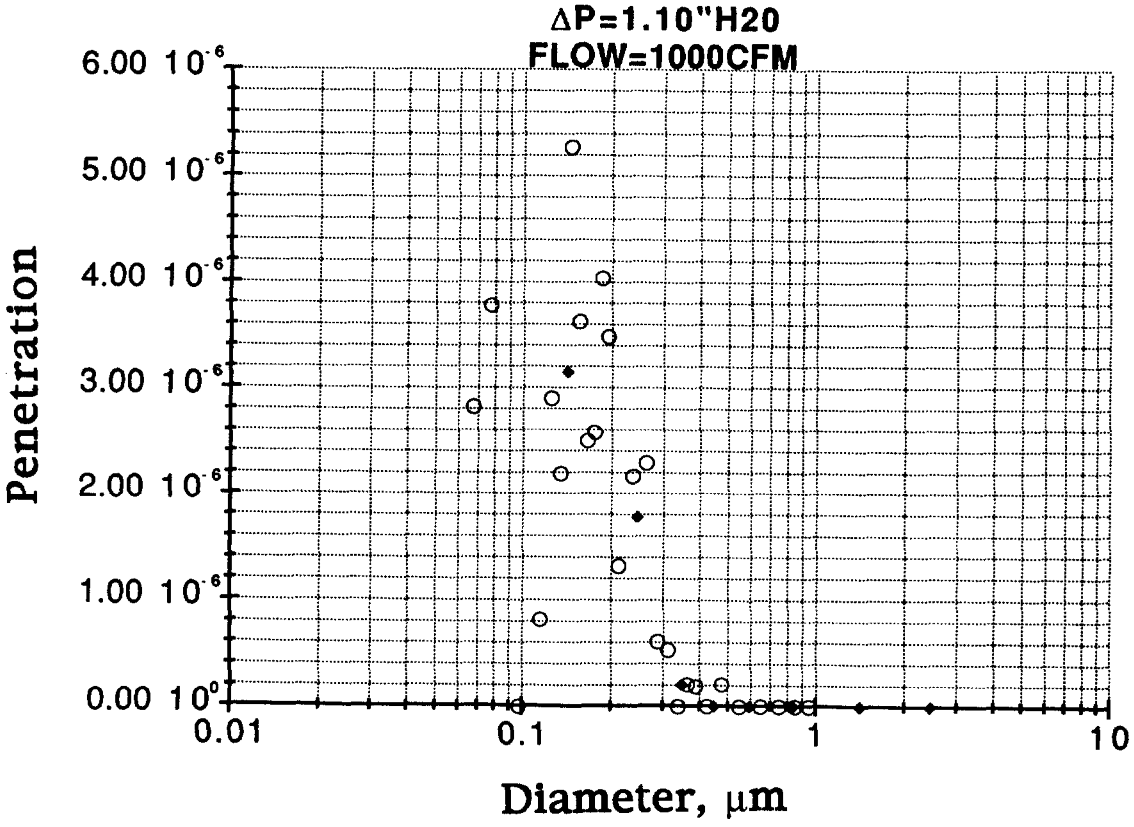

Figure 7. Filter penetration as a function of aerosol diameter for a single HEPA filter system using the in-place penetration measurement with a 100:1 diluter. Open data was generated with HS-LAS, closed data with LASAIR. In-place leak test with a photometer was 6 x 10^{-5}.

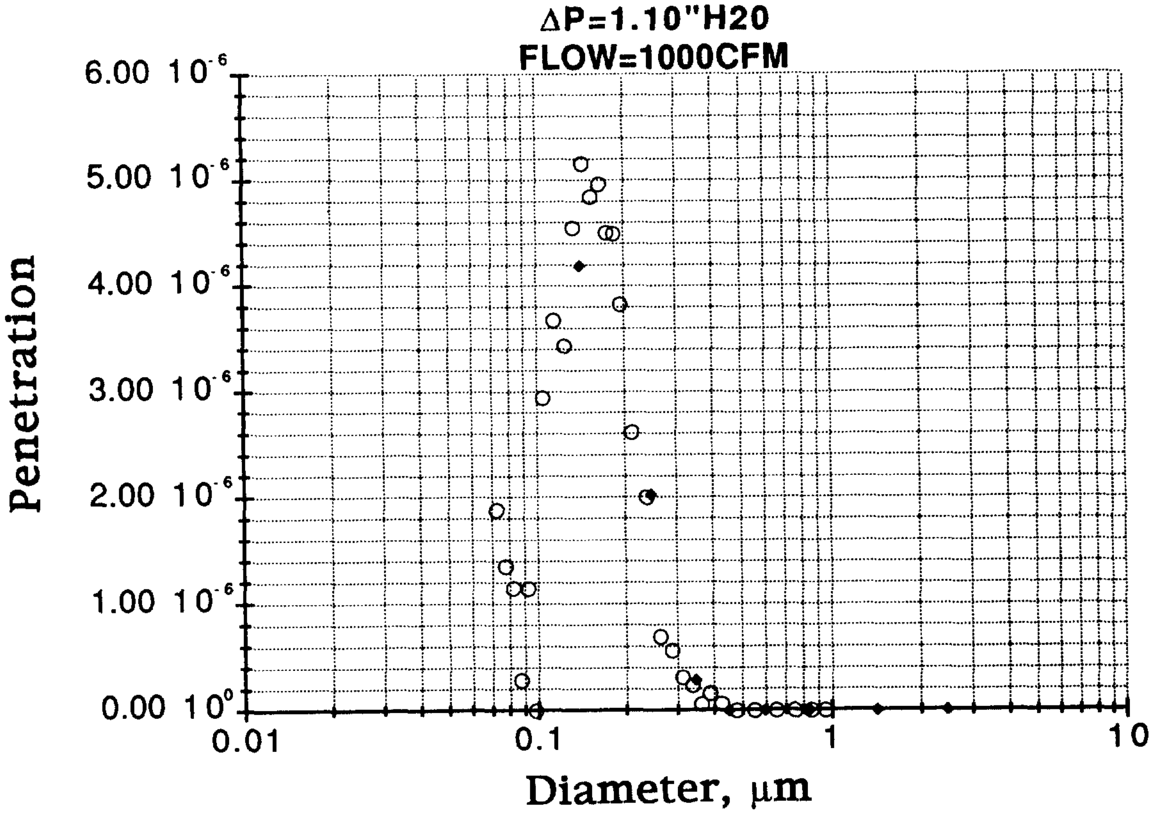

Figure 8. Filter penetration as a function of aerosol diameter for a single HEPA filter system using the in-place penetration measurement with a 1,000:1 diluter. Open data was generated with HS-LAS, closed data with LASAIR. In-place leak test with a photometer was 6 x 10^{-5}.

A detailed comparison of the time requirements for the in-place leak and the in-place penetration test is given in Table 2. The increased time to carry the penetration equipment was due to the additional laser counter, the diluter and pumps and miscellaneous items. After the in-place penetration equipment and procedure is finalized, the time for carrying the equipment will be the same for both in-place tests. The much longer test time for the penetration test can be reduced to be comparable to the leak test once the optimum diluter is developed.

Table 2. Comparison of time requirements for in-place leak and in-place penetration measurements on a single HEPA filter installation.

Task	Leak Test	Penetration Test
Carry equipment to roof	2 min.	10 min.
Set up equipment	2 min.	3 min.
Set up generator	8 min.	8 min.
Test filter	2 min.	12 min.
Total	14 min.	33 min.

We repeated the in-place penetration test two additional times to assess the repeatability of the test. Figure 9 shows the three in-place penetration tests on the single HEPA filter installation are very repeatable.

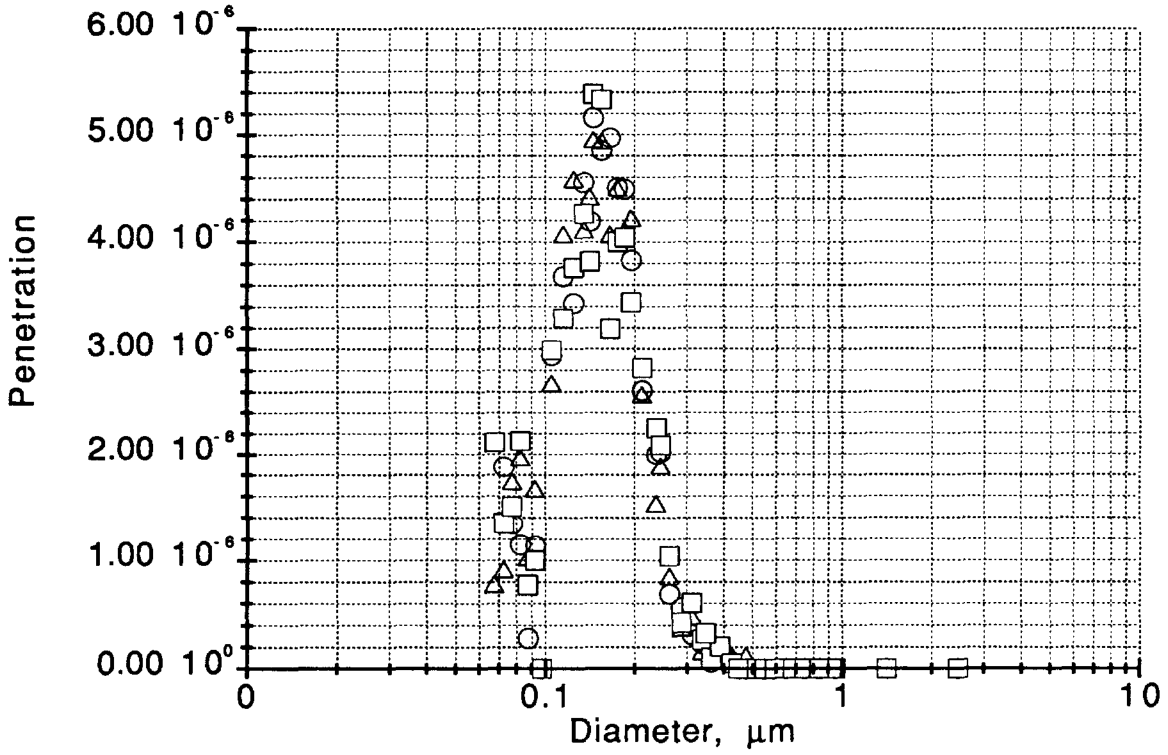

Figure 9. Measurements of the filter penetration obtained with the in-place penetration test apparatus shown in Figure 6 repeated three times.

The second field evaluation of the in-place penetration measurement was in a two-stage HEPA filter plenum using the shroud sampling method. The shroud sampling method allows individual HEPA filters to be leak tested independent of the other HEPA filters in a filter bank. This is done by placing shrouds on the upstream and the downstream side of individual HEPA filters to effectively isolate the HEPA filter from all others in the filter bank. Each shroud is a sheet metal duct that is held against the HEPA filter or frame on one end and has a reduced 1' x 1' section on the other end. The upstream shroud is used for injecting aerosols, and the downstream shroud is used for sampling the downstream aerosols. Figure 10 shows the front (A) and rear (B) sides of the upstream shroud, that is used to expose a HEPA filter to a uniform aerosol concentration. Figure 10 B shows the rear side of the upstream shroud with the 9 point aerosol injection manifold. The aerosols are then mixed by a baffle plate seen in Figure 10 A and B and further dispersed by a screen seen in Figure 10 B. The upstream shroud also has a sample port for sampling the challenge concentration. The downstream shroud, shown in Figure 11, has a 9 point sampling manifold and no internal mixing devices. The filter leak or penetration is obtained by simultaneously placing the upstream and downstream shrouds against the HEPA filter or frame as shown in Figures 12 and 13 respectively.

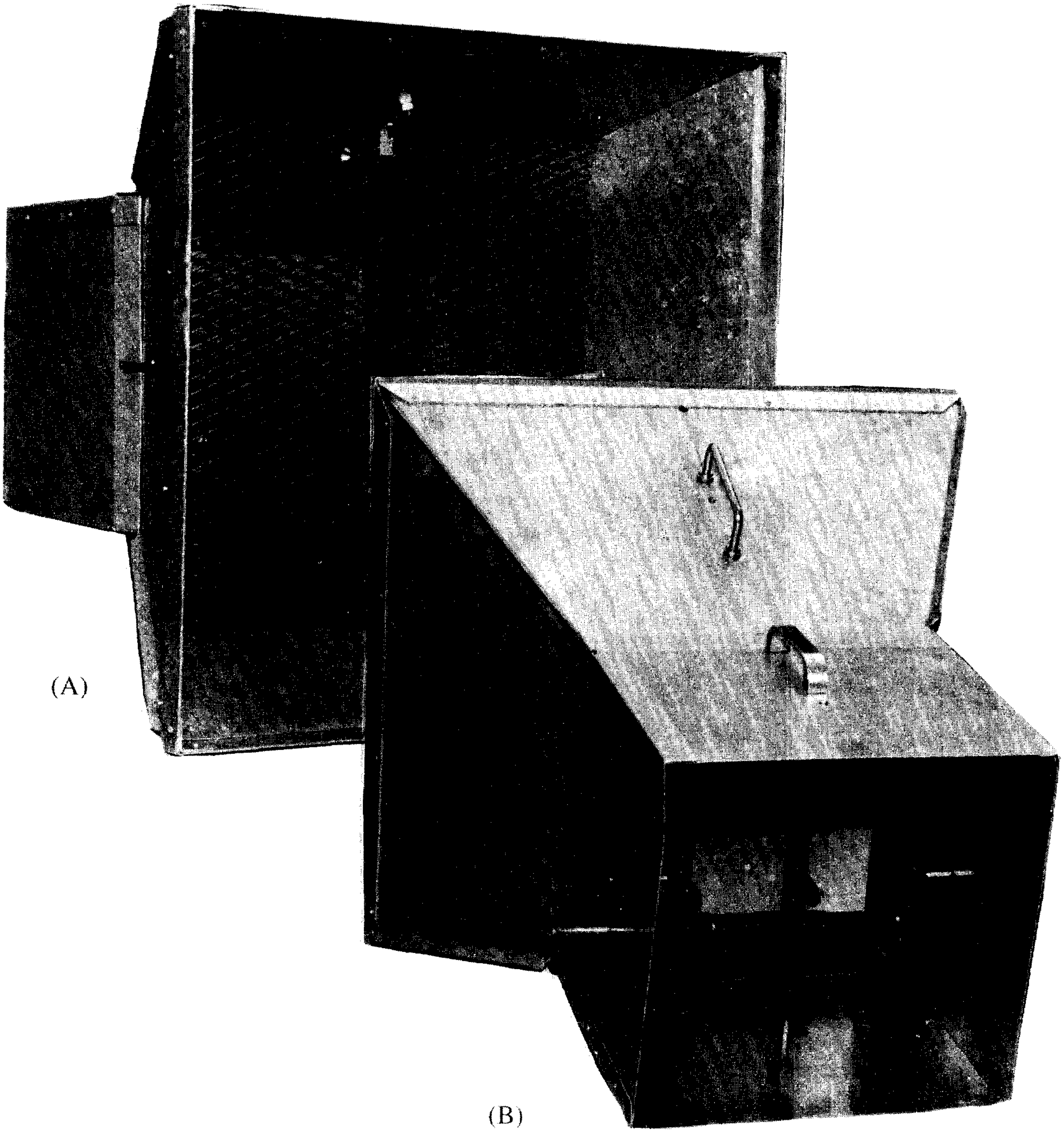

10. Upstream shroud for exposing individual HEPA filters in a filter plenum to challenge aerosols. (A) shows the front side, (B) shows the rear side.

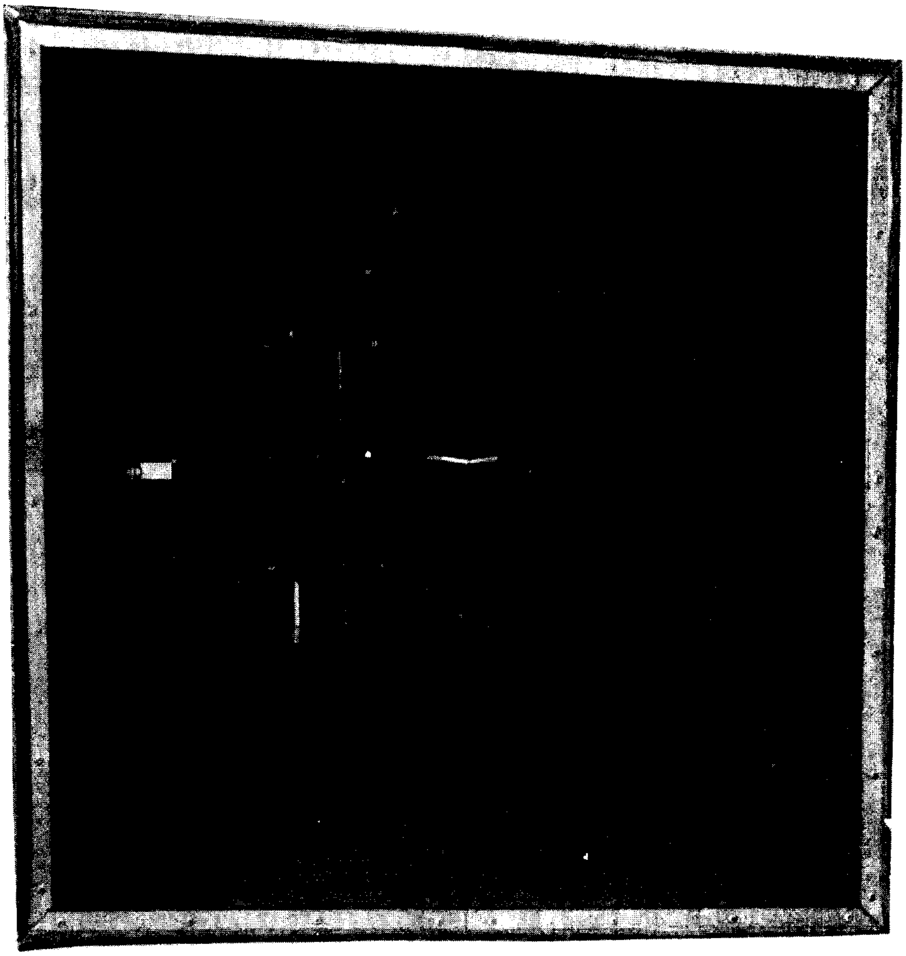

Figure 11. Downstream shroud for sampling filter penetration or leak. Nine point sampling manifold is seen from the inlet side facing the HEPA filter.

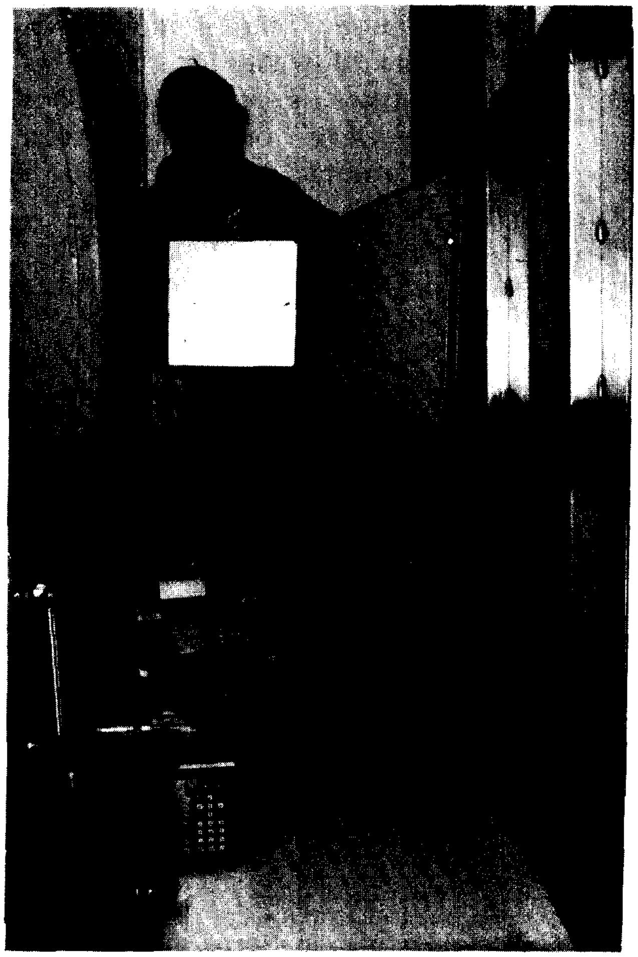

Figure 12. Downstream shroud for sampling aerosol penetration from individual filter. In-place penetration equipment used in this test.

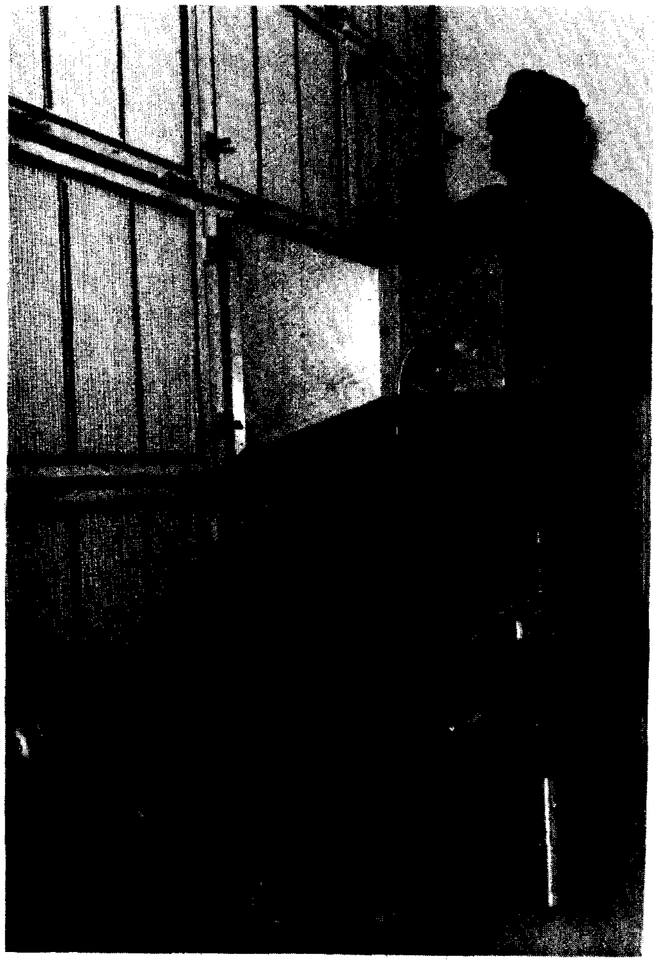

Figure 13. Upstream shroud for generating challenge aerosols. Laskin nozzle aerosol generator used in this test.

The result of the in-place penetration measurement on one filter in the plenum is shown in Figure 14. We were unable to generate the required high concentration of challenge aerosols to use the 10,000:1 diluter because the compressor shown in Figure 13 could not supply sufficient pressure to the Laskin nozzle aerosol generator. As a result, we used the 100:1 diluter with a lower aerosol concentration. This resulted in lower precision and a longer sampling time than would be required with a higher aerosol concentration and a 10,000:1 diluter. The upstream and downstream sample times were 2 and 8 minutes, respectively. The equipment used for the in-place penetration measurement using the shroud method was the same as previously described for the single filter test.

Since the shroud method only measures the penetration or leaks through the filter, and not around gasket leaks, a separate leak test is performed on each filter. This is done by directing a concentrated aerosol challenge around the perimeter of the upstream side of the filter using a long tube. Another person samples the perimeter of the downstream side of the filter using a long probe that is moved in syncronization with the upstream challenge tube. If the downstream leak is greater than 0.03% of the upstream concentration, then the filter is replaced. This traverse leak test is far more conservative than the leak or penetration measurement through the filter because no significant air volume passes through the leak compared to that flowing through the filter. Since the air flow through a gasket leak parth is not known, the traverse leak test is not quantitative, but rather a qualitative test. When using the laser counter in this leak test, the counter output is set to the concentration mode and not the count mode.

The conventional in-place leak test indicated the filter in Figure 14 had a leak of 2 x 10^{-4}. We used a TDA-2EN photometer and a TDA-5B aerosol generator, both from ATI, for the in-place leak test. The test aerosol for the in-place leak test was Emery 3004.

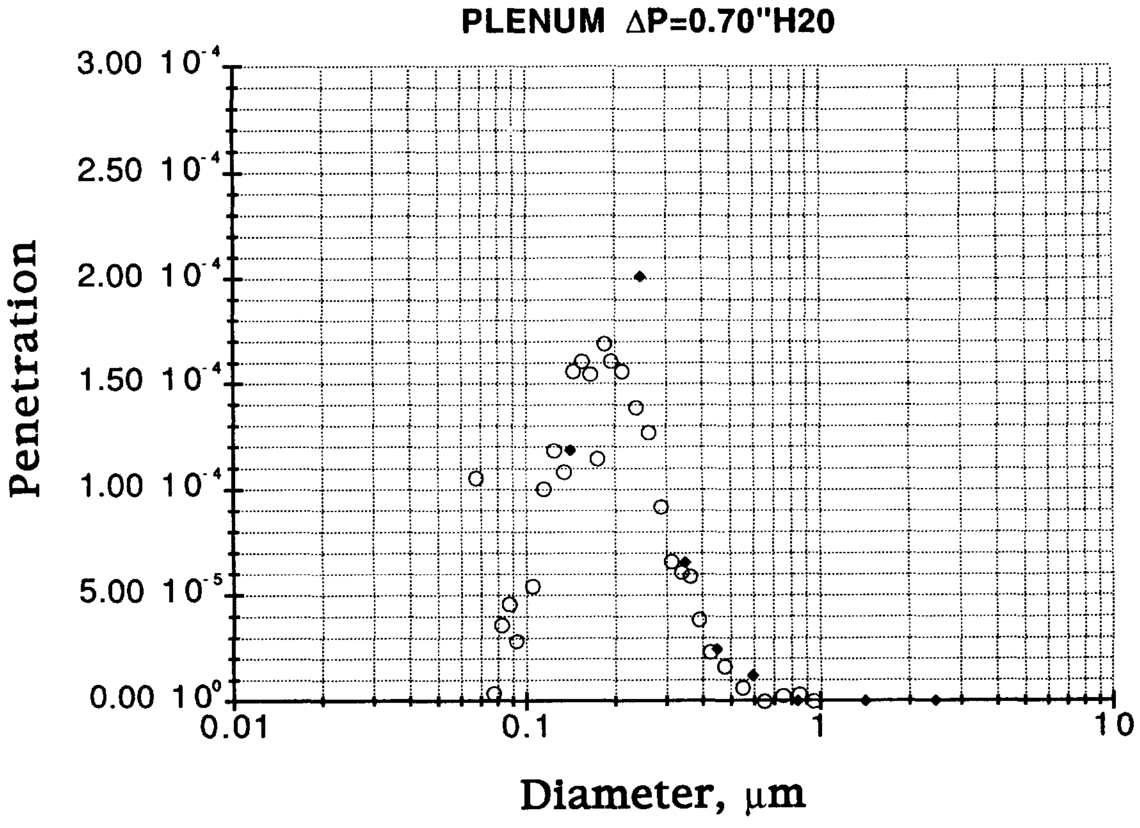

Figure 14. In-place penetration measurement of a HEPA filter in a plenum using the shroud sampling method. Open data obtained with HS-LAS, closed data with LASAIR.

We performed a detailed analysis of the time requirement for the in-place leak and the penetration test using the shroud method and tabulted the results in Table 3. The time requirements for all of the tasks except for the downstream measurements are comparable for the two in-place tests. As noted before, the long downstream sampling times was primarily due to the inability to generate a sufficient concentration. We anticipate that the in-place penetration measurement would not require much more time than the in-place leak test once the experimental test system is optimized.

Table 3. Comparison of time requirements for in-place leak and in-place penetration measurements on a HEPA filter bank using the shroud method.

Task	Leak Test	Penetration Test
Equipment set up	10 min.	15 min.
Equipment warm up	10 min.	10 min.
Upstream meas./filter	(5 min.)	(4 min.)
Upstream bank (16 filters)	80 min.	64 min.
Downstream meas./filter	(0.3 min.)	(10 min.)
Downstream bank(16 filters)	5 min.	160 min.
Tear down	30 min.	30 min.
Total	135 min.	279 min.

VI. Conclusions

We have demonstrated the feasibility of conducting in-place penetration tests on high efficiency particulate air (HEPA) filters as installed in nuclear ventilation systems. The in-place penetration test, which is designed to yield equivalent penetration measurements as the standard DOP penetraton test, is based on measuring the aerosol penetration of the filter installation as a function of particle size using a portable laser particle counter.(1) Additional tests are required to confirm that the in-place penetration test yields identical results as the standard DOP penetration test for HEPA filters with controlled leaks in the filter and gasket and duct by-pass leaks. Further development of the procedure is also required to reduce the test time before the in-place penetration test is practical.

VII. Acknowledgments

We gratefully acknowledge the assistance Mr. Wayne Krause and Mr. Donald Beason in the shroud tests.

VII. References

1. MIL-STD-282 Filter Units, Protective Clothing, Gas-Mask Components and Related Products: Performance-Test Methods, Method 105.9, Military Standard MIL-STD-282, Commanding Officer, Frankford Arsenal, Navy Department, ATTN: SMUFA-N1100, Philadelphia, PA, 19137, (1974)

2. American Society of Mechanical Engineers, "Testing of Nuclear Air Treatment Systems", ASME Standard N510-1989, The American Society of Mechanical Engineers, 345 47th Street, New York, N.Y. 10017, (1989)

3. American Society of Mechanical Engineers , Code on Nuclear Air and Gas Treatment, ASME AG1-1994, The American Society of Mechanical Engineers, 345 47th Street, New York, N.Y. 10017, (1989)

4. Burchsted, CA, Kahn, JE, and Fuller, AB, “Nuclear Air Cleaning Handbook”, ERDA 76-21, National Technical Information Service, 5285 Fort Royal Rd, Springfield, VA 22161, (1976).

5. Parrish, EC and Schneider, RW, “Review of inspection and testing of installed high-efficiency particulate air filters at ORNL”, in Treatment of Airborne Radioactive Wastes, International Atomic Energy Agency, Vienna, pp 243-264, (1968)

6. W. Bergman, A. Biermann, W. Kuhl, B. Lum, A. Bogdanoff, H. Hebard, M. Hall, D. Banks, M. Mazumder, and J. Johnson, "Electric Air Filtration: Theory, Laboratory Studies, Hardware Development, and Field Evaluations", LLNL Report, UCID-19952. January 9, (1984)

7. W. Bergman and A. Biermann, "Effect of DOP Hetero-dispersion on HEPA Filter Penetration Measurements," in Proceedings of 18th DOE Nuclear Airborne Waste Management and Air Cleaning Conference, Baltimore, MD, Aug. 12-16, 1984, pp. 327-437, NTIS, Springfield, VA, CONF-840806, (1985)

8. Scripsick, R.C., Smitherman, R.L., and McNabb, S.A. "Operational evaluation of the High Flow Alternative Filter Test System" Proceedings of 19th DOE/NRC Nuclear Air Cleaning Conference, CONF-860820, National Technical Information Service, Springfield, VA 22161, pp 863-889, (1987).

9. Schusster, B and Osetek, D, “The use of a single particle intra-cavity laser particle spectrometer for measurements of HEPA filters and filter systems” 14th ERDA Air Cleaning Conference, p.528, CONF-760822, NTIS, Springfield, VA, (1977).

10. Ortiz, J, "In-place testing of multiple stage filter systems without disruption of plant operations in the plutonium facility at Los Alamos, 18th DOE Nuclear Airborne Waste Management and Air Cleaning Conference, CONF-840806, NTIS,Springfield, VA, p. 209, (1985).

11. Ortiz, J, Biermann, A, and Nicholson, R, "Preliminary test results of a round robin test program to evaluate a nulti-stage HEPA filter system using single particle size counts" in Advances in Filtration and Separation Technology, 4, 213, American Filtration Society, Gulf Publishing Co., Houston, Texas (1991).

12. ASTM Standard Test Method for "Air cleaning performance of a high-efficiency particulate air filter system", F-1471-93, ASTM, 1916 Race St. Philadelphia, PA, 19103, (1993).

13. Martinez, V. '"Procedure for in-place filter testing" Los Alamos National Laboratory, Operating Manual, (1995).

14. Biermann, AH and Bergman, W, "Filter penetration measurements using a condensation nuclei counter and an aerosol photometer" J. Aerosol Sci., Vol. 19, No. 4, pp 471-483, (1988).

DISCUSSION

FRANKLIN: On the DOP feed of the sampler, was that downstream of the grid? I could not tell where you were sampling the concentration of the DOP feed.

BERGMAN: The upstream sample was measured through a single probe that was inserted through a porthole in the shroud just before the HEPA filter. A single probe is sufficient at this point because the Emory 3009 aerosols were well mixed. The aerosols are injected through a nine-port manifold within a one foot by one foot area. The aerosols then hit a baffle that covers about 70% of the open area and is further mixed by a grid. The sample is then taken after the grid.

KOVACH, B: I have one question . When you tested with the shroud method I understand how you calculated the average leak with the shroud, but how did you add the gasket leakage to the efficiency?

BERGMAN: The shroud method only allows you to measure the average leak if the HEPA filter is mounted on the upstream, dirty side of the frame. In this case, the shroud is placed against the frame on the downstream side. Penetrations through gasket leaks and the filter are measured together as a single measurement. If the HEPA filter is mounted correctly on the downstream, clean side of the frame, it is not possible to quantify the leak through the gasket. The shroud is placed over the HEPA filter and only measures the leak through the filter. Leaks through the gasket are determined in a separate test in which a probe is traversed around the perimeter of the gasket. If the aerosol penetration at any point exceeded 0.03% the filter was removed.

METHOD FOR HEPA FILTER LEAK SCANNING WITH DIFFERENTIATING AEROSOL DETECTOR

Bela J. Kovach, Eric M. Banks, Walter O. Wikoff
NUCON International, Inc.
Columbus, Ohio

Abstract

While scanning HEPA filters for leaks with "Off the Shelf" aerosol detection equipment, the operator's scanning speed is limited by the time constant and threshold sensitivity of the detector. This is based on detection of the aerosol density, where the maximum signal is achieved when the scanning probe resides over the pinhole longer than several detector time-constants.

Since the differential value of the changing signal can be determined by observing only the first small fraction of the rising signal, using a differentiating amplifier will speed up the locating process. The other advantage of differentiation is that slow signal drift or zero offset will not interfere with the process of locating the leak, since they are not detected.

A scanning hand-probe attachable to any NUCON® Aerosol Detector displaying the combination of both aerosol density and differentiated signal was designed.

Introduction

The scanning of HEPA filters is described in numerous articles and the general conclusion is that the size of the smallest leak detected is the function of the threshold sensitivity, reduced by the photometer response time versus scanning speed of the operator. The explanation is that the bell shaped curve of the aerosol concentration behind the pinhole is the highest in the center of the hole. Consequently, while scanning, the probe should reside over the center of the hole long enough to build up the maximum aerosol concentration in the optical chamber of the photometer. Since this is seldom the case, the conclusion is that with any given photometer there is a compromise between "missing some of the holes or working unnecessary long hours." Instead of such compromising, a mathematical solution of "enhancing" the data by differentiation of the exponential response curve was suggested.

The Method of Measuring the Aerosol Density and its Limitations

An isokinetic sampling probe for 100 feet per minute (fpm) face velocity using the 1 CFM pump was designed with an opening of 3" long and 0.5" wide. At a scanning speed of 10 fpm., it passes the pinhole leak in 0.5 sec

The response curve of the aerosol detector to a sudden increase of the aerosol concentration is an exponential function. The time constant of this function is independent of the pulse height. (3) The time constant of the NUCON® aerosol detector used for our experiment on the sensitivity range of 0.1 microgram/ liter is 0.62 sec. The detected pulse, with previously mentioned scanning speed of 0.5 seconds, reached approximately 30% of the maximum value. Scanning over the pinholes where this signal value is equal to the drifts generated by the detectors electrical system and/or drift of the aerosol concentration, no leaks were detected. To improve the threshold sensitivity, the following steps could be taken:

1. Slow the scanning speed
2. Decrease the time constant of the aerosol detector
3. Decrease the electrical drift

As neither of those should significantly improve the threshold sensitivity, the logical approach was to use a differentiating "enhancing" amplifier.

The Differentiating Method: Advantage and Limitations

The differentiating amplifier does not recognize the constant signal value; in our case it is the analog value of the background aerosol concentration combined with the slow electronic drift. The time constant chosen for this amplifier selectively enhances the functions, having the rise time similar to the optical chamber. This approach ensured the recognition of aerosol concentration increase in the optical chamber, while suppressing all other slow drifts signals.

The output signal of this amplifier is displayed on a 99 segment LCD display. The display is electrically preset to 50% value to allow movements in both positive and negative directions. When the scanner approaches the vicinity of the hole, the meter moves first in one direction, returns to zero and, as the probe is moved away from the hole, moves in the other direction. Due to the long sample line, this reading is delayed and the operator has to practice using the hand probe.

The Combination of Measuring the Aerosol Concentration and Differentiated Signal

As a final solution, a double display fast LCD meter was built in a hand-probe with two operational amplifiers. The first meter displays the aerosol concentration transferred from the aerosol detector meter. The second meter, adjusted to the 50% value, makes positive and negative movement only during changes of the aerosol concentration. The operator, observing this movement, returns on the same path to locate the hole and read the concentration on the first meter.

Conclusion

Tests performed using a NUCON® aerosol detector with the added differentiating hand-probe confirmed that the time spent scanning for leaks can be decreased by as much as 50-90% of the standard scanning method. The benefit of this is a reduction in the total time spent in radiation fields and confined spaces, and an increase in the total number of filters scanned in any given time.

References

1. Nuclear Aircleaning Handbook
ERDA 76-21

2- Procedure Standards for Certified Testing of Cleanrooms.
NEBB 1988

3- Scanning HEPA Filters with Photometers
Bruce McDonald, Donaldson Co., Inc. Minneapolis, Minnesota,
JOURNAL OF THE IES, Sept./Oct 1994

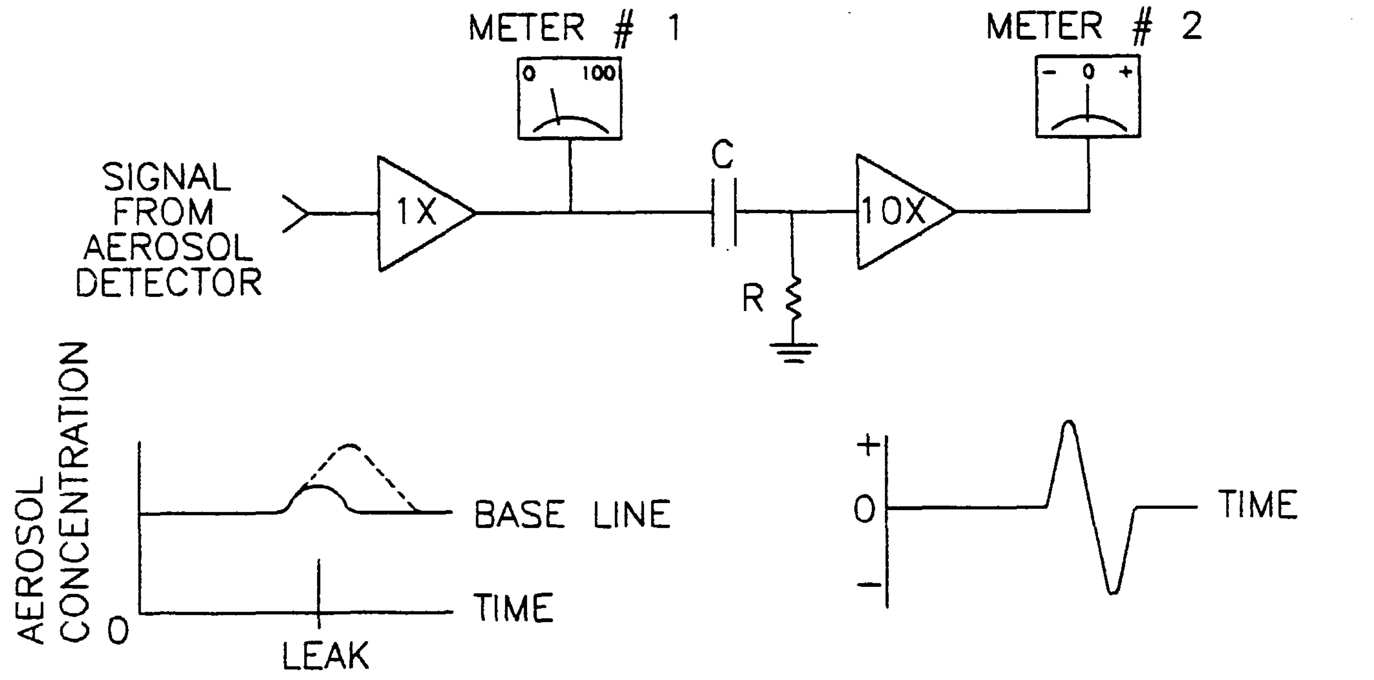

SCANNER SIGNAL WAVEFORM WHILE PASSING OVER A LEAK

DIFFERENTIATED SIGNAL WAVEFORM OF THE SCANNED LEAK

__FIGURE 1__

DIFFERENTIATING HEPA SCANNER HANDPROPE

DISCUSSION

RICKETTS: You mentioned that if you stay at the location of the leak long enough, after you have found it, that you can make an absolute measurement. Do you have to switch modes, somehow?

KOVACH, B: No, both instruments are on the same probe. You can see the display on both sides. One is a differential display which has the zero in the middle and the other is the number reading, the absolute value.

UNCERTAINTY IN IN-PLACE FILTER TEST RESULTS*

Ronald C. Scripsick[1], Richard J. Beckman[2], and Brian V. Mokler[3]

Abstract

Some benefits of accounting for uncertainty in in-place filter test results are explored. Information the test results provide relative to system performance acceptance limits is evaluated in terms of test result uncertainty. An expression for test result uncertainty is used to estimate uncertainty in in-place filter tests on an example air cleaning system. Modifications to the system test geometry are evaluated in terms of effects on test result uncertainty.

Introduction

In-place tests are performed on high efficiency particulate air (HEPA) filter systems to evaluate system performance. Test results are compared to system performance limits to judge acceptability of system performance relative to requirements of system design that assure health and environmental protection. In the absence test result uncertainty, acceptance limits on test results coincide with limits on system performance (see Figure 1). Uncertainty in test results has the effect of offsetting test result acceptance limits from acceptable system performance limits. Test results below test result acceptance limits provide clear evidence that system performance meets acceptance limits.

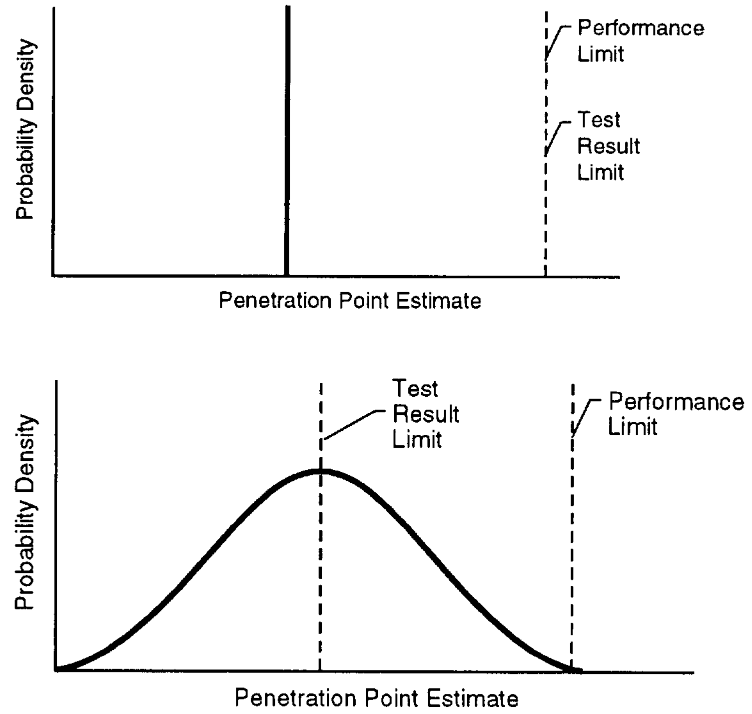

Figure 1 Two plots showing relation between system performance acceptance limit and test result acceptance limit for the case where test result uncertainty is zero and for the case where test result uncertainty is greater than zero.

---

[1] Los Alamos National Laboratory, Industrial Hygiene and Safety Group, Los Alamos, NM 87545

[2] Los Alamos National Laboratory, Statistics Group, Los Alamos, NM 87545

[3] Consultant

*Support for this work comes from the US Department of Energy, the office of Defense Programs (DP-451) and the office of Nuclear Energy (NE-30). The program managers are James Slawski and George Sherwood.

Recently an expression for uncertainty in in-place filter test results for a single HEPA filter bank was developed using error propagation analysis[1]. The expression uses indices of spatial variation of test aerosol concentration, flow velocity, and penetration to estimate test result uncertainty. These indices are referred to as heterogeneities and are defined in terms of relative standard deviations. In this paper, the uncertainty expression is used to evaluate the benefit modifications to test geometry might have in reducing uncertainty of in-place filter tests on a HEPA filter system.

An illustration of the geometry of in-place filter tests is presented in Figure 2. Test aerosol is injected into the ventilation system upstream of the HEPA filter bank at the injection plane. Aerosol concentration is sampled upstream of the filter bank in the challenge plane and downstream of the filter bank in the downstream sample plane. Concentration heterogeneity of the challenge aerosol is reduced by an upstream mixing factor, h_U, between the injection and challenge planes. Heterogeneity of aerosol penetrating the filter banks is reduced by a downstream mixing factor, h_D, between the downstream plane and the downstream sample plane.

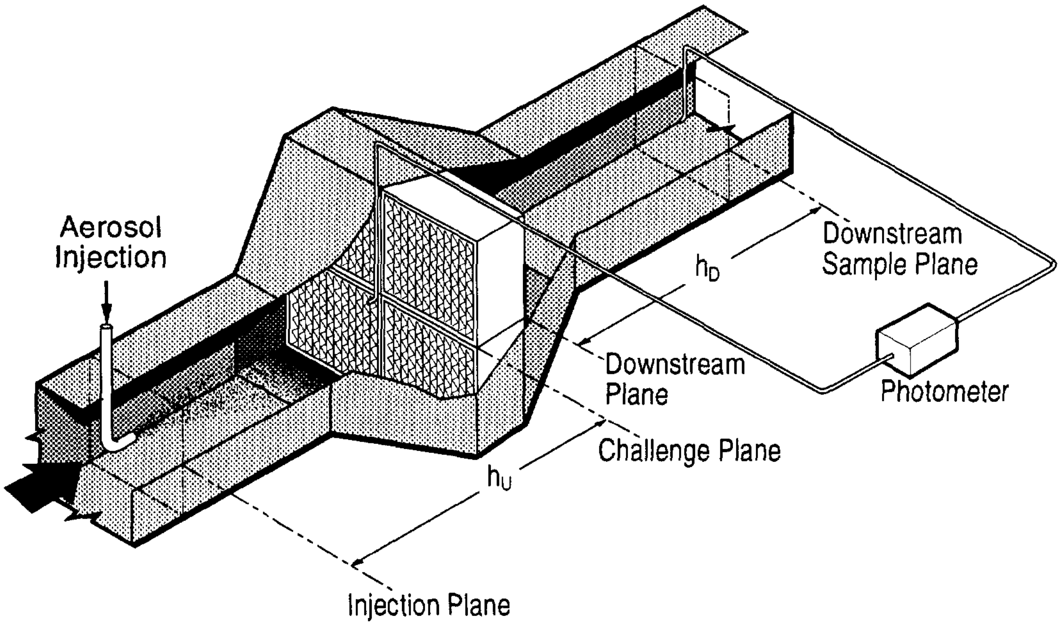

Figure 2 Generalized HEPA filter system showing in-place filter test geometry and mixing factors.

An estimate of aerosol penetration through the bank is given by:

$$\hat{P} = \frac{X_{DS}}{X_{US}} \tag{1}$$,

where,

$\hat{P}$ = penetration point estimate,
X_{DS} = the downstream sample concentration, and
X_{US} = the upstream sample concentration.

Error propagation analysis yielded an approximate expression for the uncertainty in $\hat{P}^1$:

$$H_{\hat{P}} = \left[\frac{\left(\frac{1}{X_U} - 1\right)}{h_U^2}\left(\frac{1}{h_D^2} + 1\right) + \frac{\left(\frac{1}{\hat{P}} - 1\right)}{h_D^2} + \frac{H_Q^2}{h_D^2} \right]^{1/2} \qquad (2),$$

where,

$H_{\hat{P}}$ = heterogeneity of the penetration point estimate or estimate of test result uncertainty,

X_U = dimensionless test aerosol challenge concentration, $= \frac{Q_{inj}}{Q}$,

Q_{inj} = volume flow rate of injected test aerosol,

Q = total HEPA filter system volume flow rate, and

H_Q = heterogeneity of the challenge flow velocity.

Analysis and Results

The expression for test result uncertainty (Equation 2) was used to estimate uncertainty in in-place filter tests on an example HEPA filter system. Example system design is based on an existing system at the Mound Facility in Miamisburg, Ohio[2]. A diagram of the example system is shown in Figure 3. The system has two air flow entries immediately upstream of the HEPA filter bank. Test aerosol is injected in the primary entry. There is no aerosol injection in the secondary entry.

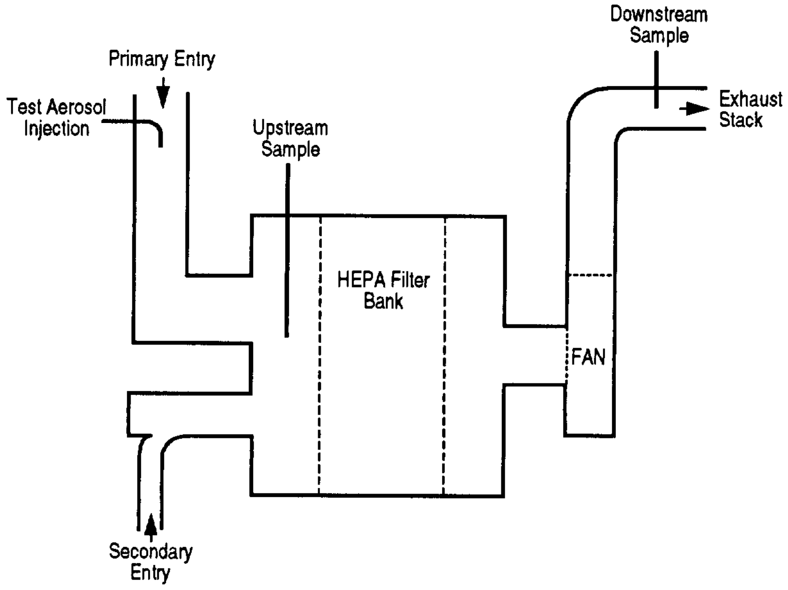

Figure 3 Example exhaust filtration system with two entries. In-place filter testing injection and sampling locations are shown.

For this analysis, Q_{inj} will be 2 cfm and Q will be 30000 cfm; both values are within the range of values observed for nuclear facility HEPA filter systems[2]. Test aerosol is assumed to be well mixed in the primary entry to the filter plenum. However, because no aerosol is injected in the secondary entry, the challenge concentration is almost certainly not the same for all filters. Consequently, h_U for this analysis was estimated to be 150, which is a tenth of the value needed for this system to meet the ASME N510 'air-aerosol mixing uniformity' requirements[3]. Because flow downstream of the filter bank passes through a fan prior to being sampled, h_D is certainly much greater than h_U. For this analysis h_D was estimated to be 1500. The division of the air flow between the two entries is assumed to be balanced such that the system meets ASME N510 'airflow distribution' requirements[3].

Values of test result uncertainty predicted from Equation 2 are shown in Figure 4 for test aerosol injected in the primary entry. At a typical system performance acceptance limit of 0.05% penetration, the predicted uncertainty was 0.82.

One potential method to reduce uncertainty in test results for this system is to inject aerosol into both entries. If aerosol injection rates are adjusted so that the average concentration is the same in both entries, the value of h_U would be increased, thus decreasing the uncertainty estimate. To illustrate this point, the analysis was repeated with test aerosol injection in both entries. This modification was assumed to increase h_U by a factor of five to 750. Uncertainty estimate predictions for this test aerosol injection configuration are shown in Figure 4. At the penetration point estimate of 0.05%, the uncertainty prediction is reduced to 0.17, almost a factor of five less than that for injection in the primary entry only.

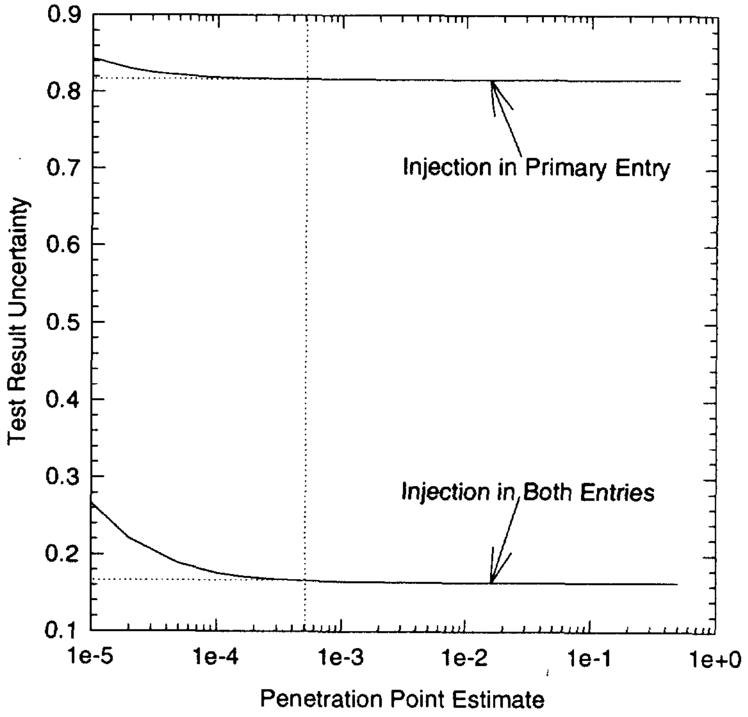

Figure 4 Values of test result uncertainty plotted against the penetration point estimate.

The uncertainty estimates were used to predict test result acceptance limits. The test result limits were determined using an offset below the system performance acceptance limit equal to three times the uncertainty estimate. Results of this analysis for both test aerosol injection configurations are shown in Figure 5. For injection in the primary entry, the test result acceptance limit was approximately 0.014% at the system performance acceptance limit of 0.05% penetration. The analysis indicates that test results below 0.014% provide clear evidence that system penetration is no greater than 0.05%. For test aerosol injection in both entries, this performance is assured by test results of 0.033% or less.

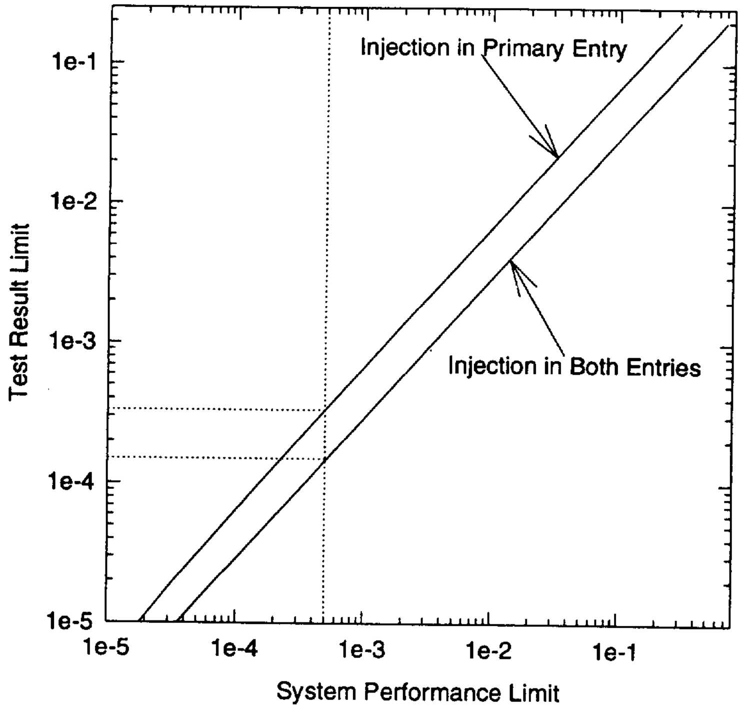

Figure 5 Test result acceptance limit plotted against system performance acceptance limit.

Discussion and Conclusions

The method presented here to account for uncertainty in in-place filter tests provides an objective rationale to judge whether tests results support the conclusion that system performance meets acceptance limits. Test result acceptance limits coincide with system performance acceptance limits only when there is no uncertainty in test results. Uncertainty in test results can be accounted for by offsetting test result acceptance limits below system performance acceptance limits by an increment related to the uncertainty. Here this increment was set equal to three times the test result uncertainty estimate. By this rationale, penetration point estimates below the test result acceptance limit are judged to provide clear evidence that limits on system performance are being met.

In addition to providing a rationale to judge acceptable HEPA filter system performance, test result uncertainty estimates can provide a metric to assess potential benefits of test geometry modifications. In the example described here, the test result acceptance limit could be increased by more than a factor of two through a modification in the test procedure. This metric provides facility managers a means to evaluate whether benefits from such modifications are cost effective. In this example, the facility manager could assess whether the extra cost of injecting test aerosol in both entries is offset by reducing the number of times system performance is rejected. If no test results have been reported in the 0.014% to 0.033% range, then the analysis indicates the modification would not be cost effective. However, if even a few test results are expected in this range, then the modification may be cost effective in delaying such costly system maintenance actions as filter replacement.

The utility of the uncertainty estimates may increase when ventilation system modifications are considered to reduce test result uncertainty. Such modifications can be costly, especially for systems contaminated with hazardous materials. Ventilation system modifications are among those being considered to establish compliance of existing systems with standards that post-date system design and construction. A number DOE nuclear air cleaning systems are in this category. The uncertainty estimates can help identify what system modifications might be needed to reduce overall test result uncertainty to levels that assure performance equivalent to that provided by tests on fully compliant systems. The estimates can also help identify costly modifications that contribute little to establishing this equivalency. Systems that pass these equivalent tests can be reasonably expected to provide levels of health and environmental protection equivalent to that provided by the fully compliant systems.

References

[1] R. C. Scripsick, Beckman, R. J., Mokler, B. V., Hinds, W. C., Martinez, V. A., "In-place filter testing geometry effects on test result uncertainty: Single stage systems", submitted to American Industrial Hygiene Association Journal, 1996.

[2] Los Alamos National Laboratory, "High efficiency filter systems-general observations, 1992-1993" by B.V. Mokler and R.C. Scripsick (LA-12763-SR), Los Alamos, New Mexico: Los Alamos National Laboratory, 1994.

[3] The American Society of Mechanical Engineers, "Testing of nuclear air treatment systems: An american national standard" (ASME N510-1989), New York: The American Society of Mechanical Engineers, 1989.

DISCUSSION

DAUBER: I am intrigued by this method and I wonder if you have applied it to the testing of adsorbers as well as to HEPA filters and, if so, could you elaborate?

SCRIPSICK: I have not done it and did not think about it until you just asked. I do not see anything right off that would prevent it. I am not as familiar with the requirements of the adsorber test as I am with the in-place filter test. From a statistics point of view, I think that it could be applied.

GRAVES: The view graph you presented showed a two entry system. Why wouldn't you just qualify the system and inject in both places according to N-510 and be done with it?

SCRIPSICK: They have tested that system that way for a number of years. However, there is a cost associated with injecting in both systems but I would opt for injecting in both. The point I was trying to make is that this gives the cost-benefit information that a manager needs to have to justify a decision like that. There will be additional costs in injecting both because the injections are remote from the plenum. You would have to add at least one person to the test team. So there would be some costs, minor ones, I think.

GRAVES: Injecting at a single point, that is not even a test. There is a cost associated with a system that might leak because people get hurt, or contamination spreads, or something like that. But I do not see any guesswork in the one you showed. The single injection is not a test of that system, it is somebody doing an exercise, but it is certainly not a test.

DORMAN: I have some comments on in-place testing but I would not want to say my comments applied to bad testing or to Scripsick's or Bergman's presentations. They are general so I will make them in the chairman's including remarks

VALIDATION TESTING OF RADIOACTIVE WASTE DRUM FILTER VENTS

Lawrence D. Weber, Ph.D.
Scientific and Laboratory Services Department
Pall Corporation
25 Harbor Park Drive
Port Washington, NY 11050

Riazuddin S. Rahimi
Process Equipment Development Department
Pall Corporation
3669 Route 281
Cortland, NY 13045

Don Edling
Edling & Associates, Inc.
P.O. Box 1252
Russell Springs, KY 42642

ABSTRACT

The minimum requirements for Drum Filter Vents (DFV's) can be met by demonstrating conformance with the Waste Isolation Pilot Plant (WIPP) Trupact II Safety Assessment Report (SAR), and conformance with U.S. Federal shipping regulations 49 CFR 178.350, DOT Spec 7A, for Type A packages.

These together address a number of safety related performance parameters such as hydrogen diffusivity, flow related pressure drop, filtration efficiency and, separately, mechanical stability and the ability to prevent liquid water in-leakage.

In order to make all metal DFV technology (including metallic filter medium) available to DOE sites, Pall launched a product development program to validate an all metal design to meet these requirements. Numerous problems experienced by DOE sites in the past came to light during this development program. They led us to explore enhancements to DFV design and performance testing addressing these difficulties and concerns.

The result is a patented all metal DFV certified to all applicable regulatory requirements, which for the first time solves operational and health safety problems reported by DOE site personnel but not addressed by previous DFV's. The new technology facilitates operations (such as manual, automated and semi-automated drum handling/re-drumming), sampling, on-site storage, and shipping. At the same time, it upgrades filtration efficiency in configurations documented to maintain filter efficiency following mechanical stress.

BACKGROUND

A great number of TRU radioactive waste packages have been generated throughout the DOE weapons complex. Condition of these packages varies widely. In addition, DOE sites continue to produce significant quantities of TRU waste, and will do so for the foreseeable future.

Hydrogen and other gasses are radiolysis products of several materials under alpha particle bombardment within the drums. This can result in flammable/explosive mixtures within the packages and/or their pressurization. The gasses must be vented while maintaining absolute containment integrity, in an environment also subject to fluctuating ambient temperature and weather conditions, and normal handling and transportation.

DOE's objective is to protect the public by consolidating these TRU waste packages in the WIPP underground repository. To meet this objective, DOE plans to ship packages in good condition, properly overpacked, with each container having at least one Drum Filter Vent (DFV), all conforming to regulatory requirements for transport and subsequent final storage. DFVs are required on all drums and boxes of TRU waste.

Several years ago, the Pall Corporation was asked by waste management personnel at the Idaho National Engineering Laboratory (INEL) to explore design possibilities of an all stainless steel DFV filter as an alternative to those in use, principally relying on a carbonaceous filter medium bonded to its mounting hardware. Availability of a qualified DFV with improved damage resistance was INELs principal objective. Pall's stainless steel filter medium at HEPA grade efficiency had been certified to a number of MIL-F-51079 performance criteria(1). It was an obvious candidate technology for use in these new designs.

DFV RATIONALE

To guide the DFV development process, Pall engineers extensively contacted DOE TRU waste management personnel. During the ensuing site visits and discussions, a number of additional concerns about existing DFV's surfaced:

1. Preliminary testing at INEL indicated that reliable head gas sampling for VOC's could not be achieved through the carbon filter medium. This was investigated by INEL because representative sampling through the filter would significantly simplify the WIPP Waste Acceptance Criteria (WAC) certification process. In order to satisfy this component of the WAC, methods were adopted in certifying waste packages which required destruction/replacement of the carbon based DFV.

2. Questions were raised concerning the effective lifetime of adhesives used in manufacturing the carbon based DFV filter medium. Compounding this concern was the varied temperature, radiation, chemical, and climatic environments to which these TRU waste packages would be exposed, in conjunction with their intended lengthy periods of service.

3. In-leakage of water through DFV's with carbon based filter medium was reported at several DOE sites. At one site, over 4,000 drums were re-processed and de-watered because of concerns arising from up to 14 gallons of water having entered each drum. Mechanism of entry: ambient temperature cycling and associated temperature/pressure variations within TRU waste drums having accumulated water on their covers (e.g. rain, or melted snow).

This in-leakage and its potential to re-occur was of concern to criticality safety personnel due to water's properties as a neutron moderator.

Liquid water in-leakage also raised questions of unseen corrosion. This is important as these packages have to be "certified" safe for transport to WIPP.

4. There was a desire, common to all of the DOE contractor personnel contacted, to maximize hydrogen diffusivity, minimize pressure drop across the DFV, and to assure HEPA level filter efficiency (≥99.97% for heat-generated monodisperse 0.3um DOP smoke).

Several sites, including Savannah River, were questioning whether to install more than one DFV per TRU package, in order to increase hydrogen dissipation rates and better prevent build-up to a flammable concentration.

HEPA level filter efficiency was referred to as the recognized standard for protecting public safety, and a level of performance desirable in DFV's. DFV's are not currently required by WIPP to perform to HEPA level efficiency. However, some DOE site specifications do require HEPA filter efficiency.

5. A very small fraction of existing drums at one DOE site were found with head gasses containing concentrations of HCl significant to stainless steel from a corrosion standpoint. Where encountered, this can be addressed by polymeric and/or higher alloy metallic DFV's. Our survey of DOE sites has not encountered any other drums where HCL would be expected to present a problem.

VALIDATION TESTING

Extensive DOE site survey also revealed current dimensional needs which Pall engineers effectively embodied in an assortment of hardware designs. A variety of these (below) have now been tested in accordance with the requirements, given in Table I, and shown under DOE witness and/or third party witness to meet or exceed them.

Table 1
DFV Validation Test Requirement and their Sources

	SOURCE	TEST
	Basic Regulatory Requirements	
1.	Trupact-II SAR	Hydrogen Diffusivity Pressure Drop vs. Air flow DOP Efficiency
2.	49 CFR 178.350 DOT Spec 7A, Type A	Water Spray Drum Drop Compression Rod Penetration
	Functional Requirements Identified Through DOE Site Visits	
3.	Liquid Water in-leakage Prevention	
	Pall Laboratories	In-leakage prevention limit
4.	Representative Head Gas Sampling	
	INEL	Hydrogen, methane, and VOC Transport Test (Formal Report recently completed.)

DFV'S SUBJECT TO VALIDATION TESTING

Pall all metal DFV's tested utilize the same filter medium, and comprise stainless steel filter medium and hardware. Models tested are depicted in Figure 1, attached.

DFV #1

The Standard Design (hexagonal body, 3/4 inch thread), intended for newly generated TRU waste packages. It is also employed on boxes and 85-gal drums used to repack or overpack damaged 55-gal TRU drums of retrieved waste. Also available in round body (#5R, Appendix A); choice made based on current equipment, handling fixtures and site procedures and practices.

Note: prior to commercial production this model DFV #1 was designated by its R&D code: "625exxx," where xxx is a three digit serial number. This code appears in this report where applicable.

DFV #2

This design arises from LANL's approach to remotely venting drums being retrieved from landfills on their site. The design mates with LANL equipment that remotely inserts a DFV into the retrieved drums.

DFV #3 & 4

These are INEL designs differing only in thread size, 7/16 inch and 1/2 inch self tapping. They arise from INEL's approach to remote venting of retrieved drums. These DFV's mate with the INEL equipment that inserts the DFV into a retrieved drum.

TEST METHODS AND RESULTS

All tests reported were conducted in compliance with indicated source (Table 1). What follows are functional descriptions of the tests, and test results.

Trupact-II SAR Requirements

Tests of hydrogen diffusivity and airflow resistance at between 1 and 10 psig were performed by an independent test facility, the Westinghouse Science and Technology Center, under contract by Pall Corporation (2). Methods were exactly as previously used in qualifying conventional carbon based DFV's.

Tests of DOP efficiency, and fixed flow rate pressure drop tests were performed under witness and certified by an independent third party, ETL Testing Laboratories, Inc., under contract by Pall Corporation. All DOP tests herein reported were performed using an ATI model Q127 DOP penetrometer, delivering heat-generated monodisperse 0.3um DOP smoke.

1. Hydrogen Diffusivity Test

Results are given in Table 2, below. The minimum acceptance criterion specified by WIPP is 1.90E-06 mole/sec/mole fraction.

Table 2
Diffusion Coefficients and Standard Errors for All Filters

Filter	D' mol/mole%/sec	D' mole/mole%/sec standard error	D' mole/sec/mole fraction	D' mole/sec/mole fraction standard error
625e016	5.13E-08	9.38E-10	5.13E-06	9.38E-08
625e046	5.33E-08	2.01E-09	5.33E-06	2.01E-07
625e010	4.96E-08	1.43E-09	4.96E-06	1.43E-07
Avg 625e's	5.14E-08	1.46E-09	5.14E-06	1.46E-07

2. Pressure Drop vs. Air Flow Test

Results are given in Table 3, below. The minimum specification established by WIPP is one LPM at one psi gauge pressure drop across the DFV (or 200 cc/min at one "H_2O gauge pressure drop; see also Table 5, below).

Table 3
Flows versus Pressure Drop at 1.0 psig

FLOW, SLPM AIR, at ΔP = 1.0 psid

625e016	625e010	625e046
10	11	10

Plots of pressure drop across the filters vs. flow for all filters were prepared from a series of measurements up to 10 psig. These were linear with correlation coefficients greater than 0.99 for each filter. The relationship between flow and pressure drop may also be expressed as the flow coefficient, C_f= flow/pressure drop, where flow is in standard liters per minute air and pressure drop is in psig. Since the graphs were linear, the flow coefficients are the slopes, shown in Table 4:

Table 4
Flow Coefficients for All Filters.

Filter	C_f, slpm air/psig
625e016	14.5
625e010	14.9
625e046	13.5

3. Pressure drop; DOP Efficiency.

The minimum flow capacity established by WIPP at one "H_2O gauge pressure drop across the filter is 200 cc/min. WIPP also specifies that each filter shall exhibit filtering efficiency >99.9% with 0.3 - 0.5 um particles of DOP smoke.

Filter pressure drop and aerosol Penetration were measured at 200cc/min flow of hot-generated 0.3um monodisperse DOP, and certified under third party witness: ETL Testing Laboratories, Inc. The results are given in Table 5, below.

TABLE 5
DOP Penetration and Filter Pressure Drop at Fixed flow Rate

	Filter	Flow Rate		Air ΔP, in. H_2O	% Penetration
Model	Part Number	SCCM	ACCM		
DFV #1	Log 916E #049	200	208	0.55	0.005-0.008
DFV #1	Log 916E #047	200	208	0.55	0.004-0.007
DFV #1	Log 916E #032	200	208	0.60	0.004-0.005
DFV #2	Log 180F #39	200	208	0.80	0.002-0.003
DFV #2	Log 180F #39	200	208	0.80	0.002-0.003
DFV #2	Log 180F #51	200	208	0.75	0.002-0.003
DFV #3	Log 216F #1	200	208	0.75	0.001-0.003
DFV #3	Log 216F #4	200	208	0.75	0.001-0.003
DFV #3	Log 216F #12	200	208	0.75	0.002-0.005
DFV #4	Log 215F #2	200	208	0.75	0.002-0.004
DFV #4	Log 215F #6	200	208	0.80	0.001-0.002
DFV #4	Log 215F #5	200	208	0.65	0.002-0.003

DOT Spec 7A., Type A Requirements

DOP penetration testing is not specified as a DOT Spec 7A performance requirement, however, this was performed as added demonstration of DFV robustness before and after the mechanical tests specified for Type A packages, items 2, 3, and 4, below.

1. Water Spray Test, performed under witness by: INEL personnel, and Edling & Associates, Inc.

The purpose of this test is to demonstrate that "rain" will not adversely affect the containment integrity and that there will not be any in-leakage of liquid water under rainy out-door storage conditions. It probes in-leakage resistance of the filter medium, DFV construction, and seals. Note: Passing this test has no bearing on the ability of the DFV to allow the passage of water in its gaseous or vapor state.

Four DFV's, one each of the four types tested, were installed into a drum lid, 90° from one another. Blotter paper was placed under the DFV inlet (drum contents side of lid) so that should liquid water enter the drum it would be captured by the paper, providing an easily detected, visual indication of even small quantities of liquid in-leakage. The blotting paper was affixed to the inside surface of the lid securely with standard duct tape, and drum assembly then completed. All DFV's and the lid were affixed using applicable torque as specified in the "DOT Spec 7A Evaluation Documents."

Following drum assembly per above, shower heads were used to deliver "rain" uniformly over the drum lid for a period of an hour. Upon completion of the water spray, in further accordance with test requirements, the package was allowed to stand two hours without draining or other disturbance prior to examination for in-leakage or other detrimental effect. At this point, water was standing on the drum lid to its height of overflow. A rain gauge placed on the lid during the shower showed overflow beyond its 5.5" capacity, demonstrating that "rain" had been well beyond the 2" per hour minimum required.

The water was drained off the lid, the lid removed, and the blotting paper thoroughly inspected for evidence of water. To pass this test, there must be no water detectable. Duplicate trials were run, each utilizing different drums and DFV's. Results are given in Table 6, below.

Table 6
Water Spray Test Results

	PASS/FAIL	
DFV MODEL	TEST 1	TEST 2
DFV #1	PASS	PASS
DFV #2	PASS	PASS
DFV #3	PASS	PASS
DFV #4	PASS	PASS

2. Drum Drop Test, performed under witness by: INEL personnel, and Edling & Associates, Inc.

This tests the ability of DFV's and drums to maintain integrity/containment as an assembled unit in the aftermath of a defined free fall.

A new drum was loaded to 950 lb using a gravel (bottom) and sand (top) mixture, as verified by weighing. A layer of 1 - 2" of fluorescein:flour mixture at 1:20 by weight was leveled on top of the sand. The drum was now full. Prior to installation, DFV's were tested for DOP penetration. They were required by Pall to provide efficiency at ≥ 99.97% for heat-generated monodisperse 0.3 μm DOP smoke at flow rate ≥200 sccm, producing $\Delta P \leq$ 1"H_2O. The reason for selecting flow rates in some cases higher than 200 sccm is that the INEL site imposed a condition that DOP efficiency tests of DFV's for their site be run at the flow rate generating 1"H_2O. As this flow rate was higher than 200 sccm, it presented another parameter by which testing was more stringent than required by the Trupact II SAR.

After testing for DOP penetration, four DFV's, one each of the four types tested, were installed into a drum lid, 90° from one another. This lid was then sealed to the weighted drum, such that the closure ring bolt was adjacent to one of the DFV's. The drop test was repeated four times with new drums and DFV's. In each trial, a different DFV model was adjacent to the closure ring bolt.

Once filled and assembled together with the four DFV's, the drum was hoisted upward and suspended from a wire harness such that the central drum axis was at 60° to the floor. In this orientation, the closure ring bolt was at the lowest point, 40" in height from a thick steel plate bolted to the concrete shop floor. A bolt cutter with pneumatic drive was used to cut the central suspension rod of the wire harness to initiate free fall.

To pass this test, there must be "no loss of contents," as determined by a complete absence of fluorescein. A UV lamp was shown with a known sample of the flour: fluorescein mixture to cause fluorescence of the fluorescein. This lamp was used to inspect the weighted drum-DFV assembly before and after each drop. Inspection was conducted on the drum, drum lid and drop platform both directly and by the inspection of wet swipes.

Following this inspection, the DFV's were retested for DOP penetration at 200cc/min, or at ΔP = 1" H_2O where this pressure drop was produced at >200cc/min. Abrupt drum deformation on impact appeared to have caused inlet (drum) side challenge of several DFV's by a visually significant quantity of fluorescein:flour. For this reason the DFV's were reverse-flushed with filtered isopropanol and dried prior to post-drop DOP tests. Even with flushing, some loss of flow capacity generally remained. In one case, a DFV remained completely blocked to flow, despite attempted flushing. The average decrease in flow capacity not counting this DFV was of the order of 15%. The results are given in Table 7, below.

Table 7
Drum Drop Test Results

Each drum lid containing four DFV's at 90° separation.

		DOP Efficiency, Pass/Fail at 99.97%	
DFV Model	Drop Pass/Fail	Before Drop	After Drop
DFV #1	PASS	PASS	PASS
DFV #2	PASS	PASS	PASS
DFV #3	PASS	PASS	PASS
DFV #4	PASS	PASS	PASS
DFV #1	PASS	PASS	PASS
DFV #2*	PASS	PASS	PASS
DFV #3	PASS	PASS	PASS
DFV #4	PASS	PASS	PASS
DFV #1	PASS	PASS	PASS
DFV #2	PASS	PASS	PASS
DFV #3*	PASS	PASS	PASS
DFV #4	PASS	PASS	PASS
DFV #1	PASS	PASS	PASS
DFV #2	PASS	PASS	Blocked to flow
DFV #3	PASS	PASS	PASS
DFV #4*	PASS	PASS	PASS

*At closure ring bolt (impact) position.

3. Compression Test, performed under witness by: INEL personnel, and Edling & Associates, Inc.

After testing for DOP penetration, four DFV's, one each of the four types tested, were installed into a drum lid, 90° from one another. The lid was installed on a new drum, maintained empty. A steel plate weighing 5,000lb was placed upon the drum lid for 24 hours. The DFV's were visually inspected and tested again for DOP penetration. The results are shown in Table 8, below. To pass this test, there must be no visually detectable physical distortion of the DFV's.

Before and after Compression test, the DFV's were tested for DOP efficiency at flow rate $\geq$ 200 sccm, producing $\Delta P \leq 1"H_2O$.

Table 8
Compression Test Results

DFV Model	Compression Pass/Fail	DOP Efficiency, Pass/Fail at 99.97% Before Compression Test	After Compression Test
DFV #1	PASS	PASS	PASS
DFV #2	PASS	PASS	PASS
DFV #3	PASS	PASS	PASS
DFV #4	PASS	PASS	PASS

4. Penetration Test (Dropped Rod), performed under witness by: INEL personnel, and Edling & Associates, Inc.

DFV's were installed on a drum prepared as for the Drum Drop Test, above, and evaluated in the following manner for physical penetration (damage) under the mechanically localized impact of a free falling steel rod.

A steel bar weighing 13.2 pounds was dropped from a height of 40 inches so that it impacted in the center of the "rain hat" of the DFV. This impact point was chosen because it represents the weakest point, as required in the DOT regulations.

In each case only an insignificant dent resulted from impact. Dents ranged from visually undetectable to a maximum depth of approximately 0.060".

To pass the test, there must be no "loss of contents" through the DFV. This was assessed as in the Drum Drop Test, above.

As a test beyond DOT Spec 7a., Type A requirements, DOP efficiency was measured before and after this Penetration Test at a flow rate ≥ 200 sccm, producing $\Delta P \leq 1"H_2O$. The results are shown in Table 9, below.

Table 9
Penetration Test Results

DFV Type	Penetration Test (Dropped Rod) Pass/Fail	DOP Efficiency, Pass/Fail at 99.97% Before Rod Drop	After Rod Drop
DFV #1	PASS	PASS	PASS
DFV #2	PASS	PASS	PASS
DFV #3	PASS	PASS	PASS
DFV #4	PASS	PASS	PASS

Liquid Water in-leakage Prevention.

Pall Laboratories: In-leakage prevention limit.

The "rain hats" were removed from the DFV's to be tested, revealing an unobstructed view of the outside surface of the filter medium. The DFV being tested was installed filter throughput direction vertical at the bottom opening of a J-tube, the long leg of which extended upward for ready measurement of hydrostatic head. The J-tube was filled gradually with water to a hydrostatic head of $75"H_2O$. After a 3 minute waiting period, if no liquid flow occurs, hydrostatic head is slowly increased to the first visual penetration. This is a sensitive test because once the liquid water in-leakage pressure is exceeded, flow is maintained and liquid droplet(s) accumulate on the filter medium.

The results are shown in Table 10, below.

Table 10
Liquid Water In-Leakage Prevention Test

DFV Model	No Leakage at 75" H_2O Pass/Fail	No Leakage at 85" H_2O Pass/Fail	Min. Pressure of Initial Flow, "H_2O
DFV #1	PASS	PASS	89*
DFV #2	PASS	PASS	N/A
DFV #3	PASS	PASS	89*
DFV #4	PASS	PASS	N/A

*Witnessed by INEL personnel.

INEL Selective VOC and other Gas transport.

INEL recently tested Pall all metal DFV's on the basis of hydrogen, methane, and VOC transport. A formal report is to be issued, soon. Personal communications indicate the report to confirm the all-metal filters as transparent to the cited compounds, consistent with non-adsorptive properties expected of stainless steel. Testing was performed consistent with requirements of the WIPP Quality Assurance Project Plan (QAPP).

DISCUSSION AND RECOMMENDATIONS

Test results show Pall all-metal DFV's to exceed Trupact II SAR requirements for hydrogen diffusivity, air flow ΔP, and DOP penetration. At the specified flow rate of 200cc/min, per Trupact II DOP test conditions, the all metal filters are at $\Delta P < 1" H_2O$, and efficiency >99.97% for hot-generated monodisperse 0.3um DOP smoke. These results were documented and submitted to WIPP in October, 1995.

Test results also verify conformance of Pall all metal DFV's to DOT Spec 7A, Type A.

DOP penetration measurements were added before and after the DOT test sequences. Mechanical shocks or other stress to DFV-drum assemblies will affect the rate of radiolysis and other chemical processes within sealed drums by promoting remixture of their contents. The affect will be largely unpredictable, but hydrogen evolution and/or other pressure producing reactions could be accelerated. For this reason, we recommend pre- and post-DOT test DOP/pressure drop measurements in validating DFV designs. The test data support a conclusion that the mechanical stresses specified by DOT Spec 7A produced no breach in filter integrity of the all-metal DFV's.

Liquid water in-leakage prevention results indicate minimum ΔP required to produce water flow is reliably at >85" H_2O. Ideal gas law calculations show a ΔP of 85" H_2O as corresponding to a temperature swing of 123F^O in the waste drum environment (drum temperature at 130^{O}F dropping to +7^{O}F, lid flooded), well beyond that expected by DOE facilities. It is recommended that new DFV designs be certified to such a standard of liquid water in-leakage, as environmentally non-inducible.

INEL has completed testing of VOC transport through Pall all metal DFV's. We understand from personal communications that it validates the all metal DFV's as providing VOC transport representative of head gas concentrations. This will mean that head gas sampling can for the first time be performed through the filter non-destructively, including such sampling to meet WIPP QAPP requirements..

Another result of Pall's ongoing contact with DOE site personnel is further design refinement. We opted to revise the designs and increase the variety of models available that adapt to a tool facilitating easy, non-destructive head gas sampling through the DFV. While performing this design evolution, we also found ways to improve producibility of our all metal DFV's. The updated designs are described in Appendix A, and depicted in Figure 2, both attached. No change in filter medium has been made since the testing herein described and, in some cases, design is so similar that the new models (Appendix A) may prove certified by existing test results. Pall is pleased to perform validation testing of design variants, where required.

CONCLUSIONS

In comprehensive discussion with personnel at DOE sites, we confirmed the regulatory requirements for DFV validation, and further identified practical problems hampering daily site operation and generating additional costs. In the course of testing new DFV designs for certification, we responded both to current regulatory requirements and to the practical needs presented to us for more economic site operation while maintaining public/worker safety.

As a result of this test program, we are pleased to point out that for the first time a rugged, all metal DFV is available to DOE sites which will:

1. Meet all applicable WIPP Trupact II SAR, and U.S. government DOT requirements.
2. Provide HEPA efficiency and pressure drop at the rated flow
3. Reduce criticality risk by providing a new level of liquid water in-leakage prevention.
4. Enable direct head gas sampling non-destructively through the DFV (INEL testing, to be reported). This is expected to reduce both operating and DFV replacement costs.

ACKNOWLEDGMENT

The authors gratefully acknowledge the DOE and M&O Contractor engineers who contributed their comments and time to this effort, and thank the members of Pall's DFV Team and Support personnel for their many contributions.

REFERENCES

1. Report No. 529719, "Tests of Single Stage Metal Fiber HEPA Filter Media and Filter Elements, ETL Testing Laboratories, Inc., Rendered to Pall Corporation, June 18, 1993.

2. Report No. 95-2TD2-PFILT-R1, “Evaluation of Filters for Flow and Hydrogen Diffusion Characteristics,” Westinghouse STC, April 24, 1995.

Appendix A
Updated Designs of All Metal DFV's, Comprising Stainless Steel Filter Medium and Hardware

DFV #1H

The Standard Design (hexagonal body), intended for newly generated TRU waste packages. It is also employed on boxes and 85-gal drums used to repack or overpack damaged 55-gal TRU drums of retrieved waste. Also available in round body (#5R, below); choice made based on current equipment, handling fixtures and site procedures and practices.

DFV #2L

This design arises from LANLs approach to remotely venting drums being retrieved from landfills on their site. The design mates with LANL equipment that remotely inserts a DFV into the retrieved drums.

DFV #3R & 4R

These are INEL designs differing only in thread size. They arise from INEL's approach to remotely venting retrieved drums. These DFV's mate with the INEL equipment that inserts the DFV into a retrieved drum.

DFV #5R

This round body design is intended as standard design for newly generated TRU waste packages. It is also used on boxes and 85-gal drums used to repack or overpack damaged 55-gal TRU drums of retrieved waste. Also available in hexagonal body as #1H, referenced above.

The round body designs (suffix "R") mate with a sampling fixture allowing head gas samples to be taken non-destructively through the stainless steel DFV, as often as needed.

Pall's Stainless Steel Drum Filter Vents Subject to Validation Testing

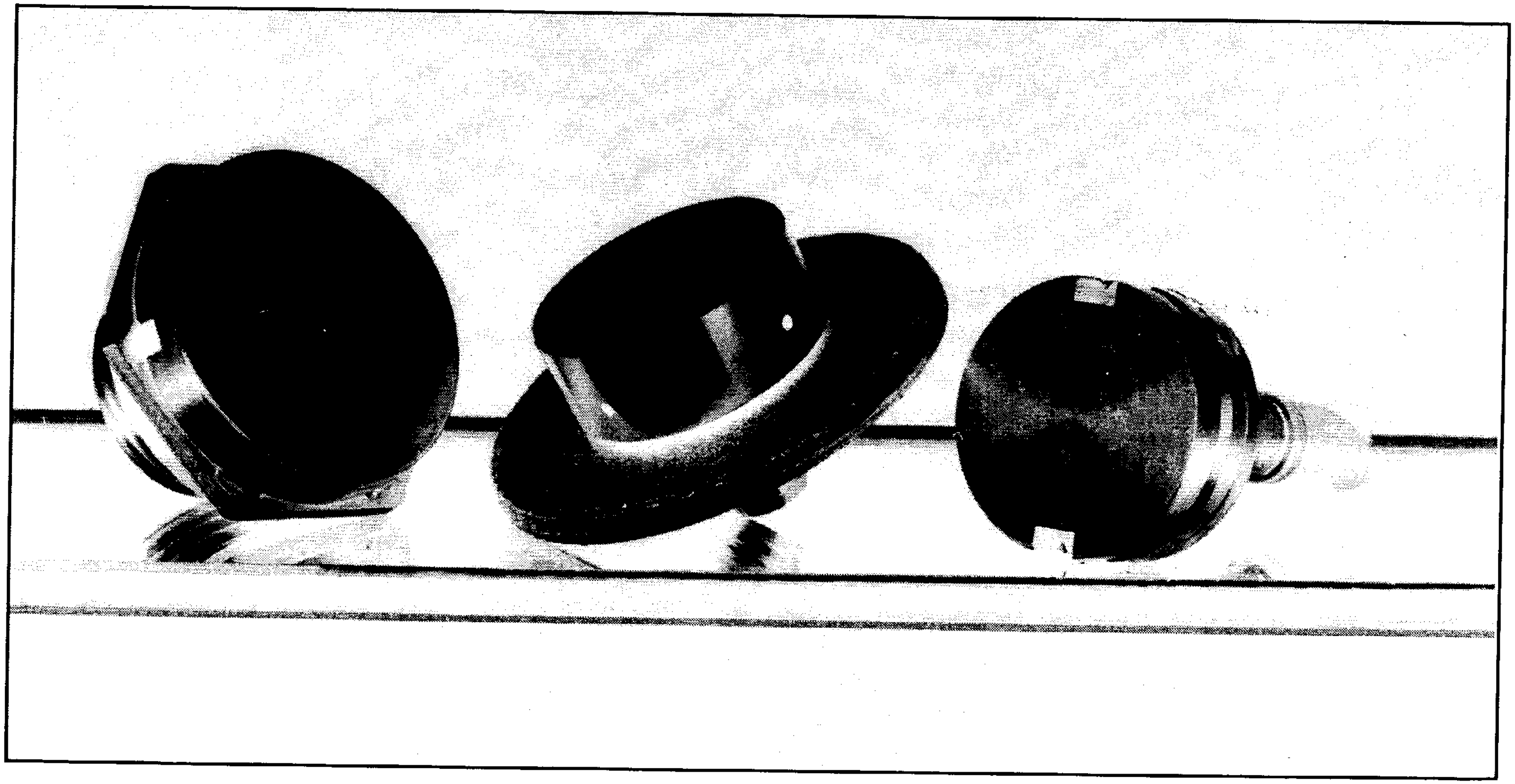

Figure 1

Pall Corporation's Family of All Stainless Steel HEPA Efficiency Drum Filter Vents for DOE Rad Waste Containers

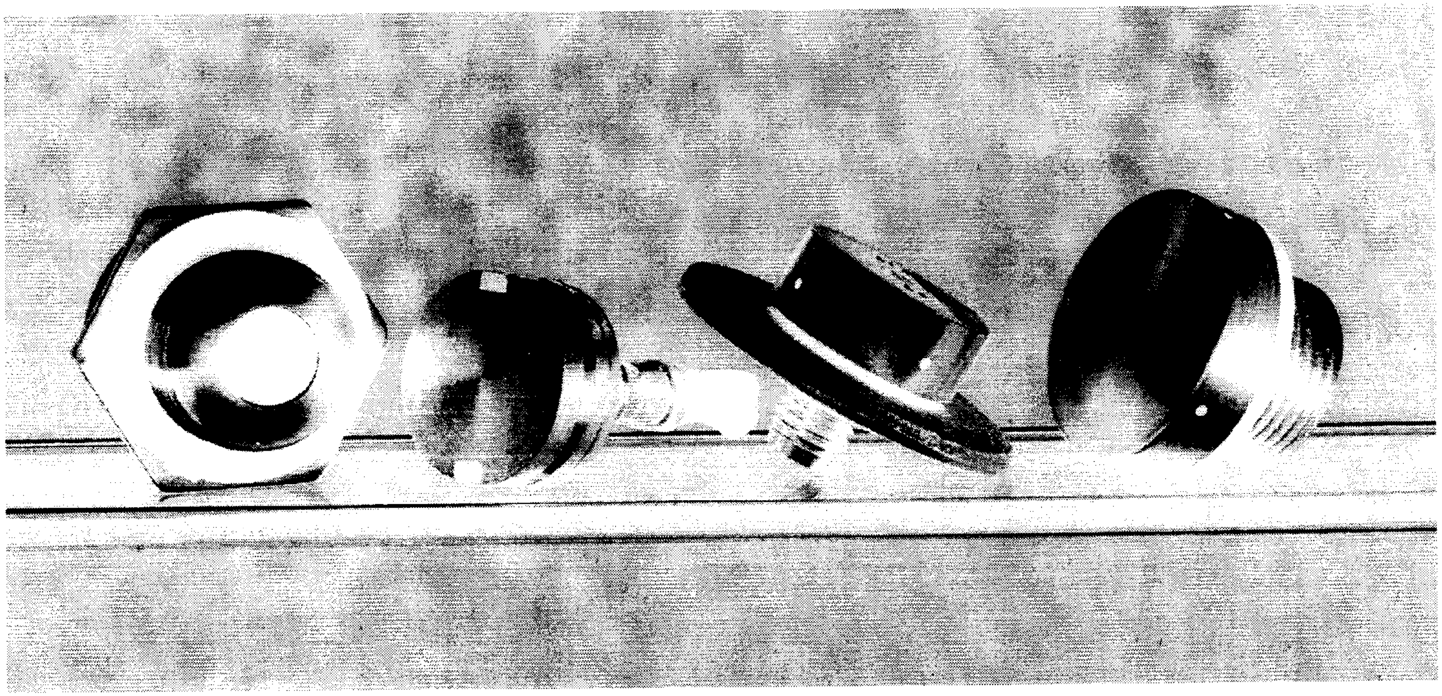

The Pall part numbers are (L to R): DFV #1H, DFV #2L, DFV #3R & 4R, DFV #5R

Figure 2

DISCUSSION

DERDERIAN: Would you discuss the simulant that you use to pressurize the drum contents?

WEBER: The simulant is specified by the DOT and the applicable CFR. It is one part fluorescein to twenty parts cooking flour by weight. The flour serves to dilute the fluorescein because there is plenty there for ultraviolet light to pick up.

DERDERIAN: But it does not pressurize the inside of the drum, is that correct or not?

WEBER: By itself, no, but when you drop the drum from a height the impact momentarily gives you quite a burst of pressure.

SCRIPSICK: Did you look at airborne fluorescein in the test? The test procedure calls for you to look on the floor. It is quite possible the dust hasn't settled yet. If you go back a week later you might find some.

WEBER: That is an interesting thought. The DOT standard used to certify the filter does not address that possibility. The DFV itself is mounted so close to the lid of the drum that you would see evidence of it from inertial impaction if it were to be true. We did not.

SCRIPSICK: On the upstream side? I assume the upstream side of the filter was coated with fluorescein.

WEBER: Yes, very much so. We saw it there and we also saw some increased resistance to flow after the test. You could also look inside to the part of the DFV that faces the contents of the drum and you could see the stuff in there. There were no measurable amounts outside.

SCRIPSICK: One of the things we found was that it is very difficult to seal up pipe threads. I wonder if the tests that you did considered that seal because it would be part of the in-place test.

WEBER: The tests were done in conformance with the existing specifications so what was tested was the assembled unit of the DFV, the drum lid, and the drum. The fact that there was no loss of contents by that test indicates that the pipe joint was not a weak point. That could be an area for additional investigation. The main seal to the drum lid is by a gasket. A lot has to do with the strength that you need to make a seal and not rip the drum lid.

MONROE: Have you done any studies on the plugging rate during normal service of these filter vents?

WEBER: We do not yet have any normal service experience with the filter vents because we have just gotten them certified. That will be a very important parameter to follow. Service does not call for extended periods of flow so I am predicting a very low plugging rate. The primary function of the filter is to dissipate by diffusion and pressure the hydrogen that is generated thermally from radiolysis inside the drum.

CONKLIN: In Washington State, drum vents that are used at Hanford must meet HEPA efficiency requirements according to Washington State regulations.

WEBER: What regulation in particular?

CONKLIN: The Washington State Clean Air Act that requires best available radionuclide control technology.

A GENERAL CORRELATION OF MPPS PENETRATION AS A FUNCTION OF FACE VELOCITY WITH THE MODEL 8140 USING THE CERTITEST 8160

Norman Lifshutz and Mary Pierce
Hollingsworth & Vose Company
West Groton, Massachusetts

Abstract

The CertiTest 8160 is a Condensation Nucleus Counter (CNC) based filtration test stand which permits measurement of penetration as a function of particle size. The Model 8140 is also a CNC based filtration test stand which provides a single penetration measurement for a fixed particle distribution aerosol challenge. A study was carried out measuring DOP penetration on a broad range of flat filtration media at various face velocities to compare these two instruments. The tests done on the CertiTest 8160 incorporated a range of particle sizes which encompassed the most penetrating particle size (MPPS).

In this paper we present a correlation between the MPPS penetration as measured by the CertiTest 8160 and the penetration values obtained on the Model 8140. We observed that at the lowest air face velocities of the study the Model 8140 tended to overpredict the MPPS penetration as measured by the CertiTest 8160. We also present a correlation of MPPS penetration with face velocity which may be of use for extrapolation purposes.

1. Introduction

It is a well-known phenomenon that the penetration of aerosol particles through a fibrous filtration medium is a sensitive function of the particle diameter, peaking at the most penetrating particle size (MPPS). Over the years there has been increasing emphasis by both filter element manufacturers and filter media manufacturers on measurement and specification of filter media penetration performance at the MPPS. Two recent documents that have referenced reporting the MPPS and its penetration at application velocity are IES-RP-021(1) and CEN/TC 195(2). While this can readily be carried out using a flat sheet test stand such as the CertiTest 8160, it is a relatively slow, time-consuming process, requiring tests at a number of particle sizes. These tests are not suitable as real time quality control tools in a media manufacturing environment. An alternative is the use of a flat sheet test stand such as the Model 8140 which uses a fixed challenge aerosol having a mean particle size diameter of 0.18 micrometers and geometric standard deviation of 1.6. The test time of the 8140 is a fraction of the test time of the 8160. Thus, the first objective of this study was the comparison of the penetration performance reported by these two test instruments.

The "Holy Grail" of filtration is the simultaneous achievement of lower particle penetrations at lower filter resistance. This has led filter manufacturers to design elements operating at lower air face velocities relative to media area, with greater emphasis on measurement and specification of filter media penetration performance at these low velocities. This is again a challenge to the penetration measuring stands because the low face velocities frequently involve flow rates at the measurement limit of the equipment, and because the particle count rates require longer and longer sample times for statistical confidence. It would be desirable to measure penetration performance at higher face velocities and be able to extrapolate to the lower face velocities of interest. Thus the second objective of this study was the establishment of a correlation between MPPS penetration and face velocity which might be used for such an extrapolation.

2. Experimental

Two different flat sheet test stands were used for this study. The more sophisticated is the TSI CertiTest 8160(3) which is shown schematically in Figure 1. A fine particle aerosol of dioctylphthalate (DOP) is generated by atomization and evaporation of a dilute solution of DOP in isopropyl alcohol. This aerosol then encounters an electrostatic classifier, which permits only a tunable monodisperse aerosol of the desired particle size to proceed to challenge the test media. Samples of aerosol are withdrawn upstream and downstream of the test media and fed to

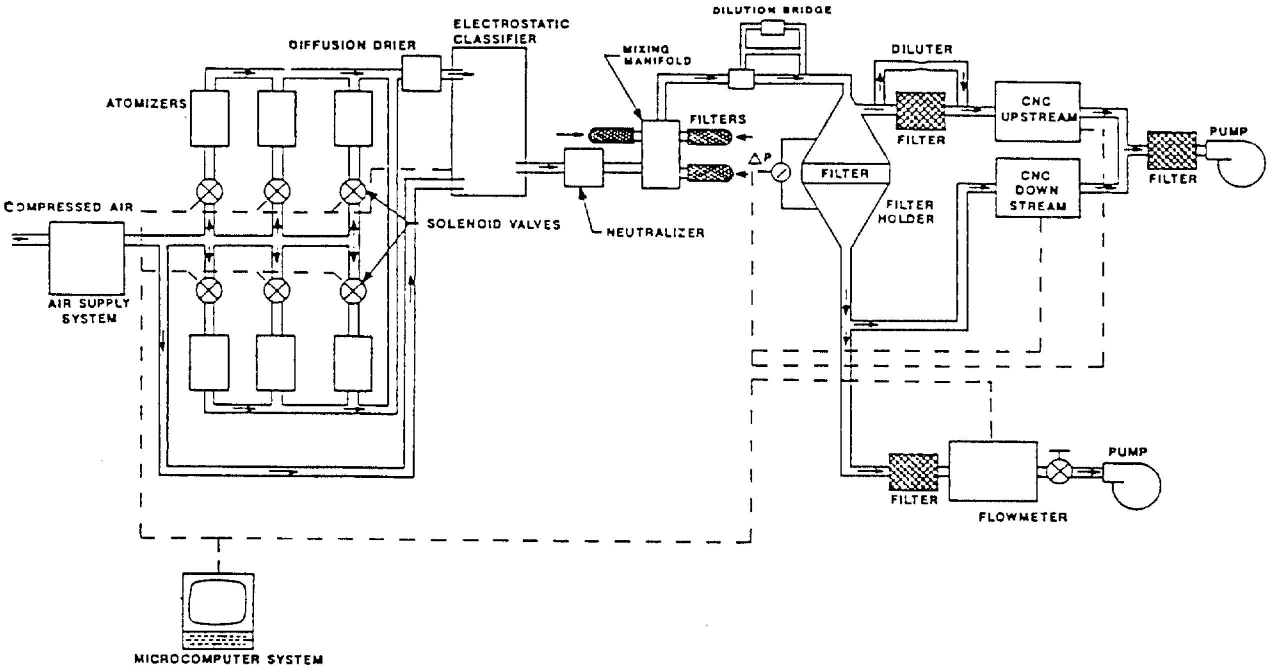

Figure 1.
Schematic of TSI Model 8160 Automated Filter Tester

separate CNC's for determination of the penetration for that particle size. To obtain a full curve of penetration for a range of particle sizes encompassing the maximum penetration, a series of particle sizes is selected and the individual penetration measurements are determined sequentially. With this equipment penetration can be reported to a precision of 10^{-8} percent over a particle size range from 0.015 to 0.40 micrometers at flow rates from 5 to 100 liters per minute.

The less sophisticated test stand is the TSI Model 8140, which is shown schematically in Figure 2(4). This instrument generates a polydisperse aerosol of DOP by atomization. This aerosol then passes through a coarse fibrous prefilter intended to narrow the particle size distribution. The aerosol then proceeds to challenge the test media. Samples of the aerosol are withdrawn upstream and downstream of the test media and fed to CNC's for determination of penetration. With this equipment penetration can be reported to a precision of 10^{-7} percent at flow rates from 15 to 100 liters per minute.

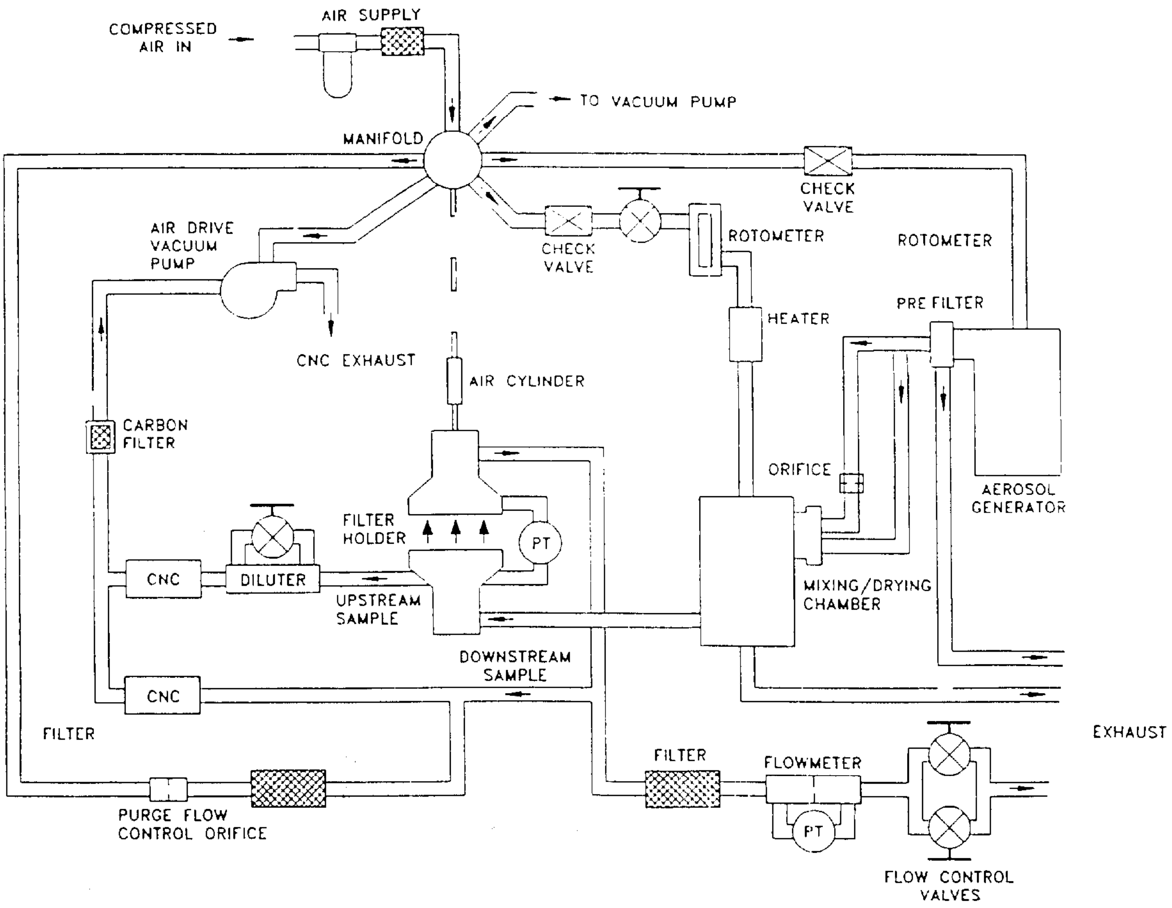

Figure 2.
Schematic of TSI Model 8140 Automated Filter Tester

With both instruments it is necessary to use purge times long enough to guarantee achievement of steady state, and sampling times long enough to provide satisfactory counting statistics. The normal sample area for both instruments is 100 cm^2, but on the 8140 we use a 333 cm^2 sample area for face velocities below 1.8 cm/sec in order to maintain flow rate accuracy.

Multiple samples of ULPA, HEPA, Sub-HEPA, and 95% DOP efficiency media were obtained. These were first tested in the 8160 using face velocities of 1.0, 1.2, 1.8, 2.5, 3.5, and 5.35 cm/sec for 0.075, 0.10, 0.12, 0.15, 0.18, 0.22, 0.26, 0.30, and 0.35 micrometer particle diameters. The same area of each sample was then retested at the same velocities using the 8140 tester Each 8160 data set was subjected to regression analysis to fit the data to the model:

$$\ln(\mathrm{Pen}) = A(\ln D)^2 + B(\ln D) + C \qquad (1)$$

Where Pen = Penetration fraction

and D = Particle diameter

The MPPS is then easily determined by setting the derivative equal to zero, so that:

$$\ln(\mathrm{MPPS}) = -B/2A \qquad (2)$$

where MPPS = Most penetrating particle size

and substituting back into the model we get:

$$\ln(\mathrm{Pen}_{\mathrm{MPPS}}) = C-(B^2/4A) \qquad (3)$$

3. Results and Discussion

Figures 3, 4, 5, and 6 are typical 8160 curves for the ULPA, HEPA, Sub-HEPA and 95% DOP efficiency media along with the 8140 results for the same samples. In general the quality of the fit to this simple model is quite good, with an average R^2 value of 0.98 for roughly 72 data sets of six points apiece. Thus the model provides a simple objective way of treating such a data set in order to abstract an MPPS value and a $\mathrm{Pen}_{\mathrm{MPPS}}$ value.

It is clear from these graphs that the curves are tangent to or just below the 8140 lines shown. It is noted that at the lower test velocities the 8140 values tend to overpredict the 8160 MPPS values by an appreciable percentage. Since the particle size distribution in the 8140 is certainly not monodisperse, one would expect that the 8140 should give penetration values somewhat below the $\mathrm{Pen}_{\mathrm{MPPS}}$, but our experimental results do not confirm this. From a media specification point of view, however, the 8140 penetration is a conservative estimate of the MPPS penetration. Areas we suspect to be possible causes for these results are diluter

FIGURE 3
PENETRATION CURVES OF ULPA MEDIA

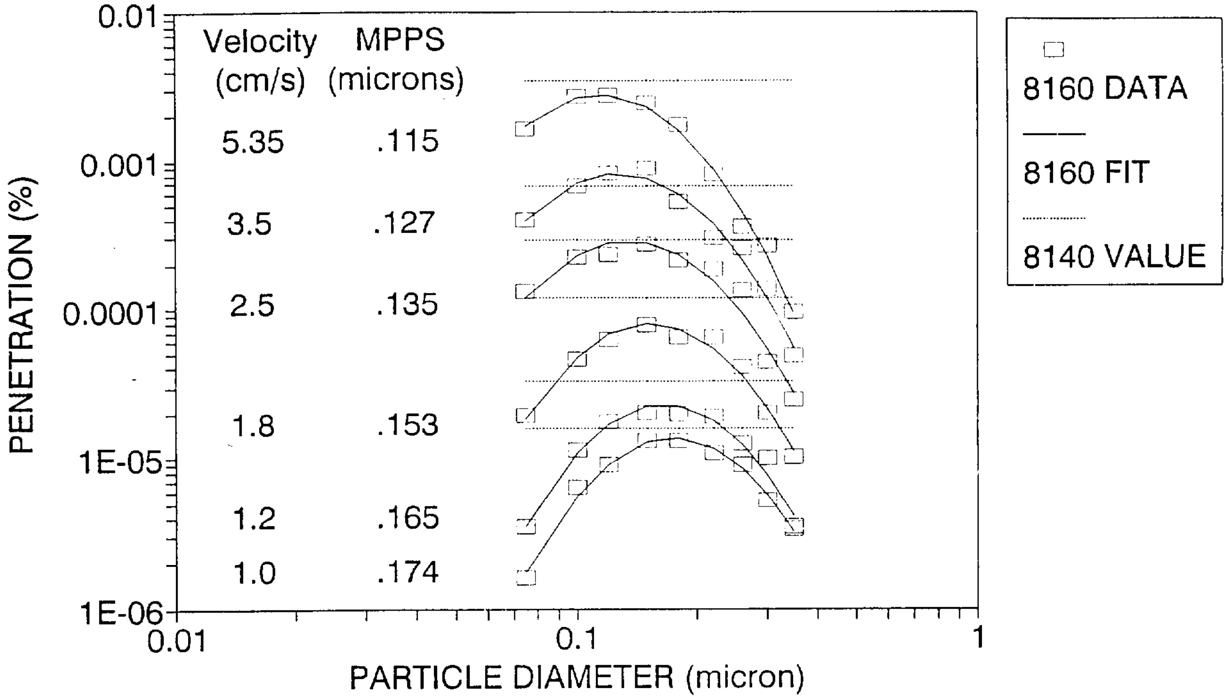

FIGURE 4
PENETRATION CURVES OF HEPA MEDIA

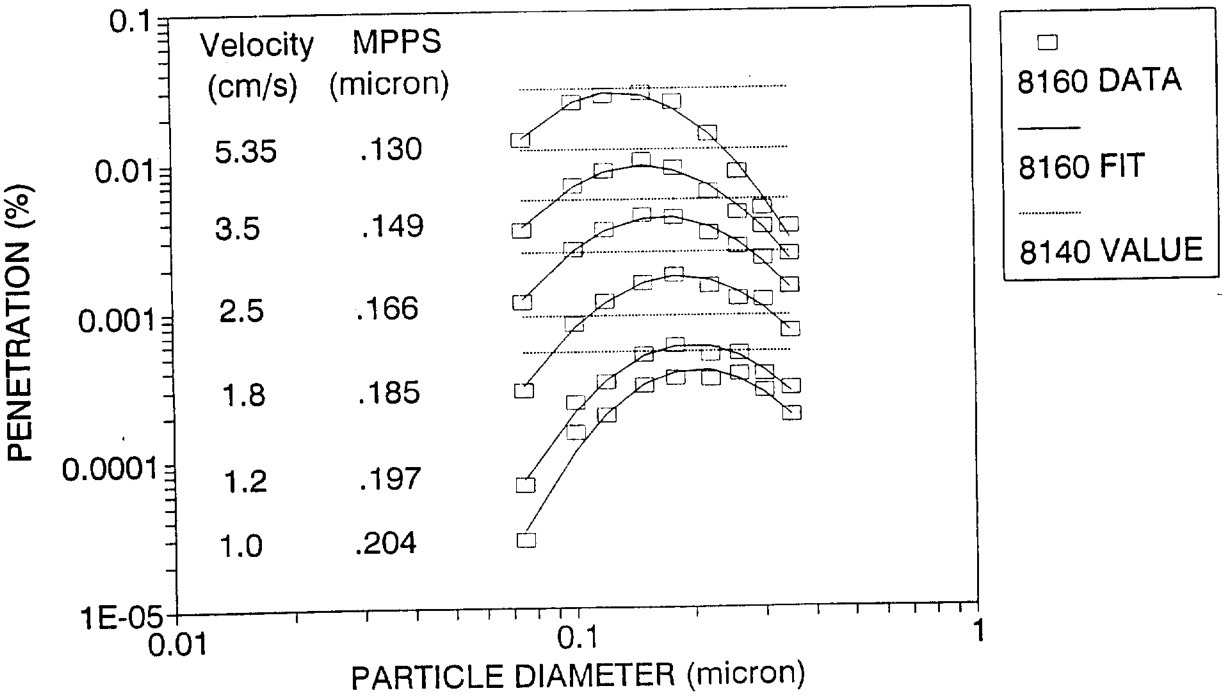

FIGURE 5
PENETRATION CURVES OF SUB-HEPA MEDIA

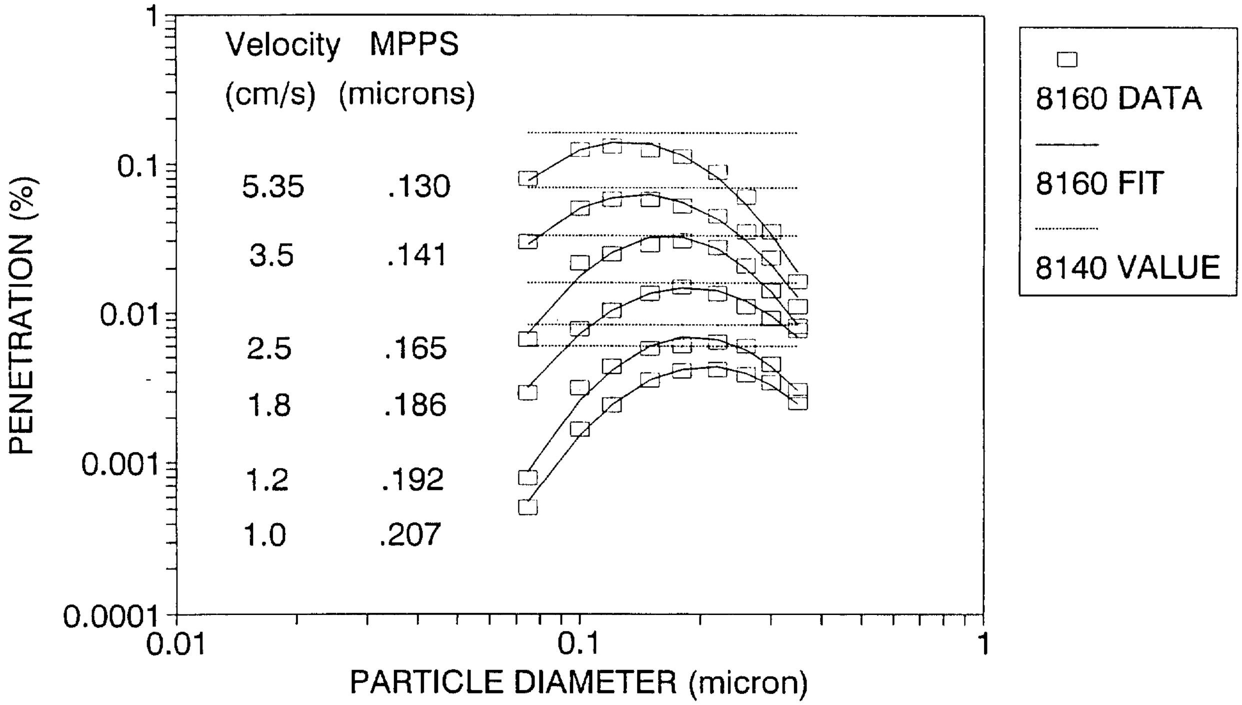

FIGURE 6
PENETRATION CURVES OF 95% DOP MEDIA

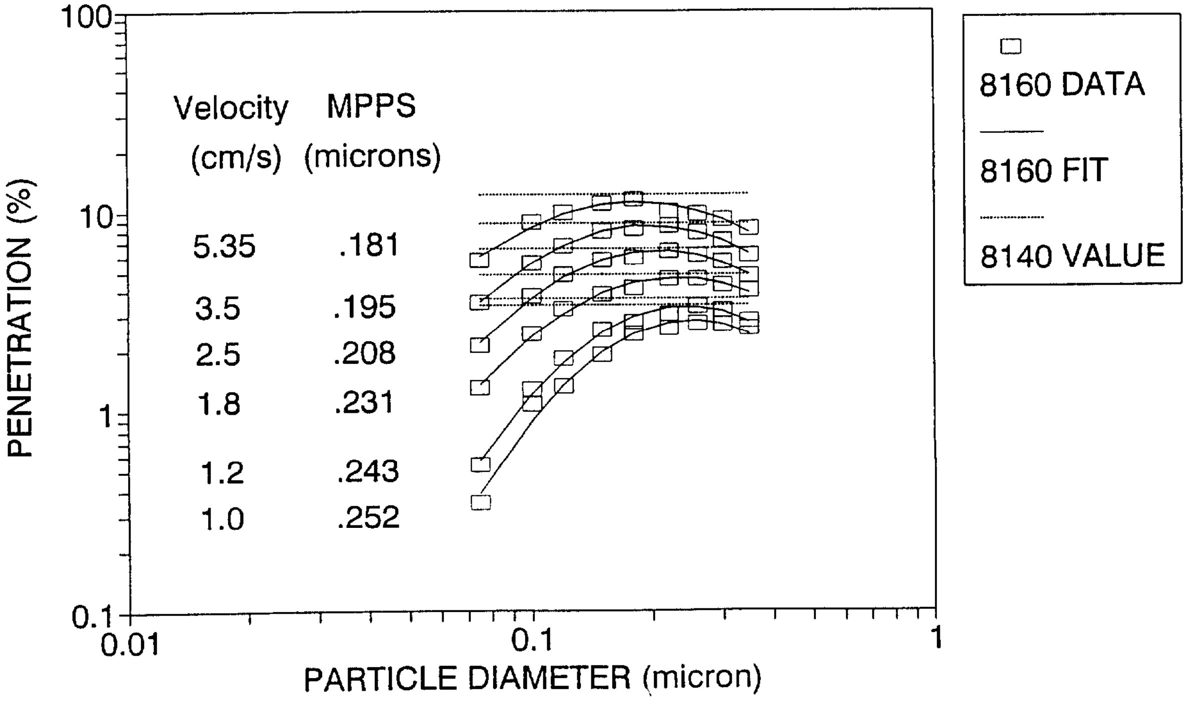

differences between the instruments, individual CNC response differences, adequate purge time at low velocity, and flow measurement precision at low velocity.

Figure 7 is a plot of Pen_{8140} values against Pen_{MPPS} values obtained from the fits to the 8160 data. Over seven orders of magnitude the two measures of penetration agree very well.

Since the 8140 gives penetration values that correlate so well with the MPPS penetration, a correlation of 8140 penetration with velocity would be useful. The 8140 data for each sample was fit to the power model for filter media penetration previously presented at this conference(5):

$$\ln Pen = \ln Pen_r (V/V_r)^N \tag{4}$$

Where Pen = Penetration fraction at face velocity, V

and Pen_r = Penetration fraction on the same sample at the reference velocity, V_r

The R^2 values obtained from these regressions were all above 0.98. Figure 8 is a graph showing the velocity dependence of 8140 penetration for the typical media samples shown earlier. The ULPA, HEPA, and Sub-HEPA curves are parallel having N values equal to -0.24. The 95% DOP media is different, however, having a slope of -0.28.

The determination of the N value for a filter medium or filter media family allows for measurement of penetration at a reference velocity within reasonable operating parameters of the test equipment and estimation of the penetration at the low application velocities which will be encountered.

Conclusions

A comparison of the penetration performance values between the TSI CertiTest 8160 and the TSI Model 8140 has shown that the penetration value obtained from the 8140 correlates very well to the MPPS penetration obtained from the 8160 penetration curve for penetrations spanning several orders of magnitude.

The 8140 penetration is related to face velocity by a power law model. This can be a useful tool for specifying media penetration performance at reasonable test equipment operating parameters.

FIGURE 7
8140 PENETRATION VS MPPS PENETRATION

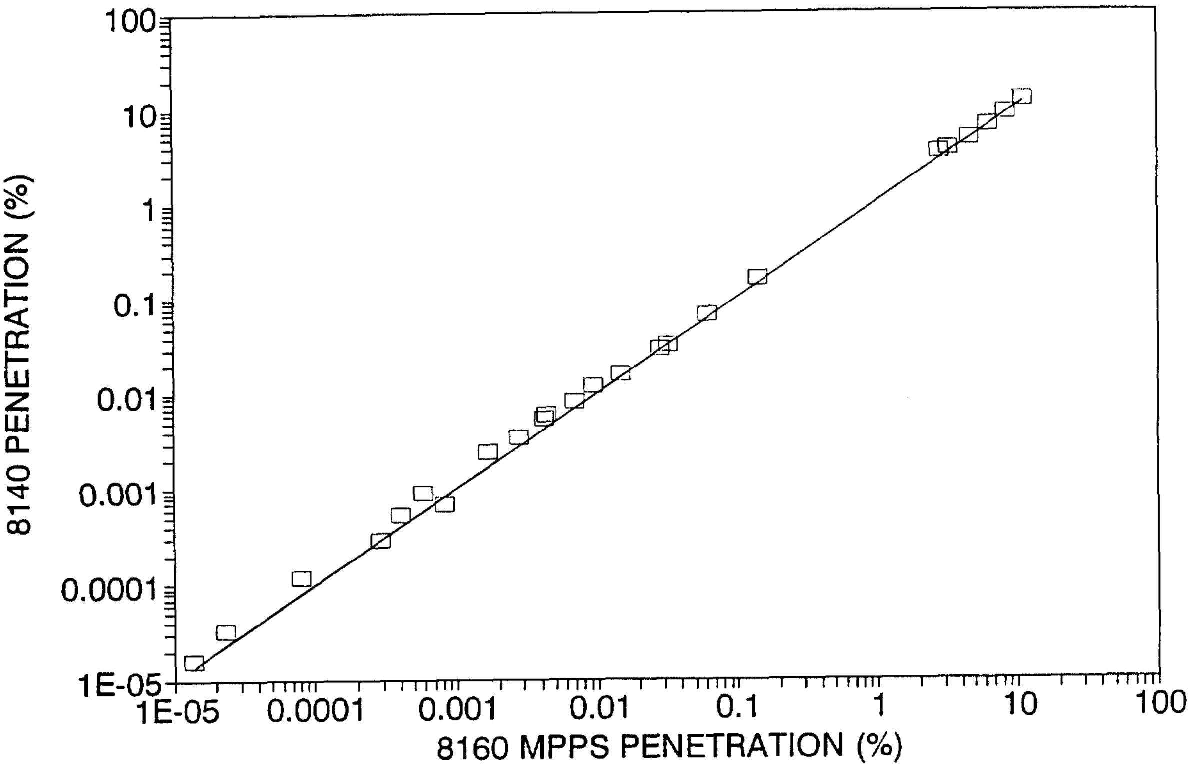

FIGURE 8
EFFECT OF VELOCITY ON PENETRATION

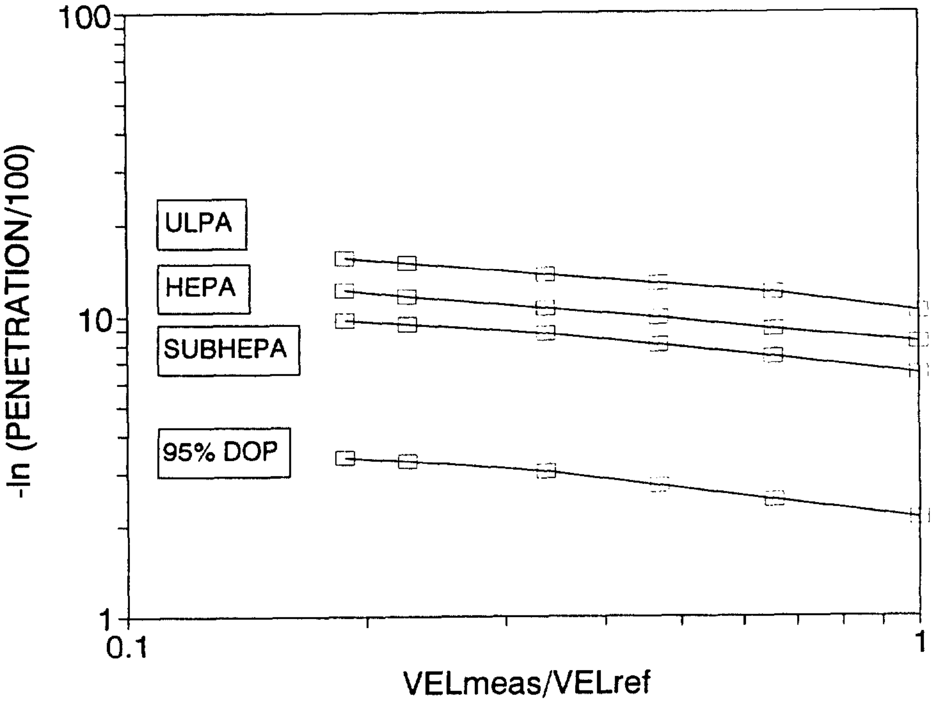

24th DOE/NRC NUCLEAR AIR CLEANING AND TREATMENT CONFERENCE

Bibliography

(1) IES-RP-CC021.1, "Testing HEPA and ULPA Filter Media", 1993. Institute of Environmental Sciences, 940 East Northwest Highway, Mount Prospect, IL 60056.

(2) CEN/TC 195/WG 1/N 023, "Final Draft Specifications for Particulate Air Filters for General Ventilation", 1991. Institute Belge de Normalisation, C/o INIEX-ISSeP - Division de Colfontaine, Sec. of CEN/TC 195/WG-1 - rue Grande, 60 - B-7340 Colfontaine, Belgium.

(3) TSI Incorporated, 500 Cardigan Road, St. Paul, MN, "CertiTest Model 8160 Automated Filter Tester Operation and Service Manual", 1993.

(4) TSI Incorporated, 500 Cardigan Road, St. Paul, MN, "Model 8140 Automated Filter Tester Operation and Service Manual", 1992.

(5) Pierce, M., Guimond, R., Lifshutz, N. "A General Correlation of DOP Penetration With Face Velocity as a Function of Particle Size Using the FTS-200", CONF-880822, pp. 973-982, Proceedings of the 20th DOE/NRC Nuclear Air Cleaning Conference, Boston, MA (1988).

DISCUSSION

SCRIPSICK: How does the particle size at maximum penetration and the penetration curve compare to theory? Did you look at that? We have seen that theory predicts much greater slope values than measurements on filters.

PIERCE: We have not compared our laboratory flat sheet results to any computer models of what the theoretical penetration would be. As a general comment, we have observed that the theoretical penetration curves tend to have steeper slopes on either side of the most penetrating particle size than test data.

DYMENT: Please comment on the relationship between the MPPS and efficiency of the different media which you chose to use.

PIERCE: Theory dictates that as face velocity is decreased, penetration will increase and the most penetrating particle size will increase. I believe this is because diffusional effects are more pronounced and inertial effects are less pronounced at lower and lower velocities, so that larger particles become more penetrating. Also, it is generally observed that as efficiency between media samples is reduced, effectively increasing the mean fiber diameter within the media samples, the MPPS increases.

FURTHER DEVELOPMENT OF THE CLEANABLE STEEL HEPA FILTER, COST/BENEFIT ANALYSIS, AND COMPARISON WITH COMPETING TECHNOLOGIES*

by

W. Bergman, G. Larsen[1], R. Lopez, K. Wilson, C. Witherell and M. McGregor
Lawrence Livermore National Laboratory
Livermore, CA 94550

ABSTRACT

We have made further progress in developing a cleanable steel fiber HEPA filter. We fabricated a pleated cylindrical cartridge using commercially available steel fiber media that is made with 1 µm stainless steel fibers and sintered into a sheet form. Test results at the Department of Energy (DOE) Filter Test Station at Oak Ridge show the prototype filter cartridge has 99.99% efficiency for 0.3 µm dioctyl phthalate (DOP) aerosols and a pressure drop of 1.5 inches. Filter loading and cleaning tests using AC Fine dust showed the filter could be repeatedly cleaned using reverse air pulses. Our analysis of commercially optimized filters suggest that cleanable steel HEPA filters need to be made from steel fibers less than 1 µm, and preferably 0.5 µm, to meet the standard HEPA filter requirements in production units.

We have demonstrated that 0.5 µm steel fibers can be produced using the fiber bundling and drawing process. The 0.5 µm steel fibers are then sintered into small filter samples and tested for efficiency and pressure drop. Test results on the sample showed a penetration of 0.0015 % at 0.3 µm and a pressure drop of 1.15 inches at 6.9 ft/min (3.5 cm/s) velocity. Based on these results, steel fiber media can easily meet the requirements of 0.03 % penetration and 1.0 inch of pressure drop by using less fibers in the media.

A cost analysis of the cleanable steel HEPA filter shows that, although the steel HEPA filter costs much more than the standard glass fiber HEPA filter, it has the potential to be very cost effective because of the high disposal costs of contaminated HEPA filters. We estimate that the steel HEPA filter will save an average of $16,000 over its 30 year life. The additional savings from the clean-up costs resulting from ruptured glass HEPA filters during accidents was not included but makes the steel HEPA filter even more cost effective.

---

[1] Present address: Kennerley-Spratling, Inc., 2116 Farallon Dr., San Leandro, CA 94577-6694

*This work was performed under the auspices of the U.S. Department of Energy by Lawrence Livermore National Laboratory under contract no. W-7405-ENG.45 and is based on the reports cited as references 1 and 2.

We also present the results of our evaluation of competing technologies with metallic and ceramic powder filters, ceramic fiber filters, and reinforced glass fiber filters. In general, the metallic and ceramic powder filters have pressure drops in excess of 25 inches of water for HEPA grade efficiencies and are therefore not viable candidates. The ceramic fiber filters cannot meet the HEPA efficiency because the fiber diameters are too large. The reinforced glass fiber filter is a promising candidate for the cleanable HEPA filter but requires additional development and testing to confirm its potential to be repeatedly cleaned.

This report is based upon material extracted from a DOE technical review of the Mixed Waste Integrated Program and from the final report of a systems analysis of cleanable steel HEPA filters.(1,2)

I. Introduction

Cleanable steel filters have been used for many years by various industries, including the nuclear industry, to provide high efficiency filtration with minimal maintenance. These filters were made from steel powder that was sintered together and formed into a hollow cylinder. Compressed air pulses were directed into the interior of the cylinder to dislodge particle deposits that had formed on the outside of the cylinder. Figure 1 illustrates the basic concept of the cleanable steel filter having multiple filter elements in a single housing, a blow-back gas for cleaning, and a hopper for collecting the particles.

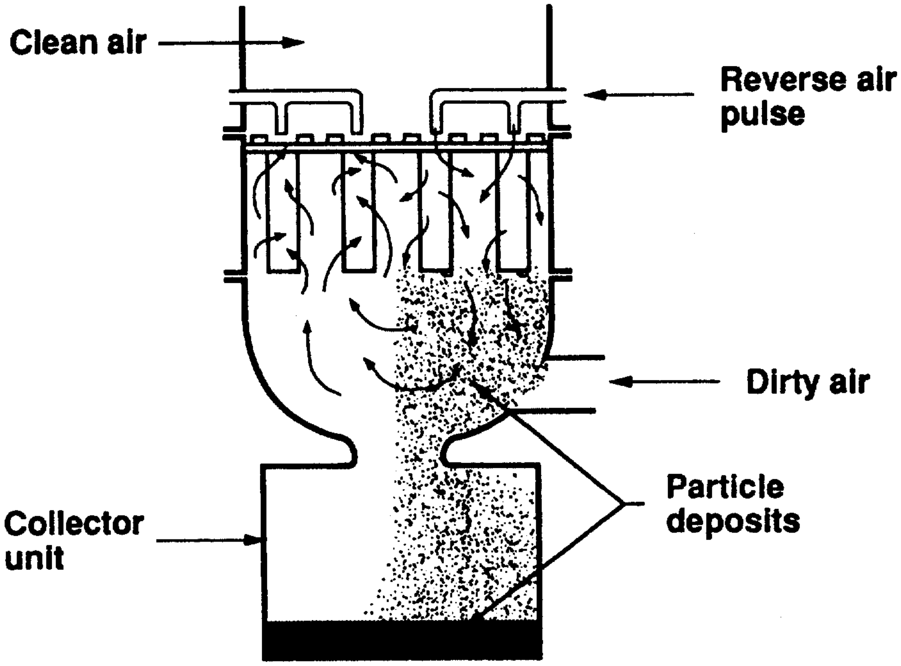

Figure 1. Typical cleanable filter with multiple cartridges and a blow-back cleaning apparatus.

The cleanable filter shown in Figure 1 is a well established design used with many other filter elements such as cloth bags, ceramic tubes, and polymeric tubes. Design variations include other filter shapes than cylinders such bayonets, stacked plates, hollow panels, etc. All filter elements have an exterior surface for collecting the deposited particles and an interior volume through which the cleaned gas exits and through which a blow-back gas is used to dislodge the deposited particles.

The applications for these filters range from recovery of catalysts in petroleum refineries to off-gas filtration in incinerators. Rocky Flats had used sintered metal filters to remove the suspended particulate from a fluidized bed incinerator that burned transuranic waste contaminated with plutonium.(3) The sintered metal filters were repeatedly cleaned by reverse air pulses. Kirstein et al also showed that sintered metal filters had excellent performance in both removal efficiency and reverse air-pulse cleaning for applications in another incinerator.(4) The filters are robust and require minimal maintenance. Despite the excellent performance of the sintered metal filters, they only had about 60% DOP efficiency when clean and had relatively high pressure drops.(5)

In the early 1980s, researchers in Europe had developed high efficiency air filters using the new filter media from Bekaert that was made from 2 µm steel fibers. Dillmann et al described the use of 2 µm stainless steel fibers to make deep bed filters for use as vent filters in nuclear power reactors.(6,7) The deep bed filters had efficiencies comparable to the glass HEPA filters but were much larger and could not be cleaned. Klein and Goossens showed major improvements in filter efficiency with decreasing diameter of the steel fibers from 12 to 4 µm.(8) However, the efficiencies were far below HEPA grade. They also showed that deposits of methylene blue aerosols could be efficiently cleaned from a cylindrical filter by washing with a water spray.

By the late 1980's, Pall Corp. had developed cylindrical filter elements using steel media having separate layers of sintered steel fibers and sintered steel powder. Randhahn et al described a stainless steel filter from Pall Corp.(9) that had efficiencies comparable to a HEPA filter, but they did not report any pressure drops. The filter consisted of two layers of 5µm fiber media and one layer of fine powder metal. Our tests showed that the filter had a pressure drop of 2.2 psi (61 inches of water) at 13 cfm, which corresponds to 1,000 cfm through a standard size HEPA filter.(10) A variation of the Pall filter with lower pressure drop and lower efficiency was installed as a prefilter in all of the French nuclear power plants.(11)

In 1990 Bergman et al showed that by eliminating the use of steel powder and using the smallest available steel fibers, filters could be made that had the same efficiency as a HEPA filter and a pressure drop only three times as great.(12) Bergman then used this new filter to begin developing a cleanable steel HEPA filter.(13)

Two designs of the cleanable steel HEPA filter have been developed to date: an assembly of multiple cartridges housed in a standard 2' x 2' x 1' frame and multiple cartridges housed in a pressure vessel. We developed the basic design parameters for the steel filter that can be retrofitted into the standard HEPA housing.(14) This filter design consists of 64 individual filter cartridges housed in a standard HEPA filter frame of 2' x 2' x 1'. We were only able to use 150 ft^2 of media in the filter instead of the minimum 200 ft^2 found in glass HEPA filters. This limitation was due to the clindrical cartridge design, that prevented more media from being used. The cleanable steel filter, shown in Figure 2, consists of 64 cartridges assembled into the HEPA filter housing.

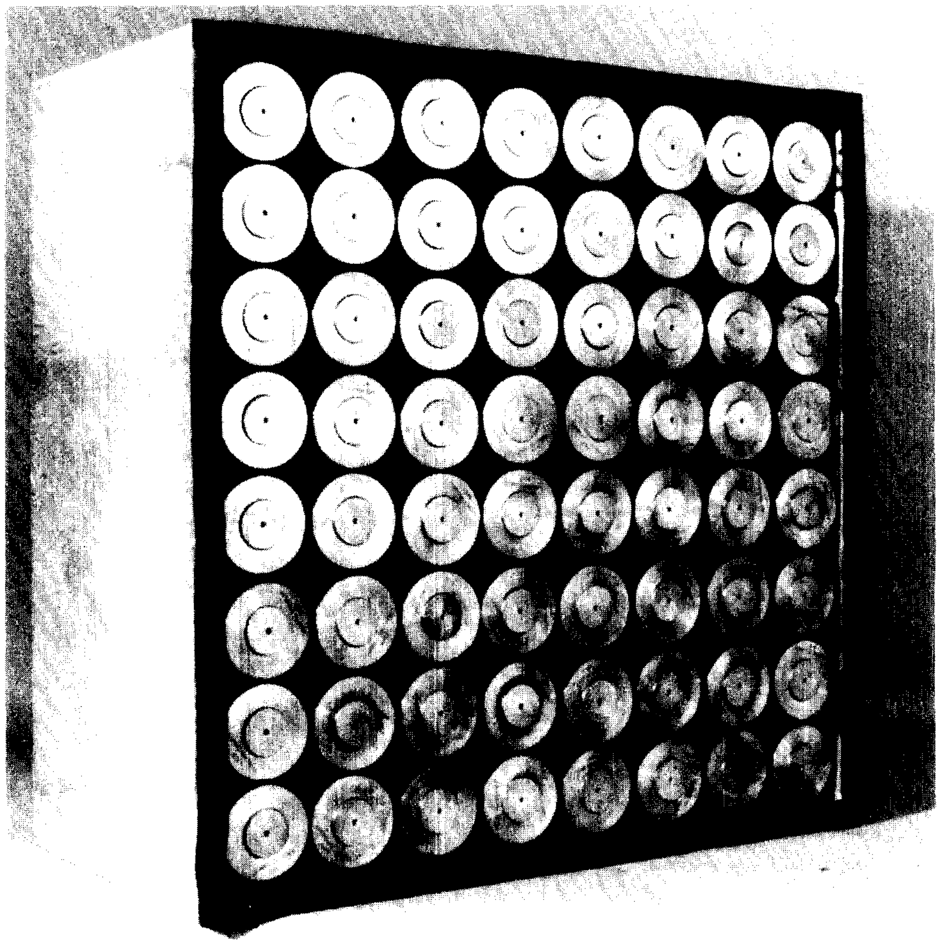

Figure 2 Photograph of the assembled cleanable steel filter using the flat panel design with 64 cartridges

We made two cleanable steel filters like that shown in Figure 2 using filter cartridges from Pall Corporation and Memtec Corporation and evaluated their performance.(14) The filter media used to make the filter cartridges was made from 2 μm steel fibers sinctered into sheets and pleted to increase the surface area. Both filters met the required 0.03 % DOP penetration, but had a pressure drop of 3 inches and weighed over 200 pounds. After a successful laboratory demonstration that the filters could be repeatedly cleaned by reverse air pulses and reused, both filter units were evaluated in the exhust stream of a uranium oxide grit blaster at the Y-12 Plant in Oak Ridge, TN.(15) The field evaluation was not completed because water accumulation in the exhaust system caused excessive pressure drop and interfered with the filter cleaning studies.(15) Since additional funds were not available to dry the wet exhaust, the field evaluation was prematurely terminated.

In addition to the panel filter design shown in Figure 2, the cleanable steel filter can be designed as a pressure vessel for use in applications that do not require retrofitting into existing housings. Pall Corp. has built several units in which multiple cartridges are housed inside a pressure vessel as shown in Figure 3. This is the design that was to be used in the vitrification plant at Hanford.(16,17) The filter in Figure 3 is cleaned using a reverse water flush. Tests by Pall using Arizona road dust show that fully loaded filters can be efficiently cleaned using the water wash.(18,19)

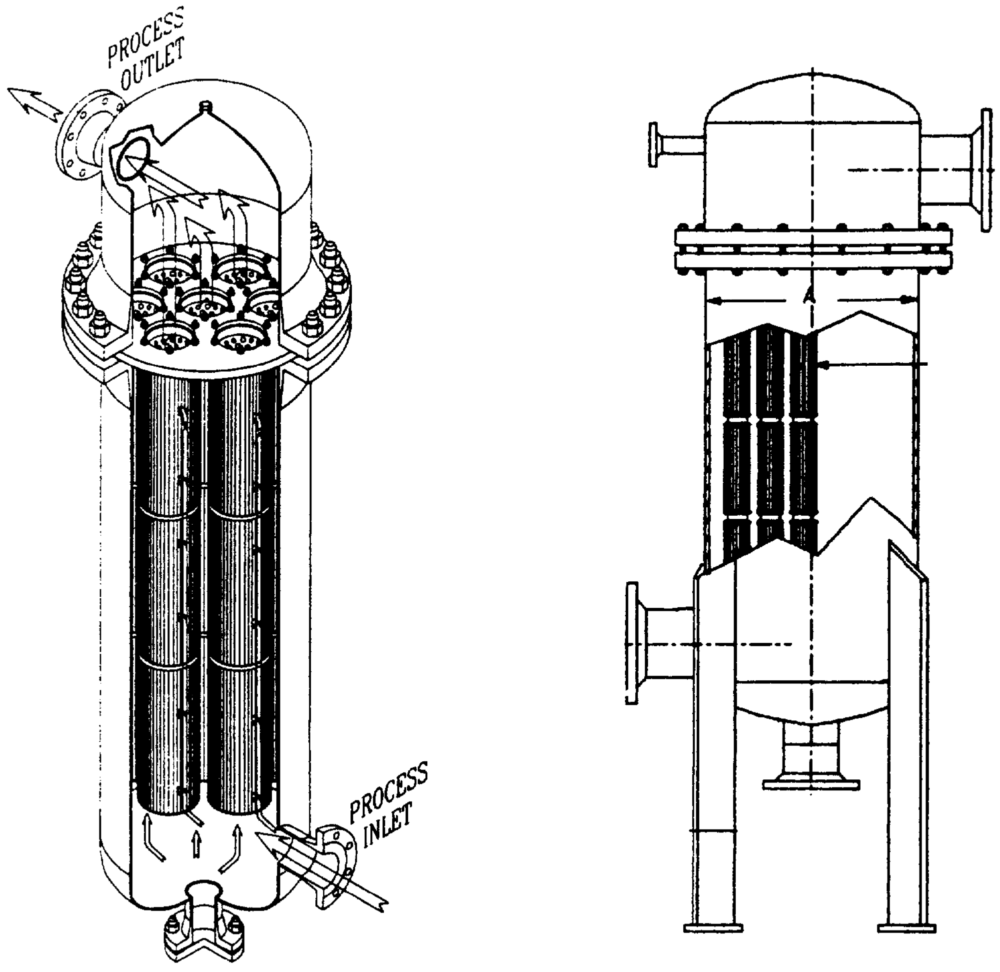

Figure 3. Drawing and schematic of the cleanable steel filter with filter cartridges housed in a pressure vessel.

Neither of the two steel HEPA designs shown in Figures 2 and 3 have been accepted by the nuclear industry as replacement for the glass HEPA filter. The cleanable steel filter shown in Figure 2, which is designed for both new and retrofit applications, has the overall dimensions of a standard glass HEPA filter, but has an unacceptable high pressure drop and weighs too much. Installing more powerful blowers to overcome the high resistance is not acceptable because of the extra cost and the misbalance introduced into existing building and system ventilation systems. In addition, special lifting and positioning equipment would be needed to install and remove the 200 pound filters. In our field demonstration of the cleanable filter, we built a specially designed alignment table and mounted it on a scissors lift in order to install the steel filter.(15) Unfortunately, this type of equipment could not be used in most existing HEPA filtration systems due to space limitations. The high pressure drop, high weight and special lifting equipment are only a problem in existing filtration systems and not in future systems that can be designed to accomodate the special requirements.

The pressure vessel design in Figure 3, which is intended for new filtration systems, also has high pressure drop, high weight and requires special lifting equipment. This design had been selected for use in a waste vitrification plant at Hanford prior to the cancellation of the plant.(16,17) The pressure vessel design was selected over a deep-bed sand filter for that application.(16) The initial cost of the steel HEPA filter was also less than the cost for the deep bed sand filter. However, both the steel HEPA and the sand filters cost far more than the conventional HEPA filter.

Another major reason why steel HEPA filters are not selected over glass HEPA filters in the nuclear industry is their high cost. The current steel HEPA filter shown in Figure 2 costs about \$70,000 compared to \$300 for the glass HEPA filter.(20) The cost for the pressure vessel design shown in Figure 3 is estimated at \$109,000.(20) These costs are for current prototype steel HEPA filters. We have estimated that the cost of the panel filter in Figure 2 could be reduced to \$5,000 with further development and with production efficiencies.(14)

Despite the much higher costs for the steel HEPA filters compared to the glass HEPA filters, the high cost of disposing of contaminted HEPA filters made the steel HEPA filters appear economically attractive. Our previous cost analysis shows that a \$5,000 steel filter would save \$54,000 over its life compared to glass HEPA filters.(14) This cost saving is due to the average cost of \$4,450 for handling and disposing of glass HEPA filters.(21) Implicit in the cost estimate was that the glass filter had a 3 year life while the steel HEPA filter had a 45 year life.(14) If the assumptions were significantly in error, then the potential cost savings could disappear. Although no additional data on the assumptions was available since our last estimate, we have performed a sensitivity analysis of the potential cost savings as a function of the assumed input parameters.(2) That analysis, which will be summarized in this report, shows that the cleanable steel HEPA filter is still cost effective under a wide range of assumptions.(2)

In order to overcome the identified deficiencies in peformance and the high cost, further development of the steel HEPA filter is required before it can replace the glass HEPA filter. We will summarize the recent developments of the cleanable steel fiber HEPA filter and compare the performance with competing technologies.

II. Reduction in Pressure Drop Achieved With Smaller Diameter Fibers

The most important parameter that controls the efficiency and pressure drop of fibrous filters is the diameter of the fibers used in the filter medium. To illustrate this point, we have plotted the minimum efficiency and the filter pressure drop in Figure 4 for typical commercial glass fiber filters as a function of the average fiber diameter used in the filter media. The minimum efficiency, pressure drop and fiber diameter for each of the filters identified in Figure 4 represent typical values for each class of filter. The filters are normailized to the same dimensions (2' x 2' x 1') and flow rate (1,000 cfm). As seen in Figure 4, the efficiency increases much faster than the pressure drop with decreasing fiber diameter. Since the filters used to generate the curve in Figure 4 represent typical commercial products, we assume that the filters have been optimized to maximize the efficiency and minimize the pressure drop. Thus filter media with smaller diameter fibers are needed for higher efficiency filters.

Using Figure 4, we can illustrate that reducing the fiber diameter is more effective than alternative approaches such as increasing the amount of fibers or the thickness of the media to obtain filters with the desired efficiency and pressure drop. For a filter medium having a fixed fiber diameter, higher efficiencies are obtained by adding more layers of media. For example two layers of a 95% efficient ASHRAE filter with 1 μm fiber media will yield a filter with a combined efficiency of 99.75% ($E= 1-(1-.95)(1-.95)= 0.9975$). The pressure drop for the combined layers is twice the single layer (0.5 inch), or 1.0 inch. Alternatively, Figure 4 shows that by using a filter media with 0.7 μm diameter fibers, we can reach the same efficiency but only have a pressure drop of 0.7 inches.

We applied the principle of reducing the fiber diameter to improve the performance of the steel filters. The commercially available steel filters shown in Figure 2 meet the HEPA filter efficiency requirement but have a pressure drop of 3 inches of water. In order to reduce the pressure drop to the required 1 inch, the steel fiber media must be made from fibers having diameters about 0.5 μm instead of the present 2.0 μm diameter.

We have fabricated and tested a filter cartridge element using steel media obtained from Tomeogawa Inc. that was made from 1 μm diameter, 316L stainless steel fibers.(1,22,23) An electron micrograph of the sintered media sheet is shown in Figure 5. Tests on the flat sheet are shown in Figure 6 where the penetration is plotted as a function of particle diameter. The face velocity is 3.5 cm/s, which corresponds to the velocity that would be obtained with 150 ft^2 of media in a full scale filter. Figure 6 shows that the 1 μm media has a penetration of 0.004% at 0.3 μm aerosol diameter and a pressure drop of 1.05 inches. Thus, the 1 μm media represents the threshold for achieving HEPA filter performance.

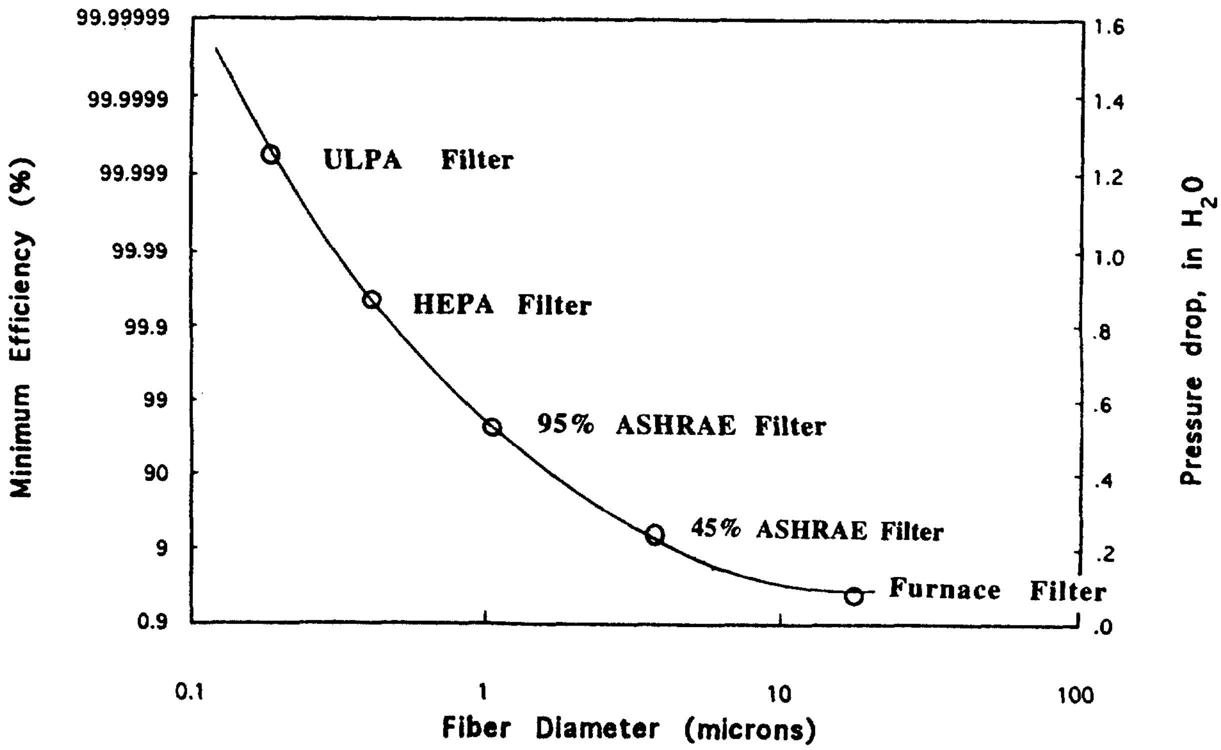

Figure 4. Relationship between the minimum efficiency, pressure drop and fiber diameter in commercial filters.

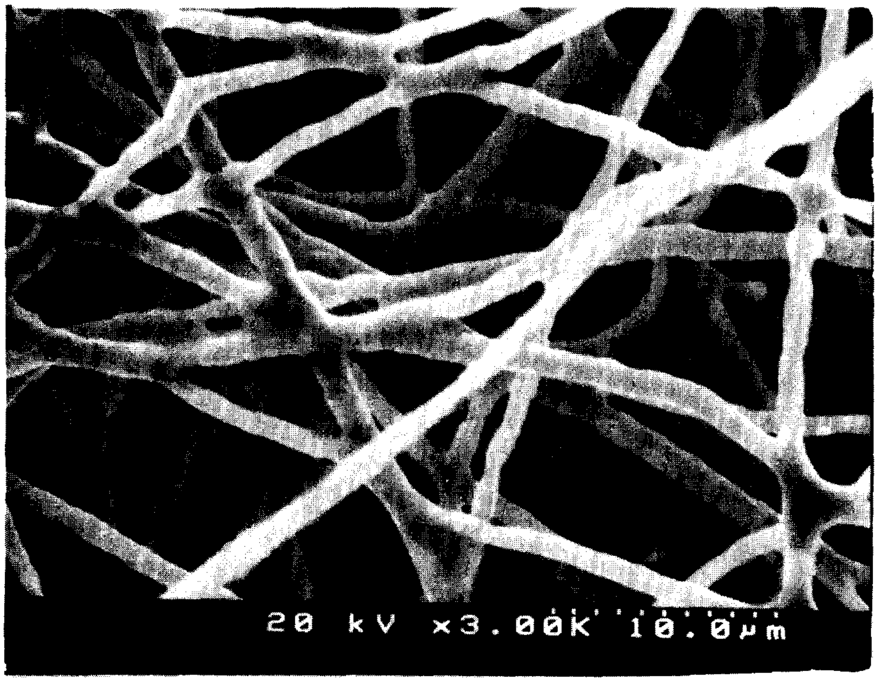

Figure 5. Electron micrograph of Tomeogawa steel fiber media made from 1 μm diameter, 316L stainless steel fibers.[23]

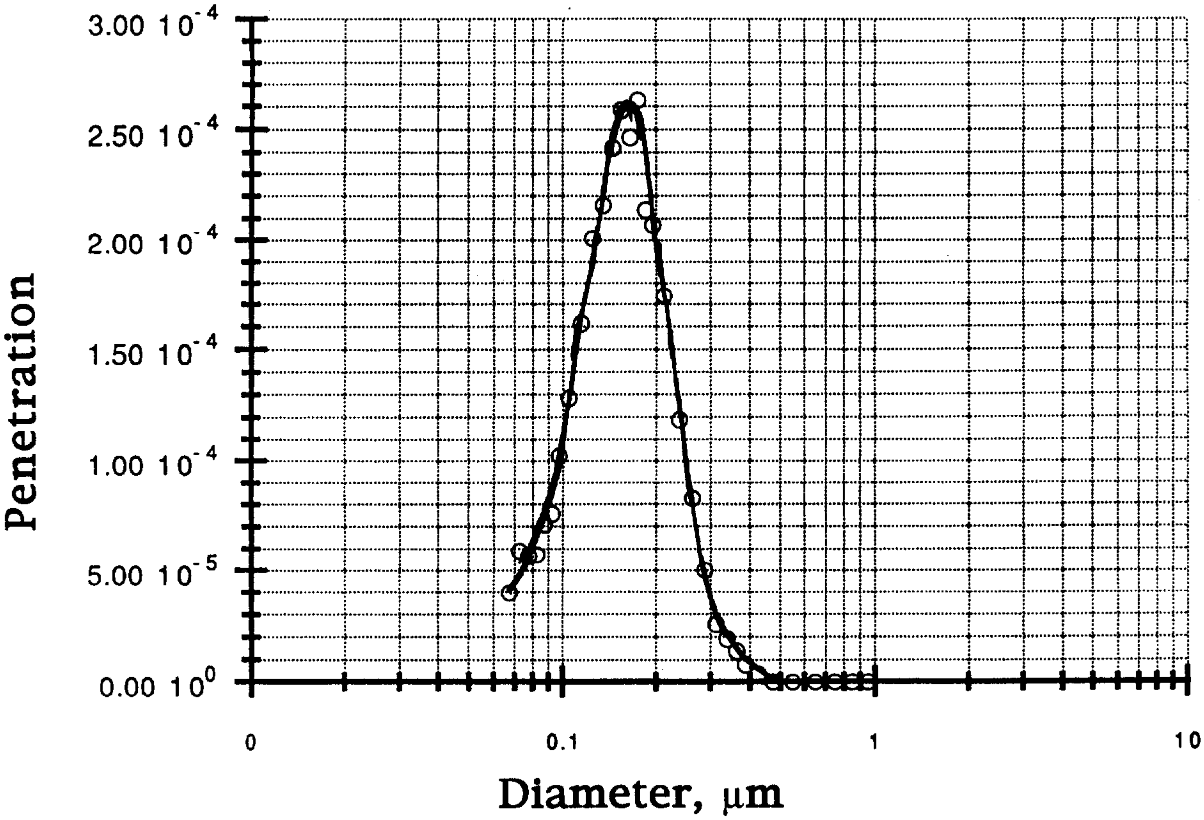

Figure 6. Penetration of DOS aerosols through 1 μm fiber media from Tomeogawa at 3.5 cm/s. Pressure drop was 1.05 inches.

The filter cartridge, shown in Figure 7, was made by sandwiching the media between support screens, pleating the composite layers, welding the composite sheet ends to form a pleated cylinder, and sealing the two, pleated, cylindrical ends in a potting compound. The pleated, cylindrical ends also could have been sealed by brazing to end caps. We used the test method and apparatus described in our previous report to evaluate the filter cartridge at 15.6 cfm to correspond to a full-scale HEPA filter.(14) Figure 8 shows the penetration of dioctyl sebacate (DOS) aerosols as a function of aerosol diameter. Although the penetration at 0.3 μm diameter is satisfactory at 0.002% , the pressure drop is 1.5 inches of water and exceeds the maximum allowable 1 inch. The major reason for the higher pressure drop in the cartridge than in the filter media shown in Figure 6 is the variablitiy in the media properties. The cartridge in Figures 7 and 8 was made from a different media batch having 50% higher pressure drop than the media in Figure 6. This variation was due to the small sample size in the media production and should not occur with larger samples. Thus, we have approached the threshold for achieving a HEPA filter using 1μm media. Steel media having fiber diameters less than 1 μm is needed for making steel HEPA filters with production variability.

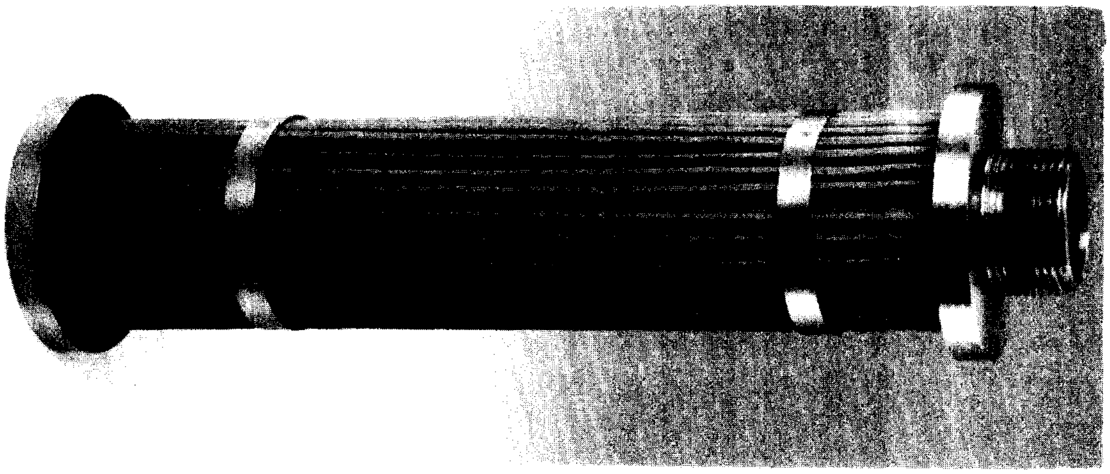

Figure 7. Pleated filter cartridge made from 1 µm steel fiber media.

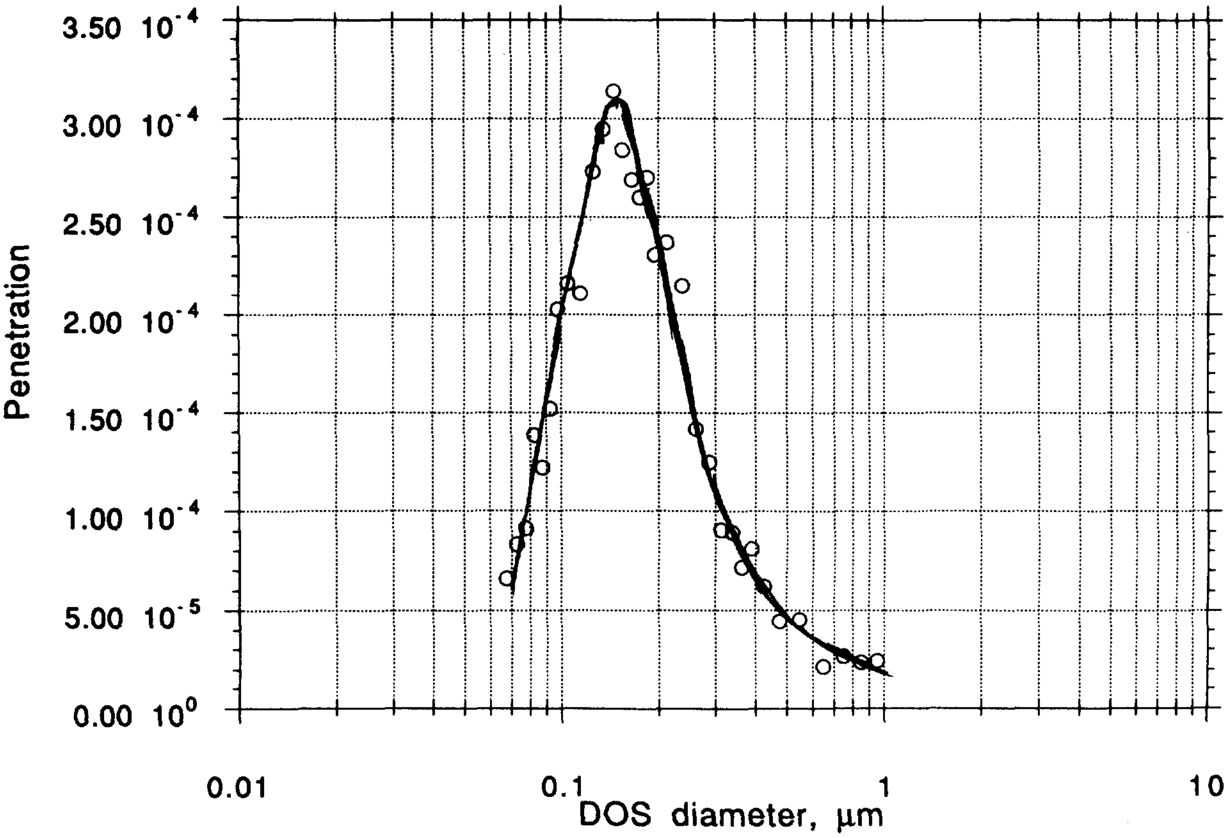

Figure 8. Aerosol penetration through filter cartridge shown in Figure 7 as a function of aerosol diameter. Pressure drop is 1.5 inches at 15.6 cfm flow.

Since the ability to clean and reuse the steel HEPA filter is an important property of the cleanable steel HEPA filter, we conducted a series of filter clogging and cleaning tests on the filter cartridge shown in Figure 7. We used AC Fine dust (Powder Technology Inc, Burnsville, MN) to load the filter and compressed air pulses to remove the particle deposits. The test system is described in our previous publication.(14) Figure 9 shows the results of loading and cleaning the filter cartridge 10 times. The test shows that the filter can be repeatedly cleaned and reused. Note that there is a small increase in the baseline pressure from 1.5 to 2.0 inches up to the fifth cleaning. Beyond that point the residual deposits in the filter remain constant.

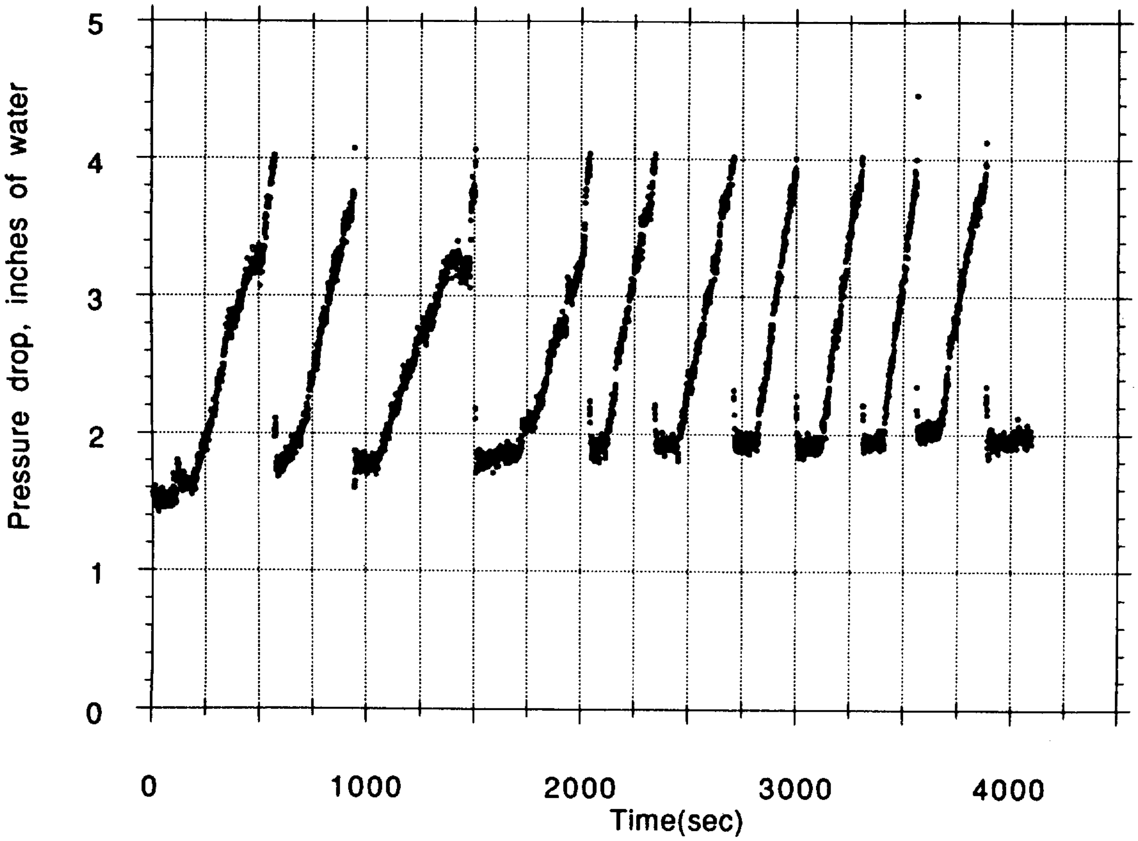

Figure 9. Filter loading and cleaning cycles using AC Fine test dust and compressed air pulses on the filter cartridge in Figure 7.

Since there are no commercial sources that can make 0.5 µm steel fibers, we used fundamental laboratory techniques based on the wire bundling and drawing process to make a small quantity of these steel fibers. The process, which is extremely labor intensive and not suitable for prototype development, involves a series of repetitive steps in which wires are bundled together into a rod and then reduced in diameter by drawing through progressively smaller dies. The starting point is a stainless steel rod that is snugly fitted inside a copper tube. We then reduced the diameter of the rod by swaging until the resulting rod could be drawn through a standard wire drawer for further size reduction. The wire drawing process was periodically interrupted to heat treat the rod to reduce the hardness induced by the drawing process. The reduced wire was then cut into fixed lengths which were then inserted into a new copper tube and the process repeated. Figure 10 shows a rod consisting of a bundle of wires being reduced in diameter through progressively smaller dies. The individual wires have a copper coating from the initial cladding operation to prevent sticking to the other wires. Figure 11 shows a cross section of the rods, starting with the original rod and going through the first, second and nth bundling. When the desired fiber diameter is reached, the copper cladding is dissolved in nitric acid and the fibers dispersed.

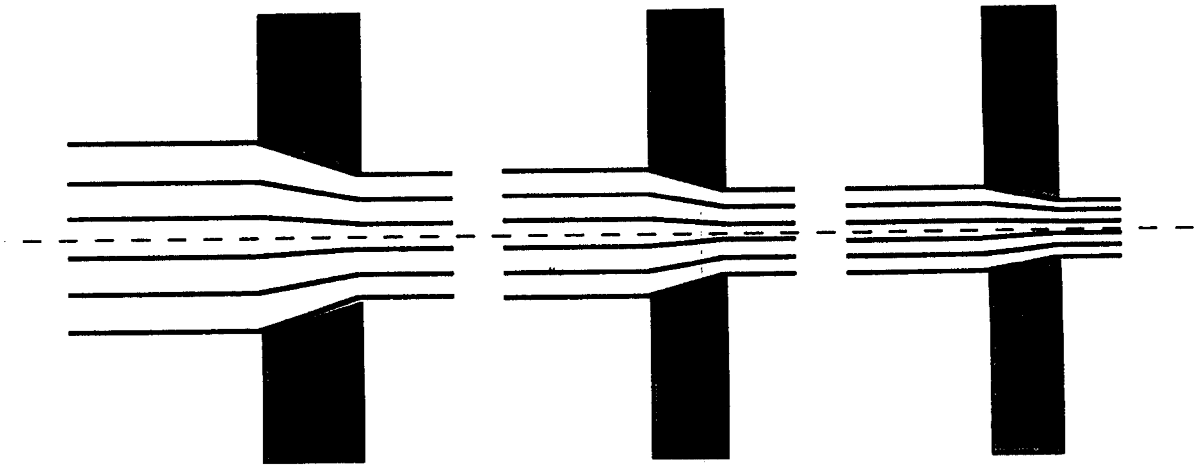

Figure 10. Wire drawing is used to produce smaller diameter steel fibers.

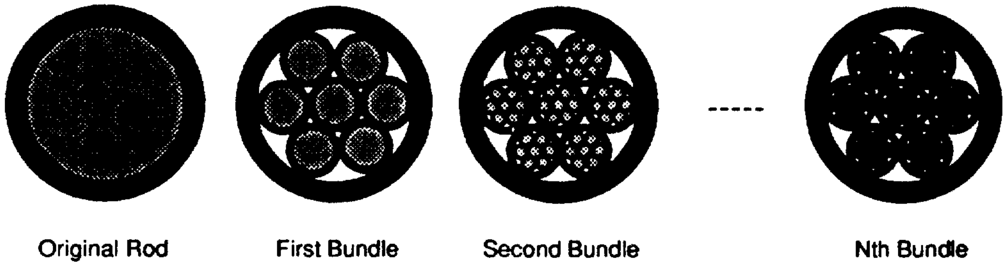

Figure 11. Cross section of steel rods from the original to increasing iterations of bundling and drawing

We then made a small sample of stainless steel fiber media from the 0.5 µm steel fibers using the paper making process followed by sintering.(1) Figure 12 shows an electron micrograph of the media. Laboratory tests at 3.5 cm/s face velocity yielded an efficiency of 99.998% for 0.3 µm dioctyl sebacate (DOS) aerosols.

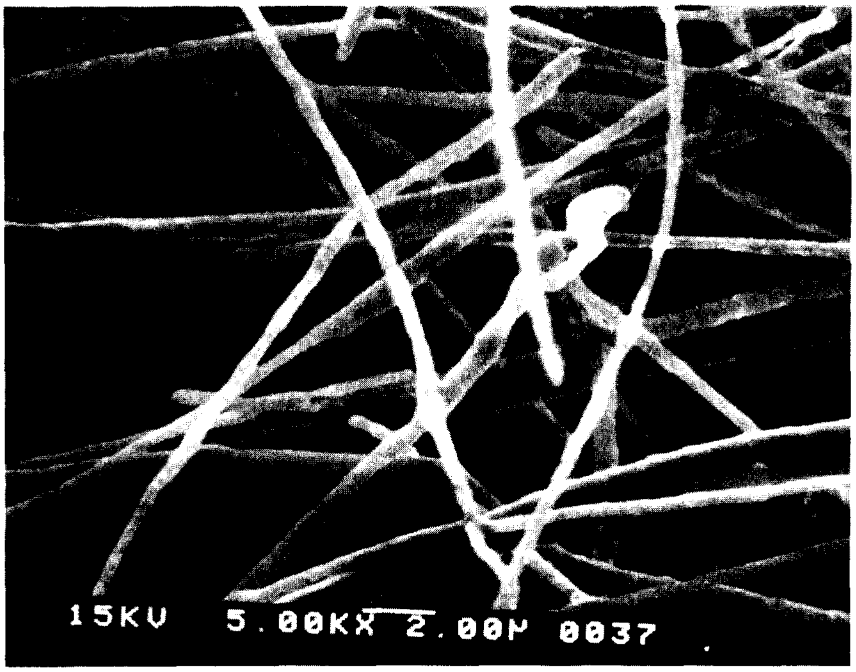

Figure 12. Electron micrograph of the steel fiber media made from 0.5 µm steel fibers.

Figure 13 shows the penetration (1-efficiency) measurement of the media as a function of particle size. The pressure drop was 1.15 inches. The media had a greater quantity of fibers than was needed to achieve the desired efficiency value. We estimate that reducing the quantity of fibers to yield an efficiency of 99.97% will result in a media pressure drop of 0.8 inches. Unfortunately, we did not have sufficient fibers to optimize the media formulation. Nevertheless, our tests have demonstrated that filter media made from 0.5 µm steel fibers will yield the desired HEPA filter performance.

We have shown the feasibility of developing a steel HEPA filter that meets the efficiency and pressure drop requirements for HEPA filters. However, the laboratory bench scale process must be scaled up in order to produce a sufficient quantity of fibers and media to make several prototype HEPA filters. This represents the next step in the development of the cleanable steel HEPA filter.

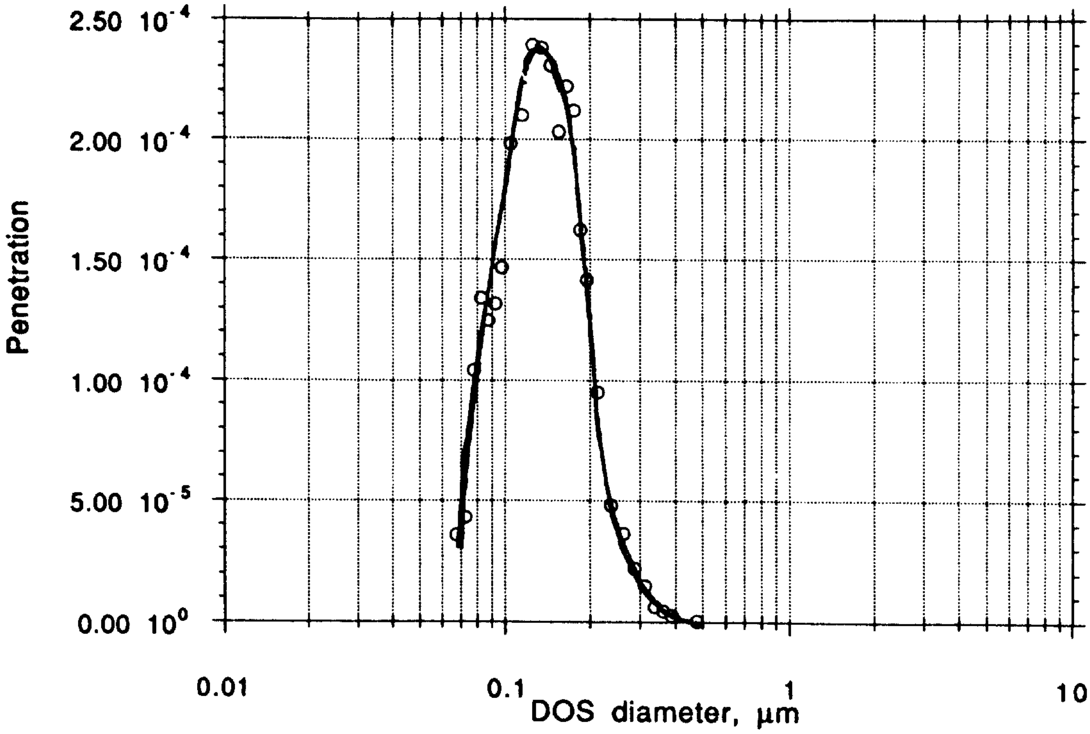

Figure 13. Aerosol penetration measurements at 3.5 cm/s face velocity through steel fiber media shown in Figure 12. Pressure drop was 1.15 inches.

III. Reduction in Weight Achieved by Using Conventional HEPA Design

Since the filter media for the steel HEPA is expected to weigh about 10 pounds for 200 square feet (glass fiber media would weigh 3.3 pounds), most of the weight is due to the support structure. The filter design that consists of multiple pleated cylinders as shown in Figure 2 would require a considerable amount of heavy metallic support elements and end plates on which to attach the cylinders. This design can not be used to fabricate a steel HEPA filter that has a comparable weight to the steel-framed HEPA with glass fiber media. To achieve the weight objective, it will be necessary to use a similar design as used for glass fiber HEPA filters. Figure 14 shows a design using corrugated separators. Since the steel media is much stronger than the glass media, it also is possible to eliminate the separators. Other designs such as the mini-pleat and Dimple Pleat™ design are also possible.(14,24) The assembly of such filters is very similar to that used for the present glass HEPA filters except that organic sealants would be replaced with a brazing compound. Any of a variety of different brazing or welding techniques can be used to seal the pleated media pack into a steel frame. The final weight of the filter is expected to be less than 60 pounds, compared to the 200 pounds for the commercial units.

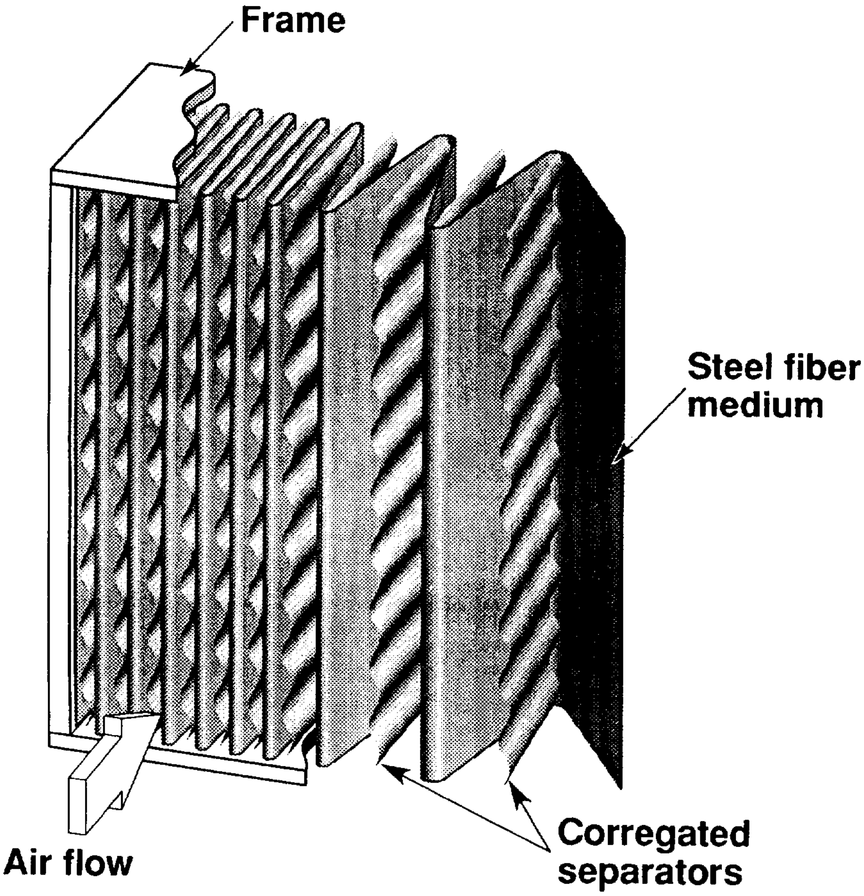

Figure 14 Cleanable steel HEPA filter with the deep pleat and separator configuration.

IV. Sensitivity Analysis Shows Cleanable Steel HEPA Flatters Are Cost Effective

The initial driver that was responsible for the early development work of the filter was the cost saving that resulted from reducing the large waste disposal costs by cleaning the filter and reusing it.(13,14) We found that during the 1987-1990 period, DOE facilities used an average of 11,478 HEPA filters per year and had an annual estimated cost of $55 million.(21) We estimated that replacing all of the glass HEPA filters with steel HEPA filters would reduce the annual costs to $13 million and save $42 million per year.(14)

Since the number of HEPA filters used by DOE facilities have decreased dramatically in recent years and the parameters used in the cost estimates are uncertain, we have performed a sensitivity analysis of the cost parameters to reevaluate the potential cost savings.(2) The annual number of HEPA filters used by DOE facilities dropped from about 12,000 in 1990 to 4,000 in 1995 as a consequence of the end of the Cold War.(2) The other major factors that determine the total cost savings from using cleanable steel HEPA filters are the average filter life for the glass and steel HEPA filters, the initial purchase price for the glass and steel HEPA filters, the installation, test, removal and disposal cost for a glass or steel HEPA filter, and the cost for cleaning the steel HEPA filter.

The average filter life for the glass-paper HEPA was estimated to be 3 years from a study of filter usage during 1977-1979.(21) If we assume that the number of facilities and operations remain constant during this period, then it is possible to estimate the total number of filters in DOE facilities by multiplying the number of filters tested each year by the average life. For the period between 1977-1979, DOE tested an average of 10,352 filters and therefore had 31,055 filters in its facilities.

Once we have the total number of filters, we can estimate the average filter life by dividing the total number of filters by the annual number tested. Assuming the total number of active filters is still about 31,000, we estimate that the average filter life is (31,000/4,000 = 7.8) 7.8 years. This estimate is reasonable based on the filter age data from Lawrence Livermore National Laboratory as of 10/13/94 that is shown in Figure 15. However, the 4,000 annual filters reflect a relatively idle DOE undergoing a major redirection following the end of the Cold War, and a large fraction of DOE operations, such as environmental clean-up , waste processing and weapons manufacturing are not yet in full operation. The number of HEPA filters used is expected to significantly increase with a corresponding decrease in the average HEPA life as DOE begins to process its radioactive waste and decontaminate and decommission its facilities. For our analysis, we will assume the average filter life will fall within the range of 3 years for full production and 7.8 years for primarily idle operation. The average is 5 years. In addition, there is a growing trend for DOE facilities to impose a 5 year life time on glass HEPA filters because of deterioration with age.(25)

The life of the steel HEPA is another uncertain parameter in the potential cost savings from using steel HEPA filters. The life of the cleanable steel HEPA filter, assumed be 45 years in our original cost savings estimate, is probably much less.(14) The 45 year life estimate assumed that the steel HEPA filter would last the life of a typical facility, hence 45 years. However, the life of the steel HEPA depends on the environment to which the filter is exposed. For a relatively clean, non-corrosive environment, this is probably still a good estimate. However, if 304 or 316 stainless steel filters are exposed to a halide salt or acid environment, then the filter will rapidly degrade due to chemical attack. In fact, these filters should not be used in those environments. For applications in corrosive environments, the fibers should be made from Hastelloy or Inconel. Unfortunately, these fibers are only available in diameters greater than 8 μm, which are not suitable for HEPA filters as seen in Figure 4.

In addition to chemical attack on the fibers, the filter life is also determined by the ability to clean the filter. If the filter cannot be effectively cleaned, then the filter life will be shortened. In our cost analysis, we have assumed a life of 30 years. This is based on having a minimum of six cleanings (i.e. six equivalent glass HEPA filters, each having a 5 year life). In our laboratory tests, we were able to repeatedly clean the steel HEPA for an equivalent of 15 glass HEPA filters.(14)

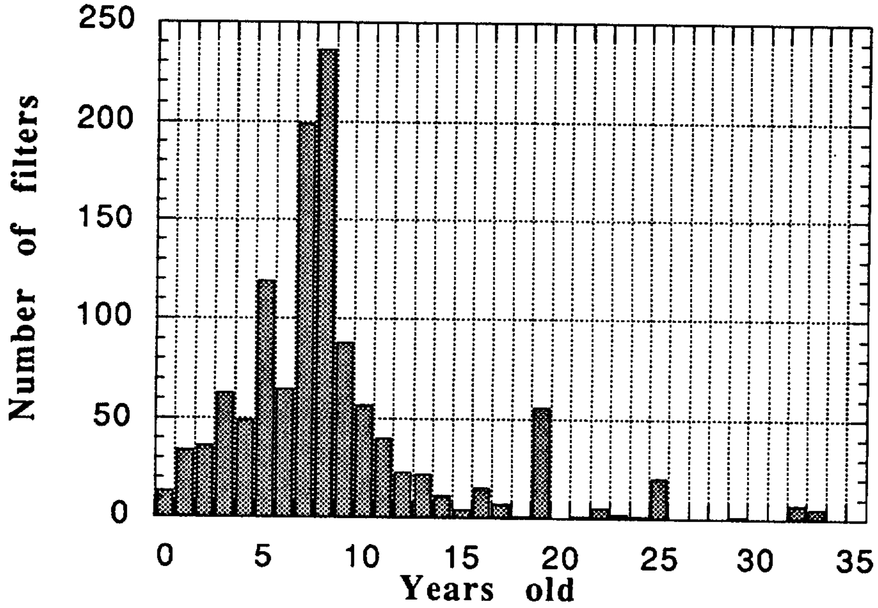

Figure 15. Distribution of HEPA filter age at LLNL as of 10/13/94. The filters are size 5.

Another uncertain parameter in the cost analysis is the final cost of the cleanable steel HEPA filter after it is completely developed and in production. We have assumed that the cost of the steel HEPA filter can be reduced to $5,000 through further development work and with efficiencies in mass production. The present cost of a cleanable steel filter with 3 inches pressure drop and weighing 200 pounds is about $70,000.(20) In contrast a standard glass HEPA filter, which weighs about 40 pounds, costs about $300.

The cost for the installation, test, removal, and disposal was $4,450 as obtained from a survey of life-cycle costs of glass HEPA filters for the period 1987-1990.(21) We assumed that this cost would be the same for both the prototype and the steel HEPA filter. The prototype steel filter would have a slightly higher cost because of its greater weight, but we have ignored that in our analysis.

The final parameter to be considered in our cost analysis is filter cleaning costs. We have assumed reverse pulse air cleaning or filter removal and off-line washing would be the primary cleaning methods. Pall has also developed and successfully tested an on-line water cleaning method for their pressure vessel design.(18,19) We have estimated that each cleaning cycle would cost $500 based on labor costs. The associated capital costs for the cleaning hardware (e.g. blow back tubes) would be lumped into the initial cost for the filter element housing or in the initial cost of the steel HEPA filter.

We have summarized the various costs and parameters for the glass HEPA filter, the commercially available steel filter, and the fully developed cleanable steel HEPA filter in Table 1. We have also computed the total filtration cost for a given HEPA filter installation over 30 years. The total filtration cost for the HEPA filters are given by:

$$C_{GT} = (30/L_{GF})(C_{GF} + C_M) \qquad (1)$$

$$C_{ST} = (30/L_{SF})(C_{SF} + C_M) + N_C(C_C) \qquad (2)$$

where C_{GT} = total filtration cost for glass HEPA in a single installation over 30 years.

C_{ST} = total filtration cost for steel HEPA filter in a single installation over 30 years.

L_{GF} = Life of glass HEPA filter, years

L_{SF} = Life of steel HEPA filter, years

C_{GF} = Initial cost of glass HEPA filter

C_{SF} = Initial cost of steel HEPA filter

C_M = Maintenance cost of installation, test, removal and disposal

C_C = Cleaning cost of filter

N_C = $30/L_{GF}$ = Number of cleanings

Equation 2 incorporates the assumption that the steel HEPA is cleaned prior to disposal at the end of its useful life. The cost of the cleaning system that is required for retrofit applications is included in the cost of the cleanable steel HEPA because it is small compared to the cost of the filter. The cleaning system would either consist of an in-duct reverse air pulse jet or the filter would be removed for off line cleaning in a liquid bath.

Once the costs for glass and steel HEPA filters are determined from Equations 1 and 2 respectively, a variety of other cost figures can be computed such as annual costs per filter location, total and annual cost savings for steel HEPA filters compared to glass HEPA filters, and total DOE filter costs and total savings. We have made these computations in Table 1.

As seen in Table 1, the commercially available steel filter is not cost effective because of the high purchase cost of $70,000 and the few cleaning cycles for applications having an average HEPA life of 5 years. This explains why these filters are not being used in applications where conventional glass HEPA filters are used. The steel HEPA filter becomes more cost effective with increasing cleaning cycles because of the $4,450 in handling and waste disposal costs that are saved with each cleaning. Table 1 also shows that the steel HEPA filter costing $5,000 is very cost effective for the given assumptions. We believe that this cost reduction is achievable with additional development and improvements in production methods.

To assess the sensitivity of the filtration costs and cost savings to variations in the key parameters in Table 1, we used Equations 1 and 2 to determine the total cost as a function of the glass HEPA life (or cleaning frequency), the purchase cost of the steel HEPA filter, and the service life of the steel HEPA. Details of the sensitivity study are presented in our previous report.(2)

Table 1. Comparison of costs and parameters for glass HEPA and cleanable steel HEPA filters.

	Glass-paper HEPA	Stainless steel HEPA	
		Commercial	After Development
Filter element (1000 ft^3/min)	$300	$70,000	$5,000
Installation, test, removal, and disposal	$4,450	$4,450	$4,450
Cleaning	$0	$500/cleaning	$500/cleaning
Average filter life	5 years	30 years	30 years
life costs for one location(30 years)	$28,500	$77,450	$12,450
life savings per location	$0	-$48,950	$16,050
cost per location per year	$950	$2,648	$415
annual savings per location	$0	-$1,698	$535
total DOE cost per year (31,055 filters)	$29.5M	$82.2M	$12.9M
total DOE savings per year (31,055 filters)	$0	-$52.7M	$16.6M

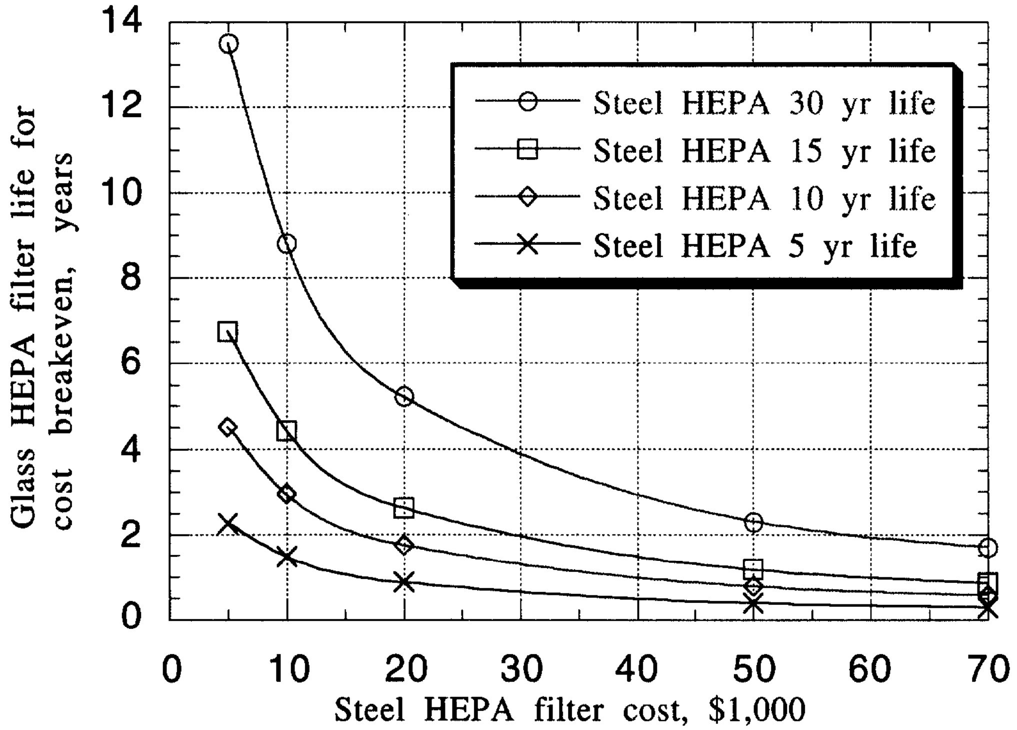

Figure 16 Break-even costs for cleanable steel HEPA filter having different filter lives as a function of purchase cost.

The results of our sensitivity analysis are summarized in Figure 16 which defines the break-even costs as a function of glass HEPA life, steel HEPA cost, and steel HEPA life. Using a cleanable steel HEPA filter will be cost effective for any combination of glass HEPA life and steel HEPA cost that lies below the curve defining a given steel HEPA life. Figure 16 shows that more expensive steel HEPA filters are only cost effective with long steel filter life and short glass HEPA life. Conversely, lower cost steel filters can be cost effective with higher glass HEPA filter lives and lower steel HEPA lives.

In addition to the direct cost savings shown in Table 1, there are additional cost savings due to the increased reliability of the steel HEPA filters. Steel HEPA filters have a much higher reliability than the present glass HEPA filter, which can be damaged or destroyed under a number of operational and accident conditions involving fires, explosions, tornadoes, or water exposure.(26) When the HEPA filters are damaged, radioactive contaminants can escape and cause environmental contamination. The typical consequence of a accidental release is a facility shut down and an environmental clean-up operation, both of which are very expensive.

V. Evaluation of Competing Technologies for Cleanable HEPA Filter

The major competitors of the sintered steel fiber filter are the metal and ceramic sintered powder filters and the reinforced glass fiber HEPA filter. In fact, the early high efficiency metal filters used in nuclear air cleaning applications were sintered steel powder filters.(3-5,9) Currently, both steel and ceramic sintered powder filters are used extensively in high efficiency filtration applications in which the filters are repeatedly cleaned and reused. Most of the applications involve filtering gas and liquid process streams at relatively low flow rates and have high pressure drops across the filters.

We have evaluated sintered metal and ceramic powder filters and concluded that these filters have much higher pressure drops than fibrous filters with the comparable efficiency. Figure 17 illustrates the general structure of a sintered powder filter which consists of several layers of different size powders that are sintered together.(27) The layer having the smallest size particles performs the basic filtration, while the intermediate layers and substrate provide structural support to the filtration layer. In order to minimize the pressure drop, the thickness of the filtration layer is made as small as possible.

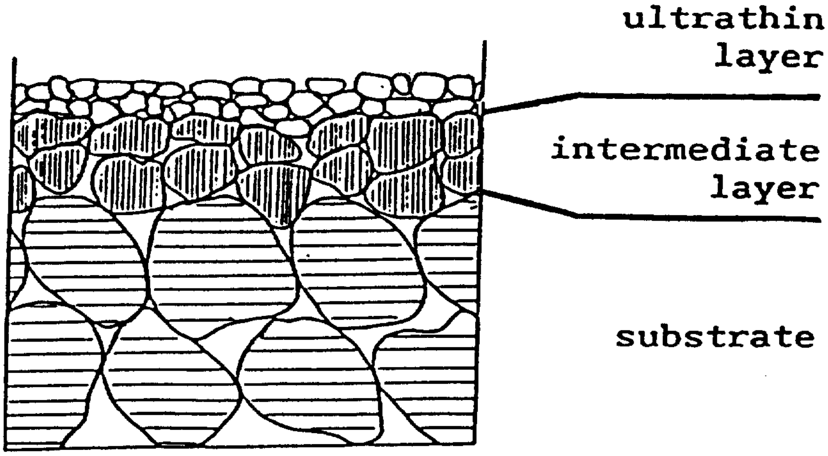

Figure 17. Typical structure of a ceramic powder filter having multiple layers of different size powder.(27)

An example of a typical ceramic powder filter is illustrated in Figure 18 which shows electron micrographs of the cross section of the French KERASEP filter.(28) The substrate layer of 5 µm aluminum and titanium oxide powder and the surface layer of 0.8 µm zirconium or titanium oxide powder are seen in the two photographs. In addition to the filter with a surface layer of sintered 0.8 µm powder, we also obtained KERASEP filters with a surface layer of 1.4 µm powder and one filter having only the substrate with no surface layer. This filter was used by the French Atomic Energy Agency for isotope separation.

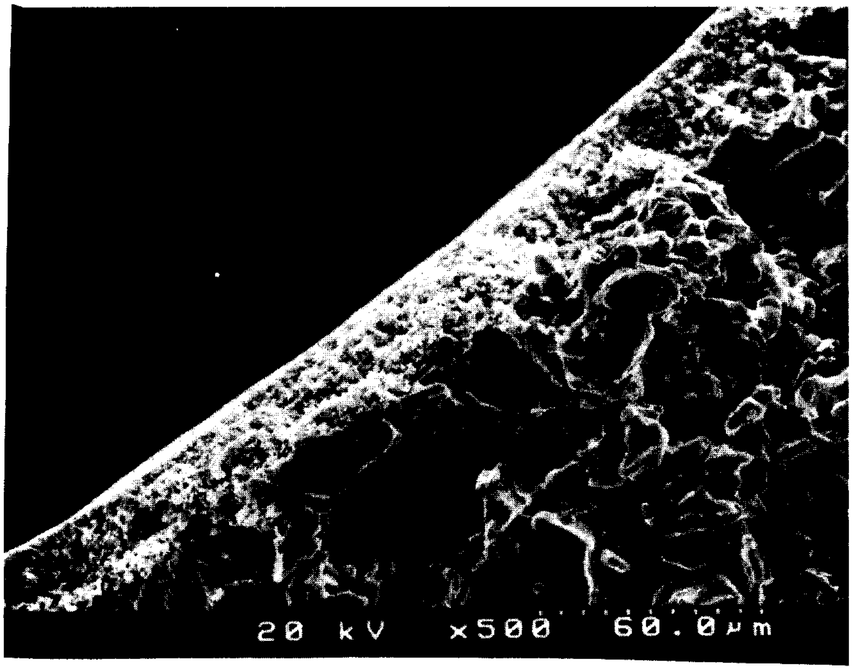

(A)

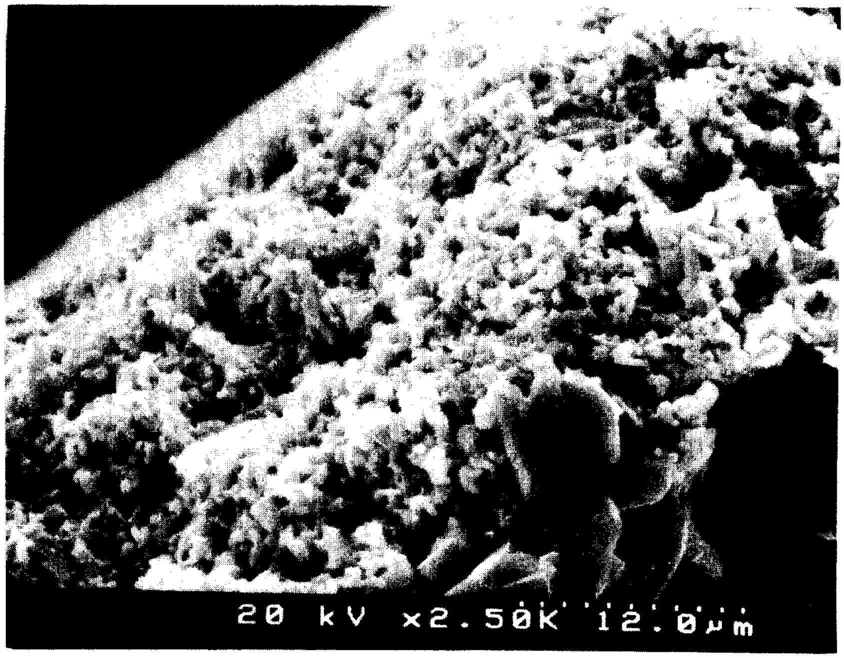

(B)

Figure 18. Electron micrographs of the cross section of the KERASEP ceramic powder filter having a surface layer of 0.8 µm powder. B is a magnification of A.

We measured the penetration of DOS aerosols and the pressure drop of the three different KERASEP filter elements at 1.3 cfm, which corresponds to a flow rate of 1,000 cfm if the maximum number of KERASEP elements were packaged into the standard HEPA frame of 2' x 2' x 1'. The KERASEP filter elements are cylinders with multiple interior channels that are parallel to the cylindrical element. Figure 19 shows the KERASEP filters have an excessive pressure drop, even with only the pure substrate. The filter with a layer of 1.4 µm powder meets the HEPA penetration requirements but has an excessive pressure drop of 25 inches of water.

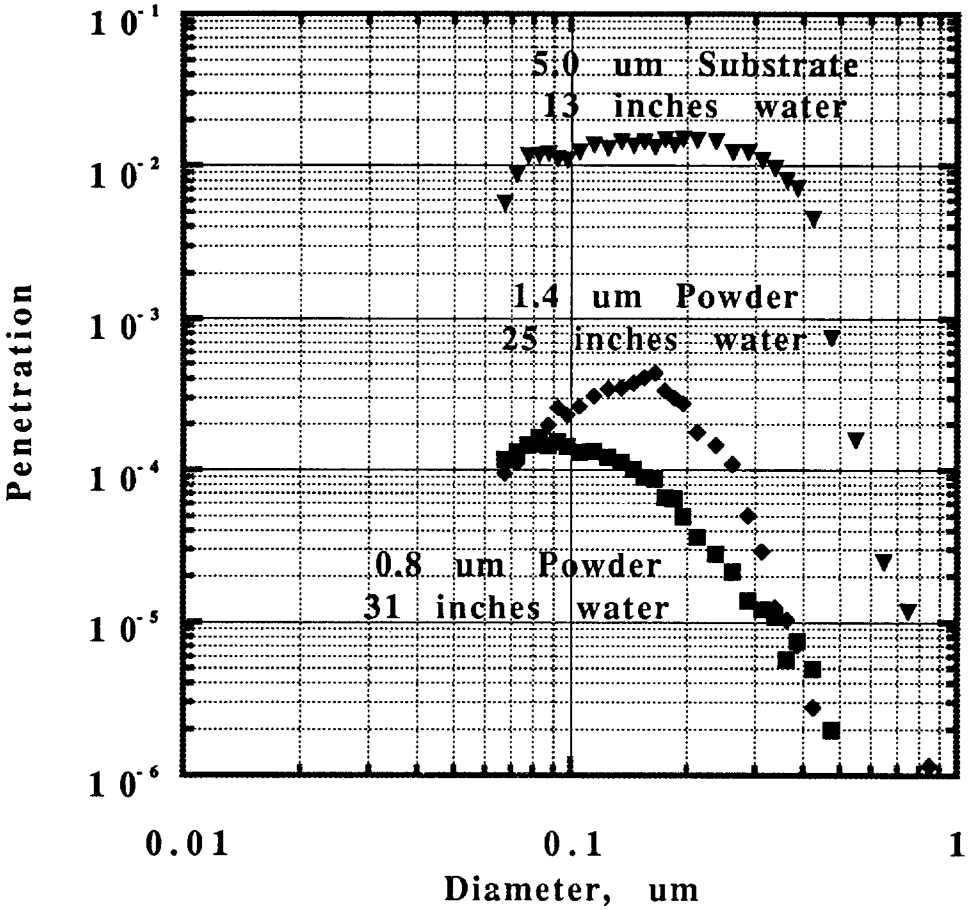

Figure 19. Penetration of DOS aerosols as a function of diameter for three different KERASEP ceramic powder filters.

Another multi-layer ceramic filter that we evaluated was a honeycomb ceramic monolith with a surface layer of fine ceramic powder deposited by a slurry and sintered.$^{(29)}$ This filter element from the CeraMen Corporation had high efficiency and relatively low pressure drop. We tested the filter sample at 50 cfm to correspond to the 1,000 cfm flow for a 2' x 2' x 1' standard HEPA filter. Figure 20 shows that the penetration at 0.3 µm was 0.06, and the pressure drop was 4.0 inches. These values are not close to the HEPA filter requirements.

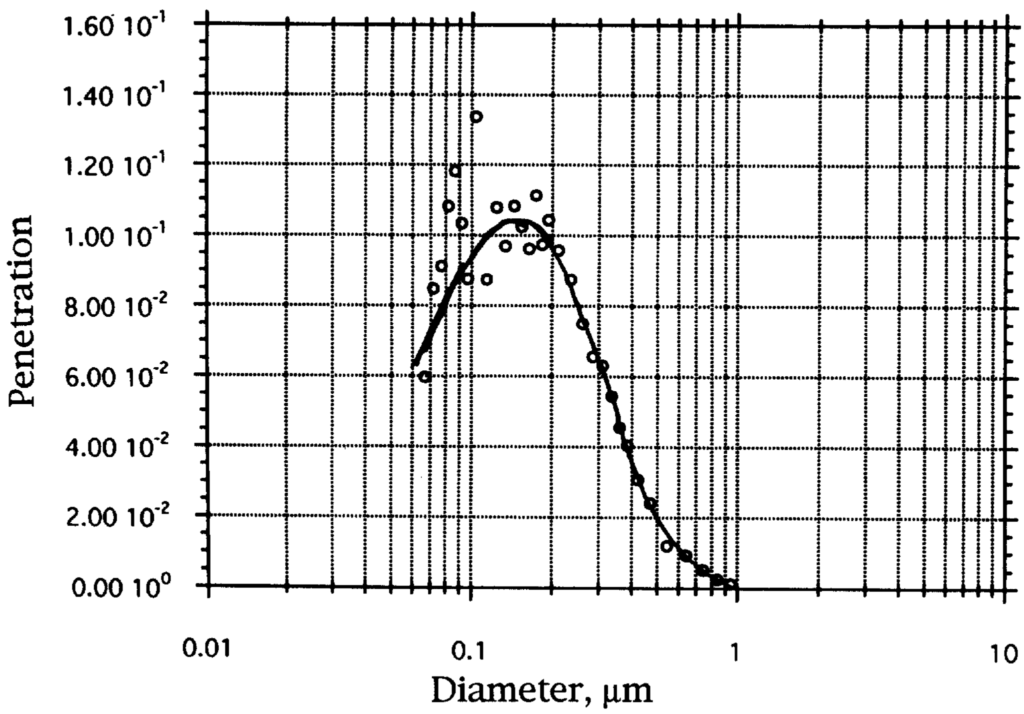

Figure 20. Penetration of DOS aerosols through CeraMen ceramic filter at 50 cfm. The pressure drop was 4.0 inches.

Sintered powder metal filters have a similar performance as the powder ceramic filters because the basic structure of the medium is the same. The powder metal filters are made with either multiple layers of graded powder as in Figure 17 or with uniform size powder throughout. The configuration of the powder metal filters is generally as tubes or other rigid shapes because once the powder is sintered, the filter medium cannot be bent sharply, as required for making filter pleats, without cracking. This is true even for relatively thin sheets. An example of a powder steel filter (Mott Metallurgical, Farmington, Conn.) having 85 tubes with a nominal pore size of 0.2 μm mounted together is shown in Figure 21. We attempted to determine the aerosol penetration through the multi-tube filter, but the pressure drop was too high for our test equipment. The pressure drop across the filter at 1.9 cfm was 8 psi (222 inches). This flow corresponds to the equivalent flow through the small element that a full-scale HEPA filter would see. The full scale filter would have more than 3,800 tubes within the 2' x 2' x 1' filter housing.

Fain has developed a powder nickel filter using the tube design for potential applications as a HEPA filter.(30) The filter has 4 layers of decreasingly smaller powder diameter arranged as in Figure 17: a substrate layer of 55 μm powder, first intermediate layer of 15 μm powder, second intermediate layer of 5μm powder, and a top layer of 0.5 μm powder. The filter technology for making the multi-layer filter was used in the U.S. gaseous diffusion process for separating radioactive isotopes (analogous to the French using the KERASEP filter in the French isotope separation process). We evaluated a prototype module consisting of 10 tubes approximately 11 inches long and that represented 1/64 the capacity of a standard HEPA filter. The full scale HEPA filter would have 676 tubes.

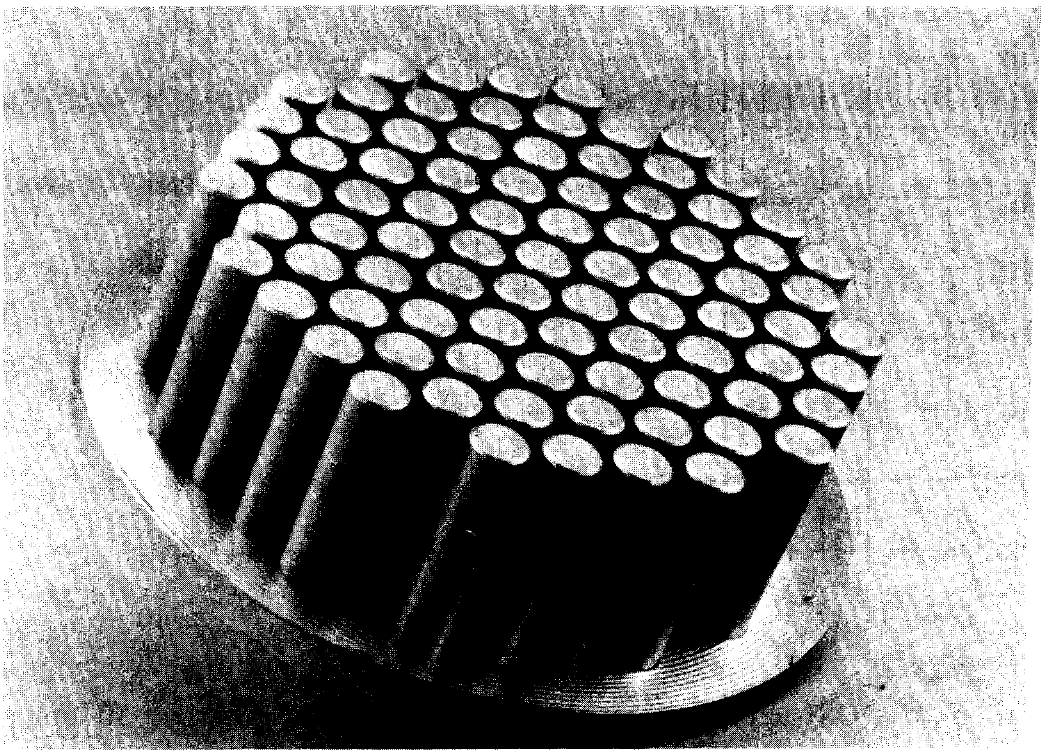

Figure 21. Photograph of sintered stainless steel powder filter from Mott Metallurgical consisting of 85 tube elements. Each tube has a diameter 0.31 inches and is 1.2 inches high.

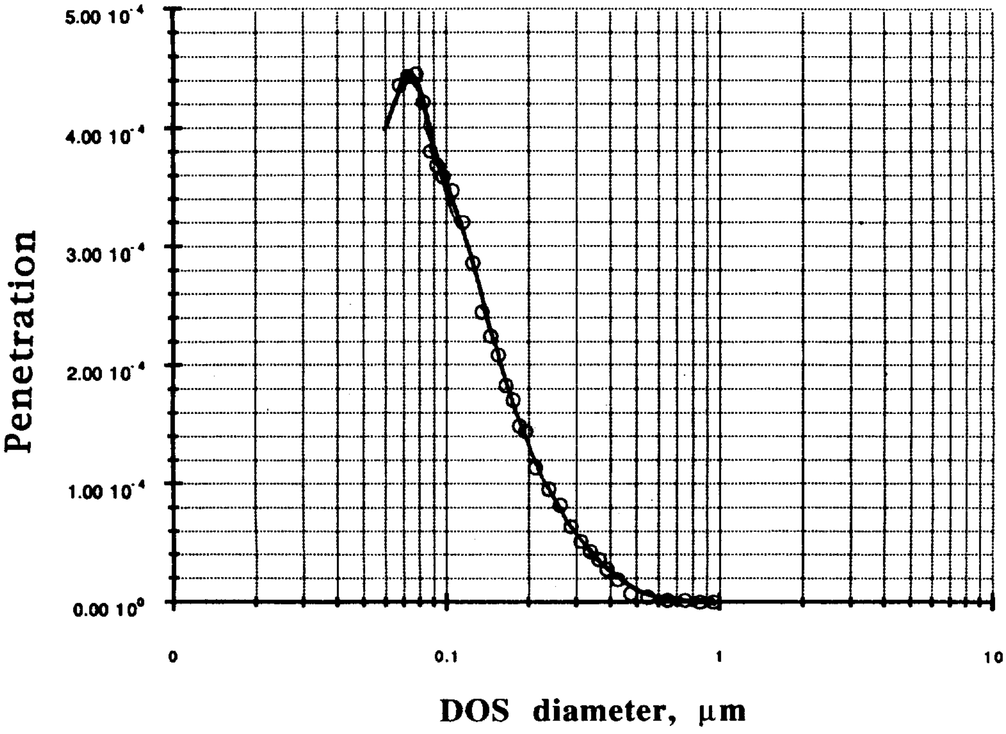

Figure 22. Penetration of DOS aerosols through sintered nickel power filter consisting of 10 tubes. Pressure drop at 15.6 cfm was 38 inches.(30)

Our test results showed the powder nickel filter had very high pressure drop and plugged rapidly with aerosols. Figure 22 shows the penetration of DOS aerosols through the filter as a function of particle size. The penetration at 0.3 µm is 0.00006, which meets the requirements for a HEPA filter. However the pressure drop at 38 inches greatly exceeds the maximum 1 inch. Since the filter pressure drop increased from 38 to 45 inches within 5 minutes of aerosol exposure, we were careful to measure the aerosol penetration for the clean filter within the first 60 seconds before the particle loading could affect the filter penetration. Attempts to reduce the pressure drop by reducing the powder layers is futile as seen with the French KERASEP filter in Figure 19 because the aerosol penetration will increase beyond the maximum 0.0003 at 0.3 µm. Thus we conclude that the sintered powder filters are not a viable competitor of the steel HEPA filter.

The reason why the sintered powder filter cannot compete with the sintered steel fiber filter is the more restrictive structure of the powder filter. Figures 23 and 24 show cross sections of a steel fiber and a steel powder filter respectively. These cross sections are perpendicular to the air flow and represent the environments particles would see at the fixed depth within the filter. Figure 23 shows the fibers occupy a small volume fraction of the filter and result in relatively open region for air and particles to pass. In contrast, Figure 24 shows the powder occupies a large volume fraction and results in a relatively closed region for air and particles to pass.

This difference in fraction of occupied space accounts for the observed differences in filtration performance between the fibrous and powder filters. Because of the open space in a fibrous filter, the average internal air velocity is not much greater than the external air velocity. Particles therefore have a long residence time within the filter and result in high particle capture due to Brownian motion. The relatively few restrictions to the air flow also result in a low pressure drop for the fibrous filter. In contrast, the small volume of open space in the powder filter forces the air to flow at very high velocities through the powder filter matrix. The high velocity forces the particles through the filter very quickly with little residence time for Brownian motion to capture the particles. A high pressure drop is also required to force the air flow through the small open areas of the filter.

We have measured the aerosol penetration and the pressure drop through a sintered powder and fiber filter having the same powder or fiber dimension to illustrate the difference between the two filters. Figure 25 shows the resulting penetration of DOS aerosols and the pressure drop through a sintered powder filter made from 5 µm steel powder and a sintered fiber filter made from 5 µm steel fibers. We see that the powder filter has a much higher aerosol penetration and a higher pressure drop than the fiber filter. Note also that the peak aerosol penetration occurs at 0.17 µm for the fiber filter and at 0.11 µm for the powder filter. The shift in maximum penetration to smaller particle sizes with increasing filtration velocity is well known in the field and occurs because of lower residence time and the resulting decrease in Brownian capture.

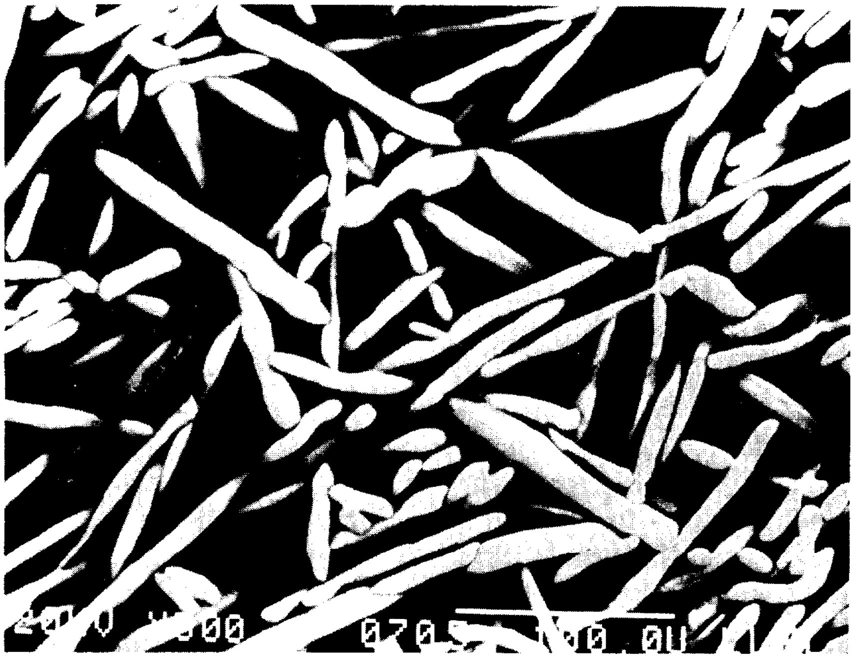

Figure 23. Electron micrograph of a cross section of a steel fibrous filter in a plane perpendicular to the air flow.

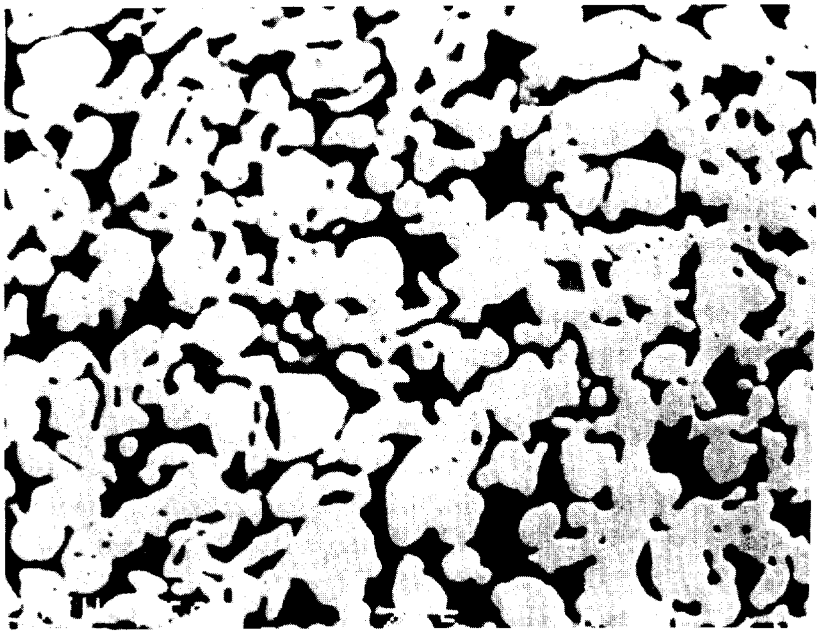

Figure 24. Electron micrograph of a cross section of a steel powder filter in a plane perpendicular to the air flow.

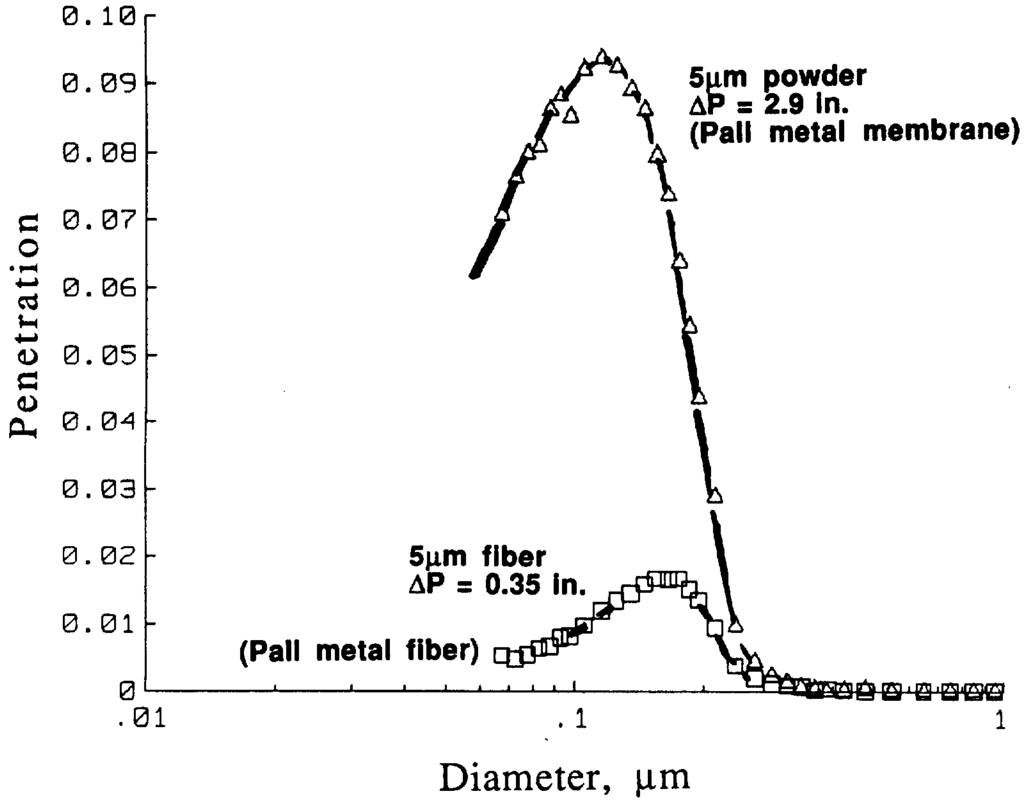

Figure 25. Penetration of DOS aerosols through sintered fiber filter made from 5 µm steel fibers and sintered powder filter made from 5 µm steel powder tested at 1.25 cm/s.

Another technology that we reviewed for potential application as a cleanable HEPA filter was ceramic fiber filters. These filters would have the same geometry advantages as the steel fiber filter. However ceramic fiber filters do not appear promising as a candidate for cleanable HEPA filters for several reasons. One of the major problems is the large diameters of most ceramic fibers. As seen in Figure 4, it is necessary to have fibers substantially less than 1.0 µm diameter to be considered for use as a HEPA filter. One of the smallest diameter ceramic fibers are the Saffil (ICI, England) aluminia fibers shown in Figure 26. These fibers range from 2-4 µm and are available in felts, although sheets could be made in the wet paper making process. We measured the penetration of DOS aerosols on the Saffil felt and found the filter has an unacceptable high penetration for consideration as a HEPA filter. Figure 27 shows the penetration at 0.3 µm is 0.33 and the pressure drop is 0.49 inches at a velocity of 4 cm/sec. Even with two layers, the penetration would only drop to 0.10 while the pressure drop increases to 0.98 inches.

Assuming that ceramic fibers smaller than 1 µm become available, the resulting filter media would be too brittle to be used as a cleanable HEPA filter. The fibers would have to be either sintered together or bonded together with a ceramic glue, both of which would result in easilv fractured media. Using an organic binder as done with glass HEPA filters would allow the media to be flexible for pleating, but would not withstand the high temperature. We do not believe that the ceramic fiber media in flat sheets would have the required strength to survive repeated cleanings.

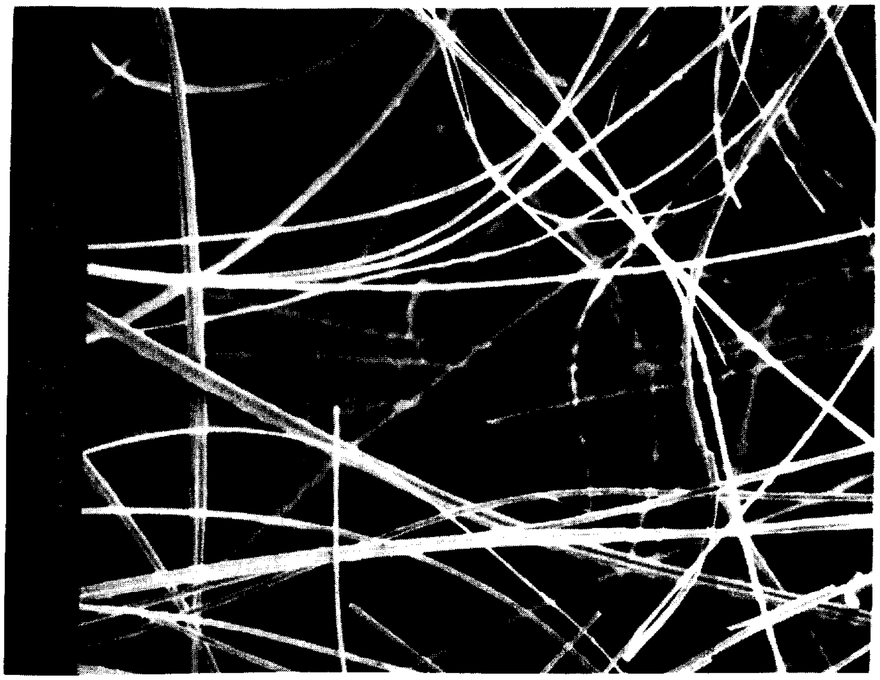

Figure 26 . Electron micrograph of Saffil alumina fiber media.

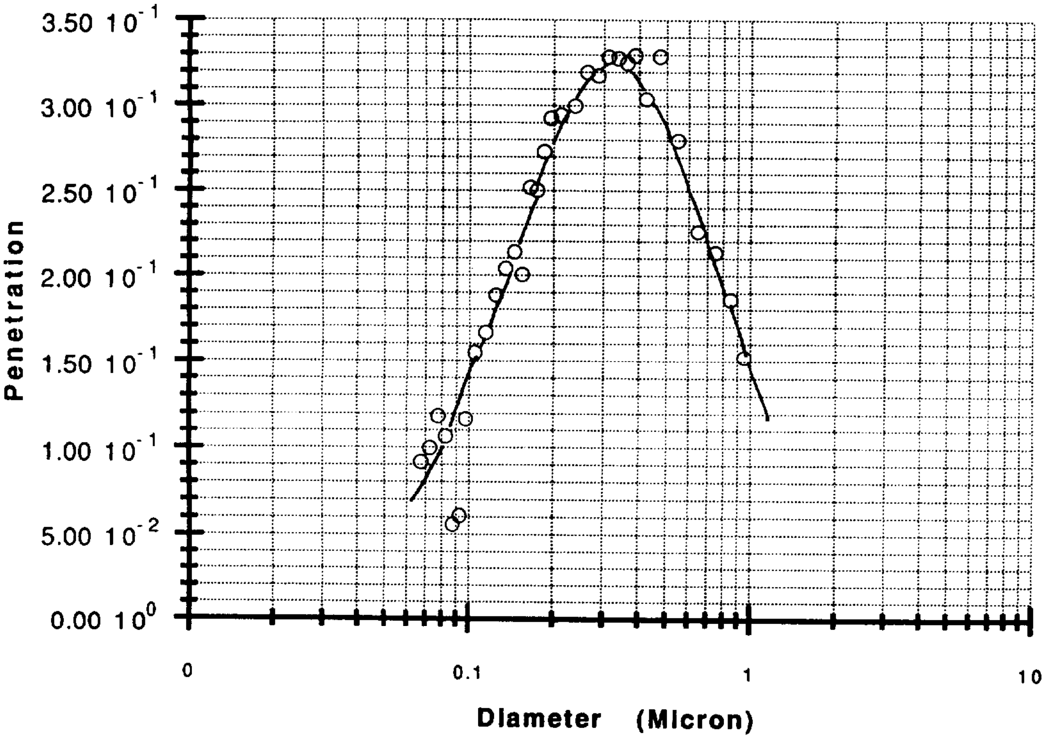

Figure 27. Penetration of DOS aerosols through Saffil alumina fiber medium at 4 cm/s. Pressure drop was 0.49 inches.

The final potential candidate for a cleanable HEPA filter that we reviewed is the reinforced glass fiber HEPA filter.(31) This filter has a glass scrim laminated on the back of the HEPA media to provide extra strength to the medium. Test results have shown the reinforced media is very effective in preventing filter blow out during heated air and water exposure tests.(31) However, the filter was designed to withstand a single accident condition and not for repeated cleanings by reverse air pulses. To survive repeated reverse air pluses, the glass HEPA medium should have glass scrim laminated on both sides of the medium. Without this reinforcement, the glass fiber medium could be blown out. Although a HEPA filter with a single layer of reinforced medium can meet the one inch pressure drop requirement, it is not known whether the same holds for two layers. In addition, tests need to be conducted to establish that the reinforced glass fiber filter can be repeatedly cleaned as was demonstrated for the steel fiber filter in Figure 9 for the single cartridge and in our previous report for the full scale HEPA filter.(14) Other cleaning methods such as liquid washings also have to be evaluated for those applications where reverse air pulses are not effective. Since a cleanable glass HEPA filter is expected to cost about $500 compared to $5,000 for a cleanable steel HEPA filter, the reinforced glass HEPA filter has the potential to be a viable candidate for the cleanable HEPA filter.

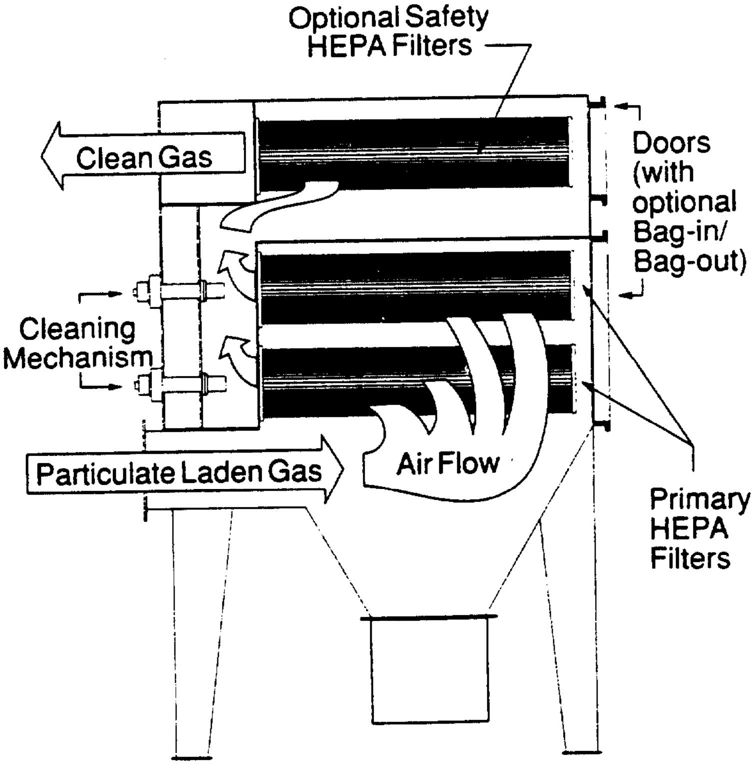

Figure 28. Cleanable HEPA filter using reinforced glass HEPA medium and manufactured by MAC Environmental.(33)

Cleanable HEPA filters using the standard and the reinforced glass fiber HEPA medium and a gentle reverse air pulse are being developed for various applications.(32,33) Leibold et al have described the use of reverse air flows in the pockets of deep pleated HEPA filters to dislodge particle deposits for renewing clogged HEPA filters.(32) They were able to clean standard, deep-pleated HEPA filters using several different dusts. Morgan described a cleanable HEPA filtration system using HEPA filters with reinforcement scrim on both sides of the HEPA media.(33) The commercially available unit uses cylindrical cartridge HEPA filters in a conventional blow-back air cleaning unit. Figure 28 shows the commercially available cleanable HEPA filter system manufactured by MAC Environmental (Kansas City, MO). This system functions in a similar to the cleanable steel HEPA filter system shown in Figure 1.

VI. Conclusion

We have made further progress in developing a cleanable steel fiber HEPA filter. We fabricated a pleated cylindrical cartridge using commercially available steel fiber media that is made with 1 µm stainless steel fibers and sintered into a sheet form. Test results at the DOE Filter Test Station at Oak Ridge show the prototype filter cartridge has 99.99% efficiency for 0.3 µm dioctyl phthalate (DOP) aerosols and a pressure drop of 1.5 inches. Filter loading and cleaning tests using AC Fine dust showed the filter could be repeatedly cleaned using reverse air pulses. We also produced 0.5 µm steel fibers using the fiber bundling and drawing process and sintered the fibers into small filter samples. Test results on the sample showed a penetration of 0.0015 % at 0.3 µm and a pressure drop of 1.15 inches at 6.9 ft/min (3.5 cm/s) velocity. Based on these results, steel fiber media can easily meet the requirements of 0.03 % penetration and 1.0 inch of pressure drop by using less fibers in the media.

A cost analysis of the cleanable steel HEPA filter shows that, although the steel HEPA filter costs much more than the standard glass fiber HEPA filter, it has the potential to be very cost effective because of the high disposal costs of contaminated HEPA filters. We estimate that the steel HEPA filter will save an average of $16,000 over its 30 year life. The additional savings from the clean-up costs resulting from ruptured glass HEPA filters during accidents was not included but makes the steel HEPA filter even more cost effective.

We also present the results of our evaluation of competing technologies with metallic and ceramic powder filters, ceramic fiber filters, and reinforced glass fiber filters. In general, the metallic and ceramic powder filters have pressure drops in excess of 25 inches of water for HEPA grade efficiencies and are therefore not viable candidates. The ceramic fiber filters cannot meet the HEPA efficiency because the fiber diameters are too large. The reinforced glass fiber filter is a promising candidate for the cleanable HEPA filter but requires additional development and testing to confirm its potential to be repeatedly cleaned.

VII. References

1. Bergman, W, Larsen, G, Lopez, R, Wilson, K, Witherell, C, and McGregor, M, "Feasibility demonstration of a steel HEPA filter," in Mixed Waste Integrated Program, Mid-Year Technical Review, Volume 5, Off-Gas Treatment, Available from DOE, EM-50, 1000 Independence Ave, Washington, DC 20585, Document WPI.94-0159-5, April 21, (1994).

2. Bergman, Werner "Requirements for a cleanable steel HEPA filter derived from a systems analysis" Lawrence Livermore National Laboratory Report UCRL-ID-125048, Available from NTIS, 5285 Port Royal Rd, Springfield, VA 22161, June (1996).

3. Ziegler, D.L., and Johnson, A.J., "Disposal of HEPA filters by fluidized bed incineration" in Proceedings of 15th DOE Nuclear Air Cleaning Conference, CONF-780819, NTIS, Springfield, VA 22161, pp.111-116, (1979).

4. Kirstein, B.E., Paplawsky,W.J., Pence,D.T., and Hedahl, T.G., "High efficiency particulate removal with sintered metal filters" in 16th DOE Nuclear Air Cleaning Conference, CONF-801038, pp. 719-744, (1981).

5. Bergman, W., "Comments to paper by Kirstein" in 16th DOE Nuclear Air Cleaning Conference, CONF-801038, pp. 742-744, (1981).

6. Dillmann, H.G., and Pasler, H., "Experimental investigations of aerosol filtration with deep bed filters" in Proceedings of 17th DOE Nuclear Air Cleaning Conference, pp. 1160-1174, CONF-820833, (1983).

7. Dillmann. H.G., and Pasler, H., " A filter concept to control airborne particulate release due to severe reactor accidents and implementation using stainless-steel fiber filters" in Proceedings of 18th DOE Nuclear Air Cleaning Conference, pp. 1417-1428, CONF-840806, (1985).

8. Klein, M., and Goossens, W.R., " Aerosol filtration with metallic fibrous filters" in Proceedings of 17the DOE Nuclear Air Cleaning Conference, pp 504-522, CONF-820833, (1983).

9. Randhahn, H., Gotlinsky, B., and Tousi, S., "The development of all metal filter for use in the nuclear industry" in Proceedings of 20th DOE/NRC Nuclear Air Cleaning Conference, CONF-880822, pp 726-748, (1989).

10. Bergman, W.," Evaluation and modification of commercial sintered metal filters" LLNL memorandum, July 7, (1989).

11. Kaercher, M.V., "Design of a prefilter to improve radiation protection and filtering efficiency of the containment venting system" in Proceedings of the 22nd DOE/NRC Nuclear Air Cleaning and Treatment Conference, pp 443-452, CONF-9020823, (1993).

12. Bergman, W., Conner, J., Larsen, G., Lopez, R., Turner, C., Valha, G., Violet, C., and Williams, K., "High efficiency steel filters for nuclear air cleaning" , in Proceedings of 21st DOE/NRC Nuclear Air Cleaning Conference, CONF-900813, pp. 733-761, (1991).

13. Bergman, W., "Cleanable steel HEPA filters" in Environmental Technology Program Annual Report FY90, pp.44-47, Lawrence Livermore National Laboratory report UCRL-LR-105199, January 2, (1991).

14. Bergman, W., Larsen, G., Weber, F., Wilson, P., Lopez, R., Valha, G., Conner, J.. Garr, J., Williams, K., Biermann, A., Wilson, K., Moore, P., Gelner, C., Rapchun, D., Simon, K., Turley, J., Frye, L., and Monroe, D., "Development and Evaluation of a Cleanable High Efficiency Steel Filter" in Proceedings of the 22nd DOE/NRC Nuclear Air Cleaning Conference, CONF-9020823, PP586-616, July (1993).

15. Bergman, W., Larsen, G., Lopez, R., Wilson, K., Simon, K., and Frye, L., "Preliminary field evaluation of high efficiency steel filters" in Proceedings of the 23rd DOE/NRC Nuclear Air Cleaning and Treatment, CONF-940738 , pp 195-213, February , (1995).

16. Kruger, O.L., "Hanford Waste Vitrification Plant Applied Technology Plan", WHC-EP-0417, January (1992).

17. Procurement Specification, Filter, High Efficiency Metal, W-320-P3, January 24, (1995).

18. Weber, L., "Pall Technical Brief: HEMF-5, Demonstration of efficiency measurements and in-situ cleaning"Pall Corporation report, December 31, (1992).

19. Weber, L., "Pall Technical Brief: HEMF-6, Study to investigate backwash regenerability and maintenance of integrity by ASHRAE test", Pall Corporation report, December 31, (1992).

20. Dittman, P., "Cost estimate for steel HEPA filters", Pall Corporttion, Cortland, NY, May 28, (1996).

21. Moore, P., Bergman, W., and Gilbert, H., "Survey of Life-Cycle Costs of Glass-Paper HEPA Filters" in Proceedings of the 22nd DOE/NRC Nuclear Air Cleaning Conference, Denver, Co, August 24-27, 1992. UCRL-JC-109768, December, (1992).

22. Stepuszek, D and Hirose, J "High performance functinal paper for use as filter media" in Advances in Filtration and Separation Technology, Vol. 7, System Approach To Separation and Filtration Process Equipment. W.W-F Leung, Editor, pp. 111-114, The American Filtration Society, P.O. Box 6269, Kingwood, Texas 77325, April (1993).

23. Tomeogawa High-Performance Sheet, SS, Specification brochure for sintered stainless steel sheeet, Tomeogawa (U.S.A.) Inc., 742 Glenn Avenue, Wheeling, IL 60090 (1993).

24. Flanders Filters Catalog showing separatorless filters likethe Dimple Pleat™ and Super-Flow™ HEPA filters. Bulletins 812 and 871.

25. Air Filter Specifications, Manual No. 5Q1.10, Section 7, Westinghouse Savannah River Company, Savannah River Site, Health Protection Department, (1995).

26. Bergman, W., First, M.W., Anderson, W.L., Gilbert, H., and Jacox, J.W., "Criteria for calculating the efficiency of deep-pleated HEPA filters with aluminum separators during and after design basis accidents" in Proceedings of the 23rd DOE/NRC Nuclear Air Cleaning and Treatment Conference, NTIS, Springfield, VA, CONF-940738 , pp 563-598, February , (1995).

27. Gerster, D. "State of mineral membranes in the world" in the 1986 Fourth Annual Membrane Technology/Planning Conference, W. Shoemaker, Editor, Business Communications Co., Inc,. Norwalk, CT 06855, pp152-159, (1986).

28. Kientz, G "Industrial use of inorganic membranes in the food industry" in Advances in Filtration and Separation Technology, Vol. 8, Filtration and Separation Processes and the Environment, S.K. Sharma, Editor, American Filtration and Separations Society, PO Box 1530, Northport, AL 35476, pp 49-55, (1994).

29. Abrams, R, "High temperature filtration using ceramic membranes" in Advances in Filtration and Separation Technology, Vol. 8, Filtration and Separation Processes and the Environment, S.K. Sharma, Editor, American Filtration and Separations Society, PO Box 1530, Northport, AL 35476, (1994)

30. Fain, DE "Inorganic membrane cleanable HEPA filter" in Mixed Waste Integrated Program, Mid-Year Technical Review, Volume 5, Off-Gas Treatment, Available from DOE, EM-50, 1000 Independence Ave, Washington, DC 20585, Document WPI.94-0159-5, April 21, (1994).

31. Gilbert, H., Bergman, W., and Fretthold, J. "Development and evaluation of a HEPA filter for increased strength and resistance to elevated temperature." in Proceedings of the 22nd DOE/NRC Nuclear Air Cleaning Conference, Denver, Co, August 24-27, 1992. LLNL report UCRL-JC-110582, January, (1993).

32. Leibold, H., Doffert, I., Leiber, T., and Wilhelm, J.G., "The application of HEPA filter units in gas streams of high dust concentrations" in Proceedings of the 22nd DOE/NRC Nuclear Air Cleaning Conference, Denver, Co, August 24-27, 1992, pp 540-553, CONF-9020823, NTIS, Springfield, VA, July, (1993).

33. Morgan, L, "Ultra high efficiency dust collection" pp 30-32, in Filtration News, Vol, 12, No. 4, July/August (1994).

DISCUSSION

WILHELM: Who is producing 1μm diameter metallic fibers and what is the form in which it is delivered?

BERGMAN: Tomeogawa, a Japanese firm, produces the 1 μm stainless steel fiber media in sintered sheets. We obtained our supply from Tomeogawa (USA), Inc., Wheeling, IL.

TSENG: With any fiberized material there will be a lower limit to diameter based on practical considerations of material stability. What would be the smallest diameter in stainless steel, and how would you compare it to glass?

BERGMAN: I thought that when we had reached 2μm that we were getting close to the limit, but at this point I do not know the lower limit. We made 0.5μm fibers, and 0.1μm is not unreasonable. Glass fibers are commercially available at 0.1 - o.2μ diameters.

TSENG: With metals there is a crystalline structure and once you get down to a fiber diameter of the order of a grain boundary, you have problems. I do not know where the limits are, I was hoping you could enlighten me.

BERGMAN: I do not have the answer. As far as I am concerned, there is no limit except for time, money, and effort.

WEBER: What about glass fiber diameter?

BERGMAN: You can buy glass fibers down to 0.1μm.

BLACKLAW: What are the other important parameters in development of alternatives; for example, strength and corrosion?

BERGMAN: The strength of the steel media is due to inherent strength of the steel fibers plus the fiber-to-fiber bonds from sintering. In contrast, glass fiber media is not as strong because the fibers are held together with an organic binder, which is not only weaker, but also subject to more failure modes. However corrosion in the 300 series steels is a serious concern and one of the areas we have not studied. Corrosion resistant steels such as Hastalloy and Inconel would work, but they are only available in diameters greater than 8μm. The diameter of the Hastalloy and Inconel fibers would have to be reduced to less than 1 μm for use as HEPA filter media.

ENGELMANN: How flammable is it?

BERGMAN: The loose steel fibers are extremely flammable and will ignite spontaneously when dispersed in air. However, the sintered steel fiber media will not burn even with a flame directed on it. Direct flames will destroy the media by converting the steel alloy to oxides, which flake and crumble.

THE EFFECT OF MEDIA AREA ON THE DUST HOLDING CAPACITY OF DEEP PLEAT HEPA FILTERS

J Dyment AWE plc Aldermaston RG7 4PR United Kingdom
D Loughborough AEAT Harwell Oxford OX11 0RA United Kingdom

ABSTRACT

The high potential cost of storage, treatment and disposal of radioactive wastes places a premium on the longevity of installed HEPA filters in situations in radioactive processing facilities where dust capacity is a life determining factor.

Previous work investigated the dust holding capacity v pressure drop characteristics of different designs of HEPA filter and also the effect of using graded density papers.

This paper records an investigation of the effect of media area variation on the dust holding capacity of the "deep-pleat" design of HEPA filter. As in the previously reported work two test dusts (carbon black and sub micron sodium chloride in the range (0.15 - 0.4μm) were used. Media area adjustment was effected by varying the number of separators within the range 60 - 90.

Results with the coarser dust allowed an optimum media area to be identified. Media areas greater or smaller than this optimum retained less dust than the optimum for the same terminal pressure drop. Conversely with the finer sodium chloride aerosol the dust holding capacity continued to increase up to the maximum area investigated.

INTRODUCTION

The prime concerns of facility operators (and regulators) in the nuclear industry in respect of HEPA filter systems are their efficiency (DF) and reliability in accident conditions.

Considerations of economy in conjunction with the high potential cost of storage, treatment and disposal of radioactive wastes mean that the longevity of installed HEPA filters (in situations where dust capacity is a life determining factor) is also an important consideration.

Earlier investigations[1,2] looked at the influence of filter design viz deep-pleat vs minipleat and the use of graded papers[3] on dust holding capacity.

This paper describes an investigation into the effect of variable media area on the dust holding capacity of a particular design (the 1000cfm deep-pleat design) of HEPA filter. The media area was varied by varying the number of pleats/separators.

SCOPE OF WORK

Dust holding capacity of filter units is influenced by a number of factors, related to the nature of the airborne dust and its mode of deposition within the filter structure.
An ideal study procedure would freeze all parameters other than the one under investigation. Resource limitations constrained the present work to a limited practical investigation of real filters; procurement logistics dictated the use of filters from 3 different sources employing 2 different papers (of equivalent grade) in their construction.

In real operating situations HEPA filters encounter a whole range of conditions where they can be subject to widely varying dust burdens, both in terms of concentration and size distribution.

As in the graded media investigation[3] reported at the previous (23rd) Air Cleaning Conference, this work was carried out using two test dusts, one a fine thermally generated condensation aerosol of sodium chloride and the other a carbon black aerosol generated by dispersion of powder using a standard ASHRAE dispenser.

These two aerosols were selected partly on the basis of technology availability as established test dusts and partly on the basis of simulating widely differing operational conditions.

This approach utilised available technology to carry out a viable programme capable of producing an indicative if not a totally rigorous and comprehensive answer to the question of HEPA filter optimal dust holding capacity.

TEST EQUIPMENT AND FILTERS

Test Rig

The test rig consisted of circular ductwork with an open inlet to enable dust to be dispensed into the airstream, a filter housing and downstream ductwork connected to an extract fan. Volume flowrate was measured by BS orifice plate and controlled by adjustable damper. Filter resistance was measured using a micromanometer. The rig was identical with the one described in the graded paper work[3].

Test Filters

The deep-pleat filters were supplied by 3 manufacturers and conformed to the requirements of the British Nuclear Industry Specification[4] with media area varying from 18.8 m^2 up to 28 m^2. All filters were rated and tested at 1700m^3/h (1000 cfm) and had a minimum efficiency of 99.95% when tested by the sodium flame test[5]. They were all manufactured using either Hollingsworth and Vose Grade F39ZAE/R ("HV" in data) or Lydall grade L3255 ("L" in data). (Grades of paper currently in use in the UK nuclear industry).

Test Aerosols

The test aerosols used to load the filters were:-

(a) Sodium chloride with a MMD of 0.14μm[6]. A thermal generator was used in this work producing a condensation aerosol by vaporisation of sticks of solid sodium chloride in an oxy-propane flame; this equipment is capable of generating particulate material at rates between 0.32 and 6.7 g/min.

(b) Carbon black, acetylene, 50% compressed, with a nominal MMD of 0.6μm. Measurements carried out with an Anderson Mk III impactor[7] on airborne material dispersed with the standard ASHRAE dispenser gave an aerodynamic MMD of 2μm (35% below 1μm). These measurements are in accordance with the view that dispersion of this material by this method is far from complete. The standard ASHRAE dispenser is suitable for dispersing carbon black aerosols at rates between 0.3 and 2.4 g/min.

Test Procedure

All filters were tested at their rated flow of 1700 m^3/hr (1000 cfm). The mini-pleat filter although rated at 3000 m^3/hr (1760 cfm) was tested at 1700 m^3/hr (1000 cfm).

Dust holding capacity determinations were carried out with each filter mounted in the appropriate housing and subjected to a dust challenge at a uniform feed rate. For carbon black aerosol the feed rate to the deep-pleat filters was 2.4 g/min and to the mini-pleat unit, 1.2 g/min. For sodium chloride aerosol the feed rate was 3.6 g/min. The filter resistance was recorded against the known quantity of dust.

For purposes of comparison it is assumed that filters are changed out at a terminal resistance of 4"wg (1000 Pa), although operating practice may vary depending on other installation parameters.

CARBON BLACK LOADING RESULTS

Deep-pleat Filters

The results, (Figures 1 & 2), indicate the extent to which the carbon black dust holding capacity of this design varies with varying media area.

The current standard deep-pleat filter which has an average media area of 19 m^2 and approximately 66 media pleats (132 single sheets of media) can absorb some 470 g of carbon black before its resistance increases to 4"wg (1000Pa).

As the number of pleats increased from 66 to 80 the weight of carbon black absorbed rose to approximately 660 g for the same final resistance. Further increases in the number of pleats to

FIGURE 1 – DUST LOAD v RESISTANCE
(DEEP PLEAT FILTERS)
Carbon Black Loading

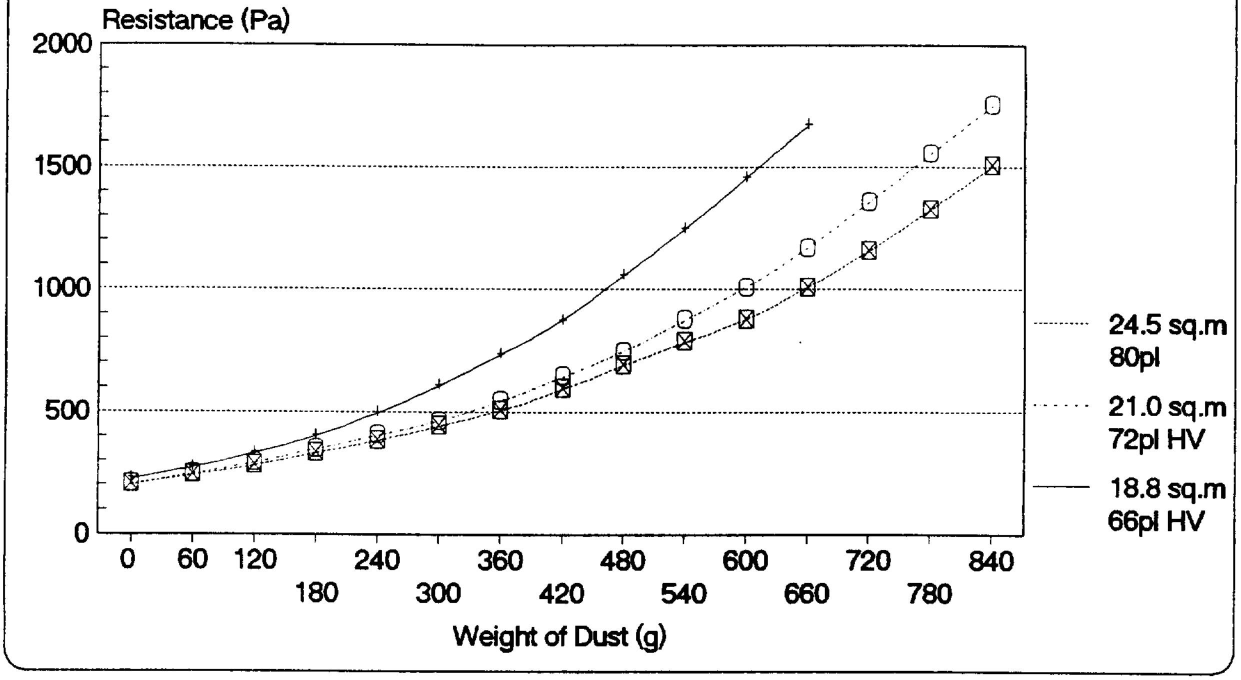

PAPER No.
DUST1

FIGURE 2 – DUST LOAD v RESISTANCE
(DEEP-PLEAT & MINIPLEAT UNITS)
Carbon Black Loading

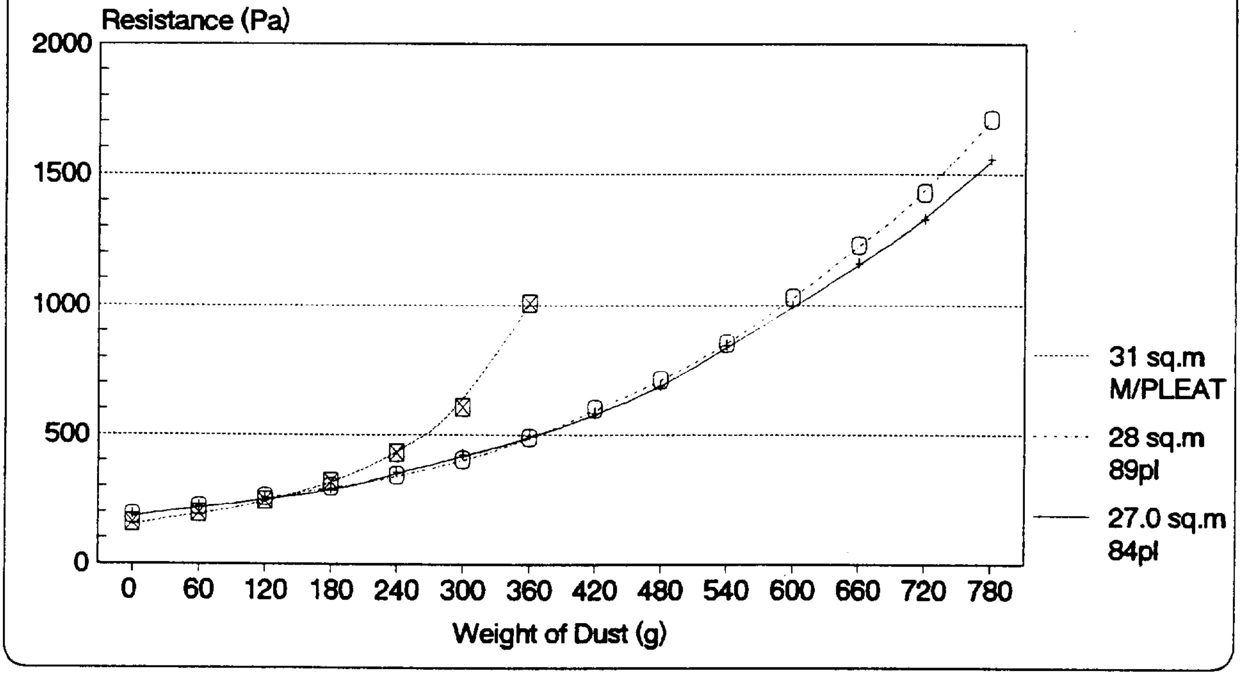

PAPER No.
DUST2

FIGURE 3 – DUST LOAD v RESISTANCE
(DEEP–PLEAT UNITS)
Sodium Chloride Loading

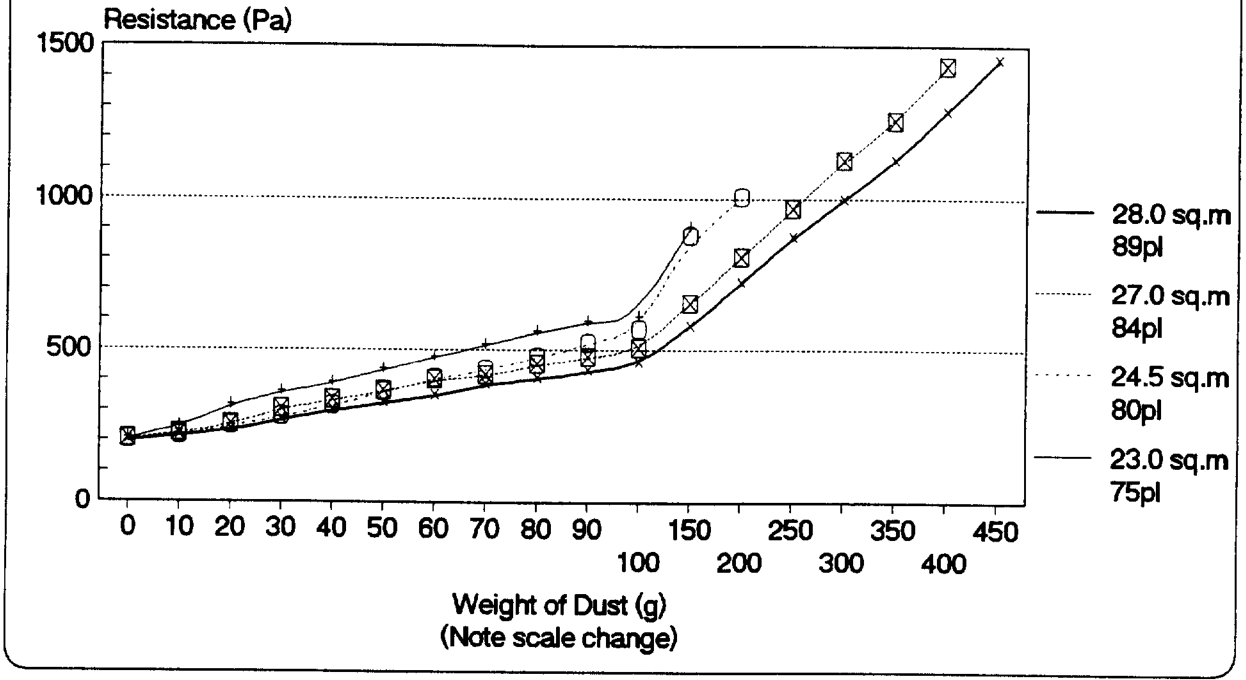

PAPER No.

DUST3

FIGURE 4 – DUST CAPACITY v No OF PLEATS
(DEEP–PLEAT UNITS)
Sodium Chloride and Carbon Black

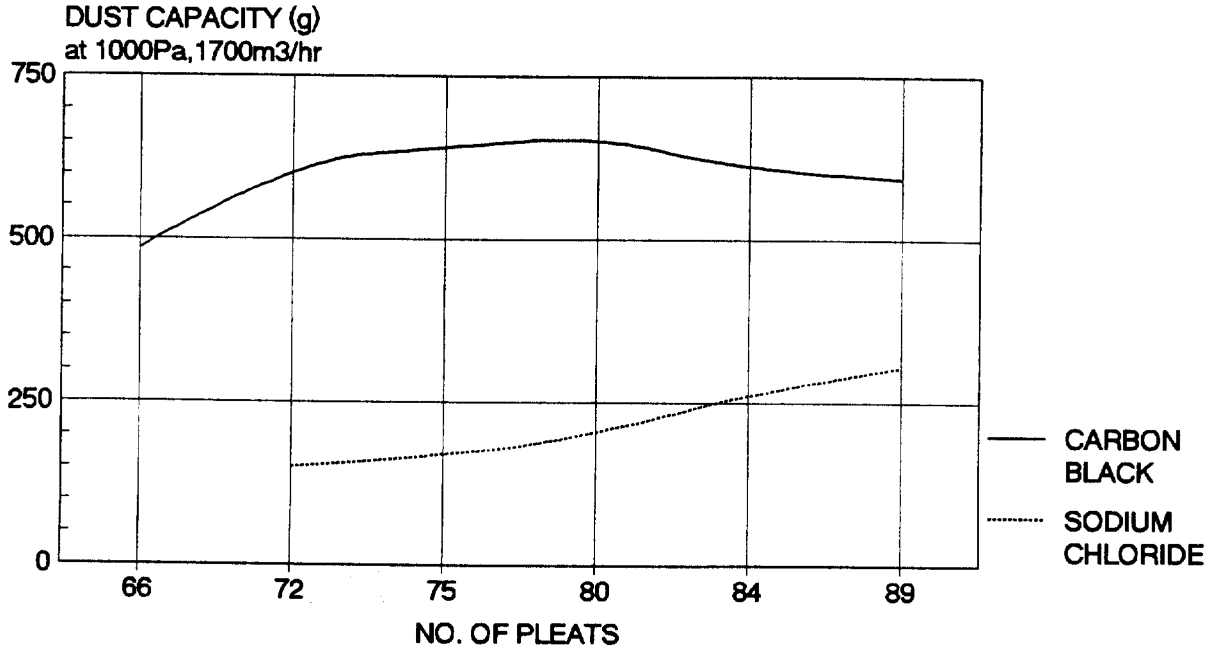

PAPER No.

DUST4

84 and 89 pleats resulted in a (small) apparent reduction in carbon black capacity.

Discussion of Results

As the number of pleats varies, different mechanisms interact to affect the filter resistance. Channel cross-sectional areas will decrease both individually and overall, so that the increased air velocity at the channel entrance will cause increased pressure losses.

The increased velocity may also in the latter stages of loading encourage a build-up of dust at the channel entrance thus further reducing the entrance cross sectional area.

It appears these effects are cumulative and more than counterbalance the advantages of the larger media area as may be seen in the results for 84 and 89 pleats, where the dust capacity of the unit is less than for 80 pleats.

This result suggests that HEPA filters having a paper area of 24-25m^2 will have an optimum capacity for dust having properties equivalent to those of carbon black.

Deep-Pleat v Minipleat Capacity (Carbon Black) at 1700 m^3/h

Figure 2 shows carbon black dust loading results obtained with a minipleat filter having some 31 m^2 of media. Although its initial resistance was well below those of all of the deep-pleat units, it rose to the terminal value, (1000Pa), with a dust load of only 360 g, approximately 55% of that obtainable (660g) with the 80 pleat deep-pleat unit. This result, which was for comparative purposes only was in line with the results of earlier tests[2] carried out on minipleat filters at a higher flowrate.

SODIUM CHLORIDE LOADING RESULTS

The results of loading the range of deep-pleat filters with the sub-micron sodium chloride aerosol are shown in Figure 3. The capacities are lower (in terms of weight) than those obtained using carbon black by a factor of about 3. As the basic particle density is similar it may be deduced that the difference relates to the greater drag engendered by the finer particle deposits.

The sodium chloride dust holding capacity of the range of deep-pleat filters increased steeply with increase in media area, in line approximately with (number of pleats)$^{3.5}$; considering that the average thickness of a continuous the dust layer would be in the region of only 5-10μm, it is apparent that a "cake" filtration regime will not have been established; thus the changes in resistance will be accounted for by a combination of increase in fibre drag from the adhering particles on the one hand and on the other by increased local velocities where the flow passages between the surface fibres are restricted.

DISCUSSION OF RESULTS

Results obtained for the two dusts vary significantly but do not necessarily represent the extremes of the whole range of operational situations.

It will be seen that the advantages of larger area HEPAs in terms of dust holding capacity are realisable principally when "fine" aerosols are involved. For aerosols having properties equivalent to carbon black there is a significant advantage in an increased area up to say 24 m^2. Increasing the area further can be counter productive.

Should a dust be coarser and even more cohesive than carbon black then the chances of covering the channel entrances become greater. The optimum HEPA design in such a case would be likely to shift towards fewer (and wider) channel entrances.

Such observations fit with the thesis that HEPA filters are far from ideal as economic collectors for significant quantities of dusts, particularly coarse and/or "sticky" dusts. They perform best as "final polishers", or the ultimate guarantee of the effective removal of airborne particulate material, when the residual airborne concentrations involved are very low.

When filter disposal costs become a major operating cost as may be the case with radioactive processing facilities it is relevant to note that the weights of dust collected (of the order 150 - 600g in the present work) are a small percentage fraction (say ~1-2%) of the total weight (20 - 30 kg) of a typical HEPA element.

Economic use of HEPAs where significant concentrations of airborne particulates are involved requires that consideration be given to the use of renewable (eg cleanable) devices to remove coarse cohesive material and thus minimise the number of HEPA changouts during the life of a system.

Enhancement of HEPA life by using increased areas of filter media within the same envelope is therefore most effective when fine well dispersed aerosols are involved; this is also reflected in the findings for graded papers[3] when optimum enhancement was obtained in the collection of the finer aerosol.

CONCLUSIONS

1 For operational situations/conditions where the challenge is predominantly a "fine" aerosol which is collected evenly throughout the whole effective media area and where there is a premium on disposal costs there would appear to be significant potential advantage in using filters with larger areas of filter media. Such conditions also favour the use of filters having "graded" paper media, and the dust characteristics conferred by a combination of such features remains

to be explored.

2 When there is a relatively cohesive and/or coarse particulate challenge to the HEPA filters, uneven dust deposition may lead to restriction and partial closure of the channel entrances. Such phenomena may cause premature resistance rises resulting in under-use of much of the media area (and consequent higher frequency of change out and accompanying elevated disposal costs).

REFERENCES

1 First, M. W., Performance of 1000cfm and 1800cfm HEPA filters on Long Exposure to Low Atmospheric Dust Loadings. 17th Air Cleaning Conference (1982) p909

2 Loughborough, D., The Dust Holding Capacity of HEPA Filters. 21st Air Cleaning Conference (1990) p

3 Dyment. J. & Hamblin, C., Development of a HEPA Filter with Improved Dust Holding Characteristics. 23rd Air Cleaning Conference (1994) p

4 AESS 30/93402

5 British Standard 3928:1969

6 Poynting, R., Comparisons of the Sodium Chloride Aerosols used by the CDE for Air Filter Tests. (U) June 1979. CDE Tech. Note No. 393

7 Hamblin, C.,UKAEA, Unpublished work.

ACKNOWLEDGMENTS

Acknowledgement is due to AAF Ltd, MC Air Filtration Ltd and Trox Brothers Ltd who supplied filters for this work. The work was carried out by AEAT Harwell under contract to the MoD.

Published with the permission of the controller of
Her Britannic Majesty's Stationery Office

DISCUSSION

DORMAN: Carbon black is notorious for forming long chains and is therefore more likely to cause "bridging"than small single particles. I am, however, somewhat surprised that relatively coarse particles size (conclusion 2) may have the effect of closing channel entrances. Cold you give a size to "relative" and also say how uneven the deposits were?

DYMENT: The aerodynamic MMD of the airborne carbon black as measured by cascade impactor was 2μm, with 35% below 1 μm, with 35% below 1 μm. The phenomenon of "uneven depostion" of test dust related to its observed tendency to accumulate more rapidly near the entrances to the pleats, causing eventual flow restriction. We are not able to quantify the degree of uneveness but we assume it results from increased local inertial deposition favored by the local flow pattern and the known cohesiveness of the dust.

POTENTIAL FOR HEPA FILTER DAMAGE FROM WATER SPRAY SYSTEMS IN FILTER PLENUMS*

by

Werner Bergman, Jan K. Fretthold[1], and James W. Slawski[2]
Lawrence Livermore National Laboratory
Livermore, CA 94550

Abstract

The water spray systems in high efficiency particulate air (HEPA) filter plenums that are used in nearly all Department of Energy (DOE) facilities for protection against fire was designed under the assumption that the HEPA filters would not be damaged by the water sprays.(1) The most likely scenario for filter damage involves filter plugging by the water spray, followed by the fan blowing out the filter medium. A number of controlled laboratory tests that were previously conducted in the late 1980s are reviewed in this paper to provide a technical basis for the potential HEPA filter damage by the water spray system in HEPA filter plenums.

In addition to the laboratory tests, the scenario for HEPA filter damage during fires has also occurred in the field. A fire in a four-stage, HEPA filter plenum at Rocky Flats in 1980 caused the first three stages of HEPA filters to blow out of their housing and the fourth stage to severely bow. Details of this recently declassified fire are presented in this paper.(2) Although these previous findings suggest serious potential problems exist with the current water spray system in filter plenums, additional studies are required to confirm unequivocally that DOE's critical facilities are at risk.

I. Introduction

One of the most serious issues dealing with HEPA filters in DOE nuclear facilities is the potential for HEPA filter rupture during accidental fires and the resulting release of radioactive smoke. This potential is not addressed in most Safety Analysis Reports (SARs) and Environmental Impact Statements (EISs) prepared for DOE facilities. The common practice in SARs and EISs is to use the HEPA filter efficiencies stated on page 22 of the Elder Report:

---

[1] Rocky Flats Safe Sites of Colorado, P.O. Box 464, Golden, CO 80402
[2] U.S. Department of Energy, Defense Programs(DP-45), Germantown, MD 20874

*This work was performed under the auspices of the U.S. Department of Energy by Lawrence Livermore National Laboratory under contract no. W-7405-ENG.45. The work was supported by DOE's Defense Program Office of Technical and Environmental Support, DP-45.

99.9% efficiency for the first stage HEPA filter and 99.8% efficiency for every filter stage thereafter under every accident condition.(3) Elder obtained these values from unpublished minutes of a meeting held in Albuquerque on December 9, 1971 to discuss HEPA filter efficiency values to be used under normal and accident conditions.(4) The selected values have no technical support and were based on the personal opinions of the twelve people attending the meeting (representatives from the Atomic Energy Commission (AEC) and the Albuquerque Operations Office). One stipulation on the use of the efficiency values, not included in the Elder report, was that "SARs show that the integrity of the filters will be maintained throughout the duration of the accident."(4) Unfortunately, most SARs and EISs use the Elder HEPA efficiency values without establishing that the filter integrity will be maintained. In contrast to the current practice of using a constant 99.9% or 99.8% efficiency for all conditions, more recent guidance recommends that the HEPA filter efficiency should be determined on a case-by-case basis and can have 0% efficiency in some cases.(5)

The use of water sprays inside HEPA filter plunums was the engineering solution to fires that had occurred at the Rocky Flats Plant. On September 11, 1957 a fire had spread through the ventilation system and threatened the final HEPA filter bank of 700, 1,000 cfm HEPA filters.(6) Firefighters used 2 1/2 inch hose lines to put out the fire. The HEPA filters were combustible and used media made from cellulose and asbestos fibers. Over 400 of the 700 HEPA filters in the final bank burned through, and almost every filter was ruined.(6) Following this fire, all combustible HEPA filters in AEC facilities were replaced with non-combustible glass fiber filters. A second major fire occurred at Rocky Flats on May 11, 1969.(6) The fire engulfed many glove boxes, burning many tons of plastic windows, and spread through the ventilation system. The fire broke through the glove box HEPA filters, intermediate filter banks, and the first stage of the final HEPA filter bank. Firemen were able to put out the fire within four hours and before the final stage was breached.(6) This fire was the most expensive ($27 million) in AEC and DOE history. Following this fire, studies were conducted to evaluate various fire protection systems for HEPA filters. These studies, which are reviewed in this paper, led to the use of water sprays inside HEPA filter plenums. However, another fire occurred at Rocky Flats on July 2, 1980 in which sprinklers were used, but the fire still resulted in extensive HEPA filter damage. An analysis of this fire in this report raises questions about the use of water sprays for protecting HEPA filters from fires.

II. Typical Water Spray System in Filter Plenums

DOE has prepared a standard on Fire Protection Design Criteria in which the water spray system shown in Figure 1 is recommended for use in HEPA filter plenums.(7) The Design Criteria document formalizes a design that has been used extensively throughout DOE facilities for many years since the 1969 Rocky Flats fire. The fire protection system consists of a heat detector at the plenum inlet, an automatic deluge spray head followed by a demister stage, and manual spray nozzles directed at the first of a two-stage HEPA filter bank. The function of the automatic deluge spray is to provide a uniform sheet of water over the entire cross section of the plenum in order to cool hot intake air. Figure 2 shows the typical spray nozzles used for the deluge spray (Figure 2A) and for the HEPA filter spray (Figure 2B). The deluge nozzle directs a flat, 180° fan-shaped spray pattern toward the floor where the water enters a drain, whereas the HEPA filter spray nozzle directs a 360° cloud of fine mist against the face of HEPA filters. Figure 3 shows a photograph of a deluge spray nozzle mounted on the ceiling of a 4x4 HEPA filter plenum and located close to the inlet of the metal mesh demisters. A second deluge spray nozzle is not seen in the photograph. The deluge spray is generated at 0.25 gpm per square foot of filter area, or 16 gpm for the 16 2'x2' demisters in Figure 3. Any water droplets carried in the air stream are removed by the demisters.

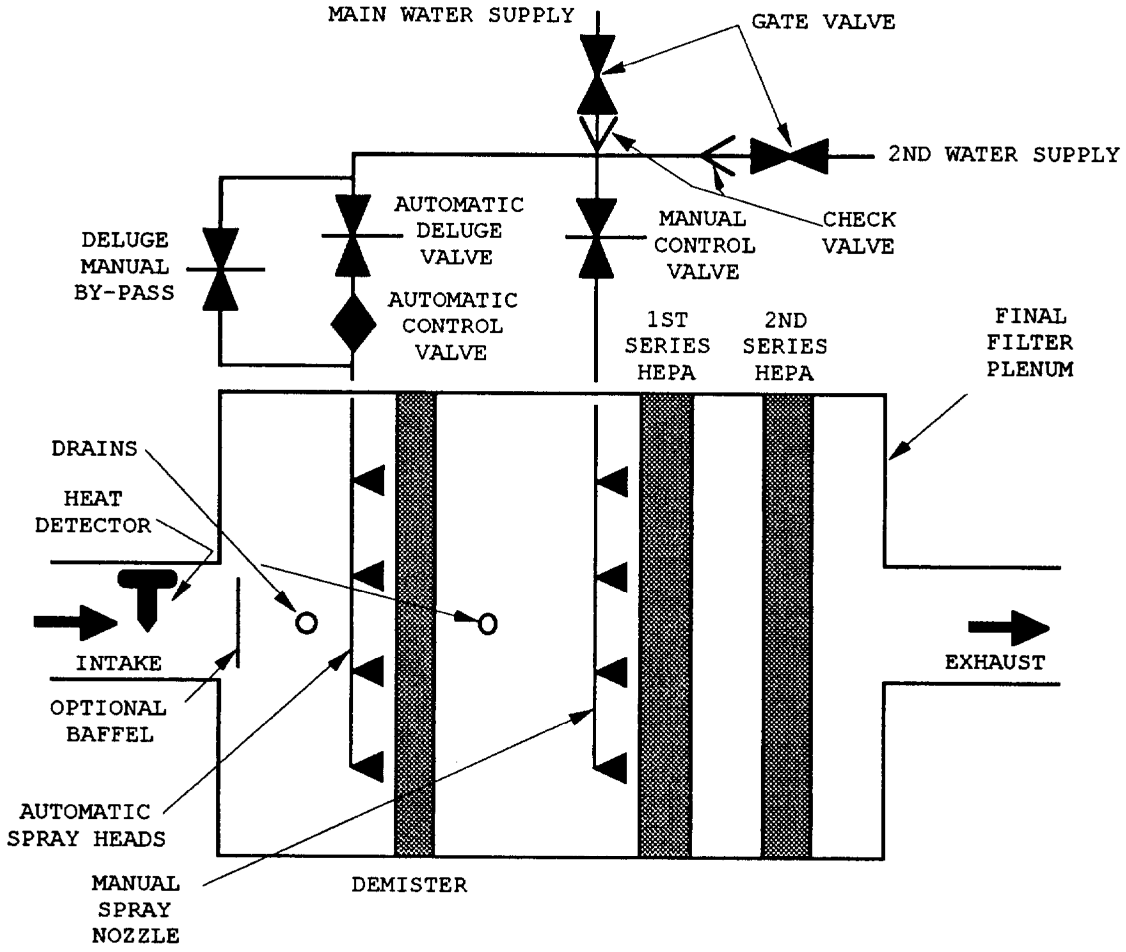

Figure 1 Diagram of the fire protection system for HEPA filter plenums widely used in DOE facilities and specified in DOE Standard on Fire Protection Design Criteria, DOE-STD-1066-XX (7)

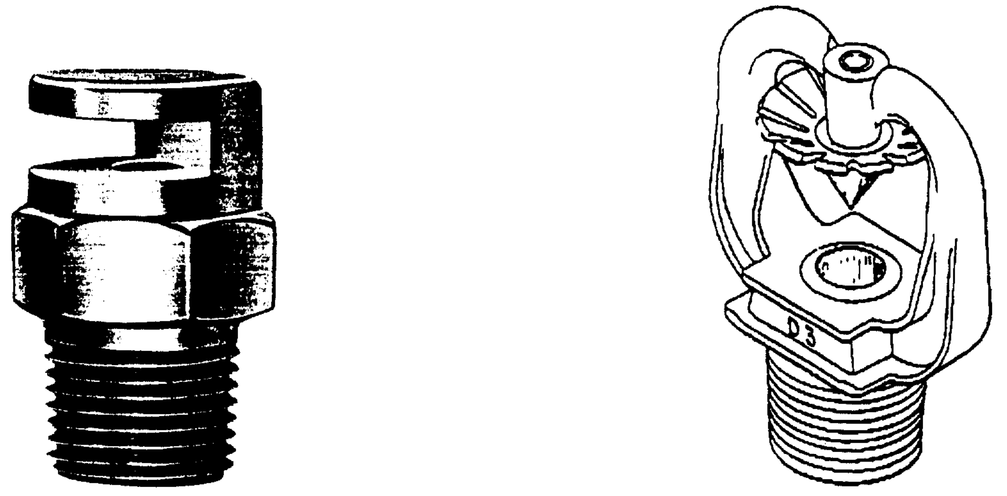

(A) (B)

Figure 2. Drawings of typical spray nozzles used for (A) the deluge spray and (B) the HEPA filter spray. The deluge spray nozzle grenerates a flat, 180° fan-shaped spray pattern. The HEPA filter spray nozzle generates a 360° cloud of fine mist.

Manual spray nozzles, like the one shown in Figure 2(B), are directed at the first stage HEPA filters to put out potential fires should they occur. However, since the HEPA filters are easily damaged by direct water sprays, the selected nozzles must generate a fine water mist. Figure 4 shows a photograph of a manual spray nozzle mounted on the ceiling of the filter plenum with the spray nozzle directed against the first stage HEPA filters. A second spray nozzle is not seen in the photograph. The water flow through both nozzles is 0.25 gpm per square foot of filter area, or 16 gpm for the 16, 2'x2' HEPA filters. Some facilities periodically test the water spray and unavoidably wet the HEPA filters. This practice reduces the strength of the HEPA media as described later in this report and should be avoided.

In preparing the Fire Protection Design Criteria, the DOE fire protection engineers recognized the potential of the water sprays to damage the HEPA filters.(7) To mitigate this potential, the standard recommends throttling back the fan controls or providing redundant filters. Unfortunately, there are no studies to support these recommendations.

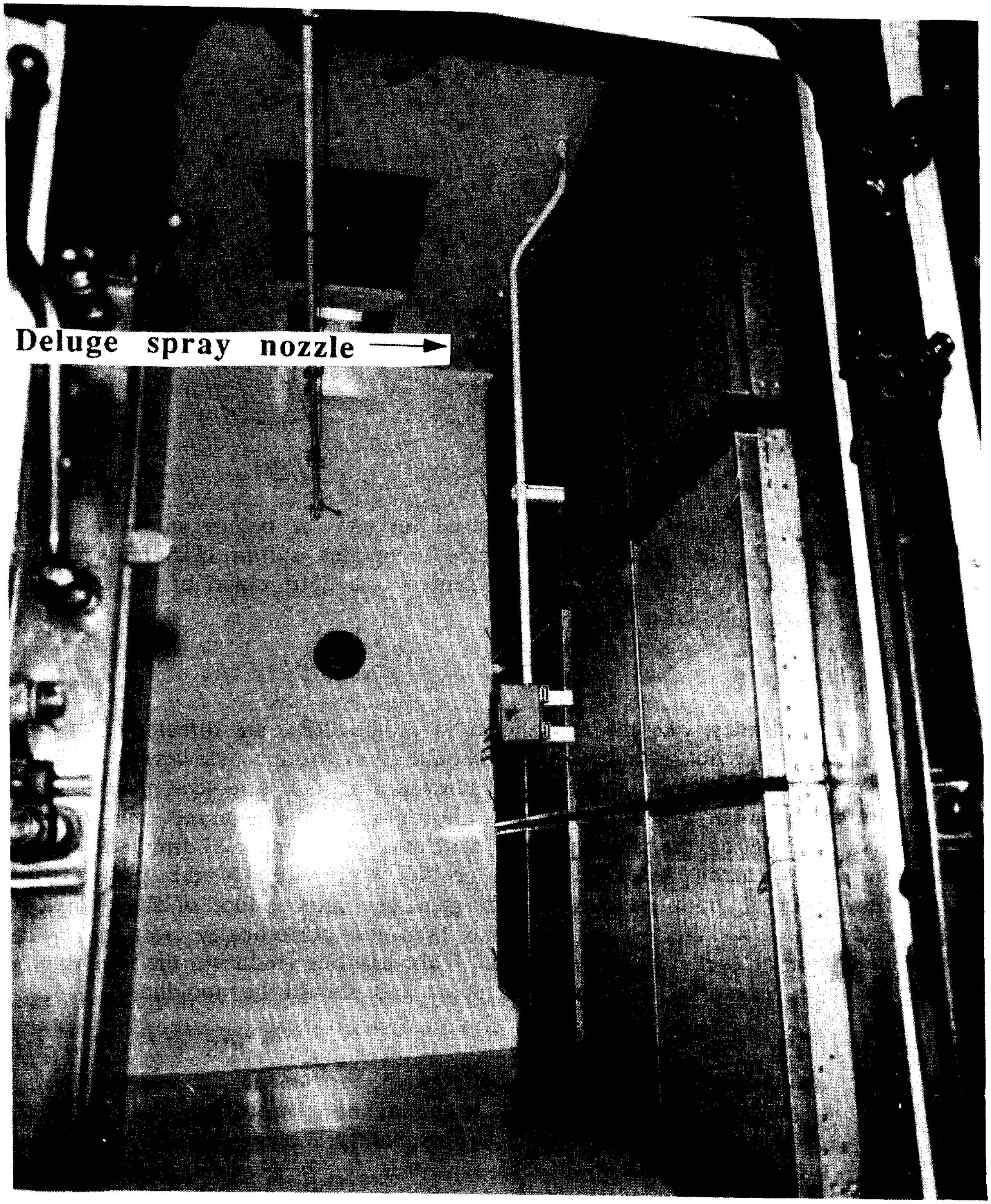

Figure 3. Photograph of a deluge spray nozzle mounted on the ceiling of a 4x4 HEPA filter plenum and located close to the inlet of the metal mesh demisters. The access door to the demister stage was opened for the photograph.

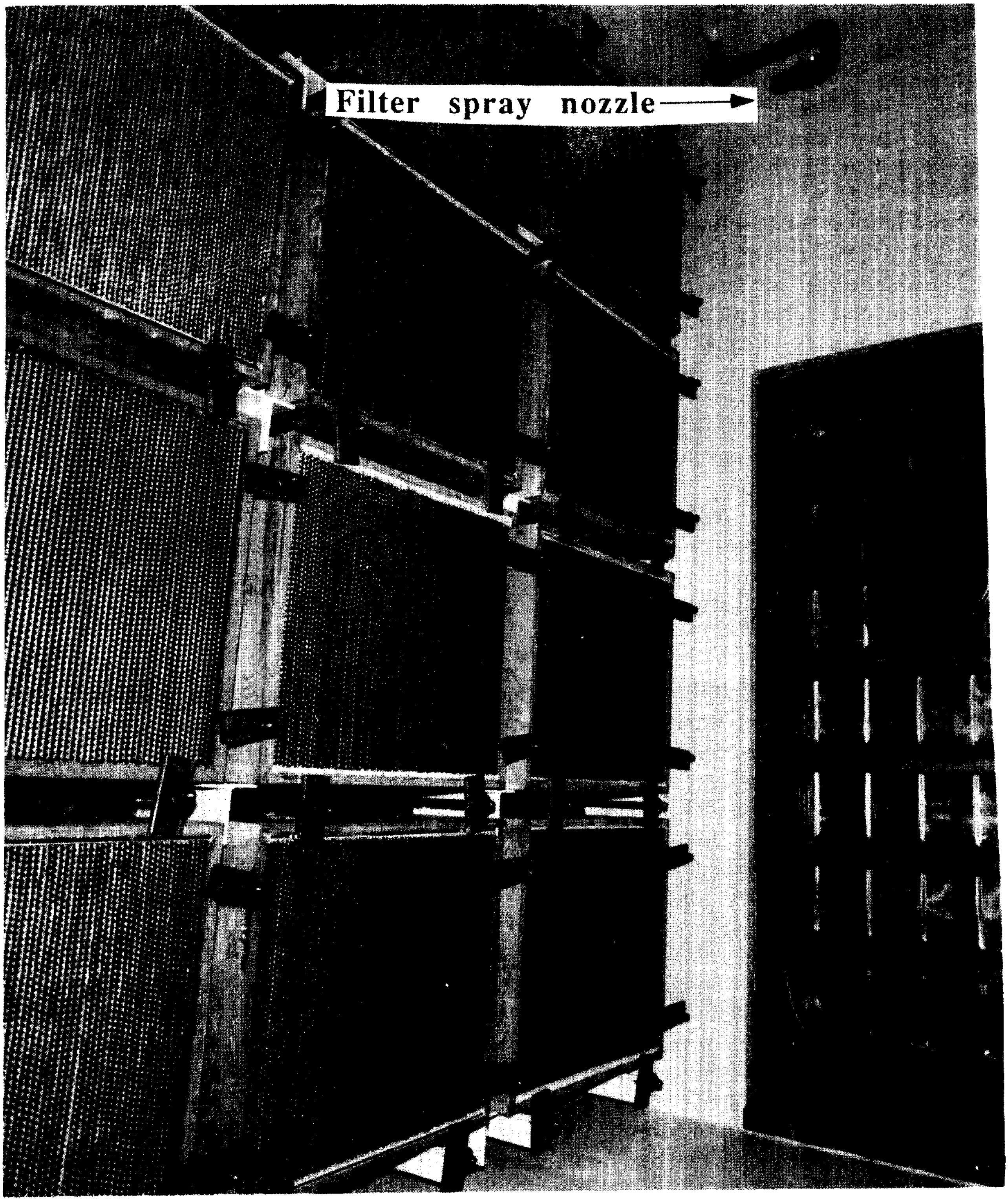

Figure 4. Photograph of a manual spray nozzle mounted on the ceiling of the filter plenum with the spray nozzle directed against the first stage HEPA filters.

III. Studies Conducted in 1970s On Water Spray Systems Were Incomplete

Several studies were conducted after the 1969 Rocky Flats fire to develop engineering solutions that prevent or mitigate the destruction of HEPA filters in filter plenums during ventilation fires. Although these studies demonstrated the performance of various technologies such as water sprays and demisters, no baseline studies were performed to attempt to destroy the HEPA filters under fire conditions that simulated the 1969 Rocky Flats fire. Thus, it was not possible to assess what benefit the fire protection counter measures had on the HEPA filters.

Cartwright et al conducted 13 full-scale tests on a 2-stage, 3x4 HEPA filter plenum (12 HEPA filters per stage) that was specially built for this study at Rocky Flats.(8) A separate structure was built to house an incinerator that injected hot exhaust into the filter plenum. Only new 2'x2'x1' HEPA filters were used in that study. The authors found that using water sprays directly on HEPA filters would soak the filter and create holes in the media and therefore recommended that direct water sprays be controlled manually and only used under extreme emergencies. They also found that a deflector plate on the inlet pipe and a water curtain followed by a prefilter reduced the gas temperature and prevented most of the sparks and water spray from reaching the HEPA filters. Unfortunately the test conditions in that study were very mild and not representative of potential, worst case conditions. The pressure drop across the HEPA filters in this study was quite low (values ranged from 0.3-0.7 inches) and could not cause any structural damage. No baseline tests were conducted to see the effect of the fire tests on HEPA filters alone.

Domning conducted full scale tests to evaluate water spray heat exchanges for protecting HEPA filters under fire conditions.(9) He conducted two tests using water sprays on a filter plenum consisting of a single stage of 12 new HEPA filters for each test. In one test, the water spray was directed against an inlet deflection plate and in the second, directly on the 12 HEPA filters. The water flow rate was 0.25 gpm per square foot of filter area. The analysis of the test results showed that the added water spray increased filter plugging compared to plugging by smoke alone. The pressure drop across the HEPA filters was so low (0.3-0.4 inches) that no structural damage was seen.

Gaskill and Murrow conducted 13 tests in which they studied cooling hot gases with various water spray and demister configurations upstream of single, new HEPA filters.(10) They used a propane burner to generate the high temperature air stream. Although they showed that a water spray with demister was effective in reducing the gas temperature, they had no baseline tests with HEPA filters without the water spray/demister system. Moreover, none of the tests showed filter plugging by water because the temperature at the HEPA filter was above the boiling point of water. In addition, since new HEPA filters were used in the study, the filters had the factory treatment of water repellency, which prevents them from plugging with water.

Based on these early studies, fire protection engineers incorporated water sprays and demisters into HEPA filter plenums to protect the HEPA filters against fires. These fire protection systems have remained essentially constant over the years and now represent the standard in DOE facilities.(1) The main attention in these early studies was focused on the high temperature aspects of the fire. Domning's finding that water sprays increased the plugging effect of smoke aerosols was not seen as an important factor for fire protection.(9) Even after Alvares et al completed an extensive study of HEPA plugging by smoke aerosols, the major concern was still high temperatures inside the filter plenum.(11) Alvares et al showed that smoke aerosols can rapidly plug HEPA filters and that water sprays accelerate and exacerbate the effect. However, the primary result of a plugged HEPA filter is the loss of ventilation. Since the plugged HEPA filter prevented radioactive particles, as well as air, from passing through, the plugged HEPA filter produced a passive containment system. Passive containment is presently used in some DOE facilities. Thus, the concerns about HEPA failures during fire conditions seemed to be generally resolved until the mid 1980s when German researchers demonstrated that water sprays and even high humidity can cause HEPA filters to rupture.(12-14)

IV. German Studies in 1980s Show Water Sprays Damage HEPA Filters

Ruedinger et al showed that high humidity can result in high filter pressure drop and decreased media strength, the combination of which can lead to structural damage and loss of filter efficiency.(12) They built a special test facility to study moisture effects on full-scale HEPA filters under various temperature and flow conditions. They found that the 11 deep pleated HEPA filters with an elastomeric sealant had structural failures at an average differential pressures of 20 inches and as low as 10 inches under wet conditions. The most frequent failure mode is the rupture of the downstream media pleats.

The filters with stainless steel frames and a glass fiber sealant were significantly weaker. The three filters tested failed at an average of 9.5 inches, and as low as 6.8 inches. The failure mode in these filters was the filter pack being pushed out of the frame, since the glass fiber sealant held the filter pack in place by friction.

For both filter types, there was no significant difference in the break pressure whether the filter was clean or had particle deposits. However, with particle deposits, the filter would absorb water at lower relative humidities and would rupture even with a demister to protect the HEPA filter. Ruedinger et al also showed that a new HEPA filter with no particle deposits would not rupture if a demister were used because not enough water would accumulate on the filter to raise the pressure drop to the failure point.(12) The filter failure under the humid air conditions occurred at differential pressures that were about 1/3 to 1/4 the comparable values for filter failure under dry conditions.

Ruedinger et al confirmed that the decreased strength of the wet HEPA filters is due to the decreased tensile strength of the glass HEPA media.(12) They showed that the tensile strength of a new filter paper is reduced by a factor of three due to humidity exposure. Ruedinger et al also conducted tests on new HEPA filters made from polycarbonate microfiber media and showed no structural damage up to the maximum pressure of 32 inches of water.(12) Although these filters do not meet the UL 586 requirements for the spot flame test, they are very resistant to water and acid exposure.(1)

Ricketts et al evaluated the structural limits of a variety of different HEPA types under high humidity conditions.(13) Ricketts et al tested 29 HEPA filters having the conventional US design (deep pleat with adhesive sealant) and found many filters failing at lower pressures than previously reported by Ruedinger et al.(12) Ricketts et al also showed that the primary failure mode is the rupture of the downstream pleats.(13) This mechanism is facilitated by the loosening of the filter pack and a ballooning of one or more pleats due to the pressure. Another failure mechanism is the tearing of the media near the sealing edges of the frame and results from a loosened filter pack. They found that the average failure pressure for the deep pleated filter with an adhesive sealant is 16 inches. Of the 29 filters tested, only three had failures less than 10 inches of water; one failed at 3.6 inches and two at 7 inches. In separate tests on HEPA filters using glass fiber sealants, they found that the breaking point was one half (8.8 inches) the breaking strength of the standard deep pleat filter with an adhesive sealant. The weakest filter design was the mini-pleat, where the structural failure occurred at an average pressure of 3.6 inches and a minimum of 1.6 inches.

Ricketts et al noted that particle deposits cause HEPA filters to fail at relative humidities less than 100%.(13) Although the average HEPA failure occurred at 97% relative humidity, two deep-pleated HEPA filters failed after exposure to 80% relative humidity for two hours. In contrast, clean filters require a water content greater than 100% relative humidity to induce structural failures. They found that the failure pressures were the same for filters with and without particle deposits as previously found by Ruedinger et al.(12)

Ricketts et al pointed out that the humidity causes HEPA filters to have structural failures at differential pressures that are 60% to 90% lower than the failure under dry conditions.(13) For example, a deep pleated, clean HEPA filter is structurally damaged at 13.7 inches under humid conditions and at 92 inches (3.3 psi) under dry conditions.

An important finding by Ricketts et al is that the combination of factors leads to an even greater filter deterioration than the cumulative effect of the individual factors alone.(13) Tests on the filter media showed that moisture causes a 60% decrease in tensile strength, creases cause a 45% decrease, moisture exposure with subsequent drying causes a 40% decrease, and dust loading on creased samples cause a 5% decrease. A cumulative effect of these factors would predict a residual tensile strength that is 13% of the value of a new, uncreased HEPA media. Experimental values for filter media subjected to the combination of exposures showed a residual tensile strength that was only 7% of its original value.

Ricketts et al extended their previous studies to show the effect of filter design, particle deposits, and the quantity and time of water exposure on the pressure drop of HEPA filters.(14) They showed that the standard, deep pleated HEPA filter loaded with dust to 4 inches, would reach a pressure drop of 10 inches in 8 minutes and 14 inches in 30 minutes when exposed to humid air with relative humidity between 96% and 99%. The major findings of this study were: (1) particle deposits greatly accelerate the increase in pressure drop due to moisture, (2) the greater the water content, the faster the rise in pressure drop for both clean and dust loaded filters, and (3) mini pleat filters have more rapid increases in pressure drop than deep pleat filters for the same moisture exposures.

The results of these German studies suggest that the water spray systems in filter plenums in DOE facilities may result in HEPA filter rupture during actual fire conditions. Surprisingly, the German studies did not stir much concern with fire protection engineers in the U.S.. Although the controlled laboratory studies were quite convincing, there were no examples of fires in any of the DOE facilities where the water spray caused HEPA filter failures. However, in 1995 Fretthold had issued a recently declassified report that described a 1980 fire at Rocky Flats involving water sprays and blown out HEPA filters.(2) That report confirmed the predictions of the German laboratory studies.

V. 1980 Filter Plenum Fire at Rocky Flats Caused Extensive Filter Damage

Fretthold described the results of a fire in a HEPA filter plenum at Rocky Flats that occurred on July 2, 1980.(2) The fire occurred in a HEPA filter plenum that filtered the exhaust from an incinerator shown in the drawing in Figure 5. The exhaust from the incinerator is treated in an off-gas system in which the hot exhaust gas is first sprayed with a caustic solution to cool the gas and to neutralize the acid gases and then passed through a wet cyclone to remove suspended particles. Figure 6 shows the off-gas system. The treated exhaust then passes through a booster blower and into the incinerator filter plenum, as shown in Figure 7. A deflector cone at the plenum inlet deflects the incoming air to distribute the air more uniformly over the HEPA filters mounted 3 high and 4 across. Note that only 600 cfm passed through the plenum that had a filter capacity of 12,000 cfm. Although the filter plenum contained 4 stages of HEPA filters, the stages were incorrectly mounted back-to-back. The incinerator plenum did not have an automatic deluge spray system or a demister stage in front of the first HEPA bank. The exhaust from the incinerator plenum then enters the main building plenum.

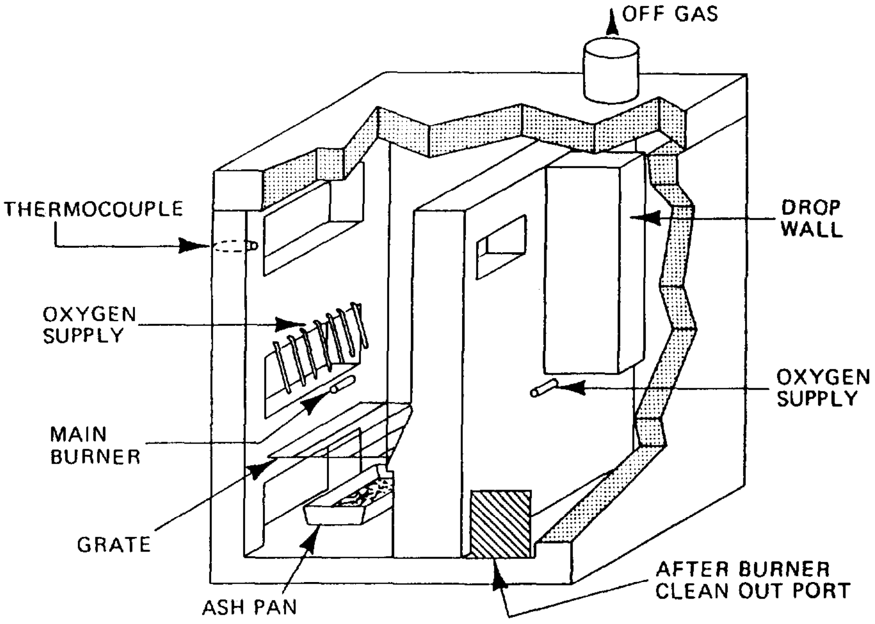

Figure 5. Drawing of the Rocky Flats incinerator.

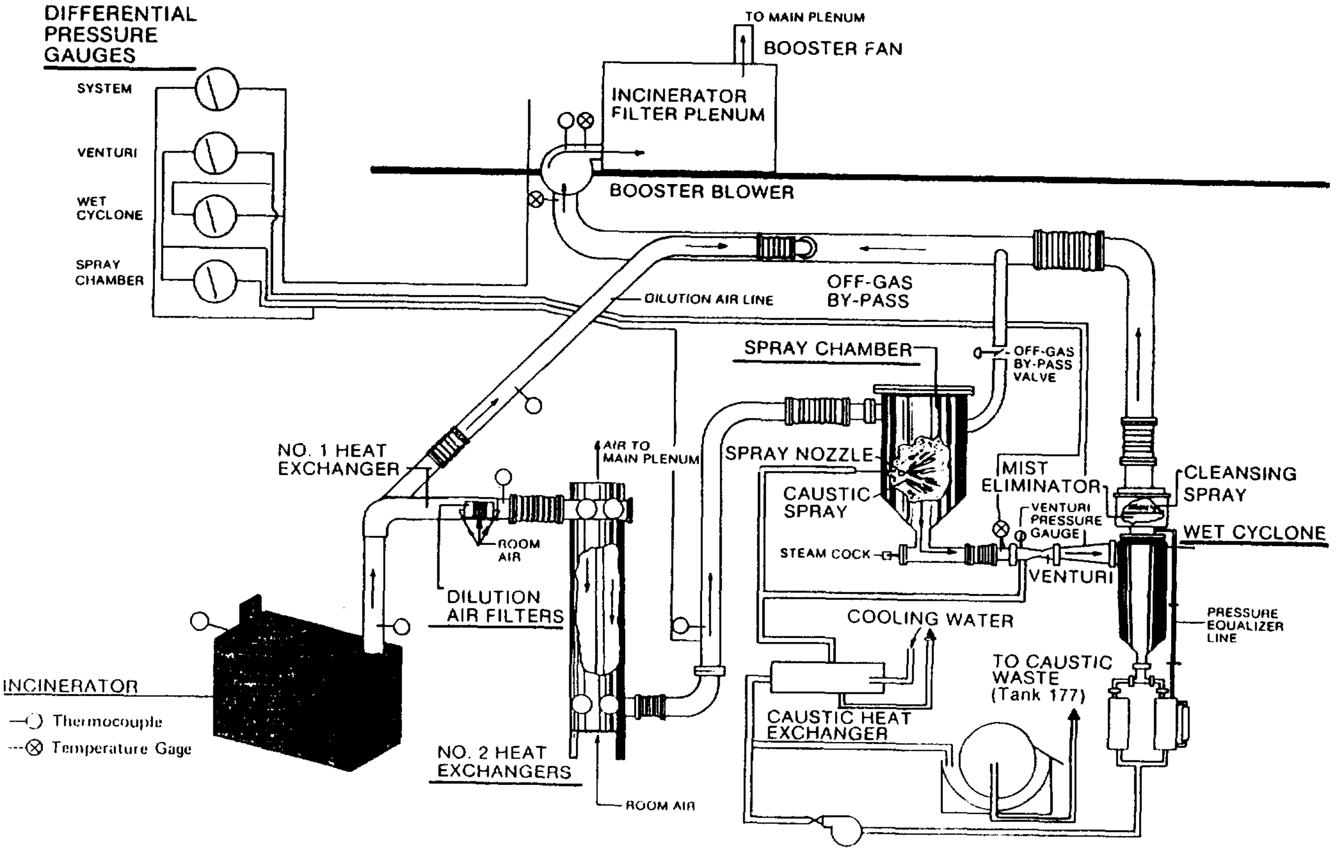

Figure 6. Schematic of the incinerator off-gas treatment system

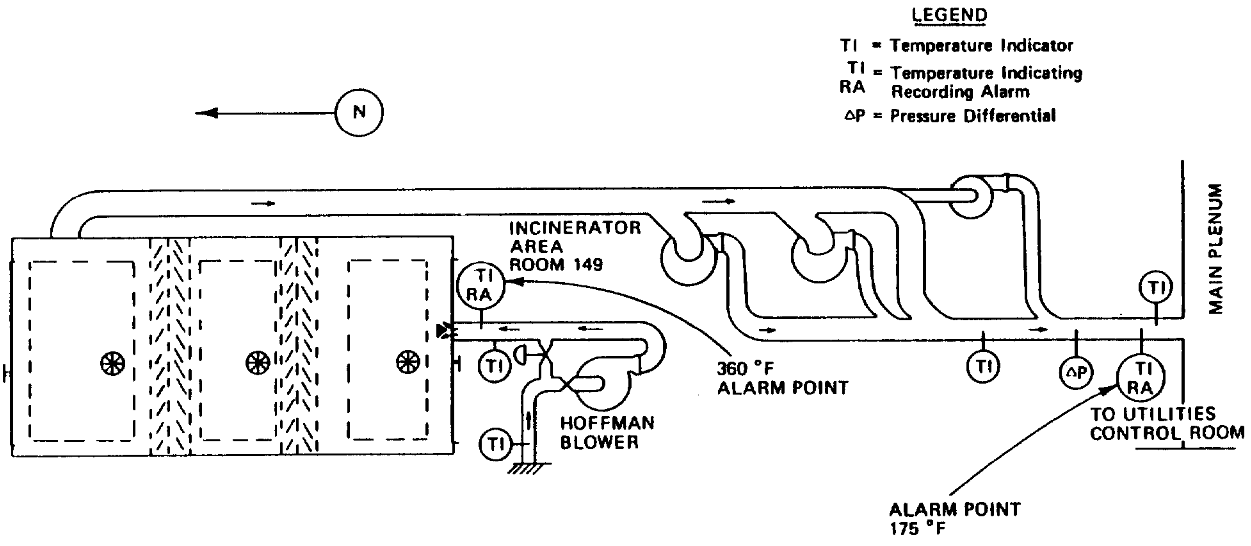

Figure 7. Incinerator filter plenum system

On July 2, 1980, a fire had occurred in the incinerator filter plenum and had extensively damaged the first three stages of HEPA filters and caused the fourth stage to severely bow.(2) A continuous recording of the plenum inlet temperature showed the temperature was constant at 100°C for several hours prior to 11:00 A.M.. At that time the inlet temperature increased linearly with time until it reached a maximum 180°C at about 12:40 A.M.. At 11:30 A.M., the production foreman inspected the filter plenum and noted the plenum inlet temperature was 70° C, the differential pressure across the HEPA filters was 0.7 inches of water, and the plenum vacuum was 7 inches of water. These were normal readings. (The automatic temperature recording at 11:30 A.M. showed the inlet temperature was 110°C, not 70°C.) At 12:34 P.M., the alarm for the incinerator filter plenum sounded as well as the main filter plenum. The deluge spray also was automatically activated in the main plenum. Responding to the incinerator fire alarm, the utilities manager observed a red glow within the incinerator plenum and then activated the manual deluge sprinklers. Shortly thereafter, firemen arrived and also noticed a red glow in the plenum and that the manual water spray had been activated. They then attempted to enter the plenum with building water hoses, but could not open the airlock doors due to the high vacuum. After reducing the air flow, the firemen entered the incinerator plenum and sprayed the HEPA filter banks with a fine water mist. Photographs of the filter plenum in Figures 8-14 showed extensive HEPA damage.

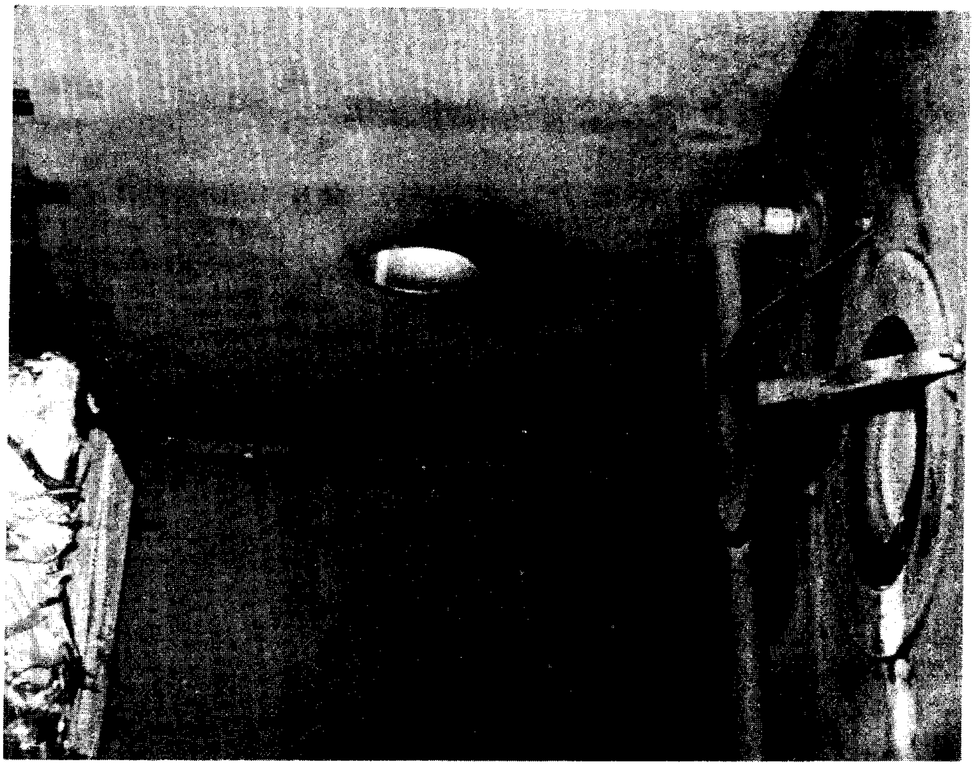

Figure 8. Photograph inside the front chamber of the filter plenum showing the air inlet with deflector cone and the damaged first stage HEPA filters.

Figure 9. Photograph showing the front side of the first stage HEPA filters.

Figure 10. Photograph inside the middle chamber of the filter plenum showing the rear side of the 2nd stage HEPA filters.

Figure 11. Photograph inside the middle chamber of the filter plenum showing the front side of the 3rd stage HEPA filters.

Figure 12. Photograph of the front side of a 3rd stage HEPA filter.

Figure 13. Photograph inside the second chamber of the filter plenum between the 2nd and 3rd HEPA stages. Note the partially melted plastic light fixture on the ceiling of the plenum.

Figure 14. Photograph of the rear side of the 4th stage HEPA filters.

The investigation following the fire concluded that the primary cause of the fire was the deteriorated off-gas bypass valve on the spray chamber shown in Figure 6.(2) The untreated hot exhaust was able to bypass the off-gas treatment and enter directly into the HEPA filter plenum. This raised the gas temperature at the plenum inlet to a maximum 180°C (356°F). In addition the investigators speculated that nitric and hydrochloric acids in the exhaust may have reacted with the urethane foam sealant used on the HEPA filters and raised the temperature even further.(2) The investigators also found metal oxide powders consisting of Cr, Fe, and Ni and as well as chlorates and nitrates on the filter media. Because the metal on the filter suggest their origin was stainless steel, the investigators concluded "This is an indication that the stainless steel duct work is being corroded by the acidic environment." From this, the investigators concluded that "All of these very fine metal particles collected on the filter media are capable of supporting combustion" and was responsible for igniting the HEPA filters.(2)

VI. Reevaluation of the Filter Plenum Fire Shows Water Sprays Caused the HEPA Filter Blow-out

Unfortunately, the investigators did not correctly assess the cause of the fire based on the evidence. They had assumed that acid had corroded the stainless steel ducting and somehow released unoxidized metal particles that were transported in the air to the HEPA filters. The problem with the investigators' assumption is that it is not possible for acid (or oxygen, salt, or any chemical) to corrode the stainless steel and release unoxidized metal particles. If acid or oxygen reacts with the stainless steel, it quickly oxidizes the iron. The oxidized iron is seen as the typical "rust powder" on the surface of steel. The "rust" will eventually ablate from the steel surface and be carried in the air stream to the HEPA filters. This is a common observation in the off-gas from incinerators.(15) In fact, so much rust had accumulated in the prefilters at the Savannah River incinerator that the prefilters had turned an orange brown color.(15) Once the metal has oxidized, it cannot be oxidized further and therefore will not support combustion.

The only combustible component in the HEPA filters used in the Rocky Flats incinerator plenum was the sealant that held the media pack to the frame. All other components were non-flammable as recognized by the fire investigators.(2) The HEPA used metal frames, aluminum separators and the standard glass fiber paper. None of these components will support combustion. Although not seen in Figures 9-14, the sealant was burnt and charred in all of the HEPA filters. However, the sealant was only exposed to the hot air flow on the top and the bottom portions of the frame. The sealant on the two sides is protected by a layer of filter media. Thus any combustion of the sealant would be confined to the upper and lower portions of the frame. This is seen in Figures 9-11, where the sides of the filter media are still attached to the frame, but the top portion of the media pack is completely separated from the frame.

We have previously shown that the urethane sealant in current HEPA filters will char and in some cases burn during the heated air qualification test.(16) Figure 15 shows a photograph of a new HEPA filter similar to widely used HEPA filters in DOE facilities following the standard heated air and overpressure test.(16,17) The urethane sealant had completely burned through from the inlet to the exit face of the HEPA filter during the heated air test. In this test, the HEPA filter is exposed to the rated air flow heated to 700 °F (371°C) for five minutes.(17) During the test, the burning urethane was seen as a red glow with only a small flame. Following the heated air test, the burnt filter had a DOP penetration of 1.24% and therefore passed the qualification test. However with the sealant burnt through, the filter pack was loose within the frame and could easily move forward or backward. The burnt filter was then placed in the overpressure test apparatus where the pressure drop across the HEPA filter was ten inches of water.(17) That pressure had displaced the HEPA filter pack about one inch in Figure 15 and was very close to blowing out the entire pack.

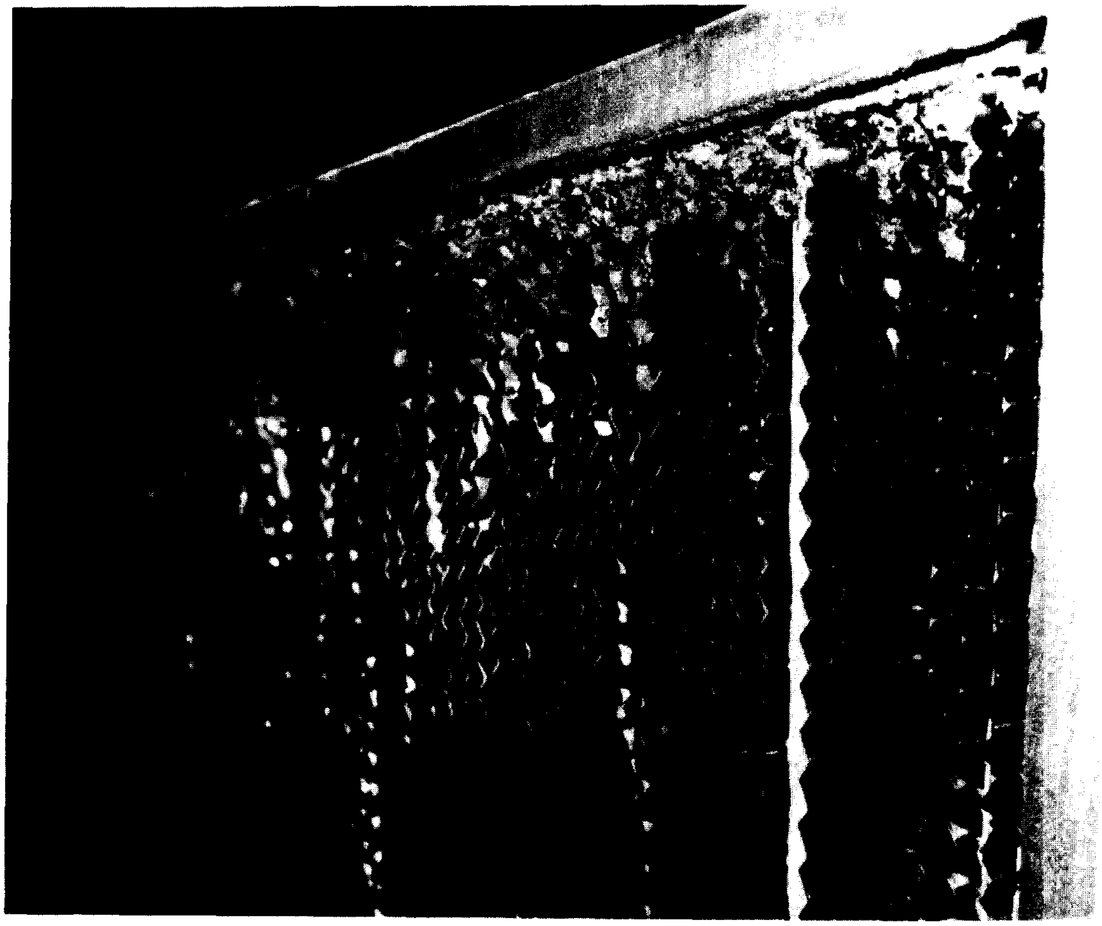

Figure 15. Photograph of the exit side of a new HEPA filter after the heated air and overpressure test. The burned urethane sealant created a separation between the filter pack and the filter frame.(16)

It is possible to reconstruct the sequence of events leading to the HEPA destruction shown in Figures 8-14 from an analysis of the photographs and the findings in previous studies. The initial step was raising the temperature of the air to a sufficient level to burn the urethane sealant. This was due to the defective by-pass valve in the off-gas treatment system. An added temperature increase may have come from the exothermic reaction between the acids and the urethane. Once the urethane sealant reached its ignition temperature, the sealant would burn. At this point, the HEPA filters would still be relatively intact. Based on our previous study, even a HEPA filter in which the sealant had burned completely through still had 99% DOE efficiency.(16) However, when the area foreman saw the red glow inside the filter plenum and turned on the water spray, the water caused the HEPA filters to plug. The effect of water plugging of HEPA filters was well documented in the German studies.(12-14) Domning and Alvares et al also showed that water sprays greatly enhance the normal filter plugging from smoke aerosols.(9,11) Bergman et al also showed that temperature or age will remove the water repellency treatment in HEPA media and thereby also result in HEPA plugging when exposed to moisture.(5) The high temperature in the filter plenum would be sufficient to drive off the water repellency treatment and result in HEPA plugging with water.

Once the filters were plugged or partially plugged, the pressure on the filters from the air flow was greatly increased and pushed against the filter pack (Recall that the firemen could not open the doors because of the negative pressure). For those filters in which the filter pack was loose from the burned urethane sealant, the pressure would cause the weakest part to be deflected. From Figures 9-12, the HEPA filter deflection began at the top of the filter where the filter pack had separated from the frame. Once the filter pack lost its integrity, blowing out the central part of the filter was easy. Note that not all of the filters suffered the same extent of destruction. Some filters showed no structural damage. The key to the filter damage was whether the filter pack was loose in the filter frame as a result of the urethane burning. Once some of the filters were blown out, the remaining filters were spared because the pressure on the filter bank was relieved when most of the air passed through the open paths.

The final filter bank was not destroyed, although some of the HEPA filters had severely bowed, as shown in Figure 14. The final HEPA stage would have experienced a lower temperature and far less water exposure then the first three banks. If the urethane sealant on the bowed HEPA filter in Figure 14 were burned out, then it would take less force to push out the HEPA pack because the top portion would be loose and not attached to the filter frame. The fact the filter pack is not blown out, but bowed, indicates the top urethane sealant was still holding the media pack to the filter frame.

Although the above scenario is consistent with the observations and previous studies, the report on the filter plenum fire stated that "the first three stages were sprayed and cooled" with fire hoses. To verify that the HEPA filter damage seen in Figures 8-14 was not due to firemen blowing out the filters with high pressure hoses, we interviewed two firemen who entered the plenum and sprayed the HEPA filters.(18) The first fireman stated that he looked through the viewing port on the inlet side of the first bank of HEPA filters and saw that the first bank was on fire, and that the HEPA filters showed large structural damage.(18) He also saw part of one HEPA filter on fire lying on the floor of the plenum. No one had entered the plenum at that time. After the air flow was turned down, he entered the downstream plenum door with a water hose having a fog nozzle, The hose was connected to the building water supply. He saw that the HEPA filters were on fire and sprayed them with the water mist, although none of the downstream HEPA filters were breached (See Figure 14). He also stated that the HEPA filter damage could not be caused by the water mist that he used.(18)

The second fireman arrived later and stated that he had entered the upstream plenum room (Figures 8 and 9) and saw the entire filter bank had been destroyed.(18) He did not spray any water on the first stage filters because there was no remaining fire. On entering the second door (Figures 10-13), he saw HEPA filters on fire and sprayed them with the water fogger. He stated that his spraying caused no further structural damage to the filters. He then entered the exhaust plenum, but since there was no fire and the HEPA filters were not damaged (Figure 14), he did not spray the filters.(18)

VII. Conclusions

The greatest damage to the HEPA filters in the 1980 filter plenum fire was due to the water spray. The high temperature from a defective by-pass valve in the incinerator exhaust was responsible for burning the urethane sealant in the HEPA filters. This, in turn, had weakened the physical strength of the filter pack because there was no longer a mechanical bond between the filter pack and the upper side of the filter frame. We speculate that the HEPA filters in this condition would have been fully operational with minimal deterioration (some filters may have reduced efficiencies to 99%). However, when the water spray was turned on, the filter began to plug with water, which raised the filter pressure drop. This increased pressure was applied to the structurally weakened filters and blew out the filter pack in several of the HEPA filters. Most of the exhaust would then pass through the blown-out HEPA filters and result in close to 0% efficiency for that filter stage. Three of the four filter stages had blown-out HEPA filters, and the fourth stage had some filters severely bowed and ready to rupture. There was no environmental contamination from the fire since the exhaust from the incinerator filter plenum was directed into the building filter plenum, which was not damaged.

The water spray inside the filter plenum was not able to put out the fire as designed. Firemen had to enter the filter plenum with spray nozzles to extinguish the flames. The ineffectiveness of the plenum water spray is due to the inaccessibility to the burning urethane sealant. Once the urethane sealant begins burning, it is not possible to extinguish the fire with ceiling mounted spray nozzles because the water cannot make contact with the burning sealant. The HEPA filter and frame protect the burning sealant from the water spray, especially on the upper side of the HEPA filter. Figures 9-12 show the complete separation of the HEPA pack from the upper frame due to the burnt out sealant.

The 1980 filter plenum fire and the German studies on filter plugging with water sprays raise serious questions about the effectiveness of the water spray system shown in Figure 1 for protecting HEPA filter plenums from fires. The omission of key experiments in the early studies that led to the present fire protection system for filter plenums have perpetuated the belief that the system will work as designed. The early studies showed that water sprays followed by demisters are very effective in lowering the air temperature, but they did not show the system could protect HEPA filters from structural damage. No baseline studies were conducted showing damaged HEPA filters. Laboratory studies show that the current HEPA filters in DOE facilities can be structurally damaged by filter plugging from moisture and/or smoke. Once a HEPA filter is plugged, it is prone to blow-out by the pull of the system blower, especially when the filter is wet.

Although the use of a metal demister, as shown in Figures 1 and 3, improves the reliability of the fire protection system by cooling the air and removing water droplets, the HEPA filters can still be blown out because of smoke and water plugging. Ruedinger et al showed that HEPA filters can rupture due to absorbed water even when protected by demisters.(12) Ricketts et al demonstrated that if a HEPA filter has particle deposits, it can rupture at relative humidities less than 100%.(13) Since smoke aerosols can easily pass through demisters, the smoke and high humidity can result in rapid HEPA plugging and subsequent rupture.

The available studies on HEPA filter performance under fire conditions suggest there are problems with the current fire protection systems in filter plenums. Unfortunately there are no studies to confirm that the current fire protection system shown in Figure 1 will prevent the extensive filter blow-out seen in the 1980 Rocky Flats fire. German studies on filter blow out suggest that smoke and moisture can rapidly plug the filter plenum system in Figure 1 and result in filter rupture. We recommend an experimental study to confirm that the existing water spray system will work in protecting HEPA filters from rupturing during fires. Until this study is completed, we recommend that 0% efficiency be assumed for each filter stage exposed to a water spray if the blower has at least 10 inches of vacuum, disregarding the presence of a demister. This recommendation had been previously made in our guide for determining HEPA filter efficiency under accident conditions.(5)

Instead of building an elaborate system to protect the fragile HEPA filters, an alternative approach would be to build high strength HEPA filters. Germany and France have installed high efficiency steel filters in the exhaust of their commercial power plants for increased reliability.(19,20) Bergman et al have developed a cleanable high efficiency steel filter for use in DOE facilities.(21) With further development, a steel HEPA filter can replace the existing glass fiber HEPA filters. Modest incremental improvements to the existing HEPA filter can also be made such as using a non-combustible sealant and reinforced glass paper.(22)

VIII. References

1. DOE (DRAFT) STANDARD : FIRE PROTECTION DESIGN CRITERIA, September 1995, DOE-STD-1060-XX.

2. Fretthold, J.K. "Summary Report of Incineration Plenum Fire, Building 771, July 2, 1980", Rocky Flats Plant Report 4969, May 31, 1995.

3. Elder, J. ,Graf, J., Dewart, J., Buhl, T., Wenzel, W., Walker, L., and Stoker, A. "A guide to radiological accident considerations for siting and design of DOE nonreactor nuclear facilities" , Los Alamos National Laboratory Report, RFP-3650, June 25, 1984.

4. Atomic Energy Commission, "HEPA Filtration Guidelines," AEC unpublished meeting notes, Albuquerque Operations Office, Albuquerque, NM, 1971.

5. Bergman, W, First, MW, Anderson, WL, Gilbert, H, and Jacox, JW, "Criteria for calculating the efficiency of deep-pleated HEPA filters with aluminum separators during and after design basis accidents" in Proceedings of the 23rd DOE/NRC Nuclear Air Cleaning and Treatment Conference, CONF-940738, NTIS, Springfield, VA, pp. 563-597, 1995.

6. Keighter, D. J. "The fire and explosion experience in filters and ventilation in U.S. nuclear facilities: a 1945-1980 review" , paper presented at CSNI Specialist Meeting on Interaction of Fire and Explosion with Ventilation Systems in Nuclear Facilities, Los Alamos, NM, April 25, 1983.

7. DOE (Draft) Standard, Fire Protection Design Criteria, DOE-STD-1066-XX, May 1996.

8. Cartwright, DR, Johnson, CM, and Thompson, MA, "Filter plenum fire tests" Dow Chemical Company Report CRD 940330-109, Dow Chemical Company, Rocky Flats Division, September 3, 1970.

9. Domning, WE, "Water spray heat exchangers for HEPA protection in accidents (heat removal requirements and the effect of smoke and water on HEPA filters), in Proceedings of 12th AEC Air Cleaning Conference, CONF-720823, NTIS, Springfield, VA, pp 755-769, January 1973.

10. Gaskill, JR and Murrow, JL, "Fire protection of HEPA filters by using water sprays" in Proceedings of the 12th AEC Air Cleaning Conference, CONF-720823, NTIS, Springfield, VA, pp 103-122, January 1973.

11. Alvares, N., Beason, D., Bergman, W., Ford, H., and Lipska, A. "Fire protection countermeasures for containment ventilation systems" in Proceedings of 16th DOE Nuclear Air Cleaning Conference, NTIS Springfield VA, CONF-801038, pp 1213-1277, 1981.

12. Ruedinger,V., Ricketts, C., and Wilhelm, J., "Limits of HEPA-filter application under high-humidity conditions", Proceedings of the 18th DOE Nuclear Airborne Waste Management and Air Cleaning Conference, NTIS Springfield VA, CONF-840806, pp 1058-1084, 1985.

13. Ricketts, C. Ruedinger, V., and Wilhelm, J. "HEPA -filter behavior under high humidity airflows" in Proceedings of the 19th DOE/NRC Nuclear Air Cleaning Conference, NTIS Springfield VA, CONF-860820, pp 319-352, 1987.

14. Ricketts, C, Ruedinger, V, and Wilhelm, J, "The flow resistance of HEPA filters in supersaturated airstreams, 20th DOE/NRC Nuclear Air cleaning Conference, CONF-880822, NTIS Springfield VA, pp 668-694, 1989.

15. Burns, DB, Wong, A, Walker, BW, and Paul, JD, "Testing cleanable/reusable HEPA prefilters for radioactive waste incinerator air pollution control systems" 24th DOE/NRC Nuclear Air Cleaning and Treatment Conference" . Portland, OR, July 15-18, 1986,

16. Gilbert, H., Fretthold, J.K., Rainer, F., Bergman, W., and Beason, D. "Preliminary studies to determine the shelf life of HEPA filters " in Proceedings of 23rd DOE/NRC Nuclear Air Cleaning and Treatment Conference, CONF-940738, NTIS Springfield, VA, pp 613-638, 1995.

17. ASME AG-1-1994, Code on Nuclear Air and Gas Treatment, The American Society of Mechanical Engineers, 345 East 47th Street, New York, NY, December 29, 1995.

18. Record of telephone conversations between Werner Bergman and Rocky Flats firemen who entered the filter plenum and sprayed the HEPA filters on July 2, 1980, September 16 and 18, 1996.

19. Kaercher, MV, "Design of a prefilter to improve radiation protection and filtering efficiency of the containment venting system" 22nd DOE/NRC Nuclear Air Cleaning and Treatment Conference", CONF-9020823, NTIS Springfield, VA, pp 443-452, July 1993.

20. Dillmann, HG and Pasler, H, "A filter concept to control airborne particulate releases due to severe reactor accidents and implementation using stainless-steel fiber filters" in 18th DOE Nuclear Airborne Waste Management and Air Cleaning Conference, CONF-840806, NTIS Springfield VA, pp 141701428, March 1985.

21. Bergman, W. et al, "Development and evaluation of a cleanable high efficiency steel filter", 22nd DOE/NRC Nuclear Air Cleaning and Treatment Conference", CONF-9020823, NTIS Springfield, VA, pp 586-616, July 1993.

22. Gilbert, H, Bergman,W, and Fretthold, JK, "Development and evaluation of a HEPA filter for increased strength and resistance to elevated temperature" 22nd DOE/NRC Nuclear Air Cleaning and Treatment Conference", CONF-9020823, NTIS Springfield, VA, pp 617-634, July 1993.

DISCUSSION

PORCO: Did the filters have face guards on them?

BERGMAN: No.

PORCO: Does that mean they were not qualified filters?

BERGMAN: I must assume that the HEPA filters were qualified to be used at Rocky Flats. The ones in Rocky Flats in 1980 did not have face guards.

PORCO: I think at that time, as well as now, the QPL requires you to have face guards.

BERGMAN: Even if you had face guards, I think the filters would still suffer significant damage. At the 1984 Nuclear Air Cleaning Conference, Ron Pratt showed a nearly complete filter collapse even with face guards after high temperature exposure. You might prevent total collapse of the entire filter pack but you would still have 50-60% penetration. To me, 60% and 100% penetration results in similar contamination.

PORCO: Face guards would add structural integrity. With high temperature you are aging the filter. Whether it is a rapid or a slow rise, binders will leave the paper and volatiles will leave the sealant. When you add a water spray, you blind the filter, increasing pressure drop, so you would expect a failure.

BERGMAN: I agree. The culprit here is the pressure drop more than the temperature. Indeed, you cause damage from the temperature but not nearly as much damage as the overpressure.

PORCO: I think the point to be made here is, if they were not qualified filters you lose your baseline of comparison.

BERGMAN: I assume that since the Rocky Flats filter test facility certifies HEPA filters for use in nuclear facilities, that the 1980 HEPA filters met all of the requirements including QPL.

FRETTHOLD: The filters were used in a system that had nitric acid in it and the galvanized face guards were literally disintegrating. Consequently, the filters were purchased minus face guards.

PYLE: Did the heated air hitting the HEPA filters exceed the temperature necessary to burn out the organic binder in the medium?

BERGMAN: Yes, the organic binders burned out immediately. Every nuclear grade HEPA filter must pass a heated air test at 750°F. At about 400°F you see a big plume of smoke in the exhaust. That is the binder, but most HEPA filters still have better than the required 97% efficiency.

WILHELM: A dust-loaded HEPA filter failed at a spray rate of around 50g H_2O/m^3 air, within 20min. A high strength HEPA filter with the Lydair medium did not fail within 20h. under the same conditions.

DERDERIAN: What is the basis of this 700°F±50°F test of the MIL Specification, and how does it represent fire vulnerability? There is a need for greater dialogue between fire protection and HEPA filter designers.

BERGMAN: That is an excellent suggestion and I recommend everyone attend Dr. Ricketts lecture tomorrow in which he addresses that very subject. I do not know the basis for the 700°F test.

DERDERIAN: I think there is also room for dialogue between the fire protection community, certainly, and the HEPA filter community in the sense that the fire people have always been concerned with deep-seated fires because in most cases they are not amenable to quenching by gaseous agents. That is a generalization that they tend to make. I am not sure it applies in this case but I think there is definitely room for dialogue between the two communities.

BERGMAN: A lot of dialogue.

ENGELMANN: Why did not the emergency response plans call for shutting down the ventilation fans before turning on the water spray?

BERGMAN: I do knot know. However, the most recent draft of a DOE fire protection standard recommends limiting the pressure drop across HEPA filters by turning down the ventilation fans.

SIMULATION TEST OF AEROSOL GENERATION FROM VESSELS IN THE PRE-TREATMENT SYSTEM OF FUEL REPROCESSING*

Sachio FUJINE, Koichiro KITAMURA, and Takehiro KIHARA
Department of Fuel Cycle Safety Research
Japan Atomic Energy Research Institute(JAERI)
Tokai-mura, Naka-gun, Ibaraki-ken,JAPAN 319-11

Abstract

Aerosol concentration and droplet size are measured in off-gas of vessel under various conditions by changing off-gas flow rate, stirring air flow rate, salts concentration and temperature of nitrate solution. Aerosols are also measured under evaporation and air-lift operation.

I. Introduction

Non-volatile radioactive elements such as Pu, Np, Am, Tc, Ru, Sr, Cs and other FPs are confined in the process under normal operation of reprocessing. Almost all radioactive non-volatile fission products are actually confined in highly radioactive liquid waste. However, there are pathways for release of these non-volatile elements to the environment through off-gas and/or aqueous effluents. Radioactivity migration of non-volatile elements takes place in the facility primarily by aerosols. Aerosol generation under normal operation are caused by liquid aeration, evaporation, transportation and other handling of radioactive solutions(1-3). Important area of facility for the radioactivity migration is particularly pre-treatment process which contains highly radioactive solutions in vessels. Not only decontamination factor of filters but also radioactivity behaviors in the process play the important role in assessment of source terms of environmental releases from large scale reprocessing plant(4). Role of aerosol behavior is significant especially for the migration of non-volatile nuclides. Influences of operation condition of vessels are studied on the concentrations and droplet size of particles of aerosols in off-gas.

II. Experimental

Experimental facility(**Fig.1**) is composed of a slab-type vessel, a condenser, an air-lift and an exhaustive blower, those are connected with pipes and valves. The slab-type vessel is aerated with air

---

* Work performed under contract with Science and Technology Agency(STA), JAPAN.

nozzle submerged in the liquid of vessel. Liquid in vessel can be heated with two 5kW electric heaters. Liquid can be circulated outside by air-lift attached to the vessel. Aerosols are sampled on off-gas pipes(Inner diameter 28mm) with Andersen sampler(AS-500). Standard sampling time is 5 hours. Nitrate aqueous solutions, listed in **Table 1**, are used as the simulated radioactive solution of reprocessing. Salts concentration of sodium, lithium, and nitrate ions are total 100 and 350 g/L. Lithium is added as tracer of the solution. Li in aerosols is analyzed by ICP.

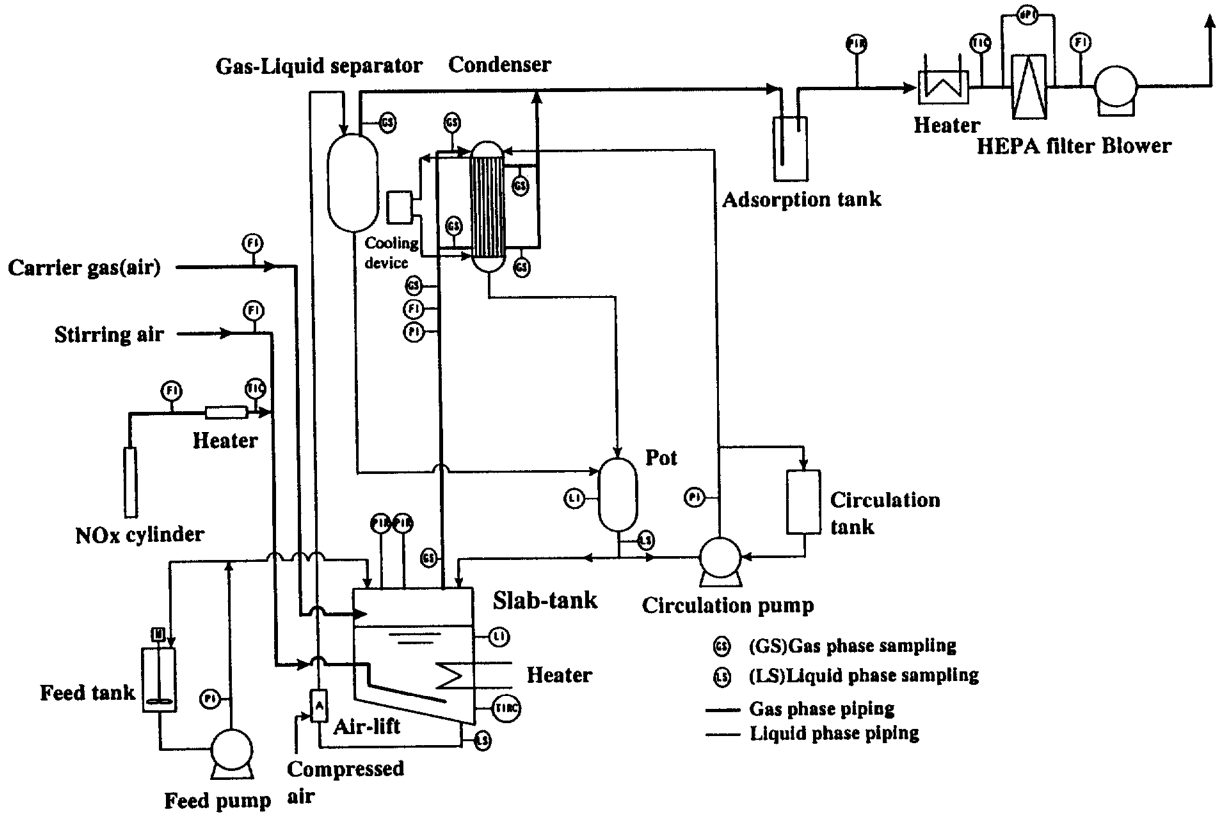

Fig. 1 Flow sheet of experimental equipment.

Liquid volume in vessel is 30L under standard condition of experiment. Distance from air nozzle submerged in solution to liquid free surface is 44cm. Distance from free surface to vessel ceiling is 55cm. Standard air stirring flow rate is 10 m^3/hm^2-free surface area of vessel which corresponds to a weak stirring condition of chemical process. Linear flow velocity of off-gas is in the range from 2 to 10 m/s. Required off-gas flow rate is adjusted by controlling sweeping air flow rate of the volume above the liquid free surface in vessel.

Aerosols in off-gas are measured at the outlet of vessels under aeration by changing the sweeping air flow rate or stirring air flow rate as operation parameters. Properties of solutions in vessel are changed in some cases. In the case of evaporation operation, aerosols in off-gas are measured at the outlet of condenser of vessels. In the case of air-lift operation, aerosols in off-gas are measured at the outlet of air-liquid separator.

Table 1 Properties of salt solutions used in the experiment.

solution	concentration g/L	density g/cm^3	viscosity cP	surface tension dyn/cm
$NaNO_3$+$LiNO_3$ in water	100	1.065	1.17	60.0
$NaNO_3$+$LiNO_3$ in 3N-nitric acid	350	1.290	2.33	50.3
$NaNO_3$+$LiNO_3$ TBP 100ppm in water	100	1.065	1.12	36.9

III. Results

Off-gas Flow Rate

Aerosol concentrations in off-gas decreases inverse proportionally to off-gas flow rate, as shown in **Fig.2**. Required off-gas flow velocity is adjusted by changing the sweeping air flow rate on the liquid free surface. Stirring air flow rate is 10 m^3/hm^2 per free surface area of liquid in slab-tank. Aerosol concentrations are observed in the range from a few to a dozen mg/m^3 under the experimental conditions. Numerical values near plots are 50% mean diameters. It is observed that mean particle size decreases from 5.3 to 2.3 μ m by increasing off-gas flow rate. There must be the bigger possibility of trapping for the larger aerosol particles near outlet of slab-tank to off-gas pipe under the higher off-gas flow rate. The outlet is located at ceiling of the tank. Saturation by humid of sweeping air influences to reduce both aerosol concentration and particle size, that is shown in Fig.2 as well.

Stirring Air Flow Rate

Aerosol concentrations in off-gas increases roughly proportionally to stirring air flow rate, as shown in **Fig.3**. This figure shows the relations between aerosol concentration at off-gas outlet of tank and stirring air flow rate for several kind of solutions. As for $NaNO_3$ 3M-nitric acid solution, aerosol concentrations are less than 10 mg/m^3 in the range of less than 30 m^3/hm^2 stirring air flow rate. A separate peak of the smaller particle size in addition to the main peak of the bigger particle size is observed in the aerosol size distribution for the higher range of stirring air flow rate in the experiment.

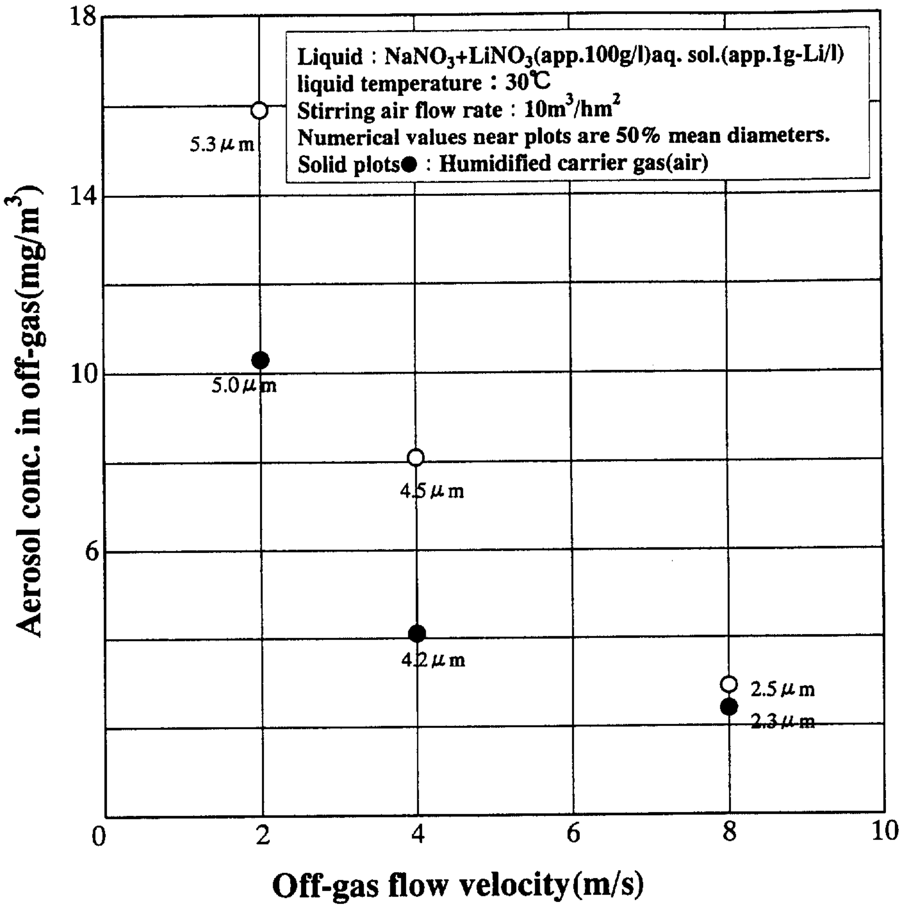

Fig.2 Aerosol concentration in off-gas depending on off-gas flow velocity

Salts Concentration

Figure 3 shows that a solution of 350 g/L $NaNO_3$+$LiNO_3$-3M nitric acid gives the smaller aerosol concentrations in off-gas approximately by half than a 100 g/L $NaNO_3$+$LiNO_3$ aqueous solution does. Both viscosity and density are bigger for 350 g/L $NaNO_3$+$LiNO_3$-3M nitric acid solution. Viscosity is 2.33 cP and density is 1.290 g/cm^3 for the solution. On the other hand, viscosity is 1.17 cP and density is 1.065 g/cm^3 for 100 g/L $NaNO_3$+$LiNO_3$ aqueous solution. Two peaks size distribution are more often observed for the higher salts concentration.

TBP Addition

Extractant TBP is added by 100 ppm to a 100 g/L $NaNO_3$+$LiNO_3$ aqueous solution. Surface tension of the solution is decreased to 36.9 dyn/cm from 60.0 dyn/cm of 100 g/L $NaNO_3$+$LiNO_3$ aqueous solution. **Figure 3** shows that aerosol concentration in off-gas increases significantly by 2 to 5 times by TBP addition.

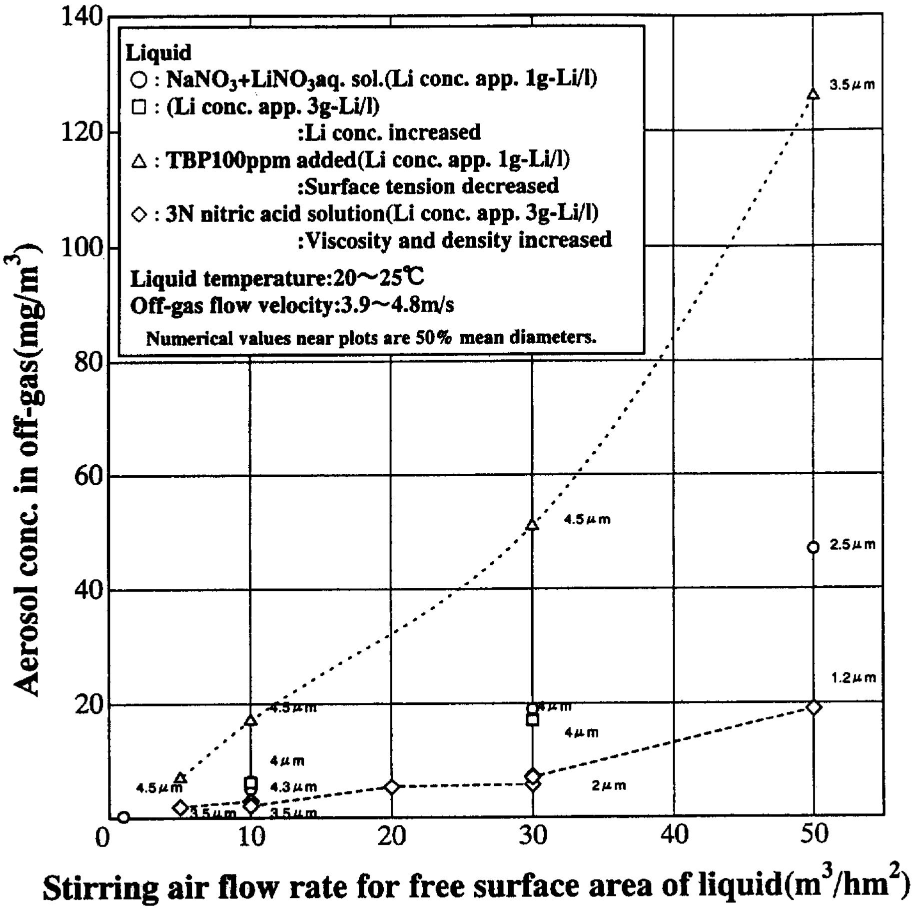

Fig.3 Aerosol concentration in off-gas depending on stirring air flow rate for different kind of solutions.

Temperature Increase

Liquid temperature in slab-tank was changed in the range from 20 to 60℃ by using two 5kW electric heaters submerged in the solution.

Aerosol concentrations in off-gas are increased by increasing temperature, as shown in **Fig.4**. Surface tension decrease by increasing temperature must be primary cause for the aerosol increase.